Elucidating the Mechanism by which KRI-1/CCM1 Regulates Apoptosis Cell Non-Autonomously in *Caenorhabditis elegans*

by

Eric Michael Chapman

A thesis submitted in conformity with the requirements
for the degree of Doctor of Philosophy

Department of Molecular Genetics
University of Toronto

Elucidating the Mechanism by which KRI-1/CCM1 Regulates Apoptosis Cell Non-Autonomously in *Caenorhabditis elegans*

Eric Michael Chapman

Doctor of Philosophy

Department of Molecular Genetics
University of Toronto

2018

Abstract

Programmed cell death initiated by genotoxic stress requires signalling from surrounding tissues, yet such mechanisms are poorly understood. The *C. elegans* germline is a powerful model to study cell non-autonomous regulation of apoptosis, since germ cells die in response to DNA damage, and because this death requires regulatory input from the soma. The scaffold protein KRI-1, a homologue of mammalian KRIT1/CCM1, was identified to promote DNA damage-induced germ cell apoptosis from the somatic tissue by an unknown mechanism. I reveal that KRI-1 is required for proper activation of MPK-1/ERK1 in the germline, and genetically up-regulating MPK-1/ERK1 restores germ cell apoptosis in the absence of KRI-1. To determine how KRI-1 signals cell non-autonomously to communicate with MPK-1/ERK1, I conducted a forward genetic screen and identified an ERK5/MAPK pathway and the KLF-3 transcription factor that function downstream of this scaffold. I have shown that like *kri-1, mpk-2*/*erk-5* is expressed in the intestine, as is *klf-3*, and that over-activation of MPK-2/ERK-5 in this tissue is anti-apoptotic. Furthermore, I found that KRI-1 interacts with K07A9.3/CCM2 and Y45F10D.10/ICAP1, which are required to regulate germ cell apoptosis. RNA sequencing of

wild type, *kri-1,* and *kri-1; mpk-2/erk5* mutants, followed by an RNA*i* screen, identified that the zinc transporter, *zipt-2.3*/*scl39,* has a role in regulating germ cell apoptosis. ZIPT-2.3 is expressed in the intestine, and reduced *zipt-2.3* expression in the absence of KRI-1 prevents proper zinc storage. This results in suppressed activation of MPK-1/ERK1 and germ cell apoptosis. Therefore, the KRI-1 scaffold protein ensures proper activation of MPK-1/ERK1 and germ cell apoptosis by regulating zinc storage.

Acknowledgments

I would like to thank everyone who helped me through the process of obtaining a PhD, without whom, this would not have been possible. To my committee members Drs. Anne-Claude Gingras and Andrew Fraser, your advice and support starting from my first committee meeting in 2013 helped me to develop my critical thinking. Our meetings were always fun and productive, and I looked forward to each one. To the Derry Lab, you have become my family and I am truly grateful to have worked alongside everyone at the bench. In particular, to those who have been with me from the beginning, Bin Yu, Ben Lant, Swati Pal, and Abigail Mateo. You helped all of the tough experiments, long nights, and busy weekends in the lab pass by with relative ease. I look forward to continuing our friendship and wish you all the best in the future. I am also glad to have worked with everyone else in the Derry lab that joined throughout the course of my studies. To the coordinators of the Department of Molecular Genetics at U of T and DSCB program at The Hospital for Sick Children, you provided an enriching environment for me to do the highest quality research, and many opportunities to develop my leadership skills. To my peers in these programs (you know you who are), thank you for being a critical sounding board when science got tough. We helped each other prevail! We also had a lot of great times outside of the lab, and you have become lifelong friends. To my scientific supervisor and mentor, Dr. W. Brent Derry, you have been a tremendous source of support throughout my studies and provided me with the best possible graduate experience. Your constant optimism is contagious and I can't thank you enough for everything you have helped me with. The best decision I made in grad school was joining your lab. I look forward to staying in touch and reading about all your future kick Ras science! To my parents and grandma, thank you for always supporting me (and for never asking when I was going to finish my PhD). Finally, to my partner Ashlee, you had to endure being with a married (to science) man for six years. You were always there for me despite my limited weekend availability and constant late nights in the lab, and provided a greater perspective when I needed it most. If that's not true love, I don't know what is.

Table of Contents

List of Tables

List of Figures

List of Definitions and Abbreviations

9-1-1 complex: Heterotrimer complex that scans DNA for DSBs, comprised of HPR-9/ RAD9, MRT-2/ RAD1, and HUS-1/ HUS1
AAK-1/2: AMP-activated kinase-1/2
ABL-1/ABL1: Related to oncogene ABL
ACT: Actin
AIF: Apoptosis inducing factor
AKT: strain AK thymoma
AMPK: 5' AMP-activated protein kinase
AMPK: 5' AMP-activated protein kinase
ANGPT2: Angiopoietin 2
APAF1: Apoptotic protease activating factor 1
AP-MS: Affinity purification-mass spectrometry
Apoptosis: Greek for “falling off” (of leaves from trees)
Apoptosome: Complex comprised of CED-4/APAF1 and CED-3/CASP9, with cytochrome c in vertebrates.
APX: Ascorbate peroxidase
AS neurons: Amphid sensory neurons
ATL-1/ATR: Ataxia telangectasia mutated-like
ATM-1/ATM1: Ataxia telangectasia mutated
Autophagy: Greek for “self-eating”
BAD: Bcl-2-associated death promoter
BAK: Bcl-2 homologous antagonist killer
BAX: BCL2 associated X protein
BCL2: B-cell lymphoma 2
BCL2L2/BCL-W: BCL2-like protein 2
BCL-xL: B-cell lymphoma-extra large
BH3-only: Proteins that contain only the third BH domain (BH3) that is found in the BCL2-family proteins
BH-domain: BCL2-homology domain
BID: BH3 interacting-domain death agonist
BIM: Bcl-2 interacting mediator of cell death
BIR-1/BIR-2: Baculoviral inhibitor of apoptosis (IAP) repeat-1/2
BMEC: Brain microvascular endothelial cells
BMK1: Big mitogen kinase-1
BSA: Bovine serum albumin
CAR-1/LSM14: Cytokinesis, apoptotis, RNA-associated-1
CARD: Caspase recruitment domain
Cas9: CRISPR associated protein 9
Caspases: Cysteine proteases that cleave after aspartate
CBP-1/CBP: CBP/p300 homolog
CBP-3/CBP: CBP/p300 homolog-3
CCM: Cerebral cavernous malformation
CDF-1/SLC30: Cation diffusion facilitator family-1
CED: Cell-death abnormal

CEH-30/BARH: *C. elegans* homeobox-30
CEM neuron: Cephalic male neuron
CEP-1: *C. elegans* p53
CGC: Caenorhabditis Genetics Center
CGH-1: Conserved germline helicase-1
CHK: Checkpoint kinase
CLK-2/TEL2: Clock abnormality-2
CNS: Central nervous system
Co-IP: Co-immunoprecipitation
COPI/II: Coatomer protein complex I/II
Core apoptosis pathway: *egl-1/BH3-only, ced-9/BCL2, ced-4/APAF1, ced-3/Caspase*
CPS-6: CED-3 protease suppressor
CRISPR: Clustered regularly interspaced short palindromic repeats
CV: Caudal vein
DAF-16/FOXO: Abnormal dauer formation-16
DAPI: 4′,6-diamidino-2-phenylindole
Dauer: German for "enduring"
DDIAS: DNA damage induced apoptosis suppressor
Death Domain: Domain able to interact with FADD
DIC: Differential interference contrast
DISC: Death inducing signalling complex
DLC-1/DYNLL: Dynein light chain-1
DLC-1: Dynein light chain-1
DRL-1: Dietary restriction like-1
DSB: Double stranded DNA breaks
DTC: Distal tip cell
E3 ligase: Ubiquitin ligase that promotes protein degradation by the proteosome
EEL-1/MULE: Enhancer of EfL-1 mutant phenotype
EFN: Eph(f)rin ligand
EGF: epidermal growth factor
EGL-1: Egg-laying defective-1
EIF: Eukaryotic (translation) initiation factor
EMS: Ethyl methanesulfonate
EndMT: Endothelial to mesenchymal transition
EndoG: Endonuclease G
EOR-1/PLFZ: EGL-1 suppressor/DiO uptake defective/raf enhancer-1
ER: Endoplasmic reticulum
ERK1: Extracellular signal-regulated kinase-1
Executioner caspases: Caspases which activate apoptosis
Extrinsic apoptosis: Death receptor-mediated apoptosis
F1/F2: First filial/second filial
FADD: FAS-associated protein with death domain
FasL: Fatty acid synthetase ligand
Fasudil: ROCK inhibitor
FBF/PUF: *fem-3* mRNA binding factor
FERM domain: 4.1 (f) protein, ezrin, radixin, moesin
GAP-2/GAP: GTP activating protein-2
GCK-1/GCK: Germinal center kinase family-1

GEF: Guanine nucleotide exchange factor
GEN-1/GEN1: GEN1 holliday junction resolvase homolog-1
GFP: Green fluorescent protein
GLA-3/TIS11: Germline apoptosis abnormal-3
GLD-1/QUAKING: Defective in germline development-1
GTPase: Enzymes that convert GTP to GDP
Gy: Gray, unit of ionizing radiation
HEG1: Heart of glass 1
HHD: Harmonin homology domain
HIF-1: Hypoxia-inducible transcription factor-1
HIP-1/HSP: Hsp-70 Interacting Protein homolog
HIZR-1: High zinc activated nuclear receptor-1
HLH-2/3: Helix loop helix-2/3
HPK-1/HIPK2: Homeodomain-interacting protein kinase
HPR-9/RAD9: Homolog of *S. Pombe* Rad-9
HR: Homologous recombination
HSN: Hermpahrdite-specific neurons
HSP-17: Heat shock protein-17
HT115: Strain of *E. coli*
HUS-1/HUS1: Human HUS1-related
IAP: Inhibitor of apoptosis proteins
ICAP1: Integrin cytoplasmic domain-associated protein 1
IGH: Immunoglobin heavy chain
Initiator caspases: Caspases which activate executioner caspases
InsR: Insulin receptor
Intrinsic apoptosis: Mitochondrial-mediated apoptosis
IR: Ionizing radiation
JNK: c-Jun N-terminal kinase
KLF: Kruppel-like factor
KRI-1: KRIT1 homolog
KRIT1: K-rev interaction trap-1
KSR: Kinase suppressor of RAS
L1 diapause: Arrested L1 larval development in the absence of food
L1-L4: Larval stages 1-4
LDL: Low density lipoprotein
LET: Lethal
LIN: Lineage abnormal
LIP-1/MKP3: Lateral signal induced phosphatase-1
MAPK: Mitogen-activated protein kinase
MCL1: Myeloid cell leukemia 1
MDM2: Mouse double minute 2
MEF-2/MEF2: Myocyte enhancer factor 2
MEK: MAPK/ERK kinase
MEKK: MAPK/ERK kinase kinase
microRNA: Small non-coding RNA of about 22 nucleotides
MLT-1/2: Metallothionein-1/2
MNK: MAPK- interacting protein kinase
MRT-2/RAD1: Mortal germline-2

Msh2: Mismatch Repair2
MT: Metallotheonein-family proteins
MTF1: Metal regulatory transcription factor 1
mTOR: Mechanistic target of rapamycin
Muv: Multi-vulva
NADPH: Nicotinamide adenine dinucleotide phosphate
NDMA receptor: *N*-methyl-D-aspartate receptor
Necroptosis: Programmed necrosis
Necrosis: Greek for "death, dying, killing"
NGF: Nerve growth factor
NGM: Nematode growth medium
NHEJ: Non-homologous end joining
NOX1: NADPH oxidase-1
NOXA: Latin for "damage"
NSM: Neurosecretory motoneuron
NUC-1/DNaseII: Abnormal nuclease-1
OP50: Strain of *E. coli*
PAC-1 : Abnormal PAR-6 at contacts-1
PAL-1/CDX2: Posterior alae in males-1
PAX: Paired box
PB1domain: Phox and Bem1
PBS: Phosphate-buffered saline
PCV: Posterior cardinal vein
PDCD10/CCM3: Programmed cell death 10
PEPT-1/SLC15 : Peptide transporter-1
PFA: Paraformaldehyde
PGP-2: P-glycoprotein related-2
Phagosome: Apoptotic cell enclosed within an engulfing cell
PHO-1: Intestinal acid phosphatise-1
PI3K: Phosphatidylinositol 3-kinases
PIKK: Phosphatidylinositol 3-kinase-related kinases
PKA: Protein kinase A
PQM-1/SALL2: Paraquat methylviologen responsive-1
PRMT-5/PRMT5: Protein arginine methyltransferase-5
PS: Phosphatidylserine
PSR: Phosphatidylserine receptor-1
PTB domain: Phosphotyrosine binding
PUMA: p53 up-regulated modulator of apoptosis
PVF-1: PDGF/VEGF growth factor related
RAF: Rapidly accelerated fibrosarcoma
RAP1: RAS-related protein 1
RAS: Rat sarcoma
RFP-1/ BRE1: Ring finger protein-1
RhoA: RAS homolog family member A
RIPK1/RIPK3: Receptor-interacting protein kinase 1/3
RME-2/LDL: Receptor mediated endocytosis-2
RNA*i:* RNA interference
ROCK: Rho associated protein (c)kinase

ROG-1/FRS: RAS activating factor in development of germline-1
ROS: Reactive oxygen species
RSK: Ribosomal s6 kinase
RTK: Receptor tyrosine kinase
SCF^{FSN-1}: F-box synaptic protein E3-ligase complex
SCRM-1: Scramblase-1
SEM-5/GRB2: Sex muscle abnormal-5
SGK-1/SGK1: Serum and glucocorticoid inducible kinase-1
SKN-1/NRF2: Skinhead-1
SLC: Solute carrier
SLC30: Family of solute carriers that generally transport zinc into the cytosol
SLC39: Family of solute carriers that generally transport zinc out of the cytosol
SMA-5: Small-5
SMAC/DIABLO: Second mitochondria-derived activator of caspases/ direct IAP binding protein with low pI
SMURF1: Smad ubiquitin regulatory factor 1
SOC-2/SHOC: Suppressor of Clr
SOS-1/GEF: SOS homologue-1
Spermatheca: Region of sperm storage
SRP-6: Serine protease inhibitor -6
STRIPAK complex: Striatin interacting phosphatase and kinase
SUR-7: Suppressor of let-60/RAS-7
TF: Transcription factor
TOL-1/TLR: Toll-like receptor
TNF: Tumor necrosis factor
TOE: Target of ERK kinase MPK-1
TRA-1: Transformer-1
TRADD: TNFR-associated death domain
TRAF: TNF receptor-associated factor
TRAIL: TNF-related apoptosis-inducing ligand
TRK: Tropomyosin receptor kinase
TSP1: Thrombospondin 1
TTM-1/SLC30: Toxin-regulated target of MAPK-1
TYR-2/TRP2: Tyrosinase-2
UNC: Uncoordinated
UV: Ultraviolet radiation
VAB-1/EphR: Variable abnormal morphology-1
VEGF: Vascular endothelial growth factor
VER-1-4: VEGF receptor family-1,2,3,4
VHL-1: Von hippel-lindau tumor suppressor homolog-1
VIT*:* Vitellogenin
WAH-1: Worm AIF homologue
WD repeat: short repeats ending with tryptophan-aspartic acid
WNT: Wingless-integration site
ZIM-2: Zinc finger in meiosis-2
ZIPT: Zrt, Irt- like protein transporter

1 Introduction

1.1 Cell Death to Promote Life

1.1.1 Why cells die

Cell viability is fundamental to all life. For single celled organisms, division creates new individuals that will continue to pass genetic material onto subsequent generations. For multicellular organisms the creation of new cells is a requirement to build and maintain complex tissues. Why then, would cells die? Sometimes, death of cells is accidental and non-controllable, such as a result of injury (Cobb, et al., 1996). Often, cell death occurs to benefit the entire organism (Renehan, et al., 2001). Such an active decision on the part of a cell or organism must be controlled. These deaths are termed “Programmed Cell Deaths”, because such a fate is coordinated genetically and biochemically, like any other cellular process. Programmed death will be the focus of this thesis and will be expanded upon in the sections below.

1.1.2 Programmed cell death

There are many situations that warrant a cell to initiate self-destruction. During development, tissue formation often requires a fine tuning of cell number. If too many cells are formed, they must be selectively removed from the body. A few well known examples of this type of developmental death include the removal of webbing between mammalian digits, and the pruning of extra neurons that form in the brain (Suzanne & Steller, 2013). It is also beneficial for cells to die in response to infection, to prevent the spread to neighbouring cells (Ashida et al., 2011). In the context of disease, cell death must occur to prevent damaged cells from usurping resources or dividing uncontrollably. The failure to remove such cells can lead to tumor formation and cancer (Brown & Attardi, 2005). The sections below outline the form of programmed cell death known as apoptosis, which is the focus of this thesis, followed by two other programmed strategies for cellular demise.

1.1.2.1 Intrinsic apoptosis: The core pathway

The term apoptosis, Greek for "falling off", was first suggested in 1972 by Kerr, Wyllie, and Currie to describe the phenomenon of cell removal in rats (Kerr, et al., 1972). This landmark report described dead cells as having condensed DNA and "blebbing" of the membrane. However, it wasn't until the late 1980s that work largely using the nematode worm *C. elegans* in the Horvitz lab determined that the process of apoptosis relied on intact genes and is therefore a genetically regulated program that is initiated by the cell (Hengartner & Horvitz, 1994b). Since the 1990s multiple groups have characterized the protein protects encoded by the conserved genes that regulate apoptosis. Not surprisingly, there are a number of steps that occur before the final result of membrane blebbing that was first described in 1972. Since *C. elegans* was instrumental in understanding the genetic cascade leading to apoptotic cell death (2002 Nobel Prize), and as the organism featured in this thesis, I will outline the apoptotic process by referencing the *C. elegans* genes that constitute the "core apoptotic cascade".

The initiation of apoptosis hinges on the activation of enzymes known as caspases, (**c**ysteine proteases that cleave after **asp**artate) and recognize substrates with a canonical D-X-X-D amino acid sequence (Li & Yuan, 2008). These killer proteases initiate the apoptotic process by cleaving structural proteins and enzymes important for DNA repair, resulting in structural degradation and nuclear fragmentation. An important aspect of apoptosis is that it does not involve the release of cellular contents, and therefore, does not elicit an immune response (Li & Yuan, 2008). This is ideal in situations when only targeted cells need to be removed from a population, leaving neighbouring cells unharmed. In *C. elegans* the main caspase involved in all cell deaths is called CED-3 (**Ce**ll-**d**eath abnormal) and was identified from a screen for genes that prevented all developmental cell deaths when mutated (Ellis & Horvitz, 1986). CED-3 is functionally related to mammalian caspases, as it was shown to induce apoptosis in mammalian cells (Miura, et al., 1993). Caspases similar to CED-3, such as mammalian Caspase-3, which activate apoptosis are termed "executioner caspases" (Li & Yuan, 2008). Given that caspases are so detrimental to the cell, how can an organism keep these enzymes on "standby", while allowing for cell survival? The answer lies in the fact that these executioner caspases exist as inactive zymogens that must be processed by "initiator caspases" upon death-inducing stimuli (Li & Yuan, 2008). Such apoptotic stimuli promote the formation of "apoptosomes" through the

interaction of the CARD (**Ca**spase **R**ecruitment **D**omain) in the long prodomain of initiator caspases with the CARD of adaptor proteins (Dorstyn et al. 2018). When the apoptosome assembles, the initiator caspases are in an orientation that allows dimerization, resulting in their activation (Dorstyn et al. 2018). The activated initiator caspase dimers are then able to process and activate executioner caspases by cleavage (Li & Yuan, 2008). In the worm, CED-3 functions as both an initiator and executioner caspase, while in mammals, the main initiator caspases include caspase-8 and capsase-9 (Li et al., 1997; Muzio et al. 1996).

The core adaptor protein of the apoptosome in *C. elegans* is CED-4, which was identified by the same screen as *ced-3/Caspase* (Ellis & Horvitz, 1986). CED-4 is homologous to mammalian **A**poptotic **P**rotease **A**ctivating **F**actor 1 (APAF1) (Zou et al., 1997), which was subsequently shown to be a component of the apoptosome in mammals (Li et al., 1997). In the worm, the apoptosome consists of CED-4 and CED-3/Caspase in an 8:2 ratio, while in mammals there are seven APAF1 molecules and three or four procaspase-9 proteins (Dorstyn et al. 2018). Intriguingly, mitochondria play an important role in apoptosome formation (Wang & Youle, 2009). In *C. elegans* the mitochondria act as a scaffold to keep CED-4/APAF1 molecules from forming the apoptosome (Chen et al., 2000; Figure 1.1C). In mammals, the process diverges, with cytochrome c being released from the mitochondrial intermembrane space (Yang et al., 1997) and binding to WD repeat motifs (short repeats ending with **tryptophan**-**aspartic acid**) of APAF1 to stimulate apoptosome assembly (Zou et al., 1997; Figure 1.1A). In both *C. elegans* and mammals mitochondrial degradation leads to the release of nucleases that facilitate DNA degradation during cell death (Figure 1.1). In *C. elegans* such proteins include WAH-1 (**w**orm **A**IF **h**omologue) and CPS-6 (**C**ED-3 **p**rotease **s**uppressor) (Wang, et al., 2002), which are functionally conserved with mammalian AIF (**a**poptosis **i**nducing **f**actor) (Susin et al., 1999) and EndoG (**Endo**nuclease **G**) (Li, et al., 2001). Therefore, while *C. elegans* mitochondria are passive scaffolds for CED-4/APAF1 during the initiation of cell death, they eventually take on an active role, similar to mammalian mitochondria, to promote apoptosis. In mammals, the proteins SMAC/DIABLO (**s**econd **m**itochondria-derived **a**ctivator of **c**aspases)/ (**d**irect **IA**P **b**inding protein with **lo**w pI) (Du, et al., 2000) and HTRA2/OMI (Suzuki et al., 2001a) are also released from the mitochondria, which promote the activation of caspases by inhibiting the function of IAPs (Inhibitor of Apoptosis Proteins) (Du et al., 2000; Suzuki et al., 2001a). These IAPs were

first identified from baculovirus genes that inhibit cell death (Clem & Miller, 1994), and are E3 ligases that promote the degradation of caspases (Suzuki et al., 2001b). While the *C. elegans* genome contains two *IAP* genes (*bir-1* and *bir-2*), their protein products have no obvious roles in apoptosis (Fraser, et al., 1999).

How do mitochondria prevent ectopic cell death? To allow cell survival, anti-apoptotic proteins in the outer mitochondrial membrane prevent precocious apoptosome formation (Willis, et al. 2003). The founding member of these anti-apoptotic proteins was BCL2 (**B-c**ell **l**ymphoma **2**), identified in patients with a chromosomal translocation t(14;18) that results in the formation of B-cell lymphoma (Tsujimoto, et al., 1984). This translocation places *BCL2* from chromosome 18 close to the immunoglobin heavy chain (*IGH*) enhancer element on chromosome 14, resulting in over-expression of *BCL2* (Hua et al., 1988). While this alone does not cause tumorigenesis, a second oncogenic mutation results in unrestricted cell growth and cancerous proliferation (Fanidi et al., 1992). Although the sequence of BCL2 was identified in the 1980s, its function remained elusive, since there was little homology to other known proteins (Schenk et al., 2017). The only clue was that BLC2 had been shown to associate with membranes (Tsujimoto, et al., 1987) including the mitochondria (Hockenbery, et al., 1990), which did not provide much insight into how BCL2 regulates cell death. The unique domains of BCL2 critical for its anti-apoptotic function were called "BH-domains" (**B**CL2-**H**omology) (Reed, 2008). BCL2 contains four of these domains, which are the defining feature of other anti-apoptotic BCL2-like proteins that comprise the "BCL2 family" including MCL1 (**m**yeloid **c**ell **l**eukemia 1), BCL2L2/BCL-W (**BCL2-l**ike protein **2**), and BCL-xL (**B-c**ell **l**ymphoma-e**x**tra **l**arge) (Reed, 2008). The protein product of one of the *"ced*" genes identified in the Horvitz Lab, CED-9, had conserved function (Hengartner, et al., 1992) and structure (Hengartner & Horvitz, 1994a) to BCL2-family proteins. This provided an opportunity *in vivo* to determine the epistatic relationship between a mitochondrial BCL2-like protein and other already identified members of the apoptotic process. This was possible because the Horvitz lab identified a gain-of-function mutation in *ced-9*, in contrast to the loss-of-function mutations in the other *ced* genes. Through genetic analysis they showed that *ced-9/BCL2* functions upstream of *ced-4/APAF1* and *ced-3/Caspase* (Hengartner, et al., 1992). This discovery was instrumental for determining that BLC2-family proteins are required to regulate apoptosome formation and caspase activation. Given that mitochondria have

disparate roles in *C. elegans* and mammalian apoptosis, it is not surprising that CED-9 functions differently from mammalian BCL2-family proteins, despite both localizing to the mitochondrial outer membrane. In *C. elegans* CED-9/BCL2 physically binds CED-4/APAF1 to prevent apoptosome formation, thus keeping CED-3/Caspase inactive (Del Peso, et al., 1998). In mammals, BCL2-family proteins function to inhibit pro-apoptotic multi-BH domain family proteins such as BAX (**B**CL2 **a**ssociated **X** protein) and BAK (**B**cl-2 homologous **a**ntagonist **k**iller) (Reed, 2008; Figure 1.1). These pro-apoptotic proteins contain three of the four BH domains that the anti-apoptotic members contain, and are important for permeabilizing the outer mitochondrial membrane to promote cytochrome c release and apoptosome formation (Schenk et al., 2017). The anti-apoptotic BCL2-family proteins bind to the pro-apoptotic members to inhibit their ability to permeabilize the mitochondrial membrane (Reed, 2008).

Since BCL2-family proteins are very effective at preventing apoptosome formation, there must be a way to relieve this inhibition to allow cell death in response to developmental cues or external stimuli. This level of regulation occurs due to the function of another family of pro-apoptotic proteins known as the "BH3-only" proteins. This group is named because members contain only the third BH domain (BH3) that is found in the BCL2-family proteins (Wang et al., 1996). The BH3-only proteins are small, and bind to BCL2-family proteins in the mitochondrial membrane to inhibit their function through conformational changes (Omonosova & Hinnadurai, 2008). In mammals, BH3-only protein binding to BCL2-family members prevents the inhibition of the pro-apoptotic BAK/BAX (Omonosova & Hinnadurai, 2008; Figure 1.1A). In some cases, BH3-only proteins can bind to BAX/BAK directly to promote pore formation in the mitochondrial membrane (Harada, et al., 2004; Wang, et al., 1996). In *C. elegans* there are two BH3-only proteins, EGL-1 (**eg**g **l**aying defective-1) and CED-13, with EGL-1 responsible for inducing all cell deaths that occur during development (Conradt & Horvitz, 1998) and in response to germline stress (Hofmann et al., 2002). EGL-1 binds to CED-9/BCL2 which results in the release of CED-4/APAF1 (Del Peso et al., 1998) and the activation of CED-3/Caspase. While *ced-13* and *egl-1* are both transcriptionally up-regulated in response to DNA-damage (Schumacher et al., 2005b), the requirement of CED-13 in promoting apoptosis is unclear. In *C. elegans*, BH3-only initiated cell death is controlled by tissue-specific or stress responsive transcription factors that regulate the levels of *BH3-only* transcript levels (Nehme & Conradt,

2008). For example, *egl-1* is regulated by the somatic tissue-specific transcriptional regulators TRA-1 (**tra**nsformer-1) (Conradt & Horvitz, 1999), HLH-2/Daughterless-like (**h**elix **l**oop **h**elix-2) (Thellmann, et al., 2003), and HLH-3/ASCL (Thellmann et al., 2003) during development, while the ***C. e****legans* **p**53 homolog CEP-1 induces the expression of both *egl-1* (Hofmann et al., 2002) and *ced-13* (Schumacher et al., 2005b) in response to radiation. Recently, it has been reported that *egl-1* can also be controlled by micro-RNAs to modulate levels of apoptosis during development (Sherrard et al., 2017), and we have confirmed that this mode of regulation occurs in the germline (Tran, Chapman, *et al.* unpublished manuscript). In mammals, the BH3-only genes *NOXA* (latin for "damage") and *PUMA* (**p**53 **u**p-regulated **m**odulator of **a**poptosis) are also transcriptionally regulated by p53 in response to stress (Nakano & Vousden, 2001; Oda et al., 2000), but post-translational mechanisms exist to regulate other BH3-only proteins. For example, BIM (**B**CL2 **i**nteracting **m**ediator of cell death) has been shown to be phosphorylated by PKA (**P**rotein **k**inase **A**) (Moujalled et al., 2011) and JNK (c-**J**un **N**-terminal **k**inase) (Lei & Davis, 2003), BAD (**B**cl-2-**a**ssociated **d**eath promoter) by AKT (strain **AK t**hymoma) (Datta et al., 1997; Del Peso, et al., 1997), and BID (**B**H3 **i**nteracting-**d**omain death agonist) is cleaved by the initiator Caspase-8 (Li, et al., 1998). While these post-translational mechanisms result in either the activation (BIM and BID) or suppression (BAD) of apoptosis, it is currently unknown if BH3-only proteins are regulated by such modifications in *C. elegans*.

All together, these components constitute a core apoptotic cascade (Figure 1.1), with mitochondria being the centre of regulation for the "intrinsic pathway". This intrinsic pathway is thought of as functioning cell autonomously, relying solely on signals from within cells. Such signals include genotoxic stress, endoplasmic reticulum (ER) stress, nutrient deprivation, enhanced cell proliferation, hypoxia, and damaged mitochondria. All of these cell stresses promote BH3-only protein activation, and/or BCL2-family protein inhibition to stimulate apoptosis. The intrinsic pathway is considered the predominant mode of regulating apoptosis, as most cells utilize this cascade.

1.1.2.2 Extrinsic apoptosis: Cell non-autonomous cues to promote death

Unlike intrinsic apoptosis, the "extrinsic pathway" relies on the stimulation of cell membrane receptors by ligands, and is therefore a cell non-autonomous process (Itoh et al., 1991). Like the intrinsic pathway, this branch of the death cascade also depends on the activation of caspases to promote death. This mechanism of initiating apoptosis is less common, as it mainly occurs in T-lymphocytes (Nagata & Tanaka, 2017) and hepatocytes (Cao, et al., 2016), requiring a specific set of ligands and receptors. The ligands involved are part of a larger TNF (**T**umor **N**ecrosis **F**actor) family (Elmore, 2007), and include FASL (**F**atty **a**cid **s**ynthetase **l**igand) (Itoh et al., 1991), and TRAIL (**T**NF-**r**elated **a**poptosis-**i**nducing **l**igand) (Pitti et al., 1996). These ligands bind to the TNF Receptor superfamily members FASR, TRAILR1, and TRAILR2 (Elmore, 2007). Once a death ligand binds to one of these receptors, a conformational change in the receptor occurs, which exposes a "Death Domain". This Death Domain is able to interact with the protein FADD (**Fa**s-associated protein with **d**eath **d**omain) (Chinnaiyan, et al., 1995; Schneider et al., 1997), which acts as an adaptor for the formation of the **D**eath **I**nducing **S**ignalling **C**omplex "DISC" (Elmore, 2007). DISC is similar to the apoptosome since it recruits the initiator caspase, Caspase-8, to be activated (Medema et al., 1997). Caspase-8 is then able to cleave and activate executioner caspases such as Caspase-3, resulting in cell death (Figure 1.1B). Interestingly, there is also cross-talk between the extrinsic and intrinsic pathways at the level of the BH3-only protein BID. In addition to cleaving and activating executioner caspases, Caspase-8 is able to cleave BID (Li et al., 1998), as previously mentioned. This results in the activation of BID, subsequent activation of BAX/BAK, and the initiation of the intrinsic apoptotic cascade (Figure 1.1B). It is possible that these two pathways are interconnected as a failsafe to ensure that apoptosis occurs when required. While TNF Receptor associated factors exist in *C. elegans* (Wajant, et al., 1998), FADD is not conserved, so the extrinsic pathway of apoptosis does not likely occur.

1.1.2.3 Apoptotic corpse engulfment: “Eat me, please”

In response to caspase activation, the lipid phosphatidylserine (PS) which is normally present on the inner plasma membrane “flips” to the outer membrane (Martin, et al., 1996). This is mediated by phospholipid scramblases such as *C. elegans* SCRM-1 (**scr**a**m**blase-1) (Wang et al., 2007), and the *C. elegans/*mammalian CED-8/XKR8 transporters which are cleaved and activated by CED-3/Caspase (Chen, et al., 2013b; Suzuki, et al., 2013). The externalization of PS is recognized by receptors expressed by engulfing cells such as macrophages in mammals (Borisenko et al., 2003), or by neighbours of the dying cell in *C. elegans* (Wang et al., 2003). This is required to prevent the cellular release of apoptotic cell corpse contents and avoids an immune response in vertebrates (Ravichandran, 2011). I will focus on the engulfment pathway in *C. elegans*, which has been instrumental for the understanding of this process. Genetic screens from the Horvitz lab identified *ced* genes that promote cell death, including *ced-4/APAF1* and *ced-3/Caspase* (Ellis, et al., 1991), while work from others identified genes such as *ced-1* that are involved in the engulfment process (Hedgecock et al., 1983). Mutants such as *ced-1* animals have persistent cell corpses due to defective engulfment. Epistasis experiments revealed that these engulfment genes define two parallel pathways that are both required for the process (Ellis et al., 1991). The first pathway consists of *ced-1/LRP1*, *ced-6/GULP*, and *ced*-7/*ABC1*, while the second pathway contains *psr-1/PSR* (**p**hosphatidyl**s**erine **r**eceptor-1), *ced-2/CRKII, ced-5/DOCK180,* and *ced-12/ELMO* (Klöditz, et al., 2017). CED-1/LRP1, and PSR-1/PSR function as receptors on the engulfing cell that recognize PS on the dying cell (Darland-Ransom et al., 2008; Wang et al., 2003). CED-6/GULP is an adaptor for CED-1/LRP1, and the ABC transporter CED-7/ABC1 is required for CED-1/LRP1 to recognize dead cells (Klöditz et al., 2017). CED-2/CRKII, CED-5/DOCK180, and CED-12/ELMO form an adaptor complex that binds to PSR-1/PSR (Klöditz et al., 2017). Both of these pathways converge on the Rho-family GTPase CED-10/RAC1 in the engulfing cell, which promotes reorganization of the actin cytoskeleton (Kinchen et al., 2005). This allows for membrane restructuring, so that the engulfing cell can surround, and enclose the apoptotic cell corpse to form the “Phagosome”. Once this occurs, lysosomal fusion results in the degradation of apoptotic corpse contents (Richards & Endres, 2014).

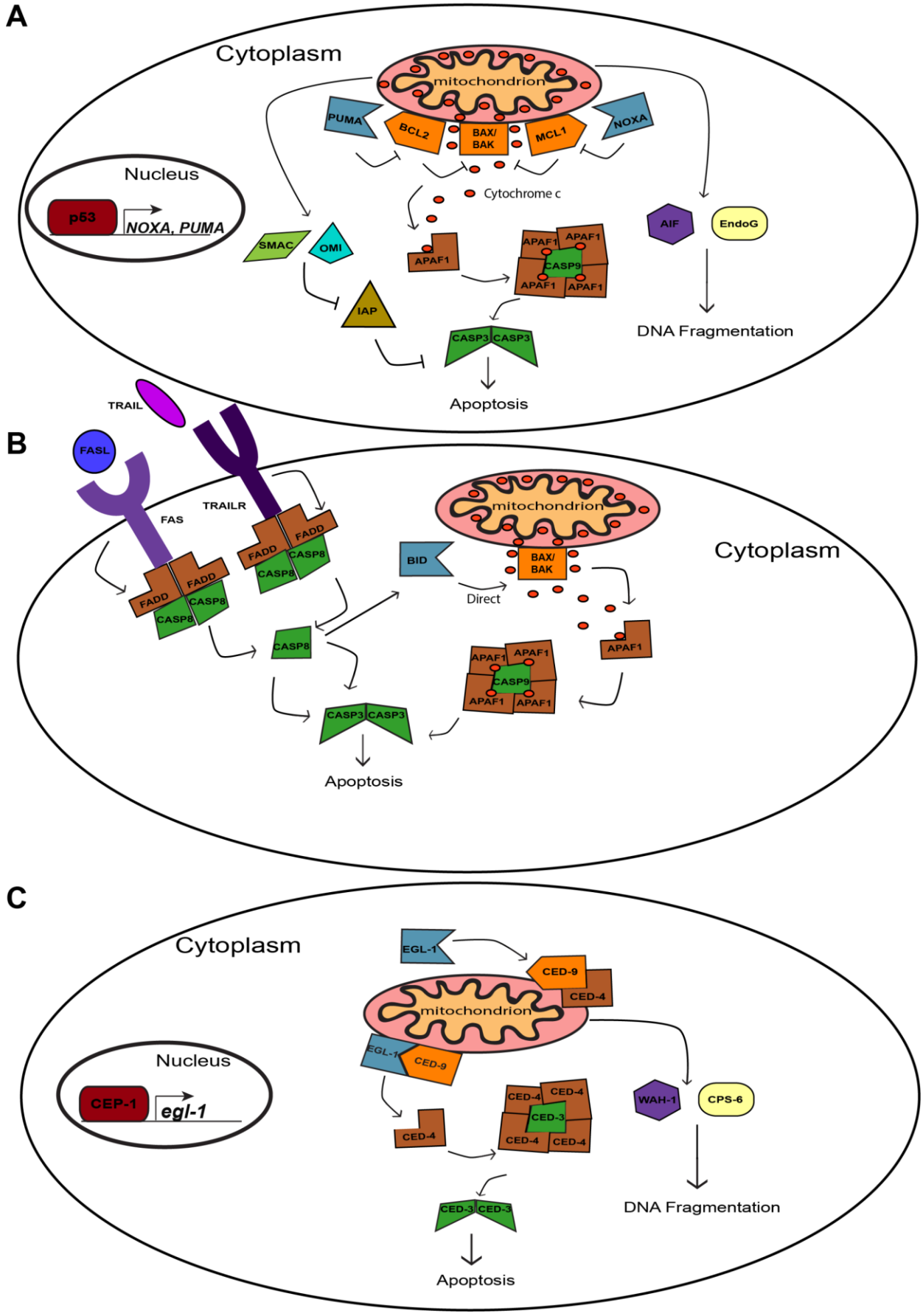
A
Cytoplasm
mitochondrion
PUMA
BCL2
BAX/
BAK
MCL1
NOXA
Nucleus
p53
NOXA, PUMA
Cytochrome c
SMAC
OMI
APAF1
APAF1
APAF1
CASP9
APAF1
APAF1
AIF
EndoG
IAP
DNA Fragmentation
CASP3
CASP3
Apoptosis
B
TRAIL
FASL
FAS
TRAILR
FADD
FADD
CASP8
CASP8
FADD
FADD
CASP8
CASP8
mitochondrion
BID
BAX/
BAK
Direct
Cytoplasm
CASP8
APAF1
APAF1
APAF1
CASP9
APAF1
APAF1
CASP3
CASP3
Apoptosis
C
Cytoplasm
EGL-1
CED-9
CED-4
mitochondrion
EGL-1
CED-9
Nucleus
CEP-1
egl-1
CED-4
CED-4
CED-4
CED-3
CED-4
CED-4
WAH-1
CPS-6
DNA Fragmentation
CED-3
CED-3
Apoptosis

Figure 1.1 Programmed cell death: apoptosis

A) Intrinsic, also known as mitochondrial apoptosis in mammalian cells. Multiple BH3-only proteins are present, and are regulated at the transcriptional level and post translation. In response to DNA damage p53 promotes the expression of *NOXA* and *PUMA* and the inhibition of BCL2 proteins and activation of BAX/BAK. This results in the permeabilization of the mitochondrial membrane, and the release of cytochrome c from the mitochondrial intermembrane space. Cytochrome c then binds to APAF1 which results in apoptosome formation and activation of Caspase-9. Caspase-9 then activates Caspase-3 and apoptosis. B) Extrinsic, also known as receptor-mediated apoptosis in mammalian T-lymphocytes and hepatocytes. Binding of the ligands FAS or TRAIL to their respective receptors results in conformational changes of the intracellular domain and recruitment of FADD to form the DISC complex. The DISC activates Caspase-8 which activates Caspase-3 and cleaves BID to promote apoptosis. C) Apoptosis in *C. elegans*. Transcription factors promote the expression of *egl-1*, such as CEP-1 in response to DNA damage. EGL-1 binds to CED-9 at the mitochondrial membrane, which results in CED-9 release of CED-4. CED-4 is then free to form the apoptosome with inactive CED-3, which results in the activation of CED-3 and the initiation of apoptosis.

1.1.2.4 Autophagy: To kill, or to protect?

Autophagy is contested as a *bona fide* cell death pathway. Traditionally, autophagy is known to promote cell survival during times of nutrient deprivation by shuttling cellular components into compartments known as autophagosomes, which fuse to lysosomes (Das, et al., 2012). This results in the degradation and recycling of cellular material, which allows for continued survival. The induction of autophagy by the mTOR (**m**ammalian **t**arget **o**f **r**apamycin) inhibitor, rapamyacin, reveals that mTor signalling is required to suppress autophagy (Jung, et al., 2010). When nutrients are low, the energy sensor AMPK (5' **AMP**-activated protein **k**inase), and AKT phosphorylate and inhibit mTor which activates autophagy (Das et al., 2012; Meley et al., 2006). In some cases, prolonged autophagy can lead to the eventual death of the cell (Amelio, et al., 2011), and suppression of apoptosis has resulted in cell death by autophagy (Yonekawa & Thorburn, 2013). In *C. elegans*, autophagy promotes animal survival during environmental stress (Meléndez et al., 2003), but also cooperates with the cell death machinery to promote (Erdelyi et al., 2011; Wang, et al., 2013) cellular demise. Thus, autophagy has evolved as a way for organisms to fine-tune their cellular life and death decisions. Interestingly, autophagy proteins in

C. elegans have been shown to have cell non-autonomous effects from neurons, muscles, and the intestine to promote the overall well-being of the animal (Ames et al., 2017; Minnerly, et al., 2017).

1.1.2.5 Necrosis: A not-so-accidental death

Necrosis as a form of "programmed cell death" is an interesting classification since it was originally thought to occur accidentally in response to injury (Golstein & Kroemer, 2007). Necrosis is morphologically distinct from apoptosis (membrane blebbing) and autophagy (large vacuoles), as cells swell until they burst, releasing internal contents. This elicits an immune response in mammals, in contrast to apoptosis (Golstein & Kroemer, 2007). Recently, genes have been identified that can promote or inhibit necrosis, revealing that this process can be genetically regulated. Necrosis has also been termed "necroptosis" (Liu, & Li, 2012) and can be activated when TNF binds to the TNFR1 receptor (Vanlangenakker, et al., 2011). When TNFR1 is activated, a complex analogous to the DISC forms, which comprises the adaptor proteins TRADD (**T**NF**R**-**a**ssociated **d**eath **d**omain), TRAF (**T**NF **r**eceptor-**a**ssociated **f**actor), and the kinase RIPK1 (**r**eceptor-**i**nteracting **p**rotein **k**inase 1) (Vandenabeele, et al., 2010). The kinase activity of RIPK1 is required for necroptosis, and inhibitors of RIPK1 such as necrostatins, block necroptosis (Xie et al., 2013). RIPK1 activates the NADPH (**N**icotinamide **a**denine **d**inucleotide **p**hosphate) **ox**idase, NOX1, leading to an increase in **R**eactive **O**xygen **S**pecies (ROS), which promotes death (Kim, et al., 2007). RIPK1 also activates the RIPK3 kinase, which promotes necroptosis by regulating metabolism (Zhang et al., 2009a). In *C. elegans*, necrosis can occur in the somatic tissue of adult animals including neurons (Xu, et al., 2001), and muscle tissue (Oh & Kim, 2013). While the core components of mammalian necroptosis (including RIPK1 and RIPK3) are not conserved in *C. elegans*, other pathways have been implicated. For example, blocking calcium release from the ER with pharmacological agents suppresses neuronal necrosis (Xu et al., 2001), and **Ins**ulin Receptor (InsR) signalling prevents necrosis in muscle tissue (Oh & Kim, 2013). Other regulators in *C. elegans* include the Serpin (**s**erine **p**rotease **i**nhibitor), SRP-6, which promotes necrosis in response to osmotic stress (Luke et al., 2007), and the autophagy pathway (Samara, et al., 2008; Toth, et al., 2007; Zou, et al., 2014). Necrotic-like features during *C. elegans* development have also been observed with linker cell death. The linker cell is important for proper male gonad positioning, and eventually dies by a process independent of

apoptosis, with features of swollenness (Abraham, et al., 2007). This necrotic-like death is regulated by WNT (**w**ingless-i**nt**egration site) signalling (Kinet et al., 2016; Malin, et al., 2016) and the *let-7* microRNA (Abraham et al., 2007).

1.2 *C. elegans* as a Model to Study Apoptosis

1.2.1 The model organism *C. elegans*

The nematode worm *Caenorhabditis elegans* is a small (1mm in length) free-living, soil-dwelling hermaphroditic animal found throughout the world (Cutter, 2015). It was established as a laboratory study specimen by Dr. Sydney Brenner who used the chemical mutagen **E**thyl **m**ethane**s**ulfonate (EMS) to study the relationship between genotype and phenotype (Brenner, 1974). Dr. Brenner's initial goal was to understand the structure and connectivity of the nervous system, and selected *C. elegans* because of its simple neural network of 302 cells (White et al., 1986). In the lab, *C. elegans* is easy to culture on agar plates supplemented with *E. coli*, which is a food source for the animal. The short life cycle of about three days, from zygote to fertile adult (Byerly et al., 1976) including four larval stages (L1-L4), allows for rapid expansion of clonal populations over several generations (Figure 1.2). This enables the isolation of chemically-induced mutations in less than two weeks as first filial (F1) heterozygotes (dominant mutations) or F2 homozygotes (recessive mutations). The short generation time also allows systematic gene knockdown experiments (Kamath & Ahringer, 2003) by **RNA i**nterference (RNA*i*) to be completed across multiple generations. Additionally, this species is sexually dimorphic with males and hermaphrodites, providing an opportunity to build compound mutant strains. *C. elegans* was the first multicellular organism to have its genome fully sequenced (The *C. elegans* Sequencing Consortium, 1998) and about 30-40% of the approximately 20,000 genes have human homologues (Shaye & Greenwald, 2011). The small size and transparency of the animal allows all tissues, and almost every cell to be observed using Differential Interference Contrast (DIC) microscopy. As such, all cell divisions during and post embryogenesis have been mapped (Sulston & Horvitz, 1977; Kimble & Hirsh, 1979; Sulston, et al., 1983) and were determined to be invariant. With GFP (**G**reen **F**luorescent **P**rotein) *C. elegans* has become a "powerhouse" for visualizing cell-specific and subcellular localization of proteins (Chalfie, et al., 1994). With respect to studying apoptosis, these features have allowed for the identification of every cell

death that occurs during development (Sulston et al., 1983), and the discovery of genes that regulate apoptosis (Ellis & Horvitz, 1986). Work using *C. elegans* has resulted in three Nobel Prizes, including the elucidation that apoptosis is a genetically regulated program (2002), gene knockdown by double stranded RNA (2006), and for demonstrating the use of GFP in molecular biology (2008).

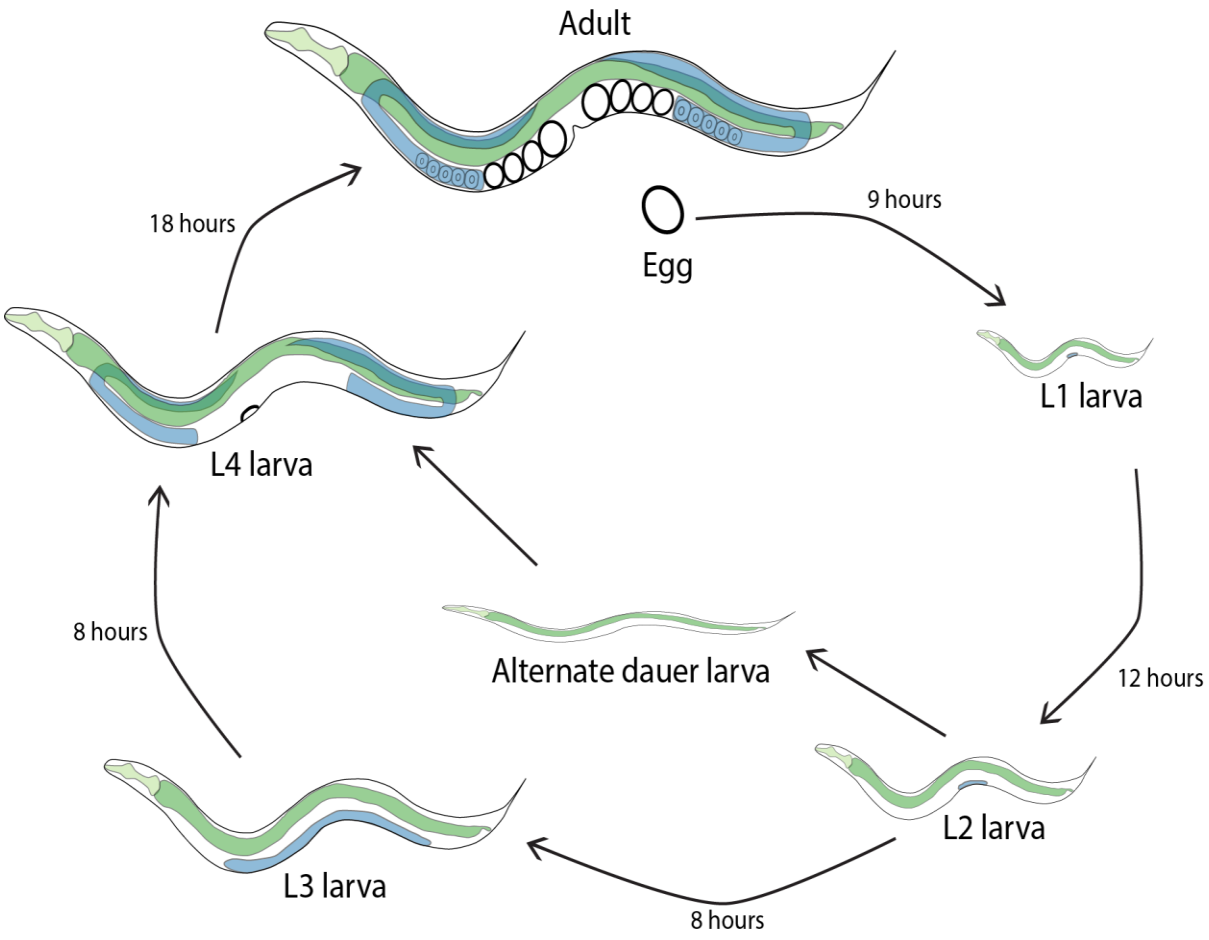

Figure 1.2 Life cycle of *C. elegans*.
The life cycle of *C. elegans* is three days starting from a fertilized zygote in the adult hermaphrodite followed by egg laying and four larval stages. In the absence of food, L1 larvae arrest in a state of diapause, and L2 larvae enter an alternative dauer life stage. When food becomes available, L1 animals continue growth to adulthood, and dauer worms molt into L4 animals eventually molting into adults. Light green represents the pharynx, dark green represents the intestine, and blue represents the germline.

1.2.2 Developmental apoptosis (somatic)

During *C. elegans* development, of the 1090 cells that arise by division, 113 undergo apoptosis during embryogenesis and 18 die during the first two larval stages (Sulston & Horvitz, 1977; Sulston et al., 1983). As previously mentioned, the invariant lineage of cell division and death facilitated the discovery of apoptosis as a genetically regulated program. This included the elucidation of the "core apoptosis pathway" components *egl-1/BH3-only*, *ced-9/BCL2*, *ced-4/APAF1*, *ced-3/Caspase*, and various regulators of *egl-1*. The activation of apoptosis occurs mainly at the level of *egl-1* with death occurring within 30 minutes (Conradt et al., 2016). An exception is tail-spike cell death, which occurs due to the unique transcriptional activation *ced-3/Caspase* by the PAL-1/CDX2 (**p**osterior **al**ae in males-1) transcription factor, and takes 10 times longer for this cell to die (Conradt et al., 2016; Maurer, et al., 2007). This demonstrates that the activation of *egl-1* is not required for every cell death during development. In addition, transcriptional regulation of *ced-3* has also been shown to regulate the death of the **Ce**phalic **m**ale (CEM) neurons (Nehme et al., 2010). Despite these examples, transcriptional control of *egl-1* is the predominant mechanism of apoptosis-initiation during development. For example, TRA-1 blocks expression of *egl-1* in the **H**ermaphrodite-**s**pecific **n**eurons (HSN) and promotes their survival in hermaphrodites, but not males (Conradt & Horvitz, 1999). Conversely, the CEM neurons die in hermaphrodites but survive in males because of the action of the CEH-30/BARH (***C. e****legans* **h**omeobox-30) transcription factor and UNC-37/TLE (**unc**oordinated-37), which repress *egl-1* expression in males (Nehme et al., 2010; Peden, et al., 2007). Regulators of *egl-1/BH3-only* transcription have also been identified in the **N**euro**s**ecretory **M**otoneuron (NSM) and its sister cell (Hatzold & Conradt, 2008; Thellmann, et al., 2003), the pharyngeal M4 neuron and its sister cells (Hirose, et al., 2010; Hirose & Horvitz, 2013), and the P11.aaap/P12.aap cells (Liu et al., 2006). The ERK1/MAPK (**E**xtracellular Signal-**R**egulated **K**inase-1/ **M**itogen-**A**ctivated **P**rotein **K**inase) pathway has been shown to regulate transcription of *egl-1* through the activation of the LIN-1/ETS (**lin**eage abnormal-1) transcription factor (Jiang & Wu, 2014).

1.2.3 Physiological apoptosis (germline)

To understand physiological apoptosis, a description of the *C. elegans* germline is required. Undifferentiated, mitotically proliferating germ cells at the somatic **D**istal **T**ip **C**ell (DTC) divide until they move away from the influence of Delta-Notch signalling, where they subsequently enter meiosis I (Austin & Kimble, 1987). As the meiotic cells migrate towards the proximal end of the germline while going through the stages of meiosis I, they encounter activated ERK1/MAPK signalling at the "pachytene region" (Figure 1.3A), which promotes exit from this stage of meiosis and differentiation into sperm (L4) and oocytes (adult) (Church et al., 1995). An alternative fate for germ cells in the pachytene region of the germline is death by apoptosis. In fact, 50 percent of germ cells are predicted to undergo apoptosis under physiological conditions, potentially to act as nurse cells for those that differentiate (Gumienny, et al., 1999). Apoptotic germ cells are morphologically similar to dying somatic cells during development, with a refractile "button-like" appearance (Figure 1.3B), cytoplasmic and nuclear condensation (Gumienny et al., 1999), and phosphatidylserine (PS) exposure on the outer membrane that serves as an engulfment signal (Wang et al., 2007). Unlike somatic apoptosis, physiological germ cell death does not depend on the activation of *egl-1* (Gumienny et al., 1999) and requires ERK1/MAPK signalling (Gumienny et al., 1999) which can enhance germ cell death when upregulated (Kritikou et al., 2006). Since the ERK1/MAPK pathway is also required for cells to exit the pachytene stage of meiosis, it is logical to speculate that these stalled cells are simply incompetent to undergo apoptosis. However, in the absence of ERK1/MAPK signalling, loss of *ced-9/BCL2* results in a restoration of apoptosis (Gumienny et al., 1999). Currently, it is unknown how ERK1/MAPK signalling induces physiological apoptosis. Additionally, the RNA-binding proteins CGH-1/DDX6 (**c**onserved **g**ermline **h**elicase-1) (Navarro, et al., 2001) and CAR-1/LSM14 (**c**ytokinesis, **a**poptotis, **R**NA-associated-1) (Boag, et al., 2005) are required to prevent excessive physiological apoptosis, possibly by repressing the translation of various mRNA transcripts. Interestingly, a genome-wide RNA*i* screen detected only four additional non-core apoptosis pathway genes that prevent excessive physiological germline apoptosis. These genes encode the RNA-binding protein CBP-3/CBP (**CBP**/p300 homolog-3), the ubiquitin-ligase RFP-1/ BRE1 (**r**ing **f**inger **p**rotein-1), the ERK1/MAPK negative regulator GLA-3/TIS11

(**g**erm**l**ine **a**poptosis abnormal-3) (Kritikou et al., 2006), and a p38 MAPK homologue (Lettre, et al., 2004).

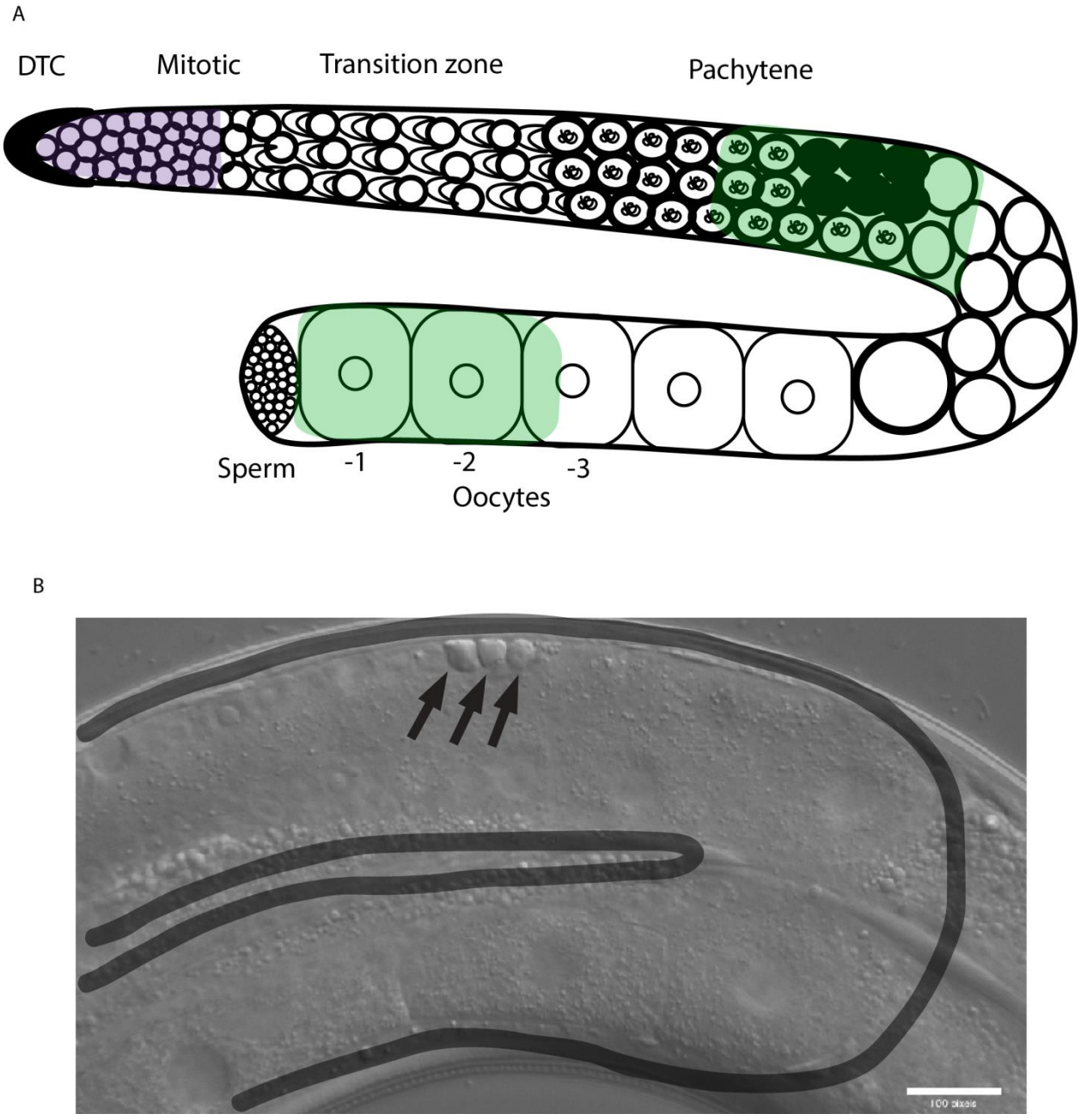

Figure 1.3 *C. elegans* germ cell apoptosis.

A) The Distal Tip Cell (DTC) promotes undifferentiated germ cells to mitotically proliferate under the control of Notch signalling (purple). As germ cells move away from the influence of Notch, they enter meiosis (I). ERK1/MAPK signalling (green) promotes exit from the pachytene stage and apoptosis (black circles). B) Apoptotic germ cells are morphologically similar to dying cells in somatic tissue during development, with a refractile "button-like" appearance compared to non-apoptotic germ cells.

1.2.4 Stress-induced apoptosis (germline)

In addition to physiological apoptosis, germ cell death can occur in response to various stresses. These include oxidative, osmotic, heat shock and starvation stresses (Salinas, et al., 2006), ER stress (Levi-Ferber et al., 2014), pathogen infection (Aballay & Ausubel, 2001), and microtubule stress (Sendoel et al., 2014). However, the best characterized is apoptosis in response to DNA damage, and is the focus of this thesis.

1.2.4.1 DNA damage and double strand breaks

The *C. elegans* germline has robust DNA damage sensing machinery. Germ cell death in response to DNA damage is important to prevent potentially deleterious mutations from being passed onto subsequent generations. When DNA damage occurs, a cell must make the "choice" to either repair the damage or initiate apoptosis if the damage is insurmountable (Stergiou & Hengartner, 2004). DNA damage can occur for a variety of reasons such as interaction with oxygen free radicals, replication errors, chemical mutagens, or insult from environmental sources of radiation (Lemmens & Tijsterman, 2011). DNA damage varies in severity, and *C. elegans* possesses multiple pathways to repair different types of DNA damage. These include nucleotide-excision repair (Lans & Vermeulen, 2011), mismatch repair (Denver, et al., 2005), **n**on-**h**omologous **e**nd **j**oining (NHEJ) (Clejan, et al., 2006) and **h**omologous **r**ecombination (HR) (Lemmens & Tijsterman, 2011). These responses rely on well-functioning DNA damage surveillance and checkpoint pathways. The most deleterious type of DNA damage is **d**ouble **s**tranded DNA **b**reaks (DSBs) (Lemmens & Tijsterman, 2011). In contrast to single stranded breaks, which are repaired relatively easily, DSBs are more complicated to resolve because a homologous template is required for faithful repair of the genomic region (Lemmens & Tijsterman, 2011). A type of insult that leads to the formation of DSBs is ionizing radiation (IR). IR is composed of high energy particles in the form of *x*-rays or γ-rays, which transfer electrons

to DNA directly or to water molecules (Close, et al., 2013). In the first scenario, the transfer of electrons directly can cause a break in DNA, and in the second scenario, the transfer of electrons to water molecules creates oxygen free radicals which can damage DNA (Close et al., 2013). If two double stranded breaks occur on the same chromosome, the consequence can include chromosomal inversions, translocations, or erroneous repair by the NHEJ pathway (Varga & Aplan, 2005).

1.2.4.2 Double-stranded breaks induce CEP-1/p53-dependent apoptosis

DNA DSBs are detected by a surveillance complex that activates a cell cycle checkpoint pathway which halts the cell cycle, providing time to either repair the damage or initiate apoptosis (Derry et al., 2007; Hofmann et al., 2002). As previously mentioned, inducing cell death is a way to prevent deleterious mutations from being passed through subsequent generations. In *C. elegans* there are two pathways that function in parallel to sense DSBs and initiate the checkpoint pathway (Figure 1.4). The first comprises the "9-1-1" complex that forms a clamp-like heterotrimer that scans DNA for DSBs, and is conserved from yeast to mammals (Hofmann et al., 2002). In *C. elegans* this complex is comprised of HPR-9 (**h**omolog of *S. **p**ombe* **R**ad-9), MRT-2 (**m**o**rt**al germline-2), and HUS-1 (human **HUS**1-related), homologous to mammalian RAD**9**, RAD**1**, and HUS**1**, repetitively (hence 9-1-1) (Hofmann et al., 2002). The second pathway is less defined, but involves CLK-2 (**cl**oc**k** abnormality-2), which is orthologous to the mammalian Telomerase TEL2, but in *C. elegans* CLK-2 does not appear to have a role in telomere maintenance (Ahmed, et al., 2001). When DSBs are detected, the 9-1-1 and CLK-2/TEL2 pathways lead to the recruitment of two **p**hosphatidyl**i**nositol 3-**k**inase-related **k**inases (PIKKs), ATM-1/ATM1 (**a**taxia **t**elangectasia **m**utated-1), and ATL-1/ATR (**a**taxia **t**elangectasia mutated-**l**ike), which are structurally similar to **p**hosphatidyl**i**nositol **3**-**k**inases (PI3Ks) (Garcia-Muse & Boulton, 2005). These PIKKs then activate the cell cycle **ch**eckpoint **k**inases CHK-1/CHK1 in response to IR (Garcia-Muse & Boulton, 2005), or CHK-2/CHK2 in response to ultraviolet radiation (UV) (Stergiou, et al., 2007), which engages CEP-1/p53 (Moser et al., 2009; Stergiou et al., 2007). Like mammalian p53, CEP-1 can promote apoptosis (Derry, et al., 2001; Schumacher, et al., 2001) by up-regulating levels of *egl-1/BH3-only* (Hofmann et al., 2002) and can promote cell cycle arrest (Derry et al., 2007). However, while mammalian p53 forms a tetramer, activated CEP-1 forms a dimer (Ou, et al., 2007). Consistent with the importance of

EGL-1/BH3-only, a gain of function mutation in CED-9/BCL2 that blocks the ability of EGL-1 to bind (Del Peso, et al., 2000), is able to suppress DNA damage-induced (Gartner, et al., 2000) and developmental apoptosis in the soma (Hengartner et al., 1992). This is not the case for physiological germ cell apoptosis, since EGL-1 is not required (Gumienny et al., 1999). In the soma, cells are able to repair DNA in response to ionizing radiation, yet apoptosis does not occur because ATM-1/ATM1 is inactivated (Vermezovic, et al., 2012). The reason for this may be to spare the limited number of post-mitotic cells that comprise the soma of the animal (Vermezovic, et al., 2012). Given the importance of CEP-1/p53 in promoting IR-induced apoptosis, a complex network exists to ensure tight control of this transcription factor. The kinases ABL-1/ABL1 (related to oncogene **ABL**) and AKT-1/AKT have both been shown to negatively regulate CEP-1, presumably to prevent apoptosis in response to minor DNA damage (Deng et al., 2004; Quevedo, et al., 2007), and there is evidence to suggest that MPK-1/ERK1 promotes CEP-1 activity (Rutkowski et al., 2011). In addition, the RNA-binding protein GLD-1/QUAKING (defective in **g**erm**l**ine **d**evelopment-1) represses *cep-1* translation in order to restrict CEP-1 protein from regions of the germline where programmed DSBs are introduced during meiosis (Schumacher et al., 2005a). In mammals, one of the primary mechanisms to inhibit p53 function is through ubiquitination by the E3-ligase MDM2 (**m**ouse **d**ouble **m**inute 2), and subsequent degradation (Moll & Petrenko, 2003). While *C. el*e*gans* does not contain an MDM2 homologue, the SCF^{FSN-1} (**F**-box **s**y**n**aptic protein) E3-ligase complex negatively regulates CEP-1 (Gao et al., 2008), and SCF^{FSN-1} was later demonstrated to regulate p53 family members in mammalian cells (Peschiaroli, et al., 2009). Finally, CEP-1/p53 also functions with two co-factors PRMT-5/PRMT5 (**p**rotein **a**rginine **m**ethyl**t**ransferase-5) and CBP-1/CBP which help to regulate CEP-1 function (Yang et al., 2009).

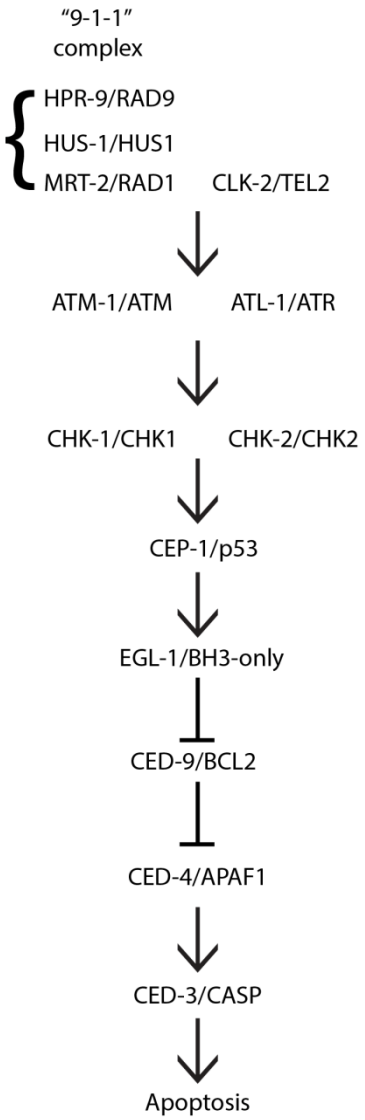

Figure 1.4 *C. elegans* DNA damage and apoptosis pathway.
The heterotrimeric "9-1-1" complex along with CLK-2/TEL2 detect double stranded breaks (DSBs) and recruit two phosphatidylinositol 3-kinase-related kinases (PIKKs), ATM-1/ATM1, and ATL-1/ATR. The activation of these two PIKKs leads to the phosphorylation and activation of the cell cycle checkpoint kinases CHK-1/CHK1 and CHK-2/CHK2 which promote cell cycle arrest, and activation CEP-1/p53. CEP-1 can induce cell cycle arrest for DNA repair or promote apoptosis by up-regulating the levels of *egl-1* to activate the core apoptotic cascade.

1.2.4.3 CEP-1/p53- independent apoptosis

In addition to CEP-1-mediated apoptosis through the induction of *egl-1/BH3-only*, additional pathways act in parallel to promote IR-induced apoptosis. A common feature of these pathways is that when they are perturbed, cell cycle arrest still occurs and CEP-1 is able to induce *egl-1/BH3-only* expression in response to genotoxic stress, yet cells do not initiate apoptosis (Ito, et al., 2010; Perrin et al., 2013). While CEP-1-independent cell death pathways mainly function within the germline, LIN-35/Rb and KRI-1/CCM1 (**KRI**T1 homolog-1) have been shown to act cell non-autonomously from the somatic tissue (discussed in the next section) (Ito et al., 2010; Schertel & Conradt, 2007). Within the germline, five pathways function in parallel to CEP-1. The Holliday Junction resolvase, GEN-1 (**GEN**1 Holliday junction resolvase homolog-1) (Bailly et al., 2010) works in parallel to the 9-1-1 complex. The ceramide biogenesis pathway (Deng et al., 2008) and the histone deacetylase, SIR-2.1/SIRT1 (Greiss, et al., 2008) are required for the normal distribution of CED-4/APAF1. The E3-ligase, EEL-1/MULE (**e**nhancer of **E**f**L**-1 mutant phenotype) (Ross, et al., 2011) functions upstream or at the level of CED-9/BLC2, and the terminal ERK1/MAPK pathway kinase, MPK-1/ERK1, functions by an unknown mechanism (Eberhard et al., 2013; Perrin et al., 2013). It remains to be determined how either IR or DNA damage activates these CEP-1/p53-independent pathways. I will now focus on MPK-1/ERK1, since it is featured in this thesis.

1.2.4.4 The ERK1/MAPK pathway and irradiation-induced apoptosis

The ERK1/MAPK pathway in *C. elegans* comprises an evolutionarily conserved kinase signalling cascade that includes the **R**eceptor **T**yrosine **K**inase (RTK) LET-23/EGFR, its EGF (**e**pidermal **g**rowth **f**actor) ligand LIN-3, the adaptor proteins SEM-5/GRB2 (**se**x muscle **a**bnormal) or ROG-1/FRS (**R**AS activating factor in development **o**f **g**ermline), LET-60/RAS (**ra**t **s**arcoma), LIN-45/RAF (**r**apidly **a**ccelerated **f**ibrosarcoma), MEK-2/MEK (**M**APK/**E**RK **k**inase), and MPK-1/ERK (Sundaram, 2013). Hypermorphic mutations in this pathway cause cell fate-specification defects resulting in the formation of ectopic vulvae (Han & Sternberg, 1990) and loss-of-function mutations prevent vulva development. These phenotypes, which are easily observed under a light microscope, led to the discovery of LET-23/EGFR (Aroian, et al., 1990), SEM-5/GRB2 (Clark, et al., 1992; Lowenstein et al., 1992), LIN-45/RAF (Han, et al., 1993),

MEK-2/MEK1 (Wu, et al., 1995), and MPK-1/ERK1 (Lackner, et al., 1994). Gain-of-function alleles of *let-60* were identified in mutants with ectopic vulvae due to constitutively active LET-60 GTPase, analogous to oncogenic RAS. This provided an opportunity to determine the epistatic relationship of the ERK1/MAPK pathway genes by observing whether ablation could suppress the *let-60(gf)* Muv phenotype. Soon after, it was demonstrated that this pathway is required in the germline to promote meiotic progression (Church, et al., 1995), as previously described. In addition to the core ERK1/MAPK kinase signalling cascade, other components such as the KSR-1 (Kornfeld, et al., 1995; Sundaram & Han, 1995) and KSR-2/KSR (**k**inase **s**uppressor of **R**AS) scaffolds (Ohmachi et al., 2002), the LET-60/RAS interacting proteins GAP-2/GAP (**G**TP **a**ctivating **p**rotein) (Hayashizaki, et al., 1998), SOS-1/GEF (**G**uanine nucleotide **e**xchange **f**actor) (Chang, et al., 2000) and SOC-2/SHOC (**s**uppressor **o**f **C**lr) (Sieburth, et al., 1998) were identified. In addition to the core kinase signalling pathway, KSR-2 was also demonstrated to function in the germline (Ohmachi et al., 2002) and is important for bridging LIN-45/RAF, MEK-2/MEK1, and MPK-1/ERK1 to facilitate the phosphorylation cascade. In the primary **v**uvlal **p**recursor **c**ell (VPC), the main targets of MPK-1/ERK1 are the EOR-1/PLFZ (**E**GL-1 suppressor/Di**O** uptake defective/**r**af enhancer-1) (Howard & Sundaram, 2002) and LIN-1/ETS (Jacobs, et al., 1998; Tiensuu, et al., 2005) transcription factors. In the germline, however, many putative targets have been proposed (Arur et al., 2009). These potential targets were identified due to the presence of conserved MPK-1/ERK1 docking sites, and the ability to be phosphorylated by mammalian ERK1 (Arur et al., 2009). Many of these proteins cause germline meiosis and physiological apoptosis defects when ablated, consistent with a role for these factors downstream of MPK-1.

Given that MPK-1/ERK is important for multiple germline processes, it is not surprising that its activation is spatially controlled in this tissue (Lee et al., 2007b). Negative regulators exist to restrict MPK-1/ERK1 activation at the translational level and post-translational phosphorylation. These include the FBF/PUF (***f****em-3* mRNA **b**inding **f**actor) (Lee et al., 2007a) and GLA-3/ TIS11 (Kritikou et al., 2006) RNA binding proteins, the phosphatase LIP-1/MKP3 (**l**ateral signal **i**nduced **p**hosphatase-1), and the kinase GCK-1/GCK (**g**erminal **c**enter **k**inase family) (Schouest et al., 2009). As a result, di-phosphorylated (activated) MPK-1/ERK is localized to the pachytene region of the germline to promote exit from this stage of meiosis I and apoptosis, and in the

proximal oocytes (Lee et al., 2007b; Figure 1.3A). When these negative regulators are ablated, MPK-1/ERK1 phosphorylation and germ cell apoptosis increases. In addition to physiological germ cell apoptosis, MPK-1/ERK1 is also required for IR-induced apoptosis, functioning both upstream (Rutkowski et al., 2011) and independently (Eberhard et al., 2013; Perrin et al., 2013) of CEP-1/p53. When up-regulated, MPK-1/ERK1 was shown to inhibit the negative regulator of CEP-1, GLD-1, allowing CEP-1 levels to increase, followed by an increase in *egl-1/BH3-only* expression and apoptosis (Rutkowski et al., 2011). On the contrary, when MPK-1 activation is reduced, CEP-1 is still able to induce *egl-1* expression, yet apoptosis does not occur (Eberhard et al., 2013; Perrin et al., 2013), revealing a CEP-1-independent role for this kinase. While it is currently not known how MPK-1 regulates the core apoptosis pathway (Figure 1.5), it is likely functioning upstream or at the level of CED-9/BCL2 (Eberhard et al., 2013; Gumienny et al., 1999; Perrin et al., 2013). How radiation-induced DNA damage activates MPK-1 is also unclear, although both the Insulin Receptor (InsR) (Perrin et al., 2013) and Ribosomal Synthesis (Eberhard et al., 2013) pathways have been implicated in this process. It is possible that InsR signalling transcriptionally regulates MPK-1/MAPK pathway components through the terminal transcription factor DAF-16/FOXO (abnormal **da**uer **f**ormation-16) (Perrin et al., 2013) and the Ribosomal Synthesis pathway might ensure proper translation of these transcripts (Eberhard et al., 2013). While DAF-2/InsR has been shown to promote MPK-1 activation (Lopez et al., 2013), it is unclear if this receptor is acting in the germline (Perrin et al., 2013). Therefore, it is possible that alternative mechanisms exist to ensure the timely activation of the ERK1/MAPK pathway in the absence of a germline receptor. Interestingly, in response to radiation, MPK-1 in the germline is required for the induction of *C17H12.8*, *K08D8.5*, and *T24B8.5*, which encode putative secreted innate immune factors. While these innate immunity genes do not have a role in IR-induced apoptosis, it is intriguing that the germline peptides they encode are required to promote somatic resistance to heat stress cell non-autonomously, presumably by being secreted (Ermolaeva et al., 2013).

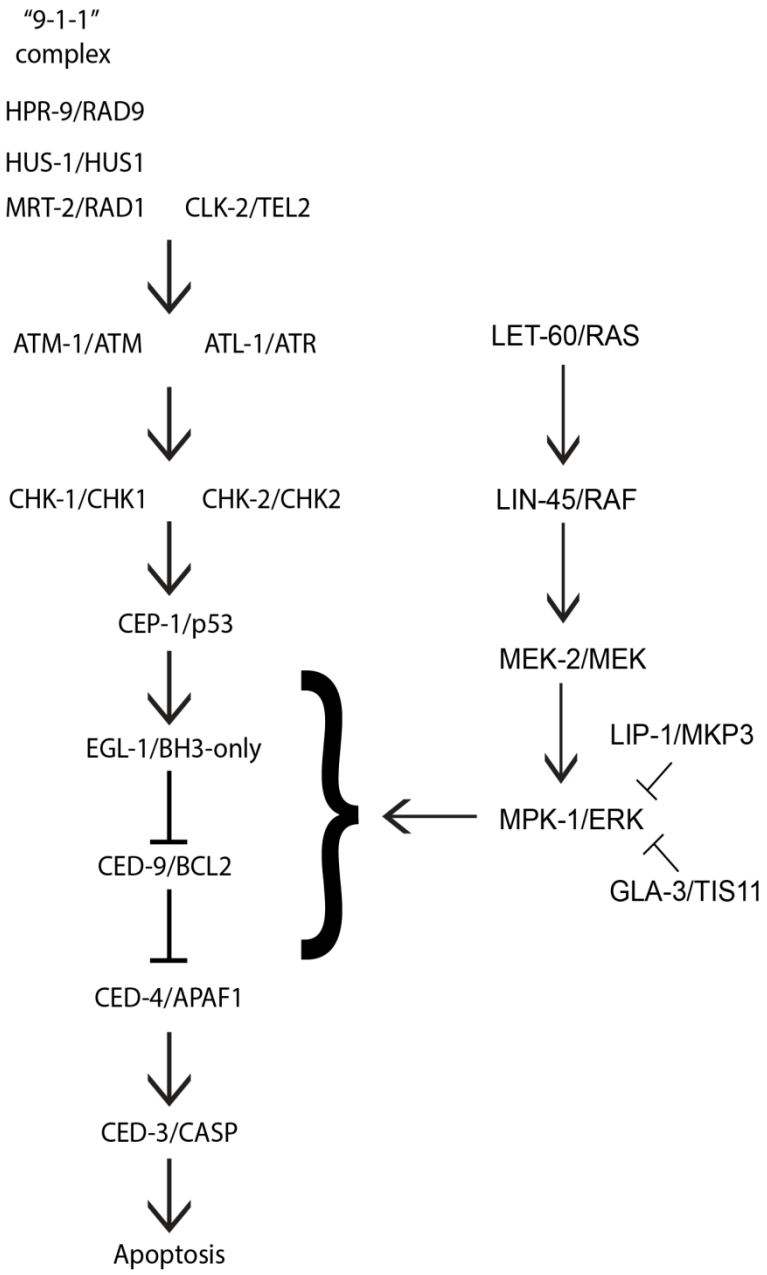

Figure 1.5 MPK-1/ERK1 promotes IR-induced germ cell death.
RAS/MAPK signalling is required to promote IR-induced germ cell death. Currently, it is not known how the terminal kinase, MPK-1/ERK1, feeds into the core apoptosis pathway, but it is likely functioning upstream of *ced-9/bcl2*.

1.3 KRI-1/CCM1 and Cell Non-autonomous Regulation of Apoptosis in *C. elegans*

1.3.1 KRI-1 regulates apoptosis cell non-autonomously

Previously, our lab discovered a novel pathway that functions in parallel to CEP-1/p53, regulated by KRI-1 (Ito, et al., 2010), which is homologous to the vertebrate KRIT-1/CCM1 scaffold protein. The *KRIT1/CCM1* gene is the most commonly mutated in familial **C**erebral **C**avernous **M**alformation disease (CCM) (Draheim, et al., 2014) and will be discussed in more detail below. In the absence of KRI-1, *egl-1* induction is unperturbed yet apoptosis does not occur in response to radiation (Ito et al., 2010), which is reminiscent of other pathways that function in parallel to CEP-1/p53. Mitotic cells arrest after radiation in these mutants, indicating that the DNA damage checkpoint pathway is active (Ito et al., 2010). KRI-1 was determined to function upstream of CED-9/BCL2 from a few key observations. First, KRI-1 does not regulate the transcript levels of *ced-4/APAF1* or *ced-3/Caspase.* Second, CED-4 levels and localization are not altered in the absence of KRI-1. Finally, ablation of *ced-9* in *kri-1* mutants restores apoptosis, confirming that CED-4 and CED-3 are theoretically able to initiate cell death in the absence of KRI-1. This places *kri-1* genetically at the level or downstream of *egl-1*, and upstream of *ced-9* (Figure 1.6). Since KRI-1 is expressed in the intestine and pharynx (Berman & Kenyon, 2006), but not the germline (Reinke et al., 2000), it must be functioning cell non-autonomously to regulate germ cell death . Indeed, this was demonstrated by tissue specific knock-down of *kri-1*. When *kri-1* was ablated in the germline, IR-induced apoptosis occurred normally, but it was completely suppressed when *kri-1* was ablated in the somatic tissue (Ito et al., 2010). Since KRI-1 has been shown to function in the intestine (Berman & Kenyon, 2006; Chen et al., 2013a; Wang et al., 2008), it is inferred that this is the tissue from which signals that promote germ cell apoptosis originate (Figure 1.6). Upstream of KRI-1, the **d**ynein **l**ight **c**hain, DLC-1/DYNLL, has been shown to regulate the levels of KRI-1 in the intestine by an unknown process (Morthorst & Olsen, 2013). To date, no mechanism has been elucidated to explain how KRI-1 regulates apoptosis cell non-autonomously, until the work presented in this thesis.

1.3.2 Additional roles for KRI-1: Lifespan extension

In addition to IR-induced germline apoptosis, KRI-1 regulates adult lifespan extension when the germline is absent. Briefly, adult animals without a germline live two times longer, possibly due to a redistribution of resources (Lin, et al., 2001). Intestinal KRI-1 mediates this response by promoting the nuclear localization of the DAF-16/FOXO transcription factor to promote the expression of lifespan-extending genes (Berman & Kenyon, 2006). One of these DAF-16/FOXO targets downstream of KRI-1 is *K04A8.*5. This gene encodes a triglyceride lipase that reduces fat storage in germline-less animals, which might produce energy to extend lifespan (Wang et al., 2008). When KRI-1 is ablated, DAF-16 remains in the cytoplasm and lifespan extension does not occur (Berman & Kenyon, 2006). KRI-1 might also mediate lifespan extension by promoting the generation of ROS. While ROS are usually thought to be detrimental to health, a recent study revealed that in animals without a germline, ablation of KRI-1 prevents the SKN-1/NRF2 (**sk**in**h**ead) transcription factor from generating ROS, which suppresses lifespan extension (Wei & Kenyon, 2016). Upstream of *kri-1*, the **pept**ide transporter PEPT-1/SLC15 functions as its transcriptional regulator. Loss of *pept-1* further extends lifespan by promoting the transcriptional up-regulation of *kri-1* (Spanier, et al., 2010). It is unknown how PEPT-1 regulates *kri-1* transcription, although it is conceivable that this transporter regulates the nuclear import of an unidentified transcription factor. The KRI-1-DAF-16 signalling pathway is also required to prevent a decline in proteostasis as germline-less animals age (Shemesh, et al., 2013). This is likely an additional mechanism by which animals with no germline are able to live longer. Currently, the germline to intestine signals that regulate KRI-1-DAF-16 have yet to be identified.

1.3.3 Cell non-autonomous regulation of apoptosis

1.3.3.1 Developmental (somatic)

In addition to KRI-1 regulating IR-induced apoptosis, cell non-autonomous regulation of cell death has been identified in *C. elegans* during development, and in mammals. For example, during formation of the mammalian nervous system, growing neurons that fail to make connections with target neurons do not receive the “pro-life” Nerve Growth Factor (NGF) signal, and die through TRKA/TRKC (**T**ropomyosin **r**eceptor **k**inase) receptor-mediated apoptosis (Dekkers, et al., 2013). In *C. elegans*, the first indication that non-autonomous cues promote

developmental death came from two studies demonstrating that engulfing cells promote the apoptotic death of their neighbours (Hoeppner, et al., 2001; Reddien, et al., 2001). This role for engulfing cells became apparent in animals with weak *ced-3/Caspase* mutations. These animals have a surviving fraction of cells otherwise fated to die, and the number of these surviving cells increases when the engulfment machinery is abrogated. The engulfment machinery was demonstrated to be required in the engulfing cells to promote death (Reddien et al., 2001), and it is hypothesized that under situations of reduced CED-3 activity, cues are emitted by the dying cell to recruit surrounding engulfing cells to aid in the killing process (Hoeppner et al., 2001). Even with fully functioning CED-3, a subset of somatic cells were identified that require the engulfment machinery for death to occur (Johnsen & Horvitz, 2016; Reddien et al., 2001). Mechanistic insight into how the engulfment machinery promotes cell death was provided by a recent study which found that the CED-1/LRP1 receptor in engulfing cells promotes a gradient of CED-3 in asymmetrically dividing cells (Chakraborty, et al., 2015). The daughter with higher levels of CED-3 undergoes apoptosis, while the sister cell survives (Chakraborty, et al., 2015).

In addition to the engulfment machinery, the DNaseII, NUC-1 (abnormal **nuc**lease-1), can function cell non-autonomously during apoptosis to promote DNA degradation in the posterior region of the embryo, when expressed anteriorly (Yu, et al., 2015). It is hypothesized that NUC-1 might be secreted in vesicles and endocytosed by cells fated to die (Yu et al., 2015), yet this remains to be validated. Finally, LIN-3/EGF acts as an extrinsic factor during development to activate LET-23/EGFR and the ERK1/MAPK pathway. MPK-1/ERK1 then activates the LIN-1/ETS transcription factor, which binds to the *egl-1/BH3-only* promoter to induce its expression and cell death. This is not conserved in germ cell death, since LET-23 does not function as a germline EGFR, and LIN-1/ETS is not a target of MPK-1/ERK1 in this tissue (Sundaram, 2013).

1.3.3.2 Physiological (germline)

During constitutive physiological germ cell apoptosis, cell non-autonomous signals from the somatic gonad are important for promoting death. The somatic gonad comprises the Distal Tip Cell, spermatheca, uterus, and five sheath cell pairs that encase the germline (Altun & Hall, 2006). The first study to describe cell non-autonomous signalling from the gonadal sheath cells identified LIN-35/RB as being required for normal physiological apoptosis (Schertel & Conradt,

2007). RB is a tumor suppressor that when mutated can result in the formation of retinoblastoma in mammals (Giacinti & Giordano, 2006). Ablation of *lin-35* results in decreased physiological apoptosis because the levels of *ced-9/BCL2* transcript, and thus CED-9/BCL2 increase. LIN-35 is therefore a transcriptional repressor of *ced-9*. Interestingly, LIN-35/RB is required in both the somatic gonad and the germline to repress the transcription of *ced-9*, and knockdown in either tissue alone does not alter *ced-9/BCL2* transcript levels (Schertel & Conradt, 2007). While transcription factors regulated by LIN-35/RB were not identified, two PAX (**pa**ired **b**ox) transcription factors, EGL-38 and PAX-2, directly activate *ced-9/BCL2* in the soma. Therefore it was hypothesized that LIN-35/RB might regulate *ced-9/BCL2* through EGL-38 or PAX-2 (Schertel & Conradt, 2007). Interestingly, LIN-35/RB also regulates IR-induced apoptosis, but independent of *ced-9/BCL2* transcriptional regulation, and through an unknown mechanism (Schertel & Conradt, 2007). In support of the model for *ced-9/BCL2* regulation by LIN-35/RB, another group found that LIN-35/RB increases in response to starvation, resulting in decreased *ced-9/BCL2* levels and apoptosis (Lascarez-Lagunas, et al., 2014). In the future, it will be interesting to determine how LIN-35/RB signals from the somatic tissue to regulate transcriptional repressors of *ced/-9/BCL2* in the germline.

Ephrin signalling from the somatic gonad is also required for physiological apoptosis to occur, while having no role in IR-induced apoptosis (Li, et al., 2012). It was shown that the Ephrin ligands, EFN-1,2,3 (**E**ph(**f**)ri**n** ligand) in the somatic sheath cells signal through the Ephrin Receptor, VAB-1 (**v**ariable **a**bnormal **m**orphology-1), in the germline to promote apoptosis. In an attempt to identify pathways regulated by VAB-1/EphR, activated MPK-1/ERK1 was quantified in the germline, but there was no significant difference in *vab-1* mutant animals compared to wild type (Li et al., 2012). VAB-1/EphR therefore regulates physiological germ cell death through a currently unidentified pathway.

1.3.3.3 Stress-induced (germline)

While the somatic gonad is an important source of signals to promote physiological apoptosis, neurons in the head have curiously been shown to regulate stress-induced germ cell apoptosis. The first of these studies revealed that the **H**ypoxia-**i**nducible transcription **f**actor, HIF-1, negatively regulates apoptosis in the germline (Sendoel, et al., 2010). HIF-1 promotes expression

of the **tyr**osinase gene *tyr-2/TRP2* in the two ASJ (**a**mphid **s**ensory **J**) neurons in the head, which are known to regulate processes such as phototaxis and exit from the starvation responsive dauer life stage. TYR-2 is secreted from these ASJ neurons, and taken up into the germline by the RME-2/LDL receptor (**r**eceptor **m**ediated **e**ndocytosis-2) expressed in the germline. Once in the germline, TYR-2 suppresses CEP-1/p53 by an unknown mechanism to inhibit germ cell death (Sendoel et al., 2010). Since *C. elegans* often encounters hypoxic conditions in the soil, it is likely that HIF-1 is important to prevent germ cell death in response to this stress (Sendoel, et al., 2010).

In response to ER-stress by genetic perturbation or pharmacological induction, the ASI sensory neurons in the head emit signals that promote germ cell death (Levi-Ferber et al., 2014). Interestingly, these neurons also induce proliferation of germ cell progenitors in larval animals (Dalfó, et al., 2012). The ability of the ASI neurons to promote ER-stress induced germ cell death is dependent on CEP-1/p53 and the core apoptosis cascade, despite ER-stress not inducing DNA damage. Currently, the mechanism by which ASI neurons signal to CEP-1 is unknown (Levi-Ferber et al., 2014). This study also ruled out a role for KRI-1 in this pathway, as ER-stress effectively induced germ cell apoptosis in *kri-1* null animals.

In addition to IR-induced apoptosis (KRI-1), the intestine is important for sending signals to the germline in response to bacterial infection. *Salmonella typhimurium* colonization in the *C. elegans* gut results in germ cell apoptosis, which promotes animal survival by an unknown mechanism (Aballay & Ausubel, 2001). While the cross-tissue communication signals were not identified, the core apoptosis pathway in the germline, including EGL-1/BH3-only, was shown to be required (Aballay & Ausubel, 2001). This suggests that germ cell apoptosis in response to *S. typhimurium* infection is dependent on CEP-1/p53, but CEP-1 had not yet been discovered (Derry, et al. 2001; Schumacher et al., 2001). This study was the first to implicate cell non-autonomous signalling in stress-induced germ cell death, and highlights the intestine as a source of such signals.

1.3.4 Intestinal to germline signalling in *C. elegans*

Given the close proximity of the intestine and germline, it is not surprising that signalling occurs between these two tissues. A well known example is communication from germ cells to the intestine to regulate lifespan, as discussed previously (Berman & Kenyon, 2006; Libina, et al., 2003). Since the focus of this thesis is intestine to germline communication, it is important to consider what is known about signalling in this direction. A well characterized process is the synthesis of yolk in the intestine and its transport into the germline to promote oocyte development. Yolk in *C. elegans* comprises lipoproteins similar to LDL (**l**ow **d**ensity **l**ipoprotein), encoded by *vitellogenin* or "*vit"* genes that are expressed in the intestine (Sato, et al., 2014). These yolk proteins are secreted from the basolateral surface of the intestine (Figure 1.6B), mediated by the COPI (**co**atomer **p**rotein) and COPII complexes, into the pseudocoelom (body cavity) (Grant & Hirsh, 1999). The LDL receptor, RME-2, is located on the surface of the germline and is required for yolk uptake to promote oocyte development (Grant & Hirsh, 1999). As previously mentioned, this RME-2 receptor is also required for the transport of TYR-2/TRP2 into the germline to suppress CEP-1/p53-dependent apoptosis (Sendoel et al., 2010). Both KRI-1 (Goszczynski, et al., 2016) and DAF-16/FOXO (Depina et al., 2011) promote *vit-2* gene expression, but KRI-1 does so independently of DAF-16 (Goszczynski et al., 2016). In addition, the mTOR pathway activates SGK-1/SGK1 (**s**erum and **g**lucocorticoid inducible **k**inase-1), which promotes the cytoplasmic localization of the PQM-1/SALL2 (**p**ara**q**uat **m**ethylviologen responsive-1) transcriptional repressor, to allow for vitellogenin gene transcription and transport of yolk from the intestine to the germline (Dowen, et al., 2016).

Another example of intestine to germline signalling occurs during a state of larval starvation, known as L1 diapause. Under such stress, the AMPK (5' **AMP**-activated protein **k**inase) catalytic subunits AAK-1 (**A**MP-**a**ctivated **k**inase) and AAK-2 function in the intestine to suppress mTOR to preserve germ stem cell progenitor quiescence (Fukuyama et al., 2012).

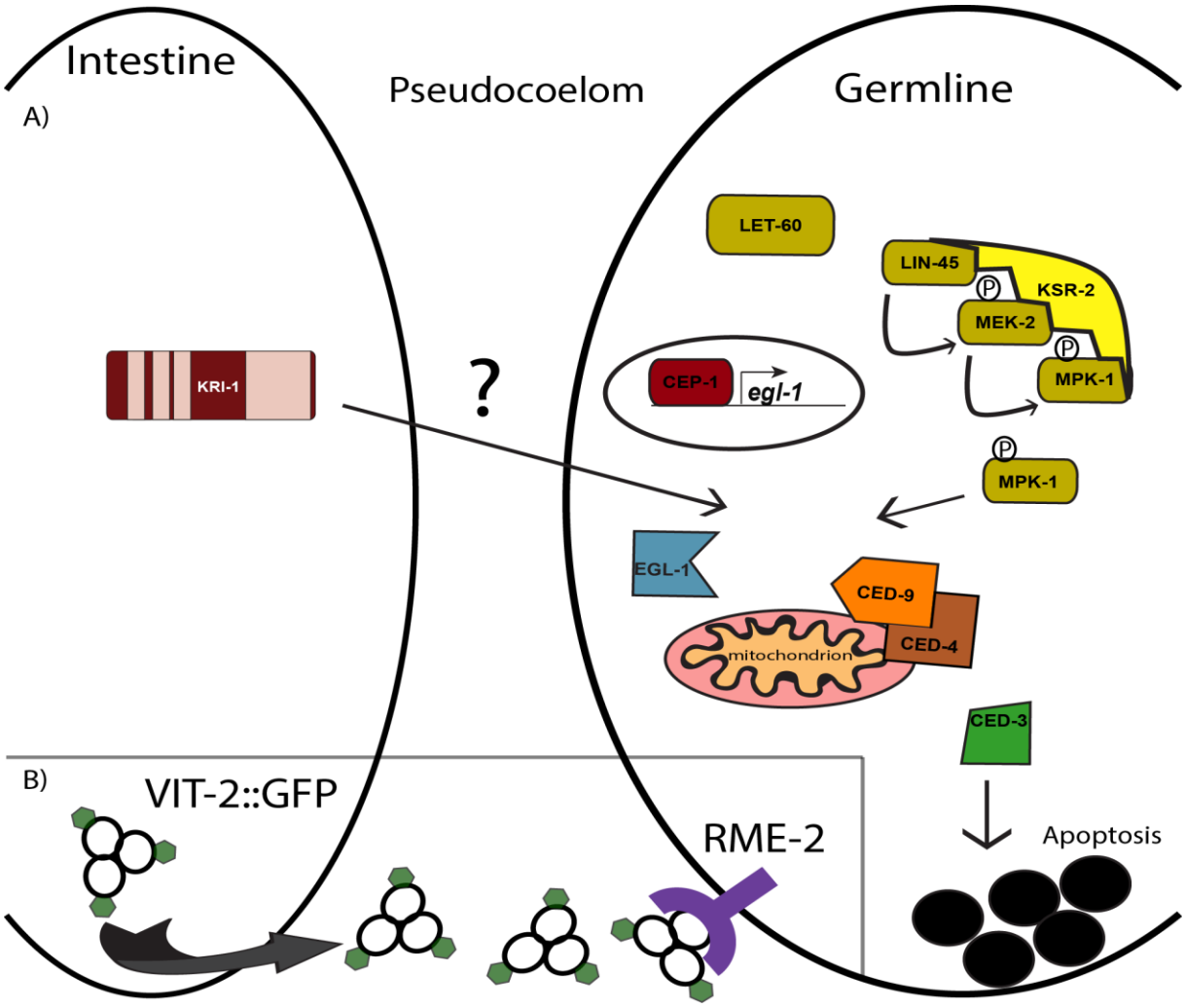

Figure 1.6 Intestinal to germline signalling in *C. elegans*

A) Intestinal KRI-1 and germline MPK-1/ERK1 are required for apoptosis in response to radiation. When KRI-1 or MPK-1 is absent, CEP-1/p53 is still able to induce *egl-1/BH3-only* expression, yet apoptosis does not occur. Additional loss of CED-9/BCL2 restores apoptosis, revealing that KRI-1 and MPK-1 feed into the core apoptotic cascade in a similar manner. The mechanism by which KRI-1 communicates to the germline is unknown. B) Yolk complexes, visualized by VIT-2::GFP, are formed in the intestine and secreted into the interstitial pseudocoelom for uptake into the germline by the RME-2/LDLR receptor to promote oocyte development.

1.4 KRI-1 homologues and Cerebral Cavernous Malformation disease

1.4.1 KRIT1/CCM1 and CCM disease

As previously mentioned, KRI-1 is the *C. elegans* homologue of the vertebrate scaffold protein KRIT-1/CCM1, and the two proteins have similar primary amino acid sequences (Mably et al., 2006). *KRIT1/CCM1* is the most commonly mutated gene in the disease **C**erebral **C**avernous **M**alformations (CCM), which affects 0.5% of the population (Draheim et al., 2014). Approximately 65% of patients with the familial form of the disease have predicted loss of function mutations in *KRIT1/CCM1*, and as a result develop anomalies in the vasculature of the **C**entral **N**ervous **S**ystem (CNS), most often in the brain (Draheim et al., 2014). These anomalies or "CCMs" have a mulberry-like appearance (Frischer et al., 2008), and occur due to weakened junctions between endothelial cells that constitute the vasculature (Baranoski, et al., 2016). CCMs are at risk of leaking blood into the brain or rupturing, resulting in headaches, strokes, or seizures depending on the number of CCMs in the brain and severity of rupture (Akers et al., 2017). Currently, invasive surgery is the main therapy for CCM patients (Akers et al., 2017), which is not viable for CCMs deep within the brain, or along the brain stem. In addition to *KRIT1/CCM1*, mutations in two other genes are associated with the familial disease. *Malcaernin/CCM2* is mutated in approximately 19% of these patients, while *PDCD10/CCM3* (**P**rogramme**d** **C**ell **D**eath 10) is mutated in about 16% of patients (Draheim et al., 2014). As with *KRIT1/CCM1*, aberrations in *Malcaernin/CCM2* and *PDCD10/CCM3* are predicted loss of function mutations (Fischer, et al., 2013). This is surprising, because CCM manifests in an autosomal dominant manner (Akers, et al., 2009). A Knudson "Two-hit" model has been proposed to explain this phenomenon (Akers, et al., 2009). Briefly, one mutant *CCM* gene copy is inherited, while loss of the second copy occurs in somatic tissue during development, most likely in the endothelium or surrounding cells.

KRIT1/CCM1 has an N-terminal Nudix domain, three NPxY/F motifs, ankyrin repeats, and a C-terminal FERM (4.1 (**f**) protein, **e**zrin, **r**adixin, **m**oesin) domain (Liu, et al., 2013). The FERM domain is further subdivided into three lobes termed F1-F3 (Zhang, et al., 2015). The F3 lobe has a PTB (**p**hospho**t**yrosine **b**inding) domain, which can bind to the first of three KRIT1 N-terminal

NPxY/F motifs, and is thought to regulate KRIT1 interactions with other proteins (Béraud-Dufour, et al., 2007). Interestingly, CCM2 binds to the second and third NPxY/F motifs of KRIT1/CCM1 through its PTB domain (Zawistowski et al., 2005) suggesting that these two proteins function together as a complex to regulate proper vasculature maintenance. CCM3, however, is mainly thought to function independently of KRIT1/CCM1-CCM2 in the **Str**iatin **I**nteracting **P**hosphatase **a**nd **K**inase (STRIPAK) complex (Goudreault et al., 2009). KRIT1 stands for "**K-r**ev **i**nteraction **t**rap-1" and was first identified in a two-hybrid screen for proteins that physically interact with the RAS superfamily protein K-rev, or RAP1 (**RA**S-related **p**rotein 1) (Serebriiskii, et al., 1997). Since the KRIT1/CCM1-CCM2 scaffold complex has no catalytic domains, it likely regulates proper vasculature maintenance through its binding partners. In addition to RAP1, proteins identified to interact with KRIT1/CCM1 include the **i**ntegrin **c**ytoplasmic domain-**a**ssociated **p**rotein 1 (ICAP1) (Zhang, et al., 2001), **S**orting **Nex**in 17 (SNX17) (Stiegler, et al., 2014), and the **he**art of **g**lass 1 (HEG1) receptor (Gingras, et al., 2012), while TRKA (Harel et al., 2009), the SMURF1 (**Sm**ad **u**biquitin **r**egulatory **f**actor 1) E3 ligase (Crose, et al., 2009), and MEKK3 (**M**APK/**E**RK **k**inase kinase) (Uhlik et al., 2003) bind CCM2. Despite the identification of these proteins, the downstream processes that are relevant to CCM disease are unclear. RhoA (**R**AS **ho**molog family member **A**) activity is suppressed by the KRIT1/CCM1-CCM2 complex by unclear mechanisms (Figure 1.7), and ablation of either KRIT1/CCM1 or CCM2 results in ectopic RhoA activation, stimulation of ROCK (**R**h**o** associated protein (**c**)**k**inase), and actin stress-fiber formation (Stockton, et al., 2010). It is possible that these stress fibers contribute to the weakened junctions between endothelial cells resulting in CCM (Stockton, et al., 2010). Interestingly, the ROCK inhibitor, Fasudil, has been shown to decrease the prevalence of CCMs in genetic mouse models of CCM disease (McDonald et al., 2011; Shenkar et al., 2017), but it is unknown whether this inhibitor will serve as an effective therapeutic for human patients.

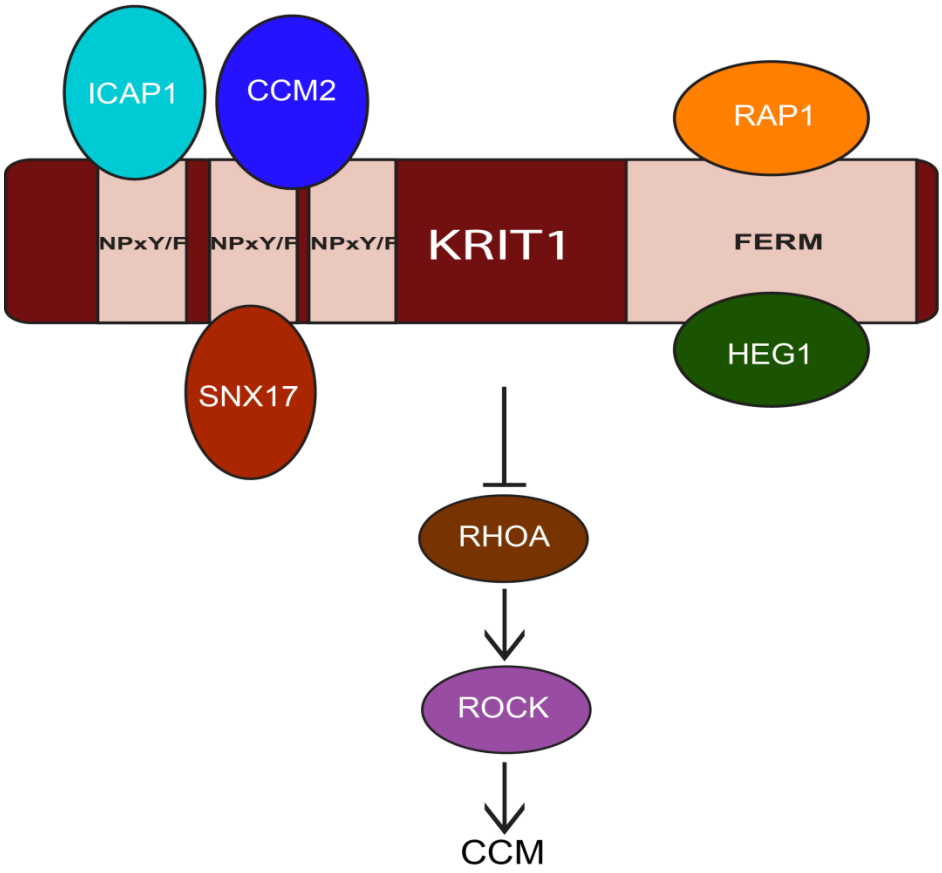

Figure 1.7 Vertebrate KRIT1 binding partners.
ICAP1 binds to the first and SNX17 the second N-terminal NPxY/F motif of KRIT1, while CCM2 interacts with the second and third NPxY/F motifs. RAP1 and HEG1 bind to the KRIT1 FERM domain, and this C-terminal region is also able to bind to the first KRIT1 NPxY motif of KRIT1. While it is unclear how these interactions ensure proper vasculature formation and maintenance, loss of KRIT1 enigmatically results in increased activation of the RHOA GTPase and RHO Kinase (ROCK) resulting in CCM formation.

1.4.2 *KRIT1/CCM1* animal models

1.4.2.1 Mouse models

Mouse models have been instrumental for the *in vivo* study of KRIT1/CCM1-CCM2. The earliest gene expression analysis of *Krit1/Ccm1* revealed ubiquitous localization early in development, with more prominent expression in the nervous system, epithelia, and select endothelial blood vessels as development progresses (Denier et al., 2002). It was later observed

that *Krit1/Ccm1* and *Ccm2* have similar expression patterns in the brain, providing the first clue that the two proteins likely function together (Seker et al., 2006). Given the broad range of *Krit1/Ccm1* and *Ccm2* expression early in development, it is not surprising that homozygous deletions in either of these two genes result in embryonic lethality (Plummer et al., 2006; Whitehead, et al. 2004), with gross defects in vascular development. These results provided an explanation as to why CCM patients inherit only one mutated *CCM* gene copy, with the second mutation occurring later during development. As such, establishing the first *Krit1*/*Ccm1* and *Ccm2* mouse models was not trivial, since heterozygotes do not develop CCMs (Akers, et al., 2009). Therefore, *Ccm1* and *Ccm2* heterozygotes were crossed into either *p53* (Plummer et al., 2004) or **M**i**s**matc**h** Repair 2 (*Msh2*) (McDonald et al., 2011) mutant backgrounds, to cause genomic instability. This created the potential for spontaneous mutations in a second gene copy in the endothelium, or surrounding tissue. Interestingly, while homozygosity in CCM tissue was confirmed in the *Msh2* mutant background supporting the "Two-hit" model (McDonald et al., 2011), the same could not be confirmed in the *p53* mutant background, suggesting that loss of p53 might contribute to CCM disease (Plummer et al., 2004). These early mouse models were not ideal, since the genomic instability likely generated many mutations, making links between CCM phenotypes and causality more difficult. Eventually, homozygous *Krit1/Ccm1* and *Ccm2* mouse models were created by conditional post-natal ablation in the endothelial tissue. This strategy allowed for the completion of embryogenesis, and these mice developed CCMs. Homozygosity of *Krit1/Ccm1* and *Ccm2* was also confirmed in the CCM tissue (Boulday et al., 2011). This new system of generating CCM knockout mice allowed for better characterization of the disease, without the potentially confounding effects of genomic instability. From these newer *Krit1/Ccm1* and *Ccm2* mouse models, important insights into the molecular causes for CCM disease were gleaned. This includes the discoveries that **end**othelial to **m**esenchymal **t**ransition (EndMT) (Maddaluno et al., 2013), bacterial infection in the intestine (Tang et al., 2017), reduced expression of the anti-angiogenesis factor, TSP1 (**T**hrombo**sp**ondin 1) (Lopez-Ramirez et al., 2017), and ectopic activation of the ERK5/MAPK signalling pathway (Zhou et al., 2016b) contribute to the development of CCMs in the absence of KRIT1/CCM1-CCM2. While likely acting distinctly from KRIT1/CCM1-CCM2, it is fascinating that tissue-specific ablation of *Ccm3* in astrocytes and glia results in the formation of endothelial CCMs (Louvi et al., 2011),

implicating cell-non autonomous signalling in the disease. Additionally, CCM3 has been shown to suppress the secretion of the angiogenesis factor, ANGPT2 (**Ang**io**p**oie**t**in 2), preventing the formation of CCMs (Zhou et al., 2016a).

1.4.2.2 Zebrafish models

The use of zebrafish to study CCM disease began during the era of heterozygous *Krit1/Ccm1-Ccm2* mouse models in the background of genomic instability. An advantage of establishing zebrafish as a CCM model was that homozygous mutants could be studied throughout embryogenesis (Mably et al., 2006). Although these mutants eventually die, the transparency of the animal allows for the visualization of cardiac and vascular defects (Donat et al. 2018), proving an opportunity to elucidate molecular pathways related to CCM proteins. The first study to assess the function of Krit1/Ccm1 and Ccm2 found that homozygous mutants for either gene fail to form a multilayered myocardium, resulting in grossly dilated heart chambers (Mably et al., 2006). This study also provided genetic evidence that *krit1/ccm1* and *ccm2* function in the same pathway (Mably et al., 2006). Shortly after the heart phenotype was identified, Krit1/Ccm1 and Ccm2 were implicated in proper vasculature development, as homozygotes were found to have severe dilations of major vessels (Hogan, et al., 2008). High resolution microscopy revealed that the microvasculature is also affected in *krit1/ccm1* animals due to the failure of vesicles to fuse during luminization (Liu, et al., 2011). Recently, two studies in zebrafish revealed that KLF (**K**ruppel-**l**ike **f**actor) transcription factors are regulated downstream of Krit1/Ccm1-Ccm2 (Renz et al., 2015; Zhou et al., 2015), mediated by the ERK5/MAPK pathway (Zhou et al., 2015). This cascade was subsequently found to regulate the formation of CCMs in mice (Zhou et al., 2016b), and initiated intense focus in the CCM research community into the function of this pathway (Cuttano et al., 2015; Donat et al., 2018, Fisher et al., 2015; Lopez-Ramirez et al., 2017). Currently, it is not well understood which targets downstream of the KLF transcription factors mediate CCM formation.

2 Materials and Methods

2.1 *C. elegans* strains

Strain	Source
C. elegans N2 (Wild Type)	Caenorhabditis Genetics Center (CGC)
C. elegans WD61 *kri-1(ok1251)*	(Ito et al., 2010)
C. elegans SD551 *let-60(ga89)*	CGC
C. elegans AH102 *lip-1(zh15)*	CGC
C. elegans WD435 *kri-1(ok1251); lip-1(zh15)*	This thesis
C. elegans WD338 *kri-1(ok1251); let-60(ga89)*	This thesis
C. elegans WD439 *kri 1(ok1251); E02D9.1a(T503del)* 4x backcrossed	This thesis
C. elegans WD440 *kri 1(ok1251); E02D9.1a(G717A)* 4x backcrossed	This thesis
C. elegans WD441 *kri-1(ok1251); mpk-2(G741A)* 4x backcrossed	This thesis
C. elegans WD442 *kri-1(ok1251); E02D9.1a(G213A)* 4x backcrossed	This thesis
C. elegans WD443 *kri-1(ok1251); E02D9.1a(C541T)* 4x backcrossed	This thesis
C. elegans WD444 *kri-1(ok1251);*	This thesis

Y106G6A.1(G1179A) 4x backcrossed	
C. elegans WD445 *kri-1(ok1251); klf-3(G749T)* 4x backcrossed	This thesis
C. elegans WD446 *kri-1(ok1251); Y106G6A.1(C1007T)* 4x backcrossed	This thesis
C. elegans WD447 *kri-1(ok1251); Y106G6A.1(C1007T)* 4x backcrossed	This thesis
C. elegans WD448 *kri-1(ok1251); Y106G6A.1(C1007T)* 4x backcrossed	This thesis
C. elegans WD449 *kri-1(ok1251); E02D9.1a(G717A)* 4x backcrossed	This thesis
C. elegans WD450 *kri-1(ok1251); Y106G6A.1(G949A)* 4x backcrossed	This thesis
C. elegans WD451 *kri-1(ok1251); Y106G6A.1(C1007T)* 4x backcrossed	This thesis
C. elegans CB1370 *daf-2(e1370)*	CGC
C. elegans WD485 *mpk-2(ok219)* 2x outcrossed	This thesis
C. elegans WD483 *kri-1(ok1251); mpk-2(ok219)*	This thesis
C. elegans WD658 *klf-3(on34)* 2x outcrossed	This thesis
C. elegans WD628 *kri-1(ok1251); klf-3(on34)*	This thesis
C. elegans MT3970 *mab-5ced-9(n1653)*	CGC
C. elegans WD682 N2 onEx93{*Pmpk-2::mpk-*	This thesis

2;myo-2::rfp;myo-3::rfp} #1	
C. elegans WD683 N2 onEx94{*Pmpk-2::mpk-2;myo-2::rfp;myo-3::rfp}* #2	This thesis
C. elegans WD684 N2 onEx95{*Pmpk-2::mpk-2;myo-2::rfp;myo-3::rfp}* #3	This thesis
C. elegans WD685 N2 onEx96{*Pelt-2::mpk-2;myo-2::rfp;myo-3::rfp}* #1	This thesis
C. elegans WD686 N2 onEx97{*Pelt-2::mpk-2;myo-2::rfp;myo-3::rfp}* #2	This thesis
C. elegans WD687 N2 onEx98{*Pelt-2::mpk-2;myo-2::rfp;myo-3::rfp}* #3	This thesis
C. elegans WD157 *kri-1(ok1251);* muEx353{*Pkri-1::gfp::kri-1;odr-1::rfp}*	(Ito et al., 2010)
C. elegans VJ268 fgEx12{P*act-5*::*act-5*::*gfp*}	(Zhang et al., 2012)
C. elegans WD688 N2 onEx99 {*Pzipt-2.3::zipt-2.3::gfp; rol-6}* #1	This thesis
C. elegans WD689 N2 onEx100 {*Pzipt-2.3::zipt-2.3::gfp; rol-6}* #2	This thesis
C. elegans WD690 N2 onEx101 {*Pzipt-2.3::zipt-2.3::gfp; rol-6}* #3	This thesis
C. elegans WD691 *kri-1(ok1251);* onEx99 {*Pzipt-2.3::zipt-2.3::gfp; rol-6}*	This thesis
C. elegans WD675 *zipt-2.3(ok2094)* 4x	This thesis

outcrossed	
C. elegans GH378 *pgp-2(kx48)*	CGC
C. elegans N2 Ex{*Pmpk-2::gfp; rol-6}* #1	This thesis
C. elegans N2 Ex{*Pmpk-2::gfp; rol-6}* #2	This thesis
C. elegans N2 Ex{*Pmpk-2::gfp; rol-6}* #3	This thesis
C. elegans RB2527 *ttm-1(ok3503)*	CGC
C. elegans WU209 *cdf-1(n2527)*	CGC
RT130 pwIs23 {P*vit-2::vit-2::gfp; unc-119*}	GCG
WD377 *kri-1(ok1251);* pwIs23 {P*vit-2::vit-2::gfp; unc-119*}	This thesis
MT2124 *let-60(n1046)*	CGC
WD502 *kri-1(ok1251);let-60(n1046)*	This thesis
WS2170 opIs110 {P*lim-7::yfp::act-5; unc-119*}	CGC
JM126 *pho-1(ca101ca102)*	CGC
HC196 *sid-1(qt9)*	CGC
CB5602 *vhl-1(ok161)*	CGC

2.2 Antibodies

Antibody	Source	Identifier
α-dpERK1 rabbit monoclonal	Cell Signalling	#4370
α-Nuclear Pore Complex mouse monoclonal (Mab414)	Abcam	#24609
goat α-rabbit Alexa 488	Invitrogen/Thermo Fisher	# A-11034
donkey α-mouse Alexa 568	Invitrogen/Thermo Fisher	# A10037
GFP-Trap_MA	ChromoTek	#gtma-10

2.3 Chemicals

Reagent	Source	Identifier
Fluozin-3	Invitrogen/Thermo Fisher	#F24195
Zinpy-1	Cayman Chemical	# 288574-78-7
ZnSO4	Sigma	#Z4750
EMS	Sigma	#M0880
Cas9	Integrated DNA Technologies	#1081060
Trizol	Invitrogen/Thermo Fisher	#15596026

2.4 Commercial assays

Product	Source	Identifier
DNeasy Blood & Tissue Kit	QAIGEN	# 69504
Invitrogen First Strand Synthesis System	Invitrogen/Thermo Fisher	#18080051
Random Hexamers	NEB	#S1330S
SYBR Green	BioRad	#1725271

2.5 Oligonucleotides

Primer	Forward	Reverse
klf-3 into L4440 vector	5’ttttttccatgggcattgctgcttgtcatcacc	5’ttttttctcgagctagattgtgctatggcgcttc
P*mpk-2* into pPD95.75 vector	5’ttttttaccggtatgagtgcgagaactacgc3’	5’ttttttgggccccagaacccctgcaaccatc3’
mpk-2 into P*mpk-2*::pPD95.75 vector	5’ttttttaccggtatgagtgcgagaactacgc3’	5’ttttttgggccccagaacccctgcaaccatc3’
mpk-2 into pJM559 (*Pelt-2*) vector	5’ttttttcggccgatgagtgcgagaactacgc3’	5’ttttttgggccccagaacccctgcaaccatc3’
P*zipt-2*.3::zipt-2.3 into	5’ttttttggatccggcatctaaactccctg	5’ttttttggtaccccggtagcccaaatcat

pPD95.75 vector	aac3’	gttgac3’
tbg-1 qPCR	5’cgtcatcagcctggtagaaca3’	5’tgatgactgtccacgttgga3’
zipt-2.3 qPCR	5’caccaacactcttcccttatt 3’	5’ cccaggcttctaagcaatc3’
klf-3 crRNA guide:	5’gcucaugagcggacucacuc3’	
dpy-10 crRNA guide	5’gcuaccauaggcaccacgag3’	
klf-3(on34) repair oligo	5’tgcgaacttccaagaacagttttgccatttgcacacaaaaggtttctcaacagagtgagtccgctcatgagctttcaaatgtgaagacttagagtatcta3’	
dpy-10 repair oligo	5’cacttgaacttcaatacggcaagatgagaatgactggaaaccgtaccgcatgcggtgcctatggtagcggagcttcacatggcttcagaccaacagcctat3’	

2.6 *C. elegans* maintenance and genetics

All nematode strains were cultivated at 16°C and maintained at 20°C for experimentation on NGM (nematode growth medium) agar plates with OP50 *E. coli* as a food source following standard procedures (Brenner, 1974). HT115 *E. coli* was used for RNA*i* knockdown. N2 Bristol was used as the wild type strain and mutant strains are listed in the above table. Compound mutants were built by crossing males of one genotype with hermaphrodites of the second genotype and double homozygotes selected in the F2 generation.

2.7 Quantification of germ cell apoptosis

Worms were irradiated 24 hours post L4 stage using a C^{137} source and apoptotic germ cell corpses quantified 24 hours post irradiation. Animals were mounted using 4% agarose pads on glass slides with 20mM L- levamisol in M9 buffer. Apoptotic cell corpses were quantified in one germline arm per animal by manually counting the number of refractile corpses (Figure 1.3B) using a 63X oil immersion lens and standard Differential Interference Contrast (DIC).

2.8 Statistical analysis of germ cell apoptosis changes

Microsoft Excel was used to determine statistical significance using a two-sided Student's *t*-test, assuming equal variance. Data was considered significant when the p-value was less than 0.05. The mean (red bar) +/- standard deviation was included in all dot plots.

2.9 Imaging

All imaging with *C. elegans* was carried out using a Leica DMRA2 system (Wetzlar, Germany) with standard DIC optics, fluorescent channels, and 10x, 40x, and 63x lenses.

2.10 RNA interference

The RNA*i* clones in this study were obtained from the Ahringer library, which contain fragments of genes representing about 85% of the *C. elegans* genome cloned into the L4440 vector and transformed into the HT115 *E. coli* strain (Kamath & Ahringer, 2003). Since *klf-3* is not included in this library, I cloned a fragment of this gene into the NcoI and XhoI sites in L4440 and transformed into HT115. Bacteria colonies were grown overnight in LB with 100µg/ml Ampicillin and 10µg/ml Tetracycline at 37°C and concentrated 10x the next day by pelleting at 10,000 rcf in a table top centrifuge. NGM plates were seeded with 100µl of the 10x concentrated culture. L1 animals were synchronized by incubating gravid adults with diluted hypochlorite to dissolve animals, while leaving the eggs intact. Eggs were hatched in M9 buffer and L1 larvae kept in a state of diapause overnight. L1 animals were plated on HT115 *E. coli* expressing double-stranded RNA the next day and grown at 20°C, irradiated 24hrs post L4, and apoptotic corpses quantified 24hrs post IR. As a control, HT115 containing the L4440 vector with a non-expressed gene was used, as previously described (Perrin et al., 2013).

2.11 Germline dissection and immunostaining

Young adult worms (24 hrs post L4) were irradiated with 60 Gy IR or left unirradiated, washed once in 1x PBS (**p**hosphate-**b**uffered **s**aline) 3hrs post IR, and transferred to 30ul 1x PBS + 4mM levamisol on slides coated with 20ul of 0.1% w/v polylysine. Germlines were dissected by removing the heads of animals, using two 27G needles. 1xPBS +4mM levamisol was replaced with 30ul fresh 2% **p**ara**f**orm**a**ldehyde (PFA) in 1xPBS for 10mins at room temperature. PFA

was prepared by dissolving 0.04g dry PFA in 1ml dH_20 +2ul 1M NaOH at 65°C for 1 hour with occasional mixing, followed by removing 500µl from the tube, and replaced with 500µl of H_2PO_4 buffer (0.004g KH_2PO_4, 0.0188g $NaHPO_4$, 500µl H_2O, pH=7.2). After germlines were isolated, a coverslip was added to each slide and placed on dry ice for at least 5 minutes, followed by freeze-cracking by rapidly removing the coverslip. Germlines were immediately fixed by immersing the slides in 100% Methanol for 5 minutes and transferred to a 1:1 mixture of Methanol:Acetone for 5 minutes. Finally, to end fixation, slides were transferred to 100% Acetone for 5 minutes. Slides were washed three times with 30µl 1x PBS + 0.1% Tween20 (PBST) for 10 minutes followed by incubation with one drop of "Image-it" added to each slide for 20 minutes. Germlines were blocked with 30ul PBST+ 1% BSA (**b**ovine **s**erum **a**lbumin) for 1hour, followed by overnight incubation with 30µl 1:100 anti-phospho- Erk-1 (Monoclonal from Cell Signalling #4370) and 1:100 anti-Nuclear Pore Complex (Monoclonal Mab414 from Abcam #24609) in (PBST +1% BSA) at room temperature with parafilm over the slide. The next day, parafilm was removed and the slides were washed three times with 30µl 1x PBST for 10 minutes. 30µl of secondary 1:500 goat anti-rabbit Alexa 488 for phospho-Erk1 and 1:500 donkey anti-mouse Alexa 568 for Mab414 in (PBST +1% BSA) were added to each slide, incubating at room temperature for 1 hour. Slides were then washed once with 30µl 1x PBST for 10 minutes and incubated with 30µl DAPI (4′,6-diamidino-2-phenylindole) for 10 minutes (1:1000 of 1mg/ml DAPI in PBST), followed by a final wash with 30µl 1x PBST for 10 minutes. PBST was removed and 5µl of Prolong Gold was added to each slide and sealed with a coverslip.

2.12 Immunoprecipitation and mass spectrometry

The following method was performed in collaboration with Christopher Go from the lab of Dr. Anne-Claude Gingras.

In biological triplicate, approximately 800,000 worms were grown on large 90 mm NGM plates with OP50 *E. coli*. Plates were prepared by transferring 5 mL of OP50 culture into 1 L of Terrific Broth and incubated overnight in a 37°C shaker. The following day, the bacteria was spun down at 4,000 rcf in 500ml centrifuge bottles for 10 minutes at 4ºC and resuspended in 5x volume of M9 Buffer. Up to 100,000 synchronized L1s were added onto each plate. Worms were irradiated with 60 Gy IR 24hrs post L4, and a corresponding set was left unirradiated. Six hours post IR,

plates were washed with M9 buffer to collect the worms in to 15 mL conical tubes followed by two more M9 washes in the tubes. The worms were then placed on a rocker for 30 minutes in 10 mL M9 buffer to rid bacteria from the intestine. Worms were washed three times in M9 followed by two washes in dH_2O and pelleted. The remaining liquid was aspirated and the worm pellet flash-frozen in liquid nitrogen. Worm pellets were later thawed on ice in a 1:1 (v/v) ratio of ice-cold DROSO lysis buffer (30 mM HEPES pH 7.4, 100 mM Potassium Acetate, 2mM Magnesium Acetate, 0.1% NP-40, 2 mM DTT; supplemented with 1 tablet/5 mL cOmplete™, Mini Protease Inhibitor Cocktail (Sigma Millipore CAT# 11836153001 ROCHE), 1:100 Sigma Phosphatase Inhibitor 2 (CAT# P5726), 1:100 Sigma Phosphatase Inhibitor 3 (CAT# P0044). Worms were lysed in a chilled Wheaton Dounce Homogenizer (metal), periodically checking 1 µL of lysate under a microscope until no worm fragments or embryos were seen. The lysate was then spun at 10,000 rcf for 30 min at 4ºC, and the supernatant transferred to a fresh tube. 10 mg of total protein for each sample was used for affinity purification. For each sample, 30 µL of a 50% slurry of GFP-Trap®_MA (ChromoTek Inc.) pre-washed in DROSO buffer was incubated with the worm lysate corresponding to 10mg of protein for 3 hours at 4ºC using a rotator. Beads were separated from the supernatant with a magnetic stand and transferred to new 1.5 mL microcentrifuge tubes in DROSO buffer. The beads were then washed once in TAP Buffer (50 mM HEPES-KOH pH 8.0, 100 mM KCl, 2 mM EDTA, 0.1% NP-40 and 10% glycerol), and once in 50 mM Ammonium Bicarbonate, pH 8. The supernatant was removed, and beads were resuspended in 10 µL of 50 mM Ammonium Bicarbonate containing 1 µg trypsin (Millipore Sigma CAT# T6567). Samples were digested overnight at 37ºC on a rotator. The next day, each sample was spun down at 400 rcf for 1 min to pellet beads and the supernatant transferred to new 1.5 mL microcentrifuge tubes. This supernatant was digested again for 4 hours with 0.25 µg of trypsin. 1 µL of 50% formic acid was used to stop the digestion, and samples were freeze dried and stored at -80ºC. Each peptide sample was resuspended in 20 µL of 5% formic acid and centrifuged at 16,000 rcf for 1 min to remove debris prior to analysis with an Orbitrap Elite Hybrid Ion Trap mass spectrometer with Xcalibur 2.0 software. Data was converted to mzML using ProteoWizard (3.0.4468) (Kessner, et al., 2008) and analyzed using the iProphet pipeline (Shteynberg et al., 2011) implemented within ProHits (Liu et al., 2010). Proteins with iProphet probability ≥ 0.95, corresponding to a false-discovery rate (FDR) of approximately 0.5% were

analyzed with **S**ignificance **A**nalysis of **Int**eractome (SAINT) scoring using SAINTexpress (version 3.6.1) (Choi et al., 2011; Teo et al., 2014) to identify true interaction partners.

2.13 EMS Mutagenesis and screening

kri-1(ok1251) late L4/young adult worms were incubated with 4ml of 50mM EMS for 4 hours in 15ml conical tubes and transferred to NGM plates for egg laying. Approximately 500,000 F1 worms (1,000,000 haploid genomes) were divided into twenty separate populations and left to lay F2 eggs. These eggs were transferred to twenty 50 ml conical tubes with liquid M9 buffer (one tube for each population) and hatched into L1 larvae. Under these conditions without food, the larvae arrest growth, and remain in a state of diapause (Johnson, et al., 1984). *kri-1(ok1251)* F2 larvae were kept in M9 for one week on a rocker at room temperature, and the entire population from each of the twenty tubes was transferred onto twenty large plates with growth media (one plate for each tube). Since *kri-1(ok1251)* L1 larvae normally do not survive a week of diapause, only *kri-1(ok1251)* animals with mutations that suppress this phenotype grew to adulthood. These survivors were singled out and clonal lines established. F3 progeny from these single survivors were assessed for a restoration of IR-induced apoptosis compared to non-irradiated controls. A single suppressor line was chosen from any given starting population, such that thirteen candidates from the twenty populations were sent for whole genome sequencing.

2.14 DNA extraction and whole genome sequencing

Mapping of whole genome sequencing reads to a reference genome and variant calling was performed by Michael Schertzberg in the lab of Dr. Andrew Fraser.

Whole genome sequencing and identification of *kri-1(ok1251)* suppressor mutations was based on the protocol described in (Burns et al., 2015). DNA was isolated using the DNeasy Blood & Tissue Kit (QIAGEN) and barcoded libraries were created for each strain using the Nextera DNA Sample Preparation Kit from Illumina. An Illumina HiSeq2500 instrument was used to produce 75 base paired-end reads. First, the sequencing reads were examined for sequence quality using FastQC up to the full 75 bases. Bases lower than a quality threshold of 30 were trimmed using Trimmomatic (Bolger, et al., 2014). Reads were aligned to the *C. elegans* N2 reference genome (release W220) using BWA-mem (Heng Li & Durbin, 2009). Alignments

were sorted by coordinate order and duplicates removed using Picard (http://picard.sourceforge.net). Before variant calling, reads were processed in Genome Analysis Tool Kit (GATK) v2.5 for indel realignment and base quality score recalibration, using known *C. elegans* variants from dbSNP build 138 (http://www.ncbi.nlm.nih.gov/SNP/). GATK HaplotypeCaller was used to call variants, and results were filtered for a phred-scaled Q score >30. For each SNP a call is made based on 1) the number of reads, 2) the phred score of the reads, and 3) how many of each alternate allele is identified. Finally, called variants were annotated using Annovar to obtain a list for each sample.

2.15 Cloning

To generate the P*mpk-2::gfp* transcriptional reporter, 6kb upstream of the *mpk-2* start codon was amplified from wild type genomic DNA and ligated into the SphI and AgeI restriction sites of the Fire Kit vector pPD95.75. The P*mpk-2::mpk-2* construct was generated by replacing *gfp* in the above P*mpk-2::gfp* plasmid with *mpk-2* amplified from wild type genomic DNA and ligated into the AgeI and ApaI restriction sites of the above plasmid. The correct sequence of *mpk-2* was verified by Sanger sequencing. The P*elt-2::mpk-2* construct was generated by ligating sequenced *mpk-2* into the EagI and ApaI restriction sites of pJM559 containing 5kb of the *elt-2* promoter (Veyhl et al., 2017). The P*zipt-2.3::zipt-2.3::gfp* translational fusion construct was generated by amplifying P*zipt-2.3::zipt-2.3* starting from 5kb upstream of the *zipt-2.3* start codon and ending after the 3'UTR of *zipt-2.3* from wild type genomic DNA. This product was then inserted into BamHI and KpnI restriction sites of the Fire Kit vector pPD95.75. The correct sequence of *zipt-2.3* was verified by Sanger sequencing. All cloning was carried out with NEB restriction enzymes and buffers, and Invitrogen T4 ligase and buffer.

2.16 Generation of transgenic strains

Constructs were injected into wild type N2 worms at a concentration of 50 ng/µl to create extra-chromosomal arrays. The plasmids pCFJ90 (P*myo-2::mcherry*) and pCFJ104 (P*myo-3::mCherry*) were used as co-injection markers for P*mpk-2::mpk-2* and P*elt-2::mpk-2* and injected at concentrations of 2.5 ng/µl and 5 ng/µl, respectively.

2.17 CRISPR-Cas9

Genome editing was performed in collaboration with Bin Yu from the lab of Dr. W. Brent Derry.

Generation of the *klf-3(on34)* strain was based on a previously reported method (Paix, et al., 2015). Wild type N2 young adult hermaphrodites were injected with Cas9-crRNA-tracrRNA RNP complexes and repair templates for *klf-3(on34)* and *dpy-10* as a marker for positive selection. Dumpy and Roller F1 worms were singled out onto individual plates, and screened for the *klf-3(on34)* mutation by PCR and sequencing. The positive candidate was outcrossed two times to remove the *dpy-10* mutation.

2.18 Total RNA extraction

In biological triplicate, 2,000 synchronized L1 worms were grown and irradiated with 60Gy 24 hours post L4 and transferred to 1.5ml conical tubes using M9 buffer 3-6 hours post IR. Worms were washed three times with M9 buffer, M9 removed, and 1ml of Trizol added. Worms in Trizol were flash frozen using liquid nitrogen and subjected to three rounds of freeze-thawing. 200µl of chloroform was added, and samples and vortexed for 30 seconds. Samples were then centrifuged at 12,000rcf for 15 minutes at 4°C. The aqueous phase was transferred to a new tube, and 500µl of 100% cold isopropanol added to samples and precipitated overnight at -20° C. The next day, samples were centrifuge at 12,000rcf for 15mins at 4°C, and supernatant was removed from the tube. The RNA pellet was washed with 1ml of 75% Ethanol in DEPC dH_2O and vortexed for 1 minute. Samples were centrifuged at 12,000rcf for 5 minutes at 4°C and supernatant discarded. The RNA pellet was air dried for 5 minutes and resuspended in 50µl of Invitrogen Ultrapure dH_20.

2.19 RNA sequencing and analysis

Mapping of mRNA sequencing reads to a reference genome was performed by Michael Schertzberg in the lab of Dr. Andrew Fraser.

mRNA was purified from total RNA by the Hospital for Sick Children Next Generation Sequencing Facility (TCAG) and reads were compared to those from the wild type N2 samples using tophat/Cufflinks (Trapnell et al., 2012). Sequencing reads were analyzed for quality with

Fastqc. Trimmomatic was used to eliminate low quality reads and remove adapters. The minimum intron length in tophat was lowered to 30bp from the default 70 due to small intron sizes in *C. elegans*. The reference genome and transcript annotations were based on release WS235 (CE11).

2.20 Quantitative PCR

To determine *zipt-2.3* mRNA levels in *C. elegans*, total RNA was extracted as described above in biological duplicate, 3-6 hours post 0 Gy or 60 Gy. cDNA was prepared from 500ng of total RNA using the Invitrogen SuperScriptIII First-Strand Synthesis System primed with a random primer mix. The reaction conditions were 25ºC for 10 minutes, 50 ºC for 60 minutes, and 85 ºC for 5 minutes. Samples were then incubated with 1U of RNaseH at 37ºC for 30 minutes. *zipt-2.3* cDNA was amplified using the following conditions: 95ºC for 30 seconds, then 95ºC for 15 seconds and 60ºC for 30 seconds repeated for 40 cycles. BioRad SYBR Green Supermix was used for quantification and the BioRad CFX96 RT-PCR system for detection. Transcripts were normalized to tubulin (Ito et al., 2010) and compared to wild type.

2.21 Zinc staining

Fluozin-3

Staining of intestinal stored zinc was based on the protocol described in (Roh, et al., 2012). 10µM Fluozin-3 was added to NGM plates with OP50 *E. coli* and left to dry in the dark for 30 minutes. L4 stage worms were added to the plates and incubated in the dark at 20°C for 24 hours. Worms were then irradiated (60 Gy) or left unirradiated and transferred to new NGM plates without dye 3-6 hours post IR to de-stain for 30 minutes, and imaged. Wild type worms without dye were used to differentiate Fluozin-3 signal from gut granule autofluorescence.

Zinpyr-1

Staining of interstitial zinc was based on the protocol described in (Roh et al., 2013). 100µM $ZnSO_4$ was added to NGM plates with OP50 *E. coli*. L4 stage worms were added to the plates and kept at 20°C for 20 hours. 20µM Zinpyr-1 was added to the plates, and worms incubated in the dark at 20°C for 2 hours. Worms were transferred to new NGM plates without dye for 30 minutes to de-stain and immediately imaged.

3 Results 1: A Conserved KRI-1/CCM Complex Regulates Intestinal ERK5/MAPK to Activate Germline ERK1/MAPK and Radiation-Induced Apoptosis

3.1 Data attribution

I'm very grateful and would like to thank Matthew Eroglu for assistance with the RNA*i* screen in section 3.6, Michael Schertzberg for aligning the whole genome sequencing reads to a reference genome for mutation identification in section 3.7, Bin Yu for generating the *klf-3(on34)* allele by CRISPR-Cas9 in section 3.8, and Chrisopher Go for helping with AP-MS in section 3.10.

3.2 KRI-1 does not regulate apoptosis through yolk secretion

To identify how *C. elegans* KRI-1 is signalling from the intestine to the germline, I became interested in yolk LDL lipoprotein secretion. Yolk is used as a source of nutrients in the germline, but the yolk complex containing cholesterol and other lipids is formed in the intestine before being secreted into the interstitial pseudocoelom, and taken up into the germline (Sato et al., 2014). I reasoned that KRI-1 might regulate the transport of apoptotic signalling molecules to the germline as part of the yolk complex. To visualize whether yolk protein expression or localization is perturbed in the absence of KRI-1, I crossed a strain that expresses the yolk protein VIT-2 tagged with GFP (Grant & Hirsh, 1999) into *kri-1(ok1251)* mutants that have a null deletion in *kri-1* (Berman & Kenyon, 2006; Ito et al., 2010). VIT-2::GFP is normally detected in the intestine and germline (Grant & Hirsh, 1999), but mutations that prevent export of VIT-2::GFP from the intestine have an increase of VIT-2::GFP in this tissue (Balklava, et al., 2007). Mutants that fail to import VIT-2::GFP into the germline accumulate this protein in the interstitial pseudocoelom (Grant & Hirsh, 1999). To determine if loss of KRI-1 results in a defect in either the secretion or uptake of yolk protein, I compared the expression of VIT-2::GFP between wild type and *kri-1(ok1251)* animals. In *kri-1(ok1251)* mutants, I observed a decrease in VIT-2::GFP levels in the intestine (Figure 3.1A-B; Table 7.1) and germline (Figure 3.1C-D). These results suggest that when KRI-1 is absent, yolk formation decreases in the intestine, resulting in reduced yolk uptake into the germline. Consistent with my observations, a recent study subsequently demonstrated that KRI-1 regulates the transcriptional activity of *vit-2* (Goszczynski, et al., 2016).

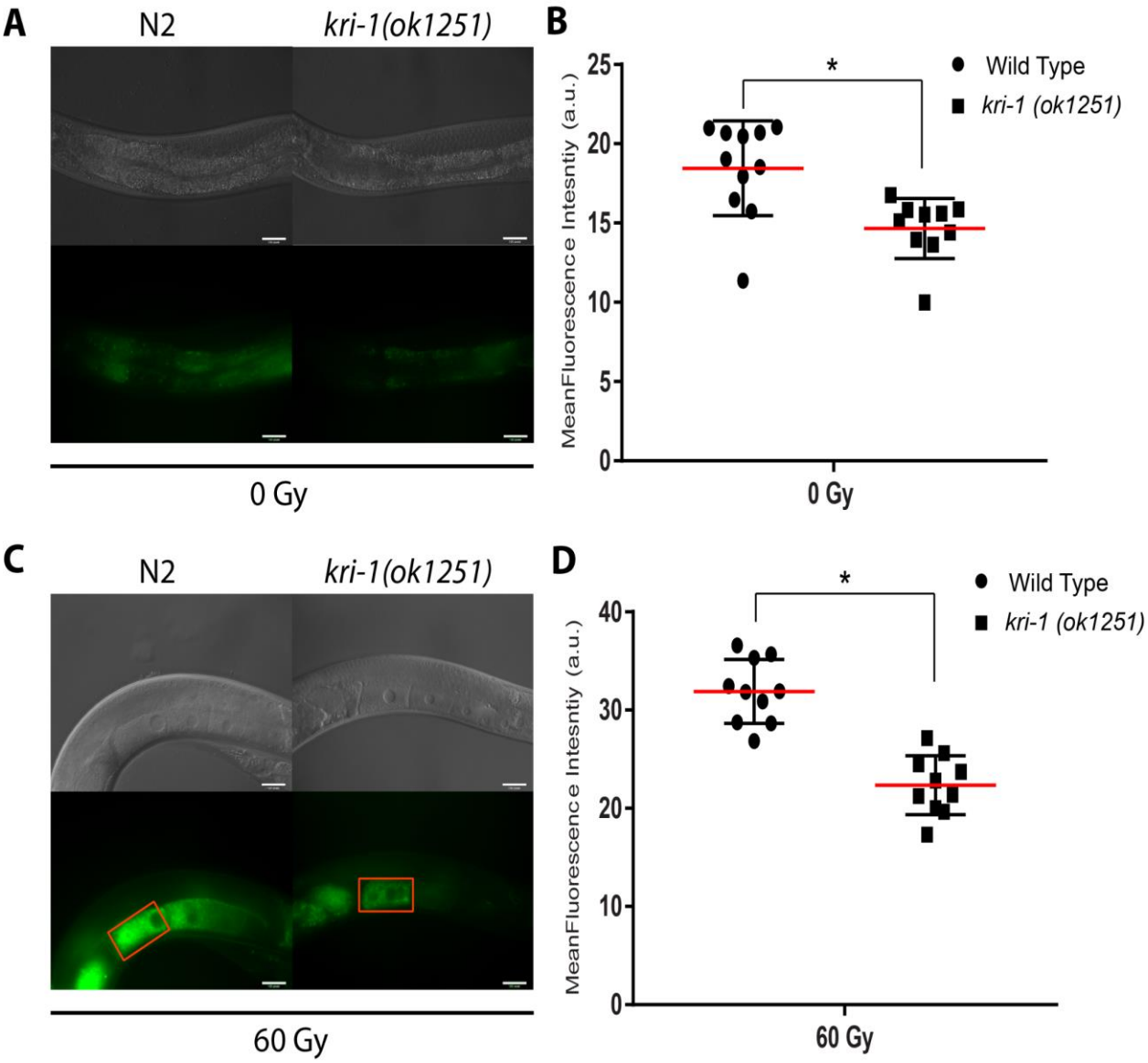

Figure 3.1 VIT-2 levels decrease in the absence of KRI-1.
A-B) Detection of intestinal VIT-2::GFP in wild type and *kri-1(ok1251)* animals 24 hrs past the L4 stage. Fluorescence was measured as a total area along the length of the intestine. Images are representative of one experiment and at least 10 worms per strain. C-D) Detection of intestinal VIT-2::GFP in the germline of wild type, and *kri-1(ok1251)* animals 3hrs post IR (60Gy). VIT-2::GFP expression is brightest in the "-1 oocyte" within the red box, and this area was used to quantify fluorescence. Images are representative of three independent replicates and at least 10 worms per strain were quantified. B&D) Red line is mean +/- standard deviation. *P<0.05, two-sided, unpaired t-test. All significant P values in this thesis are listed in Table 7.1.

Since ablation of *kri-1* results in decreased yolk production, it is possible that apoptotic factors normally loaded into the yolk complex fail to be transported into the germline. Since the RME-2/LDL receptor is necessary for the uptake of yolk (Grant & Hirsh, 1999) and apoptotic factors (Sendoel et al., 2010) into the germline, I hypothesize that ablation of RME-2 will prevent KRI-1-mediated molecules from entering the germline with the yolk complex. To test this hypothesis, I knocked down *rme-2* by RNA*i* to determine whether apoptosis is altered in wild type animals or *kri-1(ok1251)* mutants. As a positive control, I ablated *rme-2* in radio-resistant *vhl-1(ok161)* (**V**on **H**ippel-**L**indau tumor suppressor homolog-1) mutants, which restores IR-induced apoptosis by preventing the uptake of TYR-2/TRP2 into the germline (Sendoel et al., 2010). Since knockdown of *rme-2* did not affect apoptosis in wild type or *kri-1(ok1251)* mutants (Figure 3.2), I conclude that KRI-1 does not transmit apoptotic signals through the yolk complex or this receptor.

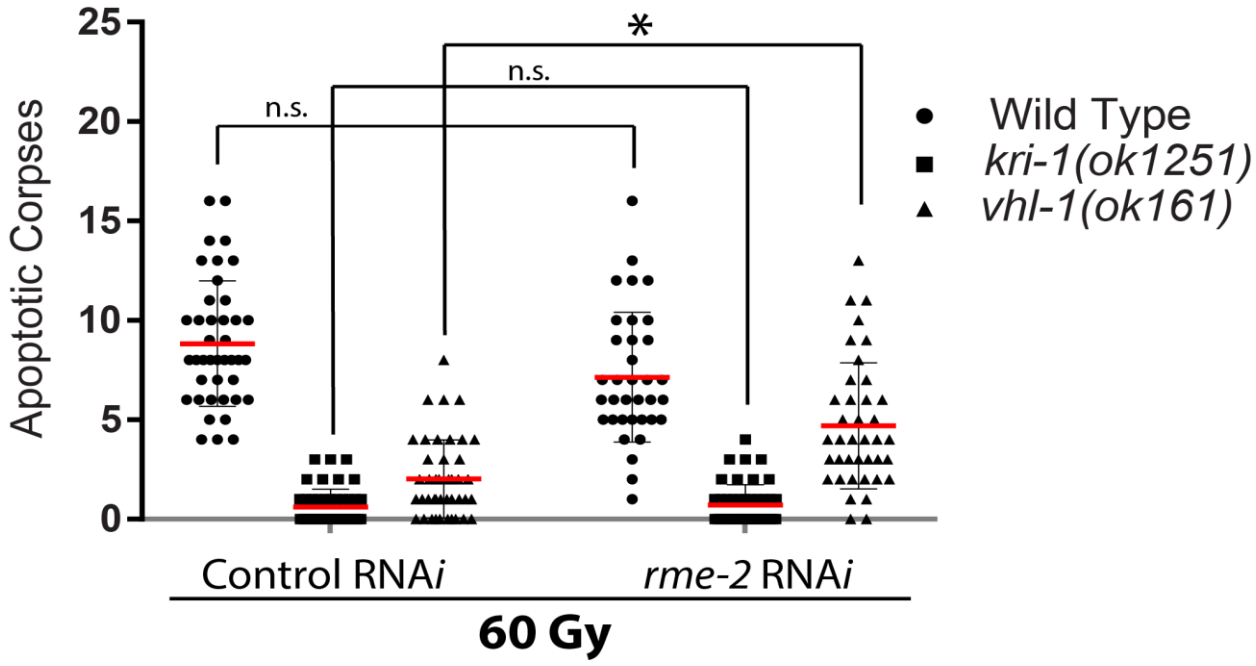

Figure 3.2 RME-2/LDLR is not part of the KRI-1 pathway.
IR-induced germ cell apoptosis quantified in wild type, *kri-1(ok1251),* and *vhl-1(ok161)* animals after knock-down of *rme-2/LDLR*. Apoptotic corpses were quantified 24 hours post irradiation (60 Gy), and the data shown represent four independent replicates. Graph represents at least 35 worms per strain, per condition. Red line is mean +/- standard deviation. *P<0.05, two-sided, unpaired t-test.

3.3 KRI-1 does not regulate apoptosis through Rho kinase

In vertebrates, loss of KRIT1/CCM1 activates the RHOA GTPase and its downstream effector Rho Kinase (ROCK) by an unknown mechanism. This activation contributes to unstable endothelium and CCMs due to actin stress fiber formation (Stockton, et al., 2010), and knockdown of either RHOA or ROCK prevents CCM phenotypes in the absence of KRIT1/CCM1 (Borikova et al., 2010). Therefore, it is possible that resistance to IR-induced apoptosis in *kri-1(ok1251)* mutants is due to increased RHO-1/RHOA or LET-502/ROCK activity. Since actin reorganization occurs in engulfing cells (Kinchen et al., 2005) that can promote apoptosis (Chakraborty et al., 2015; Hoeppner, et al., 2001; Reddien et al., 2001), it is possible that perturbation of actin in the absence of KRI-1 prevents cell death. To determine if reducing RHO-1/RHOA or LET-502/ROCK can restore apoptosis in the absence of KRI-1, I knocked down both genes by RNA*i* in *kri-1(ok1251)* mutants (Figure 3.3). Knockdown of *rho-1/RHOA* in *kri-1(ok1251)* animals results in a slight increase in IR-induced apoptosis, but cell death is not restored to wild type levels (Figure 3.3). Knockdown of the downstream effector *let-502/ROCK* did not restore IR-induced apoptosis in *kri-1(ok1251)* animals (Figure 3.3). Together, these data suggest that while KRI-1 partially regulates apoptosis through RHO-1/RHOA, LET-502/ROCK and likely actin are independent of this cascade.

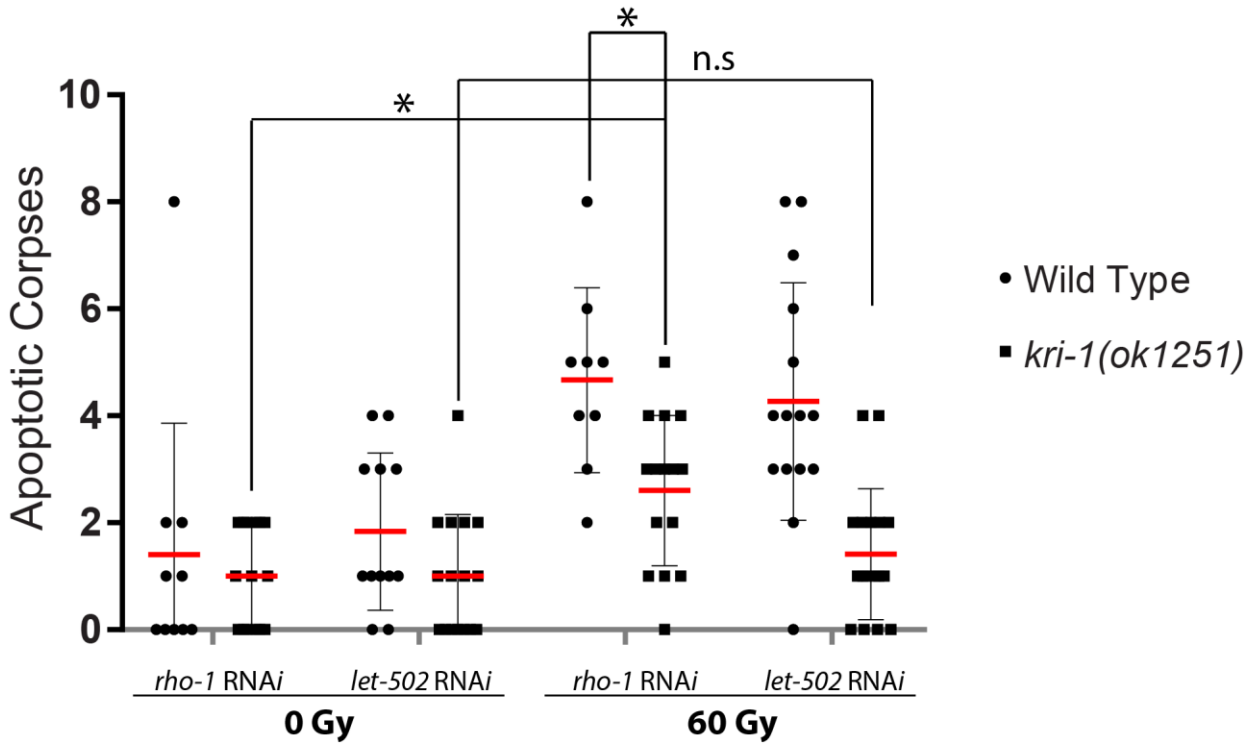

Figure 3.3 Knockdown of rho-1/RHOA or let-502/ROCK does not restore IR-induced apoptosis in *kri-1(ok1251)* animals.
IR-induced germ cell apoptosis quantified in wild type and *kri-1(ok1251)* animals after knock-down of *rho-1/RHOA* and *let-502/ROCK*. Apoptotic corpses were quantified 24 hours post irradiation (60 Gy) and represent one experiment. Graph represents at least 10 worms per strain, per condition. Red line is mean +/- standard deviation. *P<0.05, two-sided, unpaired t-test. In deviation from the protocol described in the methods section, RNA*i* treatment began at the L4 stage due to L1 larval lethality.

To visualize any potential changes in actin expression that might occur when KRI-1 is absent, I expressed YFP::ACT-5 (**Act**in) under control of the *lim-7* promoter in wild type and *kri-1(ok1251)* animals. This promoter is active in the gonadal sheath cells (Kinchen et al., 2005) that engulf germ cells (Gumienny et al., 1999). In the absence of radiation, ACT-5 localization was similar between wild type and *kri-1(ok1251)* animals, appearing as a "honeycomb" pattern (Figure 3.4A), but apoptosis was not restored in the *kri-1(ok1251)* mutants (Figure 3.5). Furthermore, in response to radiation, actin concentrated around apoptotic cells in wild type animals as previously described (Kinchen et al., 2005), and was similarly localized in *kri-1(ok1251)* mutants (Figure 3.4B). These results suggest that resistance to apoptosis in the absence of KRI-1 is not due to aberrant regulation of actin.

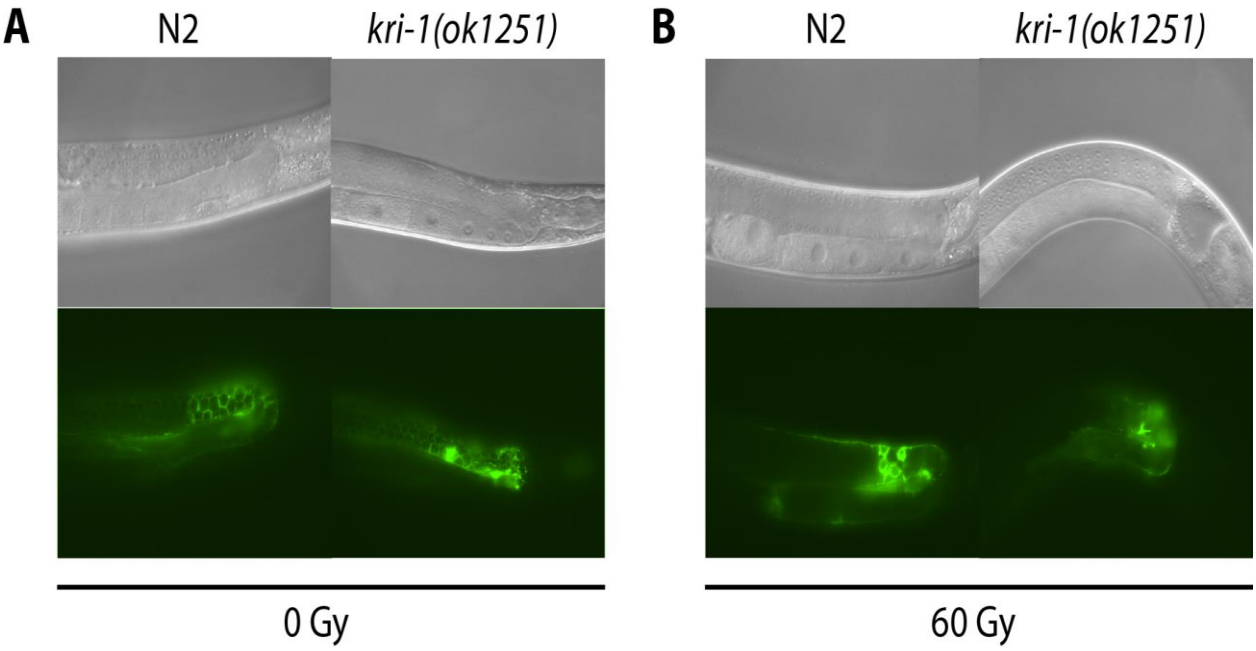

Figure 3.4 Actin localization in the gonadal sheath is not perturbed in *kri-1(ok1251)* mutants.
A-B) Detection of YFP::ACT-5 in wild type and *kri-1(ok1251)* animals in the absence of radiation (0 Gy) and 3 hrs post irradiation (60Gy). Images are representative of three independent replicates and at least 30 worms per strain, per condition.

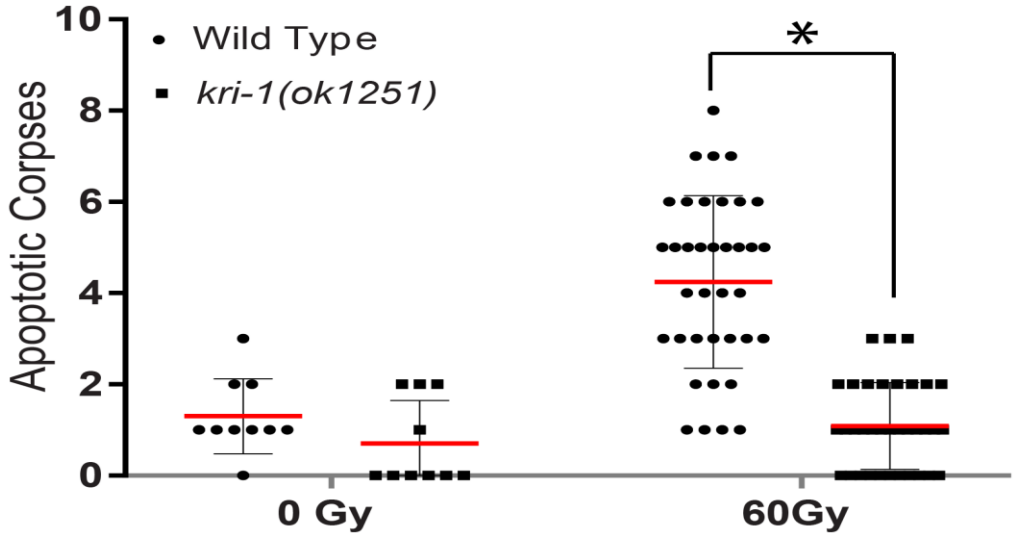

Figure 3.5 Gonadal sheath- driven actin expression does not restore apoptosis in *kri-1(ok1251)* animals.
IR-induced germ cell apoptosis quantified in wild type and *kri-1(ok1251)* animals expressing *act-5::yfp* from a gonadal sheath cell (*lim-7*) promoter. Apoptotic corpses were quantified 24 hours post irradiation (60 Gy) and in the absence of radiation (0 Gy). Graph represents three independent replicates and at least 35 worms per strain for the 60Gy treatment, and one experiment with 10 worms per strain for 0 Gy. Red line is mean +/- standard deviation. *P<0.05, two-sided, unpaired t-test.

3.4 KRI-1 does not regulate apoptosis through SKN-1/NRF2

Since the SKN-1/NRF2 transcription factor mediates lifespan extension downstream of KRI-1 (Wei & Kenyon, 2016), I wondered if this mode of regulation is important for IR-induced apoptosis. In addition, a new study showed that ablation of *skn-1/NRF2* restores IR-induced germ cell death in resistant *brap-2(ok1492)* mutants (D'Amora et al., 2018). Therefore, it is possible that KRI-1 promotes apoptosis by suppressing SKN-1/NRF2. To test this, I knocked down *skn-1* but did not observed restored apoptosis in *kri-1(ok1251)* mutants (Figure 3.6). This demonstrates

that while KRI-1 suppresses SKN-1/NRF2 to promote lifespan extension (Wei & Kenyon, 2016), the same is not true for IR-induced apoptosis. This result is consistent with KRI-1 promoting germ cell death and lifespan extension by different mechanisms (Berman & Kenyon, 2006; Ito et al., 2010).

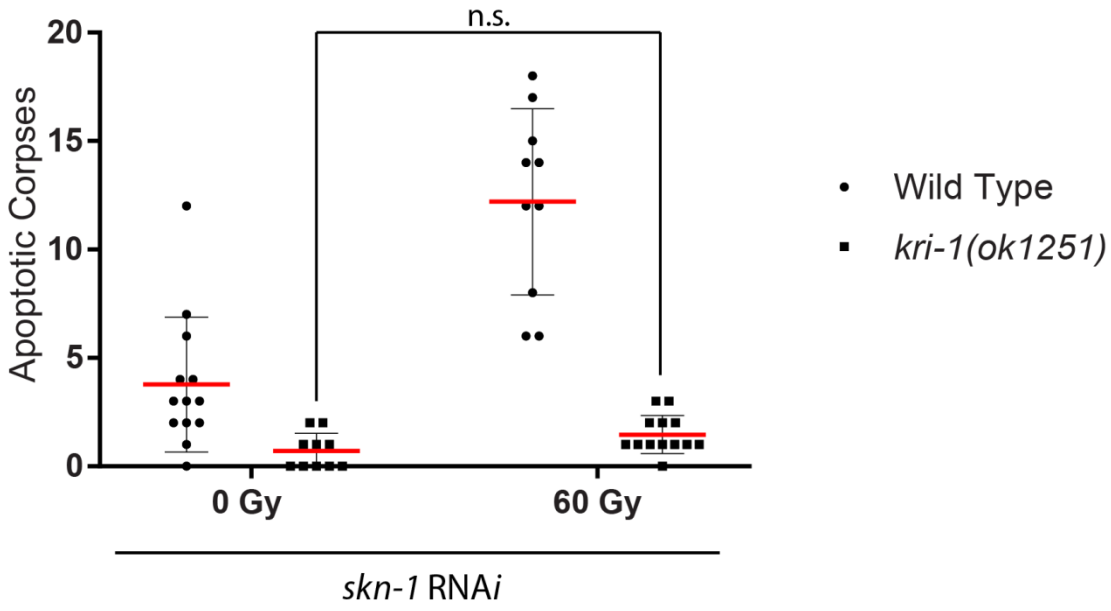

Figure 3.6 Knockdown of *skn-1/NRF2* does not restore IR-induced apoptosis in *kri-1(ok1251)* animals.
IR-induced germ cell apoptosis quantified in wild type and *kri-1(ok1251)* animals after knock-down of *skn-1/NRF2*. Apoptotic corpses were quantified 24 hours post irradiation (60 Gy) and in the absence of radiation (0 Gy). These data represent one experiment. Graph represents at least 10 worms per strain, per condition. Red line is mean +/- standard deviation. P >0.05 (n.s.), two-sided, unpaired t-test.

3.5 KRI-1 is required for the activation of germline MPK-1/ERK1 to promote apoptosis

Given that phosphorylation and activation of MPK-1/ERK1 in the pachytene region of the germline (Figure 1.3A) are necessary for IR-induced germ cell apoptosis (Rutkowski et al., 2011), I wondered if MPK-1 might be regulated by KRI-1. To test this, I isolated germlines from wild type and *kri-1(ok1251)* mutants and performed immunohistochemistry with an antibody that

recognizes di-phosphorylated MPK-1. Germlines from *kri-1(ok1251)* mutants had reduced levels of dp-MPK-1 compared to wild type animals in both non-irradiated and irradiated conditions (Figure 3.7). This indicates that KRI-1 is required for activation of MPK-1 in the germline.

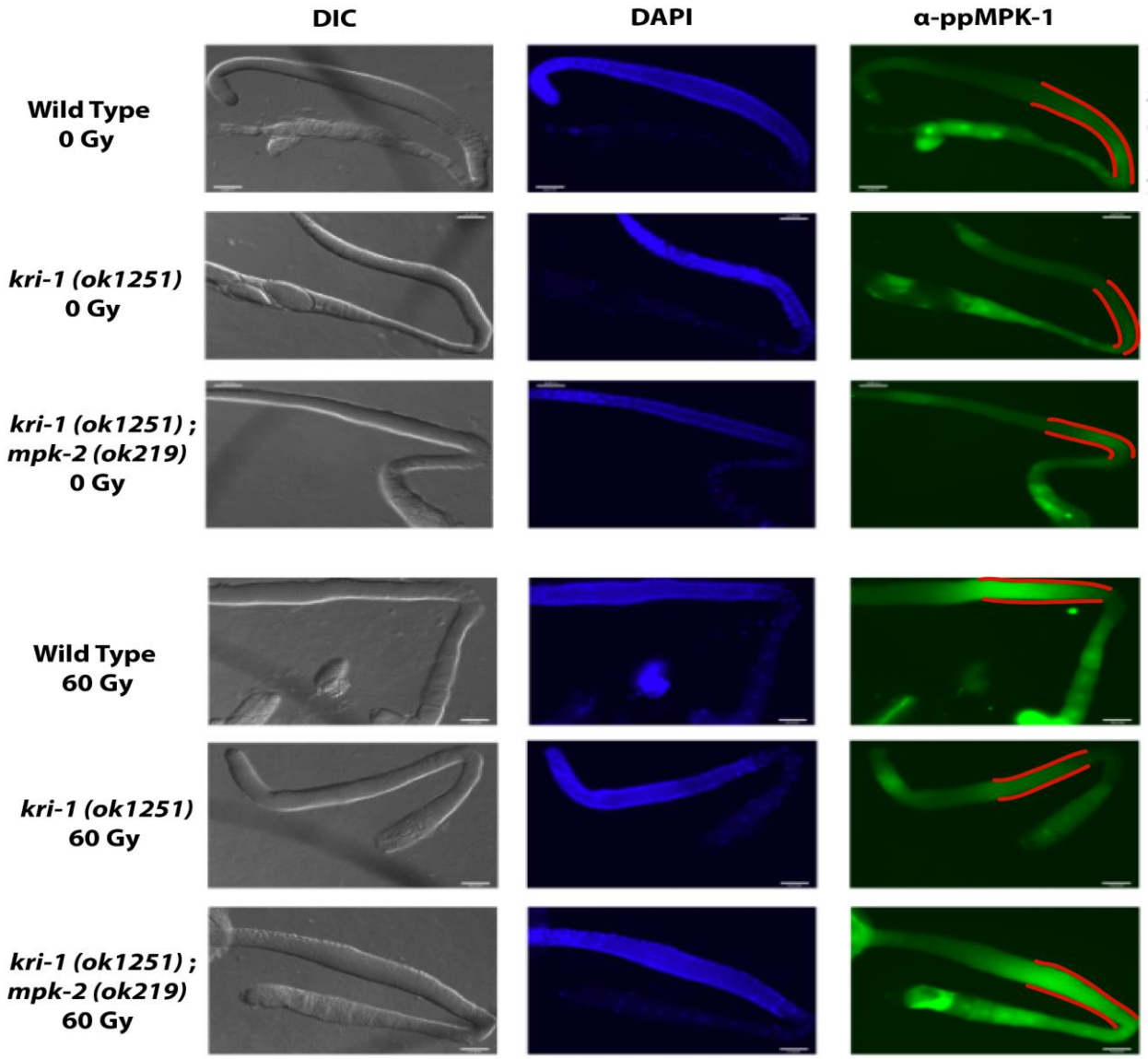

Figure 3.7 KRI-1 promotes MPK-1/ERK1 activation in the germline.
di-phosphorylated MPK-1/ERK1 in germlines of wild type, *kri-1(ok1251)*, and *kri-1(ok1251); mpk-2(ok219)* (see section 3.9) animals in the absence of radiation (0 Gy) and 3 hrs post irradiation (60 Gy). Red lines highlight the pachytene region of the germline where activated MPK-1 is required to promote apoptosis. Images are representative of three independent replicates and at least 30 worms per strain, per condition.

To determine if KRI-1 regulates MPK-1/ERK1 phosphorylation to promote germ cell apoptosis, I increased the levels of activated MPK-1 in *kri-1(ok1251)* mutants by inhibiting two negative regulators of this kinase. Knockdown of *gla-3* by RNA*i* restored IR-induced apoptosis in *kri-1(ok1251)* mutants to similar levels as knocking down *gla-3* in wild type animals (Figure 3.8A). Since GLA-3 negatively regulates MPK-1 in both the soma and germline (Kritikou et al., 2006), I crossed *kri-1(ok1251)* animals with *lip-1(zh15)* mutants that have a deletion in the *lip-1* phosphatase gene that specifically inhibits MPK-1 activation in the germline (Rutkowski et al., 2011). Consistent with my *gla-3* RNA*i* result, *kri-1(ok1251); lip-1(zh15)* double mutants have levels of apoptosis similar to *lip-1(zh15)* single mutant animals (Figure 3.8B). This demonstrates that KRI-1 regulates MPK-1/ERK1 activation to promote IR-induced germ cell death.

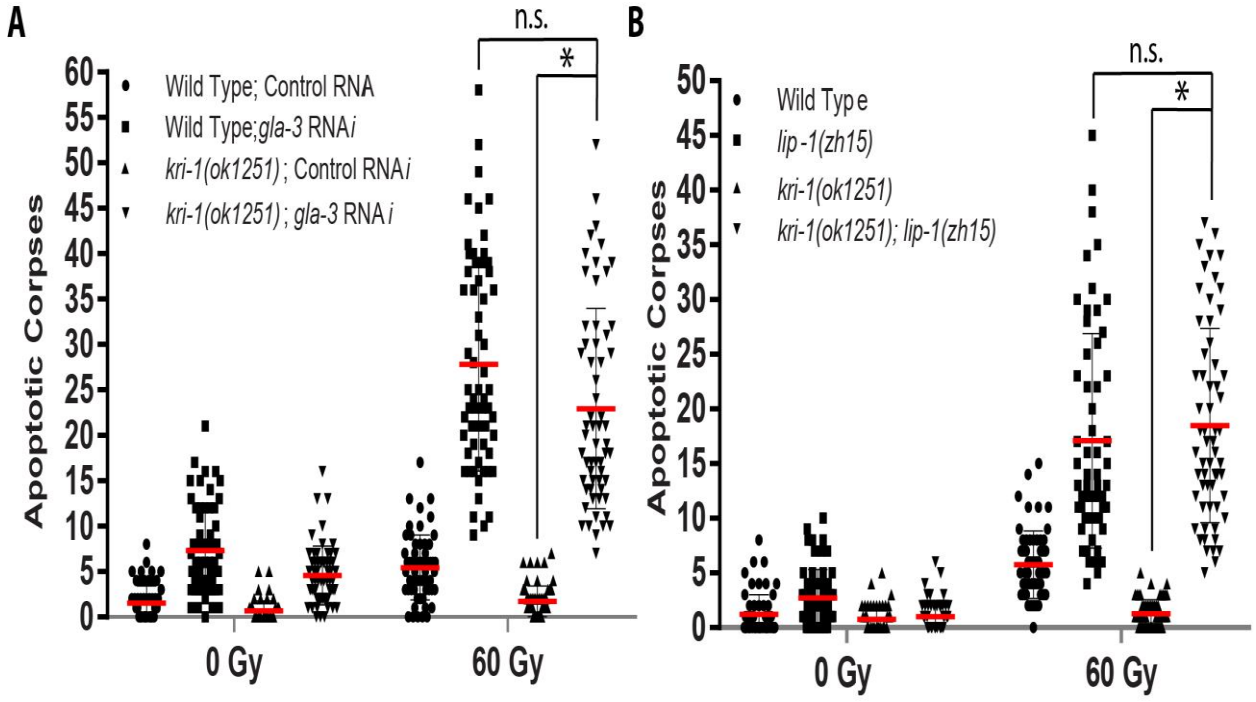

Figure 3.8 MPK-1/ERK1 activation restores IR-induced apoptosis in *kri-1(ok1251)* animals. A) IR-induced germ cell apoptosis quantified after knock-down of *gla-3* in wild type and *kri-1(ok1251)* animals. B) IR-induced germ cell apoptosis quantified in wild type, *lip-1(zh15)*, *kri-1(ok1251)*, and *kri-1(ok1251); lip-1(zh15)* animals. Apoptotic corpses in A-B) were quantified 24 hours post irradiation (60 Gy) or in the absence of radiation (0 Gy). These data represent three independent replicates, and at least 60 worms per strain, per condition. Red line is mean +/- standard deviation. *P<0.05, two-sided, unpaired t-test.

Finally, to determine where KRI-1 intersects the MPK-1/MAPK pathway, I used genetic approaches to up-regulate the levels of activated MPK-1/ERK1 by crossing *kri-1(ok1251)* worms with two different strains harbouring *let-60/RAS* gain-of-function mutations. The first allele, *let-60(ga89)*, increases MPK-1 activity more noticeably in the germline (Eisenmann & Kim, 1997; Lee et al., 2007b), and has enhanced radiation-induced apoptosis (Rutkowski et al., 2011). Interestingly, *kri-1(ok1251); let-60(ga89)* double mutants have increased IR-induced apoptosis compared to *kri-1(ok1251)* animals, but not as pronounced as *let-60(ga89)* single mutants (Figure 3.9A). The second gain-of-function allele, *let-60(n1046)*, has a stronger effect on MPK-1 activation in the vulval precursor cells (Beitel, et al., 1990; Han, et al., 1990; Lee et al., 2007b). While *let-60(n1046)* animals have increased IR-induced apoptosis (Figure 3.9A; Rutkowski et al., 2011), *kri-1(ok1251); let-60(n1046)* double mutants did not have increased apoptosis compared to *kri-1(ok1251)* single mutants (Figure 3.9A). These results suggest that KRI-1 promotes the full activation of MPK-1/ERK1 downstream or independently of LET-60/RAS (Figure 3.9B).

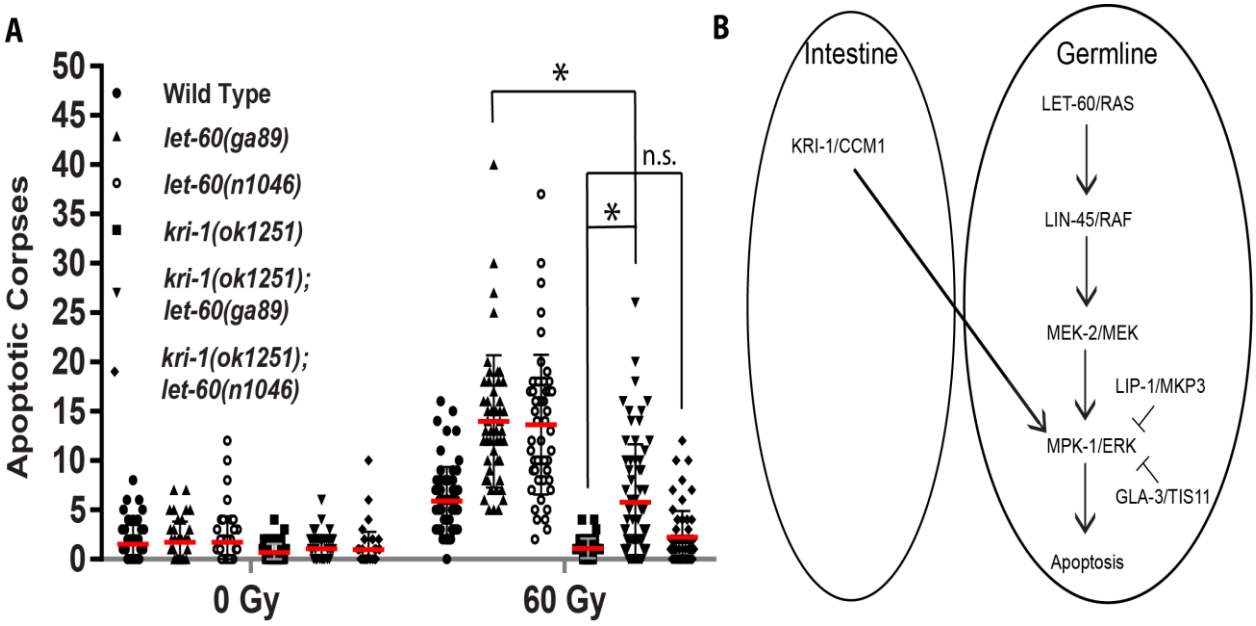

Figure 3.9 KRI-1 regulates MPK-1/ERK1 downstream or independent of LET-60/RAS. IR-induced germ cell apoptosis quantified in wild type, *let-60(ga89)/RAS(gf), let-60(n1046)/RAS(gf), kri-1(ok1251), kri-1(ok1251); let-60(ga89),* and *kri-1(ok1251); let-60(n1046)* animals. Apoptotic corpses were quantified 24 hours post irradiation (60 Gy) or in the absence of radiation (0 Gy). Graph A represent three independent replicates, and at least 60 worms per strain, per condition. Red line is mean +/- standard deviation. *P<0.05, two-sided, unpaired t-test. B) Schematic of how intestinal KRI-1 regulates MPK-1/ERK1 in the germline.

3.6 The MPK-1/ERK1 target EIF-3.D regulates IR-induced apoptosis

Since the mechanism by which MPK-1/ERK1 engages the core apoptosis pathway is unknown, I wanted to determine how this kinase downstream of KRI-1 promotes IR-induced germ cell death. Previously, 30 targets of MPK-1/ERK1 were identified based on their ability to be phosphorylated by mammalian ERK *in vitro*, and enhance or suppress the MPK-1/MAPK pathway in the germline (Arur et al., 2009). While multiple MPK-1-dependent processes were assessed, IR-induced germ cell apoptosis was not (Arur et al., 2009). Therefore, it is possible that some of these candidates might regulate cell death downstream of MPK-1/ERK1. To determine if any of these MPK-1/ERK1 targets are required for IR-induced apoptosis, I conducted an RNA*i* screen using a publicly available RNA*i* library that covers approximately 85% of the *C. elegans* genome (Kamath & Ahringer, 2003). I knocked down 27/30 genes in *kri-1(ok1251); lip-1(zh15)* double mutants that have levels of apoptosis similar to *lip-1(zh15)* single mutants (Figure 3.8B). I chose this strain because I wanted to identify genes that modulate MPK-1-depenedent apoptosis in the absence of KRI-1. Since modulation of many candidate genes causes germline defects (Arur et al., 2009), I began the RNAi treatment at the L4 stage to maintain germline integrity. In a *lip-1(zh15)* background, germ cell apoptosis begins in the pachytene region and continues throughout the proximal germline (Figure 1.3B; Figure 3.11A). Since this expanded zone of apoptosis decreases the efficiency of a cell counting screen, I focused on scoring apoptosis strictly in the pachytene region of *kri-1(ok1251); lip-1(zh15)* animals. In response to 60 Gy IR, an average of four to five apoptotic cells can be observed in the pachytene region in *lip-1(zh15)* and *kri-1(ok1251); lip-1(zh15)* animals (Figure 3.10A) compared to approximately 20 apoptotic corpses throughout the entire germline (Figure 3.8B). Focusing on the pachytene region, I screened for genes that enhance or suppress apoptosis in this region of *kri-1(ok1251); lip-1(zh15)* germlines when knocked down. While no gene knockdown enhanced apoptosis, inhibition of *eif-3.d* (**e**ukaryotic (translation) **i**nitiation **f**actor-3.d), *zim-2* (**z**inc **f**inger in **m**eiosis-2), and *pac-1*(abnormal **PA**R-6 at **c**ontacts-1) significantly suppressed IR-induced apoptosis in *kri-1(ok1251); lip-1(zh15)* animals (Figure 3.10B).

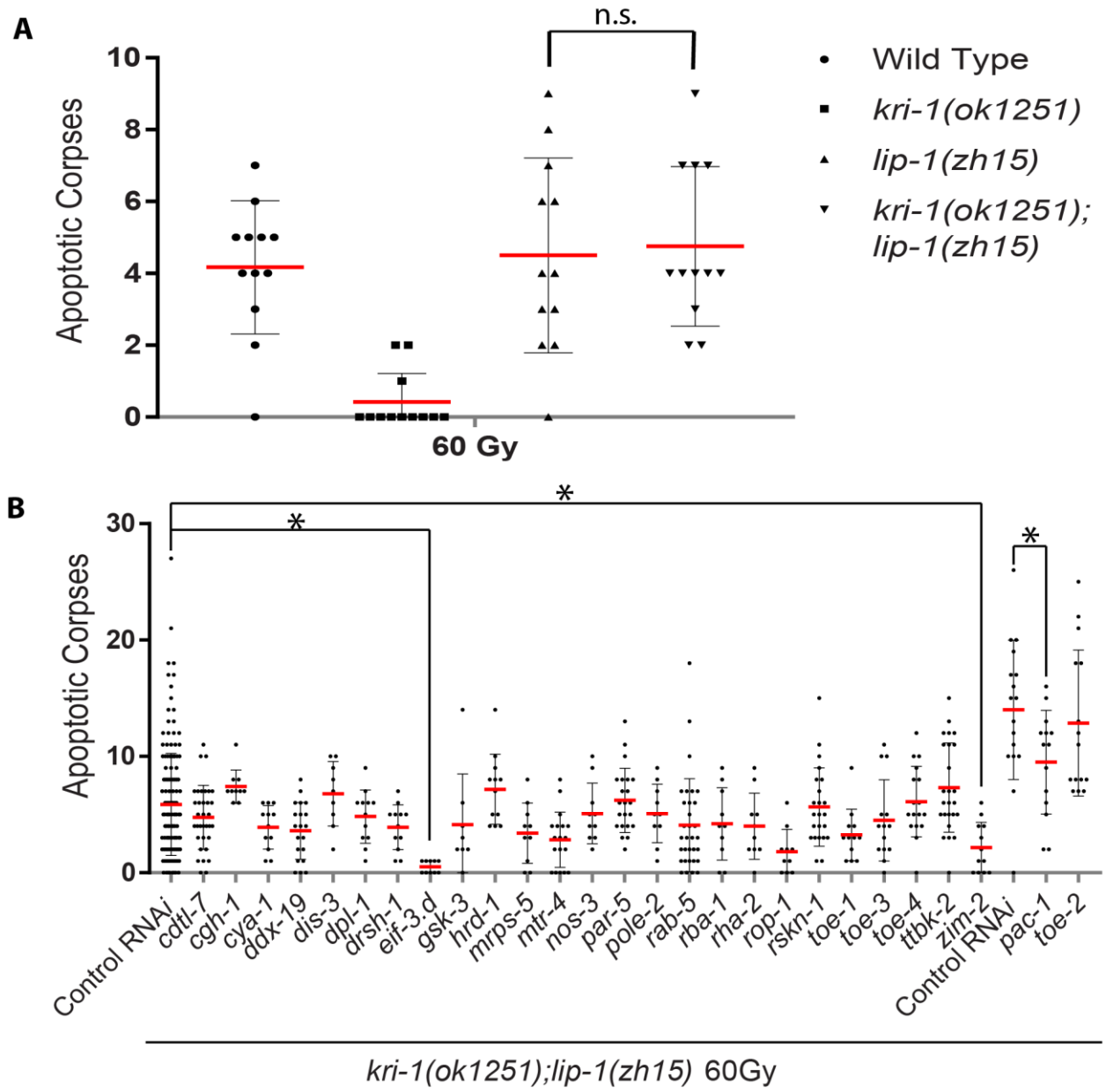

Figure 3.10 Screen of MPK-1/ERK1 germline targets for roles in IR-induced apoptosis. A) IR-induced germ cell apoptosis quantified in the pachytene region of wild type, *kri-1(ok1251)*, *lip-1(zh15)*, and *kri-1(ok1251); lip-1(zh15)* animals. B) IR-induced germ cell apoptosis quantified after knockdown of MPK-1/ERK1 germline targets in the pachytene region of *kri-1(ok1251); lip-1(zh15)* animals. Apoptosis in the *pac-1* and *toe-2* RNA*i* treatment was quantified in the entire germline. Apoptotic corpses in A-B) were quantified 24 hours post irradiation (60 Gy). Graph A represents one experiment, and at least 12 worms per strain, per condition. Graph B) represents at minimum one experiment per gene knockdown, and at least 10 worms per strain, per condition. Red line is mean +/- standard deviation. *P<0.05, two-sided, unpaired t-test. In deviation from the protocol described in the methods section, RNA*i* treatment began at the L4 stage to mitigate germline defects.

Since apoptosis was only quantified in the pachytene region of *kri-1(ok1251); lip-1(zh15)* germlines, I wanted to know if EIF-3.D, ZIM-2, and PAC-1 partially or fully promote apoptosis downstream of MPK-1/ERK1. Since cell death in the proximal germline prevents proper oocyte development (Figure 3.11A), I observed whether knockdown of *eif-3.d*, *zim-2*, or *pac-1* could suppress apoptosis in this region of the germline and restore normal oocyte morphology. Only ablation of *eif-3.d* could suppress the high levels of apoptosis in the proximal region, and restore oocyte development (Figure 3.11A). This is similar to knockdown of *mpk-1/erk1* (Figure 3.11A), confirming that reduction of *eif-3.d* phenocopies loss of *mpk-1*. Additionally, RNA*i* to *eif-3.d* reduces apoptosis in the entire germline of *kri-1(ok1251); lip-1(zh15)* animals, similar to knockdown of *mpk-1* (Figure 3.11B). Therefore the effect of knocking down *eif-3.d* are consistent with acting as a germline target of MPK-1 (Arur et al., 2009) to regulate IR-induced apoptosis.

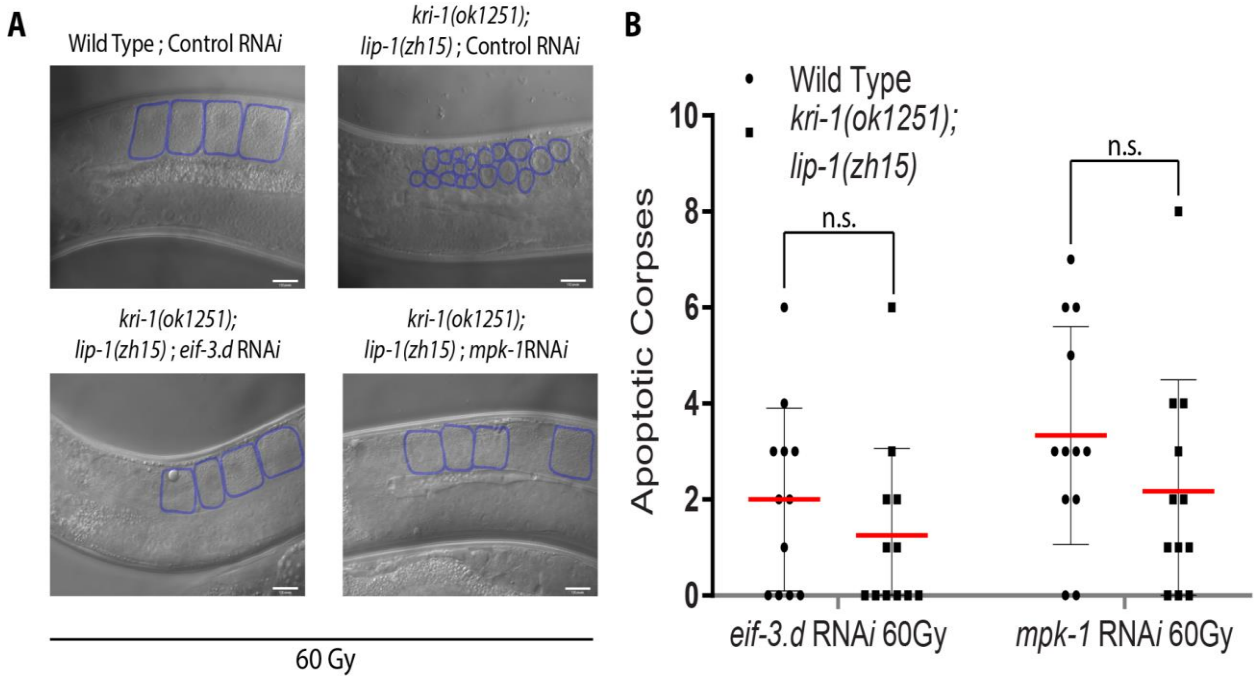

Figure 3.11 EIF-3.D regulates IR-induced germ cell apoptosis.
A) Knockdown of *eif-3.d* or *mpk-1* suppresses IR-induced germ cell apoptosis, and restores proper oocyte morphology in *kri-1(ok1251); lip-1(zh15)* animals. Oocytes are outlined in blue. B) IR-induced germ cell apoptosis quantified throughout the entire germlines of wild type and *kri-1(ok1251); lip-1(zh15)* double mutants after knockdown of *eif-3.d* or *mpk-1*. Apoptotic corpses were quantified 24 hours post irradiation (60 Gy). Graph B represents one experiment, and at least 12 worms per strain, per condition. Red line is mean +/- standard deviation. P >0.05 (n.s.), two-sided, unpaired t-test.

3.7 A forward genetic screen for *kri-1(ok1251)* suppressor mutations

Given that KRI-1 promotes MPK-1/ERK1 activation and germ cell apoptosis, I wondered how KRI-1 signals from the soma to germline. To identify genes that are downstream of *kri-1*, I conducted a forward genetic screen to restore IR-induced apoptosis in *kri-1(ok1251)* mutants using the chemical mutagen ethyl methanesulfonate (EMS), followed by whole genome sequencing (WGS). Since scoring apoptosis in single worms under a compound light microscope is rate-limiting, I took advantage of another *kri-1(ok1251)* mutant phenotype, hypersensitivity to starvation stress, to first select for *kri-1(ok1251)* suppressor candidates that survive prolonged periods of starvation. Since wild type first-stage larvae (L1) can survive more than a week of diapause arrest in liquid buffer (Johnson et al., 1984) while *kri-1(ok1251)* larvae cannot (Figure 3.12A), I reasoned that selecting mutations that restore viability of *kri-1(ok1251)* L1 larvae after a week of diapause might also restore IR-induced apoptosis. From an initial selection screen involving approximately 1,000,000 haploid genomes, I was able to isolate about 300 second generation (F2) candidate suppressors from 20 independent populations that survived this period of diapause arrest (Figure 3.12B; methods). I then established clonal populations from these survivors, and quantified apoptosis post irradiation, or without IR, and found that 13 of these suppressor strains, each from a different population, had a complete restoration of IR-induced apoptosis when compared to wild type animals (Figure 3.12C).

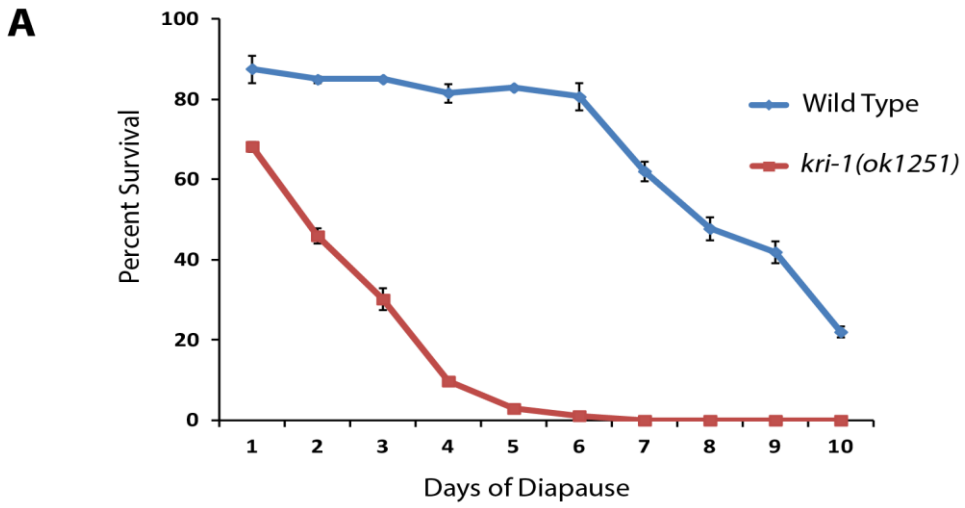

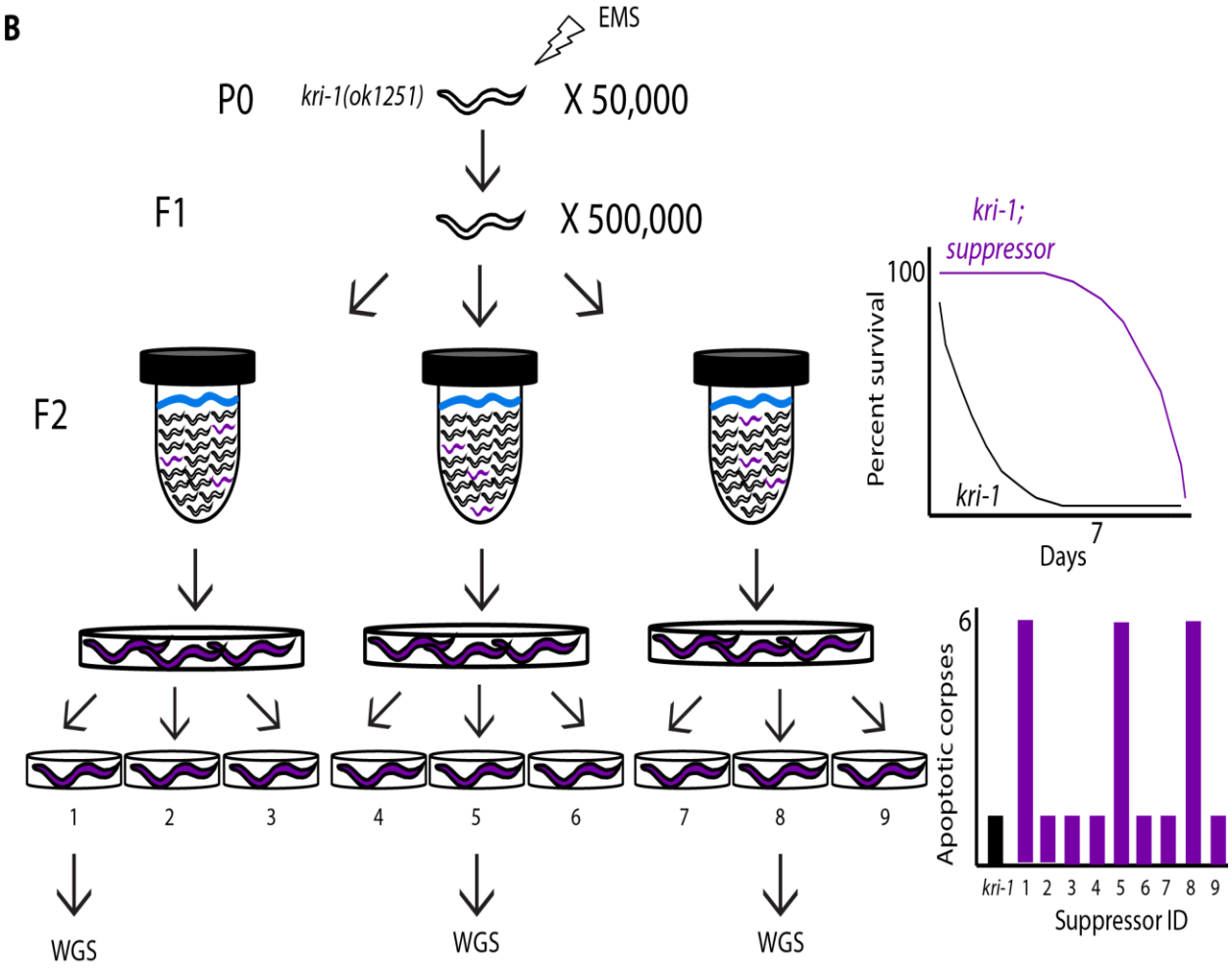
B
EMS
P0
kri-1(ok1251)
X 50,000
F1
X 500,000
F2
kri-1;
suppressor
100
Percent survival
kri-1
7
Days
6
Apoptotic corpses
kri-1 1 2 3 4 5 6 7 8 9
Suppressor ID
1 2 3 4 5 6 7 8 9
WGS
WGS
WGS

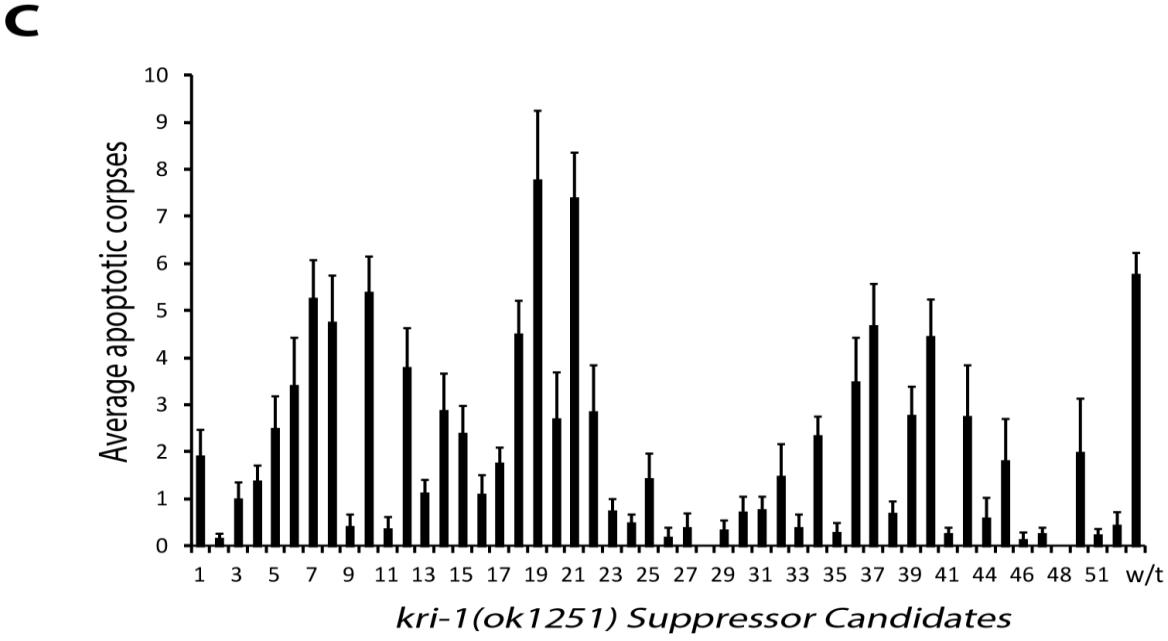
C
Average apoptotic corpses
0 1 2 3 4 5 6 7 8 9 10
1 3 5 7 9 11 13 15 17 19 21 23 25 27 29 31 33 35 37 39 41 44 46 48 51 w/t
kri-1(ok1251) Suppressor Candidates

Figure 3.12 *kri-1(ok1251)* EMS suppressor screen.
A). Survival of wild type and *kri-1(ok1251)* L1 larvae in liquid buffer (M9) without food. Graph represents three technical replicates and 600 worms per strain. B) Schematic of the *kri-1(ok1251)* suppressor screen. C) IR-induced germline apoptosis in the progeny of *kri-1(ok1251)* suppressor candidates that survived 7 days of starvation (52 of 300 candidates depicted). Apoptotic corpses were quantified 24 hours post irradiation (60 Gy) and the graph represents at least 15 worms per strain, per condition. Black bar is mean +/- standard deviation.

To remove background mutations in the thirteen *kri-1(ok1251)* suppressor strains that had wild type levels of apoptosis, I back-crossed each four times to non-mutagenized *kri-1(ok1251)* animals, selecting for progeny that had restored apoptosis and survival during L1 diapause (Figure 3.13). Since many of the *kri-1(ok1251)* suppressor candidates that survived a week of L1 diapause did not have restore apoptosis (Figure 3.12C), the KRI-1 pathway bifurcates to regulate survival during L1 diapause and IR-induced apoptosis. Therefore my selection screen enriches for mutations in genes that function downstream of *kri-1*, before bifurcation occurs.

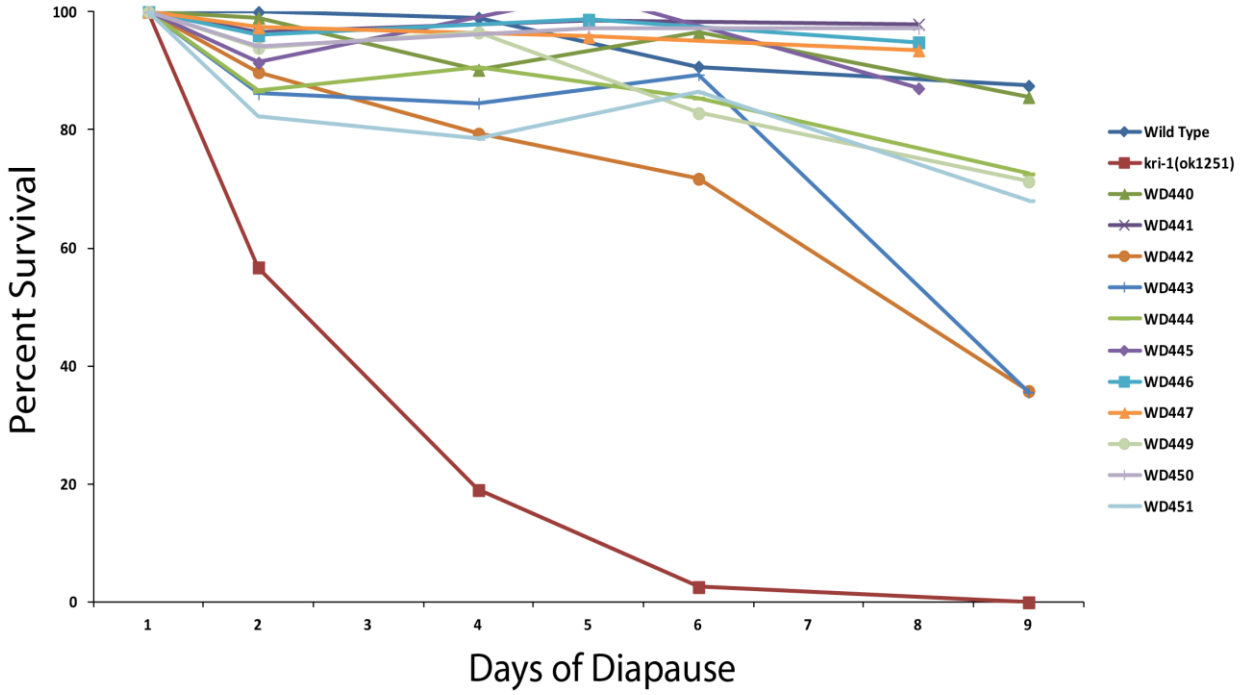

Figure 3.13 *kri-1(ok1251)* suppressor strains have restored survival during starvation.
Survival of wild type, *kri-1(ok1251)*, and 11/13 backcrossed *kri-1(ok1251)* suppressor strain L1 larvae in liquid buffer (M9) without food. Graph represents two technical replicates and 200 worms per strain.

To identify which of the thirteen *kri-1(ok1251)* suppressor strains have dominant and recessive mutations, I crossed each with non-mutagenized *kri-1(ok1251)* animals and quantified apoptosis in the F1 progeny (data not shown). Since the F1 progeny are heterozygous for suppressor mutations, those strains with apoptosis in this generation have dominant mutations, while resistance to cell death reveals recessive mutations. These crosses determined that 12 of the *kri-1(ok1251)* suppressor strains had recessive mutations, while one strain harboured a dominant mutation (Figure 3.14C). I then prepared DNA bar-coded libraries from the 13 suppressor strains and sent these samples for whole genome sequencing (WGS) to identify EMS-induced mutations. Strikingly, the 12 recessive strains had non-synonymous mutations within 3 genes that constitute the ERK5/MAPK pathway (Figure 3.14A-B). In this conserved pathway, the MAP kinase kinase kinase MEKK3 phosphorylates and activates the MAP kinase kinase MEK5 that then phosphorylates and activates the MAP kinase ERK5 (Drew, et al., 2012; Figure 3.14B). Six strains had mutations that result in single amino acid changes in *Y106G6A.1*, which is orthologous to human *MEKK3* (Figure 3.14D). Of these six strains, two had unique point mutations, while four strains contained a third point mutation (Figure 3.14A), all of which result in amino acid changes. Five strains had unique mutations in isoform "a" of the gene *E02D9.1*, which is orthologous to human *MEK5* (Figure 3.14E). Three of these mutations result in amino acid changes, one alters a splice donor site, and one is a single amino acid deletion resulting in a predicted frame-shift (Figure 3.14A). Finally, one strain had a mutation in a splice acceptor site in *mpk-2* (Figure 3.14A), which is orthologous to human *ERK5* (Figure 3.14F).

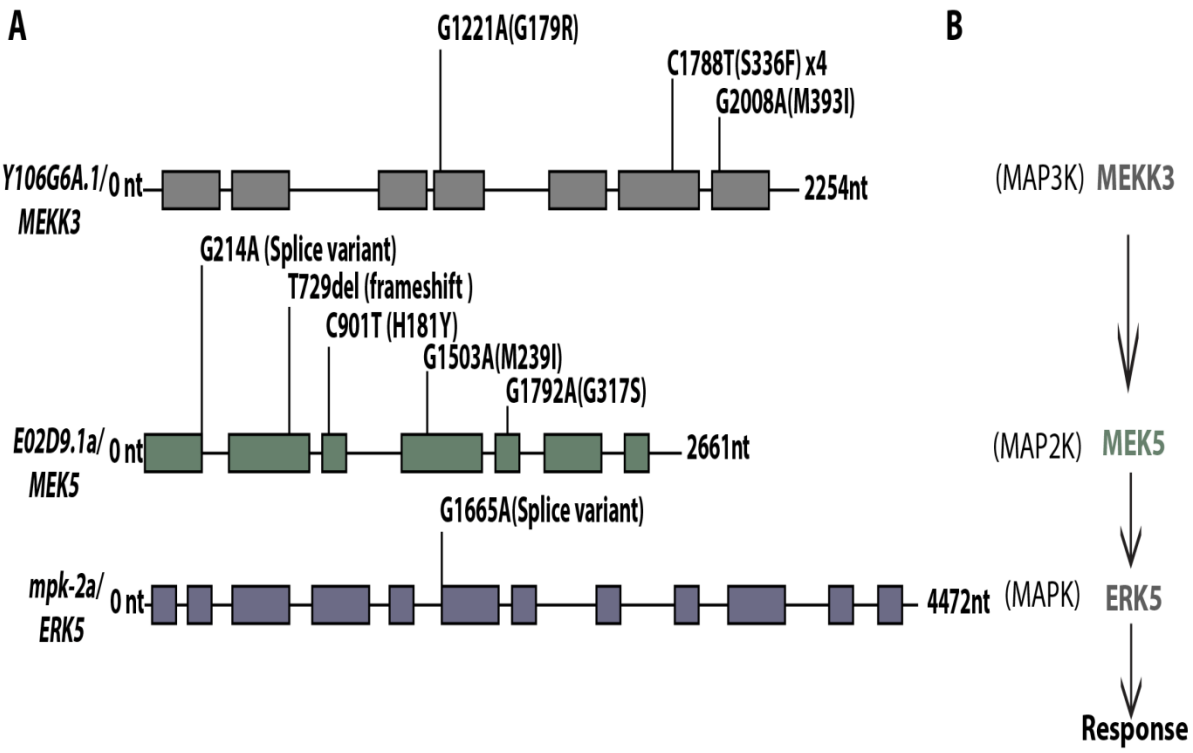

C

Strain Name	Mutated Gene	Human Homologue	Molecular Function	Chromosomal Location	Gene Region	Type of Variation	Type of Mutation
WD444	*Y106G6A.1*	MEKK3	MAP3K	ChrI: 9936362	Exon	Missense	Recessive
WD446	*Y106G6A.1*	MEKK3	MAP3K	ChrI: 9936582	Exon	Missense	Recessive
WD447	*Y106G6A.1*	MEKK3	MAP3K	ChrI: 9936582	Exon	Missense	Recessive
WD448	*Y106G6A.1*	MEKK3	MAP3K	ChrI: 9936582	Exon	Missense	Recessive
WD450	*Y106G6A.1*	MEKK3	MAP3K	ChrI: 9937149	Exon	Missense	Recessive
WD451	*Y106G6A.1*	MEKK3	MAP3K	ChrI: 9936582	Exon	Missense	Recessive
WD439	*E02D9.1*	MEK5	MAP2K	ChrI: 6802927	Exon	Frameshift Deletion	Recessive
WD440	*E02D9.1*	MEK5	MAP2K	ChrI: 6803701	Exon	Missense	Recessive
WD442	*E02D9.1*	MEK5	MAP2K	ChrI: 6802412	Intron	Splicing	Recessive
WD443	*E02D9.1*	MEK5	MAP2K	ChrI: 6803099	Exon	Missense	Recessive
WD449	*E02D9.1*	MEK5	MAP2K	ChrI: 6803990	Exon	Missense	Recessive
WD441	*mpk-2*	ERK5	MAPK	ChrII: 5106085	Intron	Splicing	Recessive
WD445	*klf-3*	Group 2 KLF (KLF1/2/4/5/6/7)	Transcription Factor	ChrII: 6621660	Exon	Missense	Dominant

D

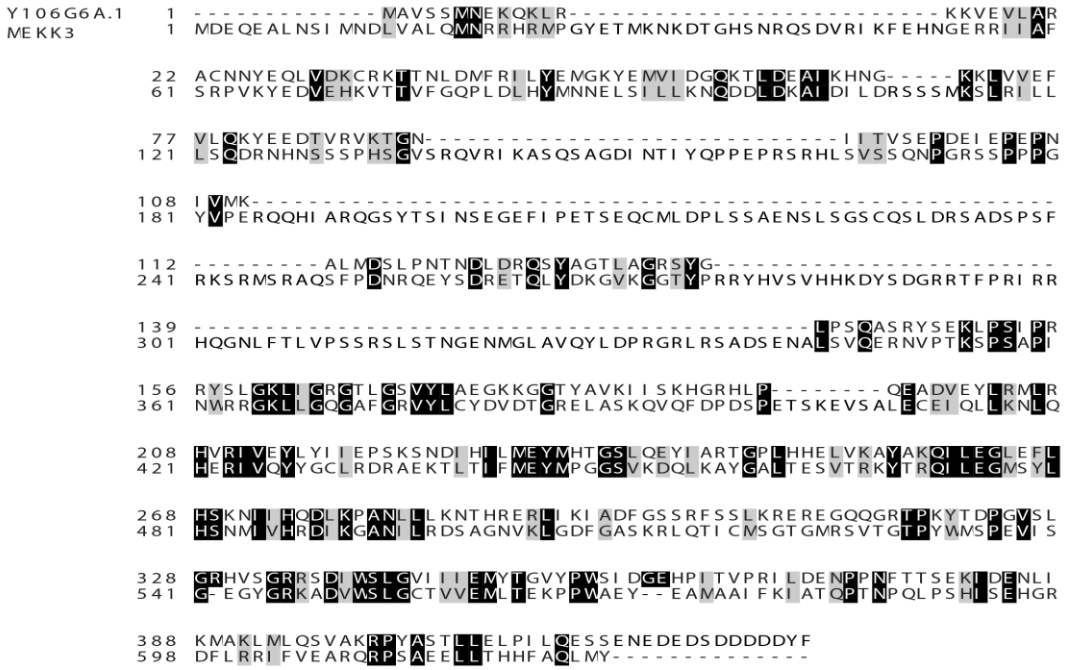

E

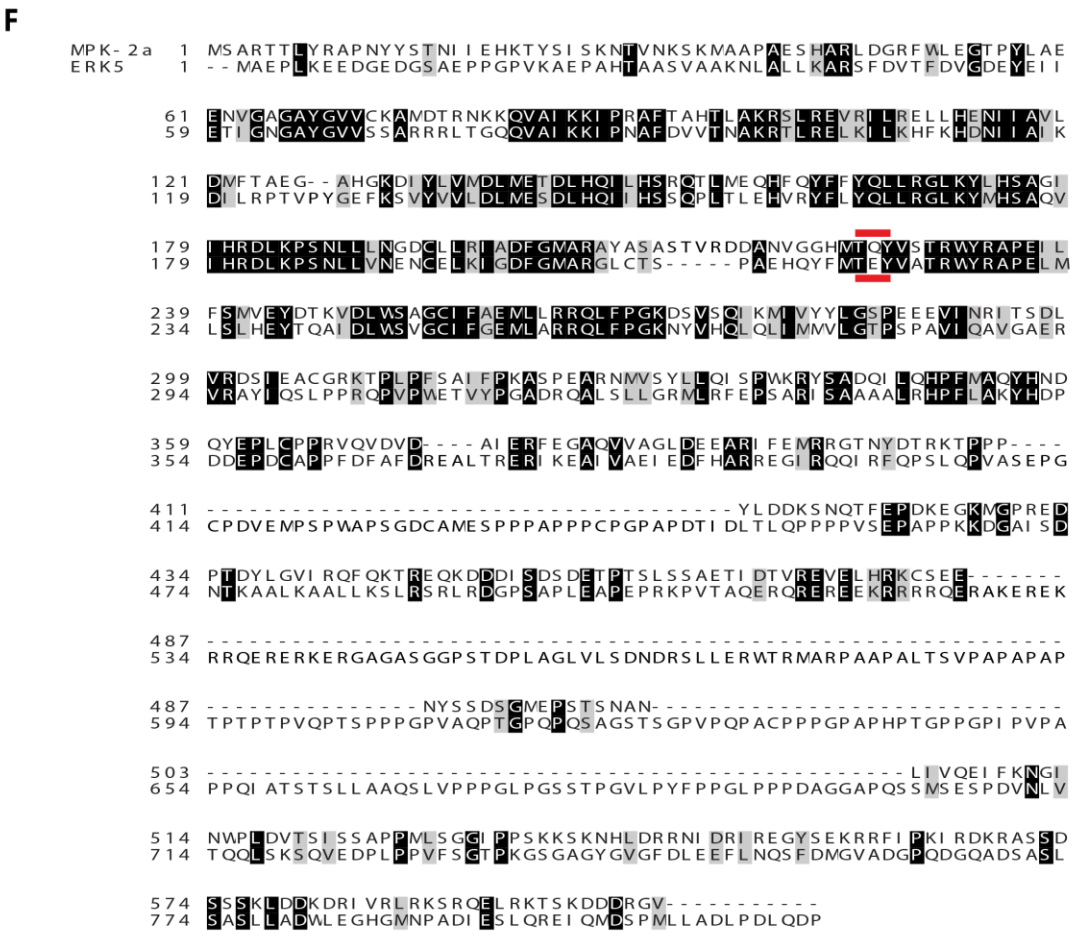

Figure 3.14 *kri-1(ok1251)* EMS suppressor screen identifies the ERK5/MAPK pathway. A) Twelve of the 13 *kri-1(ok1251)* suppressor candidates have recessive mutations in ERK5/MAPK pathway genes. B) The canonical ERK5/MAPK pathway. C) Summary of the *kri-1(ok1251)* suppressor candidates with restored apoptosis. D-F). Alignment of Y106G6A.1, E02D9.1 (isoform a), and MPK-2(isoform a) with human MEKK3 (isoform 1), MEK5 (isoform c), and ERK5 (isoform 1), respectively using ClustalW. Scores are 20.5 (D), 16.9 (E), and 29.6 (F) and represent the number of identities divided by the length of the alignment as a percent. Black background represents identical amino acids, and grey background indicates strong similarity. E) Red line represents conserved MEKK3 phosphorylation site on MEK5 (Ser311, Thr315). F) Red line represents conserved MEK5 phosphorylation site on ERK5 (Thr218, Tyr220).

The single *kri-1(ok1251)* suppressor strain with a dominant mutation (Figure 3.14C) had a non-synonymous nucleotide change in the *klf-3* gene encoding a "Group 2" KLF transcription factor (McConnell & Yang, 2010; Zhang et al., 2009b). Since vertebrate ERK5 is known to regulate Group 2 KLF transcription factors (Sunadome et al., 2011), it is possible that *klf-3* is part of the KRI-1 pathway, downstream of MPK-2/ERK5. The point mutation in *klf-3* results in a glycine to valine substitution in the second C2H2 zinc finger-DNA binding domain of KLF-3 (Figure 3.15A) and is an expected gain-of-function allele, since haploinsufficiency is very rare in *C. elegans* (Hodgkin, 2005). Taken together, the mutations identified by WGS strongly suggest that the ERK5/MAPK pathway, including the KLF-3 target, are functioning downstream of KRI-1 to regulate IR-induced apoptosis (Figure 3.15B).

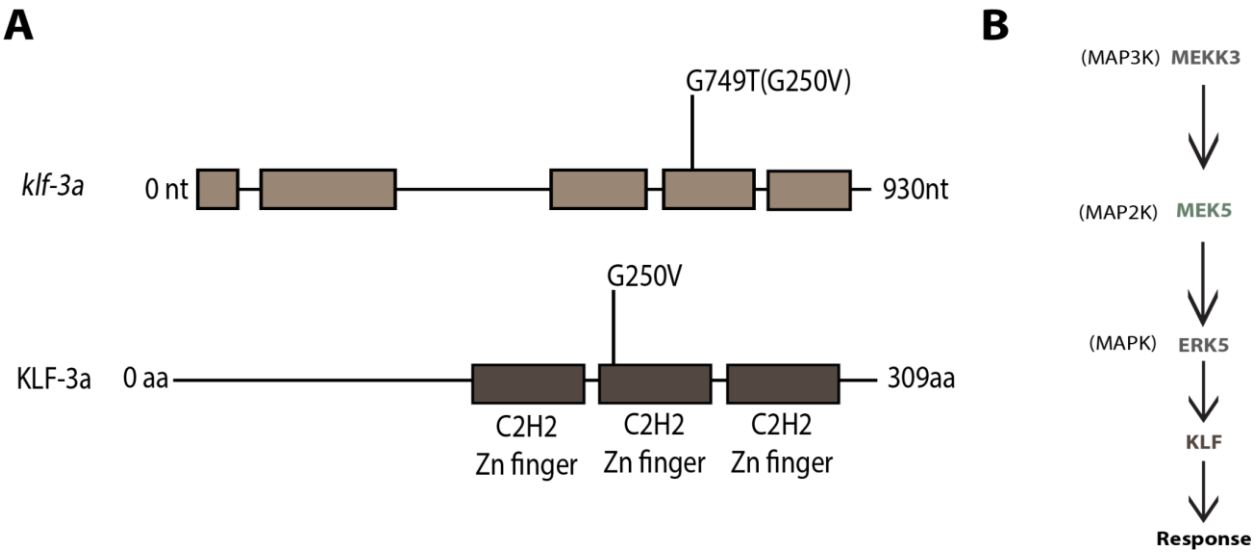

Figure 3.15 *kri-1(ok1251)* EMS suppressor screen identifies KLF-3.
A) The thirteenth *kri-1(ok1251)* suppressor candidate has a dominant mutation in the KLF transcription factor gene *klf-3*, resulting in a glycine to valine substitution in the second C2H2 DNA-binding domain. E) Depiction of the ERK5-KLF pathway.

3.8 The ERK5/MAPK pathway and KLF-3 function downstream of KRI-1

To validate that the predicted loss-of-function mutations in *Y106G6A.1*, *E02D9.1*, and *mpk-2* are indeed causing a restoration of apoptosis in the absence of *kri-1*, I knocked down each of these three genes by RNA*i* in wild type and *kri-1(ok1251)* animals. Knockdown of all three genes fully restored IR-induced apoptosis in *kri-1(ok1251)* mutants, while no further increase was observed in wild type animals (Figure 3.16A). Furthermore, knockdown of these genes did not restore apoptosis in *daf-2(e1370)* mutants (Figure 3.16A), which are also resistant to IR-induced apoptosis (Perrin et al., 2013) by a mechanism that is independent of *kri-1* (Ito et al., 2010). These results suggest that the ERK5/MAPK pathway functions specifically downstream of *kri-1* in the context of IR-induced apoptosis. Since *Y106G6A.1/MEKK3* and *E02D9.1/MEK5* are tightly linked to *kri-1* on the same chromosome, I decided to focus on the terminal MAPK gene, *mpk-2/ERK5* for compound mutant analysis. I took advantage of the previously uncharacterized, *mpk-2(ok219)* deletion allele, and determined by Sanger sequencing that *ok219* removes the 5'UTR and the first three exons of *mpk-2* (Figure 3.16B). Using this predicted null allele, I created a *kri-1(ok1251); mpk-2(ok219)* double mutant strain and found that IR-induced apoptosis was restored to wild type levels (Figure 3.16C). I also validated that the *mpk-2(ok219)* deletion functions in a recessive manner downstream of *kri-1* and fails to complement the *kri-1(ok1251)* suppressor strain with the *mpk-2* mutation (data not shown). Collectively, these results demonstrate that resistance to IR-induced apoptosis in *kri-1(ok1251)* animals is likely due to over-activation of the ERK5/MAPK pathway, and that suppression of this cascade restores sensitivity. Since MEF2 (**m**yocyte **e**nhancer **f**actor 2) transcription factors are targets of mammalian ERK5 (Drew et al., 2012), I wondered if the sole *C. elegans* MEF-2 regulates IR-induced apoptosis downstream of KRI-1 and MPK-2/ERK5. To test this hypothesis, I knocked down *mef-2* by RNA*i* but did not observe a restoration of apoptosis in *kri-1(ok1251)* mutants, or a suppression of apoptosis in wild type and *kri-1(ok1251); mpk-2(ok219)* animals (Figure 3.16D). This suggests that MPK-2/ERK5 regulates apoptosis downstream of KRI-1 through a different target, possibly a KLF transcription factor (Sunadome et al., 2011).

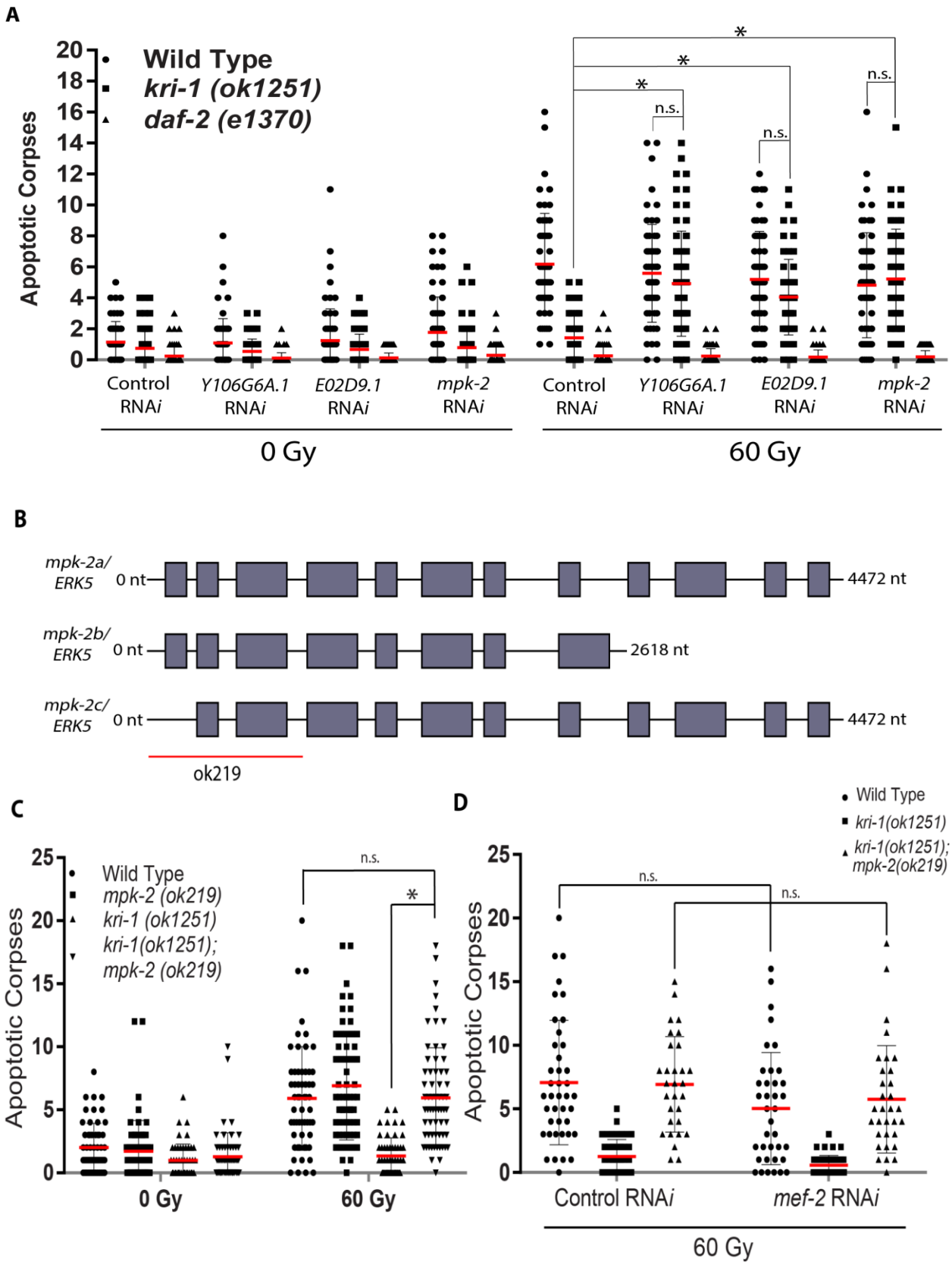

Figure 3.16 The ERK5/MAPK pathway regulates apoptosis downstream of KRI-1.

A) IR-induced germ cell apoptosis quantified after knock-down of the ERK5/MAPK pathway genes in wild type, *kri-1(ok1251)* and *daf-2(e1370)* animals. B) The *mpk-2(ok219)* allele consists of a 985 base pair out-of-frame deletion, removing the 5' UTR and the first three exons of isoform a and b, and the first two exons of isoform c. C) IR-induced germ cell apoptosis quantified in wild type, *mpk-2(ok219)*, *kri-1(ok1251)*, and *kri-1(ok1251); mpk-2(ok219)* animals. D) IR-induced germ cell apoptosis quantified in wild type, *kri-1(ok1251)*, and *kri-1(ok1251); mpk-2(ok219)* animals after knockdown of *mef-2/MEF2*. Apoptotic corpses in (A, C & D) were quantified 24 hours post irradiation (60 Gy) or in the absence of radiation (0 Gy) (A & C). The data sown represent three independent replicates (A & C) or two independent replicates (D). Graph A represents at least 60 worms per strain, per condition, graph B represents at least 50 worms per strain, per condition, and graph C represents at least 30 worms per strain, per condition. Red line is mean +/- standard deviation. *P<0.05, two-sided, unpaired t-test.

To determine if the mutation in *klf-3* was responsible for restoring apoptosis in the dominant *kri-1(ok1251)* suppressor strain, the same *klf-3* point mutation was generated by CRISPR/Cas9 (Paix, et al., 2015). I crossed the resulting *klf-3(on34)* allele into *kri-1(ok1251)* animals and found that the *kri-1(ok1251); klf-3(on34)* double mutants have a full restoration of IR-induced apoptosis (Figure 3.17A). To confirm that the *klf-3(on34)* allele functions in a dominant manner, I crossed *kri-1(ok1251); klf-3(on34)* animals with *kri-1(ok1251)* single mutants and found that the F1 progeny remained sensitive to IR-induced apoptosis (Figure 3.17B). Additionally, I assessed apoptosis in *klf-3(ok1975)* mutants that have an in-frame hypomorphic deletion in *klf-3* (Zhang et al., 2009b), because RNA*i* to *klf-3* is adult lethal (data not shown). Since *klf-3(ok1975)* animals have a minor, yet significant reduction of IR-induced apoptosis (Figure 3.17C), I conclude that the *klf-3(on34)* point mutation is a gain-of-function allele. Since the *C. elegans* genome encodes two other KLFs (*klf-1* and *klf-2*), I wondered if either of these transcription factors are also functioning in the *kri-1* pathway to regulate IR-induced apoptosis. Knockdown of these genes did not restore IR-induced apoptosis in *kri-1(ok1251)* mutants, nor was apoptosis suppressed in wild type or *kri-1(ok1251); mpk-2(ok219)* animals (Figure 3.17D). Additionally, *klf-1* RNA*i* is synthetic lethal with *kri-1(ok1251)* but not wild type L1 larvae (data not shown) and makes *kri-1(ok1251)* adults very sick when beginning knockdown from the L4 stage suggesting parallel pathways. These results indicate that while *klf-3* functions downstream of *kri-1* to regulate apoptosis, *klf-1* and *klf-2* do not.

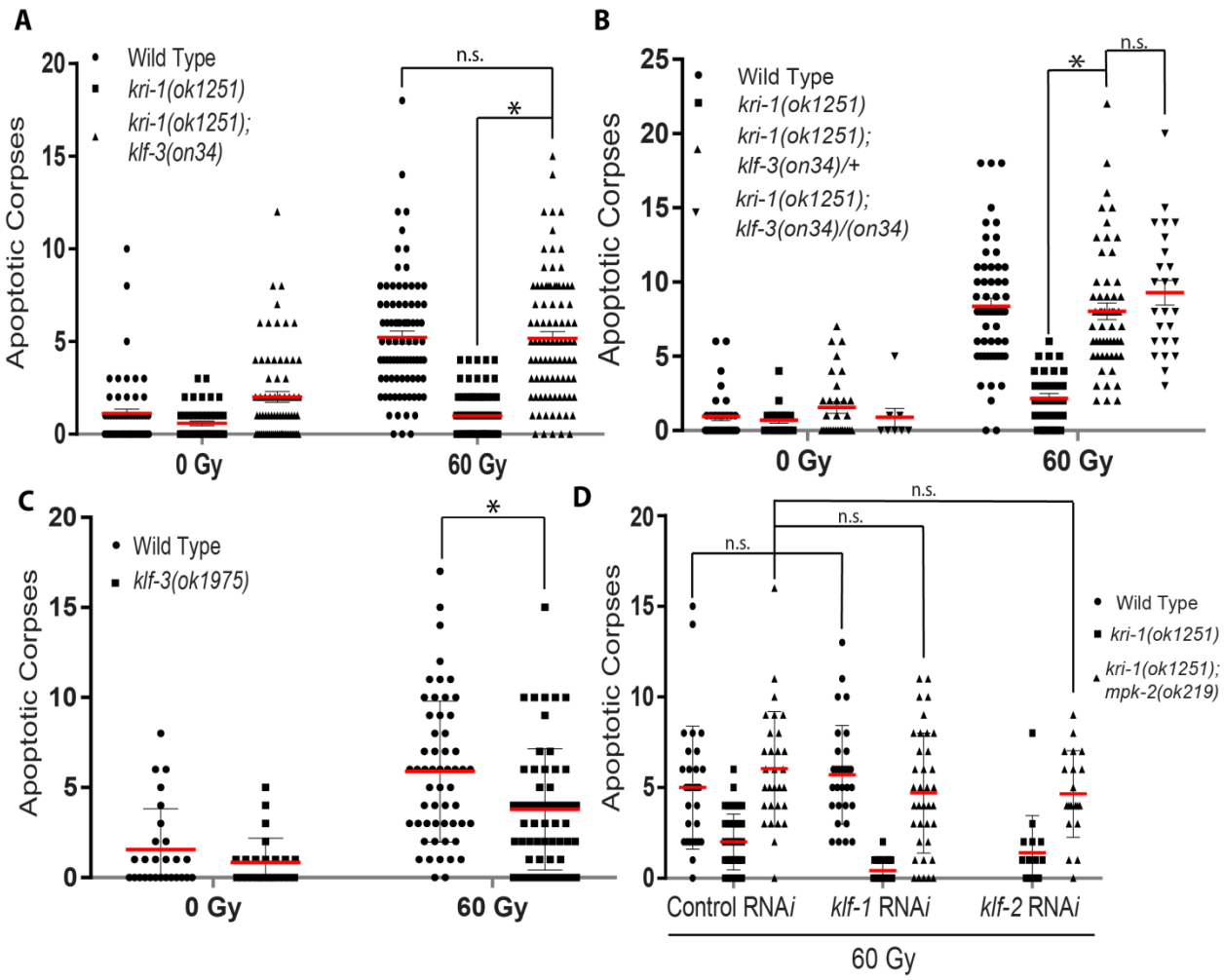

Figure 3.17 KLF-3 regulates apoptosis downstream of KRI-1

A) IR-induced germ cell apoptosis quantified in wild type, *kri-1(ok1251)*, and *kri-1(ok1251); klf-3(on34)* animals. B) IR-induced germ cell apoptosis quantified in wild type, *kri-1(ok1251)*, *kri-1(ok1251); klf-3(on34)/+* and *kri-1(ok1251); klf-3(on34)* animals. C) IR-induced germ cell apoptosis quantified in wild type and *klf-3 (ok1975)* animals. D) IR-induced germ cell apoptosis quantified in wild type, *kri-1(ok1251)*, and *kri-1(ok1251); mpk-2(ok219)* animals after knockdown of *klf-1*, and *kri-1(ok1251)* and *kri-1(ok1251); mpk-2(ok219)* animals after knockdown of *klf*-2. Apoptotic corpses in A- D were quantified 24 hours post irradiation (60 Gy) or in the absence of radiation (0 Gy) (A-C), represent three independent replicates (A & B), and four independent replicates (C). The *klf-1* RNA*i* treatment in D) represents two independent replicates. The *klf-1* RNA*i* treatment was started at the L4 stage, in deviation from the methods described in chapter 2, due to *kri-1(ok1251)* L1 larval lethality. The *klf-2* RNA*i* treatment in D) represents one experiment. Graph A represents at least 45 worms per strain, per condition. Graph B represents at least 55 worms in the 60Gy condition and 30 worms in the 0Gy condition. Graph C represents at least 55 worms per strain in the 60Gy treatment and at least 25 worms per strain in the 0Gy treatment. Graph D represents at least 30 worms per strain in the *klf-1* RNA*i* treatment and at least 15 worms per strain in the *klf-2* RNA*i* treatment. Red line is mean +/- standard deviation. *P<0.05, two-sided, unpaired t-test.

3.9 MPK-2/ERK5 regulates germline MPK-1/ERK1 and apoptosis from the intestine

To determine if *mpk-2/erk5* is expressed in the same tissue as *kri-1*, I created a transcriptional reporter consisting of about 6 kb of the region upstream of the *mpk-2* start codon, fused to *gfp*, and injected this construct into wild type worms to form extrachromosomal- "Ex-" arrays (Stinchcomb, et al., 1985). Three array-containing lines express GFP in the intestine throughout development (Figure 3.18A) similar to animals expressing KRI-1::GFP (Berman & Kenyon, 2006). Since my genetic analysis predicts that MPK-2/ERK5 is over-activated in *kri-1(ok1251)* mutants, I over-expressed *mpk-2* in wild type animals to assess whether this would confer resistance to IR-induced apoptosis. I expressed three independent Ex-array containing lines with *mpk-2* under the control of the 6 kb upstream element and observed a strong suppression of IR-induced apoptosis compared to siblings that had lost the arrays (Figure 3.18B). Since Ex-arrays are silenced in the germline (Kelly, et al., 1997), this suggests that MPK-2/ERK5 functions in the soma to inhibit germline apoptosis. To determine whether over-expression of *mpk-2* specifically in the intestine can confer resistance to IR-induced apoptosis, I expressed *mpk-2* under the control of the 5 kb *elt-2* intestinal-specific promoter from three independent Ex-arrays in wild type worms. These strains also had a reduction of IR-induced apoptosis compared to siblings that had lost the array (Figure 3.18C), confirming that MPK-2/ERK5 regulates germline apoptosis from the intestine. However, the level of suppression was not as pronounced as over-expressing *mpk-2* from its own promoter. This indicates that either the *elt-2* promoter drives weaker expression of *mpk*-2, or that MPK-2/ERK5 also functions from additional tissues. Since I was not able to establish *kri-1(ok2151); mpk-2(ok219)* animals that express these arrays, it is likely that over-expressing MPK-2/ERK5 in the absence of KRI-1 is lethal.

Given that ablation of the ERK5/MAPK pathway completely restores IR-induced apoptosis downstream of *kri-1*, I wondered whether this coincides with increased MPK-1/ERK1 activation in the germline. To test this, I immunostained germlines isolated from *kri-1(ok1251); mpk-2 (ok219)* double mutants, which had restored levels of activated MPK-1/ERK1 compared to *kri-1(ok1251)* mutants (Figure 3.7). I conclude that KRI-1 functions to subdue MPK-2/ERK5 signalling in the intestine, to facilitate the activation of germline MPK-1/ERK1 and apoptosis in response to IR.

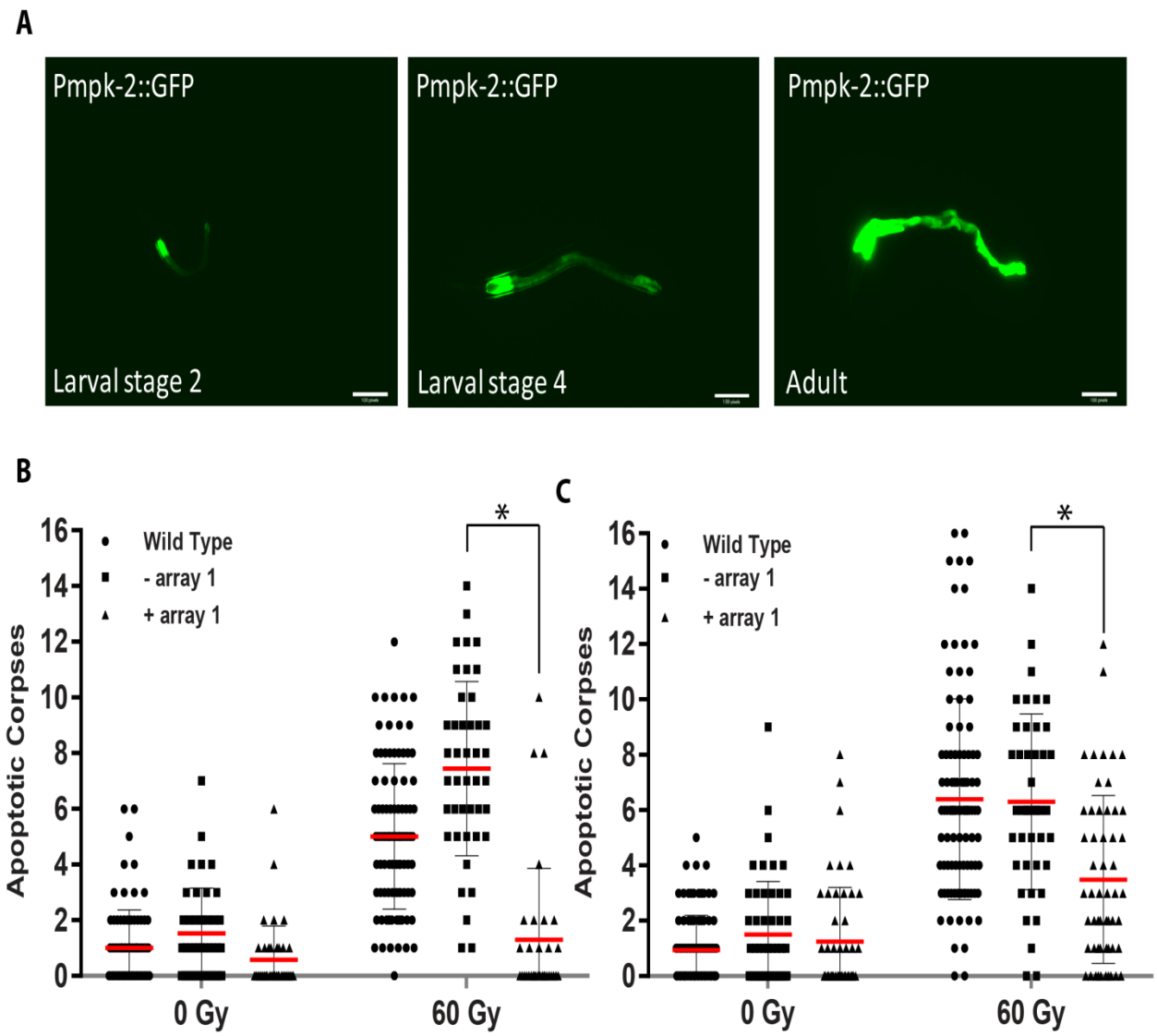

Figure 3.18 MPK-2/ERK5 regulates apoptosis from the intestine

A) Expression of *gfp* under the control of a 6 kb *mpk-2* upstream element throughout development. Images are representative of three independent lines. B) IR-induced germ cell apoptosis quantified in wild type, and *Pmpk-2::mpk-2/erk5* expressed in wild type animals (+ array) or siblings that have lost the transgene (-array). C) IR-induced germ cell apoptosis quantified in wild type, and *Pelt-2::mpk-2/erk5* expressed in wild type animals (+ array) or siblings that have lost the transgene (-array). Apoptotic corpses in B & C were quantified 24 hours post irradiation (60 Gy) or in the absence of radiation (0 Gy), and represent three independent replicates. Graphs B & C depict one of three representative array-containing lines, and at least 30 worms per strain, per condition. Red line is mean +/- standard deviation. *P<0.05, two-sided, unpaired t-test.

3.10 KRI-1 binding partners promote IR-induced apoptosis

To determine how the KRI-1 scaffold protein regulates the ERK5/MAPK pathway, I identified protein interactors by **A**ffinity **P**urification-**M**ass **S**pectrometry (AP-MS). I took advantage of a previously constructed KRI-1::GFP expressing strain (Berman & Kenyon, 2006) that restores IR-induced apoptosis in *kri-1(ok1251)* mutants (Ito et al., 2010). For controls, I used a strain that expresses actin (ACT-5) fused to GFP in the intestine (Zhang et al., 2012) and wild type worms that do not express GFP. Beads with anti-GFP antibodies were used to immunoprecipitate KRI-1::GFP fusion proteins from whole worm lysate from irradiated and non-irradiated samples. Only four proteins were identified to significantly interact with KRI-1::GFP regardless of irradiation status (Y45F10D.10, K07A9.3, F37C4.5 and HIP-1), while HSP-17 was found to interact with KRI-1::GFP post irradiation (Figure 3.19A; Table 7.2). F37C4.5 is an uncharacterized protein with no homologues outside of nematodes, while HIP-1 (**H**sp-70 **i**nteracting **p**rotein homolog-1) and HSP-17 (**h**eat **s**hock **p**rotein-17) are heat shock proteins that were also identified in control samples (last column of Table 7.2). Y45F10D.10 aligns to the mammalian KRIT1/CCM1 binding partner, ICAP1 (Zhang, et al., 2001) (Figure 3.19C), and K07A9.3 has sequence similarity with the N-terminal PTB domain and C-terminal **H**armonin **H**omology **D**omain (HHD) of human CCM2 (Figure 3.19B). These domains in human CCM2 are required to bind KRIT-1/CCM1 (Zawistowski et al., 2005) and MEKK3 (Fisher, et al., 2015b), respectively. Therefore, I propose that K07A9.3 is the *C. elegans* orthologue of mammalian CCM2. This was exciting because a *C. elegans* CCM2 orthologue could not previously be identified using standard sequence homology-based searches. Subsequent to my identification of the ERK5/MAPK pathway in the *kri-1(ok1251)* suppressor screen, KRIT1/CCM1 in vertebrates was shown to regulate the ERK5/MAPK pathway through its interaction with CCM2 (Zhou et al., 2015, 2016b), which directly binds and inhibits MEKK3 (Fisher, et al., 2015a). Therefore, I hypothesize that the KRI-1-K07A9.3/CCM2 complex inhibits the ERK5 pathway through Y106G6A.1/MEKK3, similar to vertebrates.

A

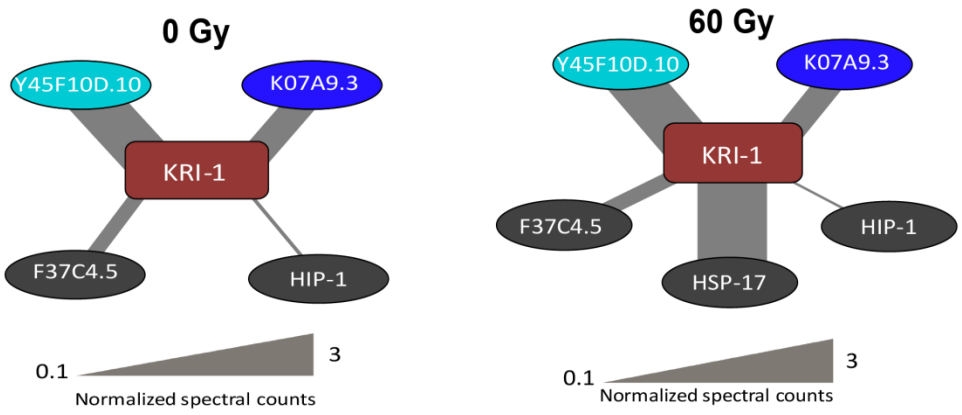
0 Gy
Y45F10D.10
K07A9.3
KRI-1
F37C4.5
HIP-1
0.1
3
Normalized spectral counts
60 Gy
Y45F10D.10
K07A9.3
KRI-1
F37C4.5
HIP-1
HSP-17
0.1
3
Normalized spectral counts

B

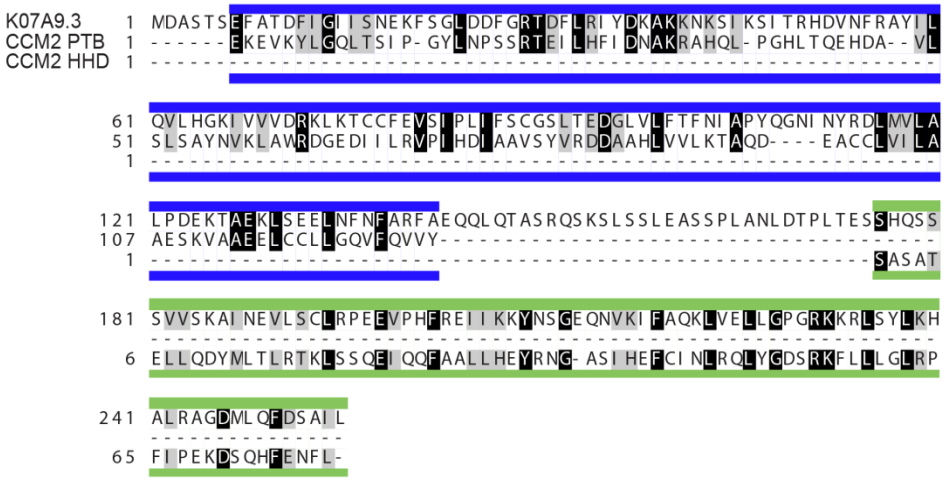
K07A9.3 1 MDASTSEFATDFIGIISNEKFSGLDDFGRTDFLRIYDKAKKNKSIKSITRHDVNFRAYIL
CCM2 PTB 1 ------EKEVKYLGQLTSIP-GYLNPSSRTEILHFIDNAKRAHQL-PGHLTQEHDA--VL
CCM2 HHD 1 ----------
61 QVLHGKIVVVDRKLKTCCFEVSIPLIFSCGSLTEDGLVLFTFNIAPYQGNINYRDLMVLA
51 SLSAYNVKLAWRDGEDIILRVPIHDIAAVSYVRDDAAHLVVLKTAQD----EACCLVILA
1 ----------
121 LPDEKTAEKLSEELNFNFARFAEQQLQTASRQSKSLSSLEASSPLANLDTPLTESSHQSS
107 AESKVAAEELCCLLGQVFQVVY----------
1 ----------SASAT
181 SVVSKAINEVLSCLRPEEVPHFREIIKKYNSGEQNVKIFAQKLVELLGPGRKKRLSYLKH
----
6 ELLQDYMLTLRTKLSSQEIQQFAALLHEYRNG-ASIHEFCINLRQLYGDSRKFLLLGLRP
241 ALRAGDMLQFDSAIL
----
65 FIPEKDSQHFENFL-

C

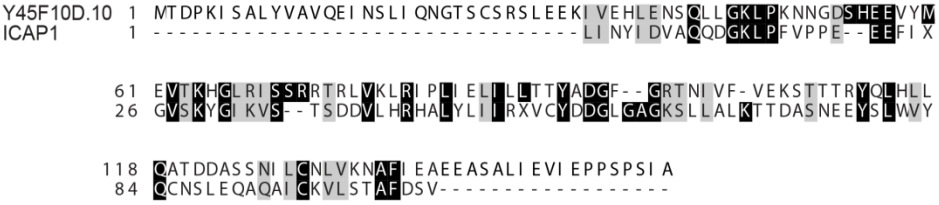
Y45F10D.10 1 MTDPKISALYVAVQEINSLIQNGTSCSRSLEEKIVEHLENSQLLGKLPKNNGDSHEEVYM
ICAP1 1 ----------LINYIDVAQQDGKLPFVPPE--EEFIX
61 EVTKHGLRISSRRTRLVKLRIPLIELLLTTYADGF--GRTNIVF-VEKSTTTRYQLHLL
26 GVSKYGIKVS--TSDDVLHRHALYLIIRXVCYDDGLGAGKSLLALKTTDASNEEYSLWY
118 CATDDASSNILCNLVKNAFIEAEEASALIEVIEPPSPSIA
84 CCNSLEQAQAICKVLSTAFDSV----------

D

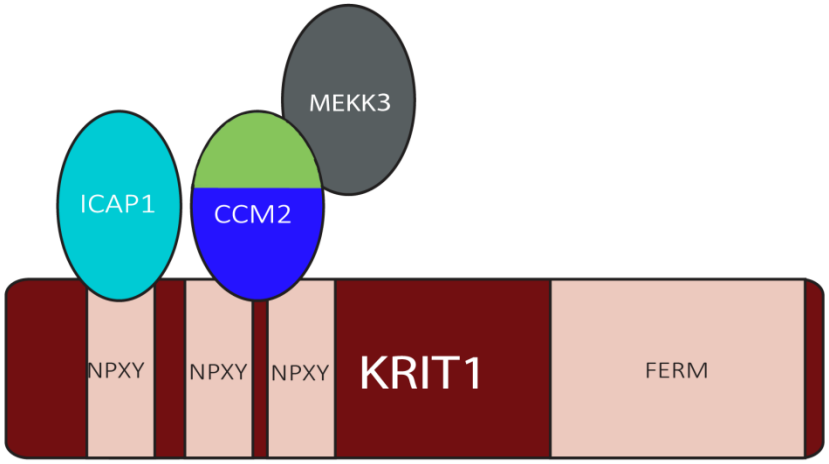
MEKK3
ICAP1
CCM2
NPXY
NPXY
NPXY
KRIT1
FERM

Figure 3.19 KRI-1 interacts with K07A9.3/CCM2 and Y45F10D.10/ICAP1.
A) KRI-1 interacting partners identified by AP-MS from non-irradiated (0 Gy) and irradiated (60 Gy) animals. Line thickness represents the average normalized spectral counts from three independent replicates (Table 7.2; Table 7.3). B) Alignment of K07A9.3 with the human CCM2 (N-terminal PTB domain underlined in blue and the C-terminal Harmonin Homology domain underlined in green). C) Alignment of Y45F10D.10 and human ICAP1. B-C) ClustalW was used for alignments. Scores are 13.3 (B), and 17.2 (C) and represent the number of identities divided by the length of the alignment as a percent. Black background represents identical amino acids, and grey background indicates strong similarity. D) Schematic of how ICAP1 and CCM2 interact with the NPxY/F motifs in mammalian KRIT1, and how MEKK3 interacts with CCM2.

To determine if any of the KRI-1 binding partners are required for apoptosis, I knocked down each gene by RNA*i* in wild type and *kri-1(ok1251)* animals. I excluded the weak binding partner HIP-1 and also HSP-17, which appears in control samples (Final column, Table 7.2) and might simply be responding to radiation stress. Knockdown of either *K07A9.3/CCM2* or *Y45F10D.10/ICAP1* suppressed IR-induced germ cell apoptosis in wild type animals, but *F37C4.5* did not (Figure 3.20A). Furthermore, knockdown of these three genes had no effect on apoptosis in *kri-1(ok1251)* mutants. Based on these results, I propose that Y45F10D.10/ICAP1 and K07A9.3/CCM2 function in a complex with KRI-1 to promote IR-induced apoptosis. Since CCM2 and ICAP1 bind separate NPxY/F motifs in mammalian KRIT1/CCM1 (Zawistowski et al., 2005) (Figure 3.19D), it is likely that these three proteins form a conserved complex in *C. elegans*. To confirm that the KRI-1-K07A9.3/CCM2-Y45F10D.10/ICAP1 complex is functioning in the intestine to regulate IR-induced apoptosis, I knocked down *kri-1*, *K07A9.3*, and *Y45F10D.10* in *sid-1(qt9)* animals (Figure 3.19C) that are only sensitive to RNA*i* in the intestine (Dowen et al., 2016). Since suppression of IR-induced apoptosis was similar to knocking down these genes in wild type animals (Figure 3.19A), the KRI-1/K07A9.3/CCM2-Y45F10D.10/ICAP1 complex functions in the intestine to promote apoptosis. Since ICAP1 inhibits β-integrin (Zhang et al., 2001) it is also possible that KRI-1 regulates integrin signalling to promote apoptosis, in conjunction with K07A9.3/CCM2 and the ERK5/MAPK pathway.

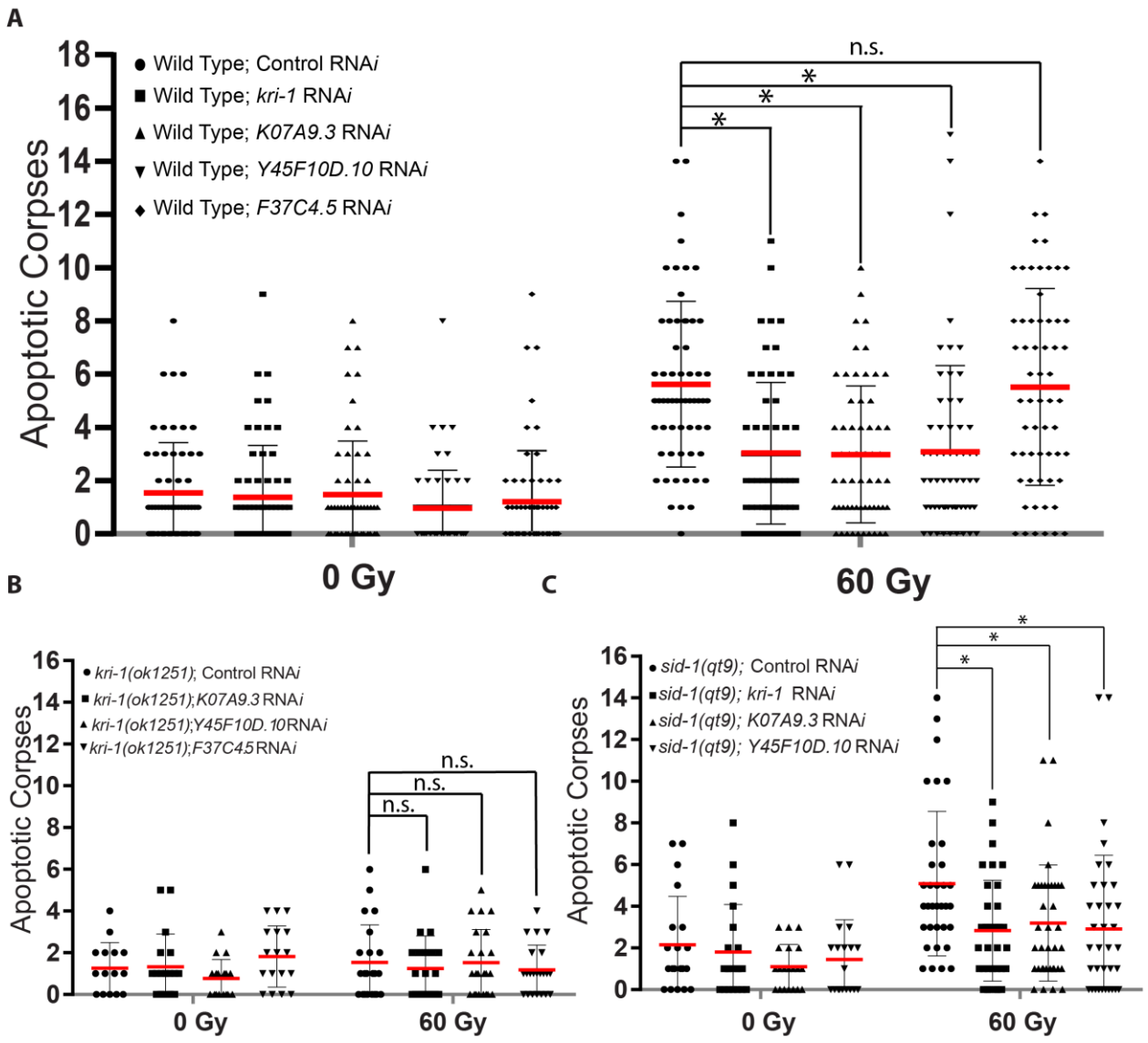

Figure 3.20 K07A9.3/CCM2 and Y45F10D.10/ICAP1 promote apoptosis.
A) IR-induced germ cell apoptosis quantified in wild type animals treated with double stranded RNA (RNA*i*) targeting a non-expressed gene (control), *kri-1*, *K07A9.3*, *Y45F10D.10*, and *F37C4.5*. B) IR-induced germ cell apoptosis quantified in *kri-1(ok1251)* mutants treated with double stranded RNA targeting a non-expressed gene (control), *K07A9.3*, *Y45F10D.10*, and *F37C4.5*. C) IR-induced germline apoptosis quantified in *sid-1(qt9)* mutants treated with double stranded RNA targeting a non-expressed gene (control), *K07A9.3*, and *Y45F10D.10*. Apoptotic corpses in A- C were quantified 24 hours post irradiation (60 Gy) or in the absence of radiation (0 Gy), and represent three independent replicates (A), one experiment (B), and two independent replicates (C). Graph A represents at least 60 worms per strain, per condition. Graph B represents at least 20 worms in the 60 Gy condition and 15 worms in the 0 Gy condition. Graph C represents at least 35 worms per strain in the 60 Gy treatment and at least 20 worms per strain in the 0 Gy treatment. Red line is mean +/- standard deviation. *P<0.05, two-sided, unpaired t-test.

4 Results 2: The KRI-1-MPK-2/ERK5-KLF-3 Cascade Regulates Zinc Localization to Permit Germline MPK-1/MAPK Activation and Radiation-Induced Apoptosis

4.1 Data attribution

I'm very grateful and would like to thank Michael Schertzberg for aligning the mRNA sequencing reads to a reference genome in section 4.2, and Yota Ohashi for assisting with the RNA*i* screen (section 4.3), survival assays (section 4.3), and cloning P*zipt-2.3::zipt-2.3::gfp* in section 4.4.

4.2 RNA sequencing reveals genes regulated by MPK-2/ERK5 downstream of KRI-1

To assess whether MPK-2/ERK5 regulates IR-induced apoptosis through a transcriptional process, I performed mRNA sequencing to determine if any transcripts are altered in *kri-1(ok1251)* mutants and return to wild type levels in *kri-1(ok1251); mpk-2(ok219)* animals. Identifying such transcripts would also provide mechanistic insight into how MPK-2/ERK5 is signalling to the germline. I treated wild type, *mpk-2(ok219)*, *kri-1(ok1251),* and *kri-1(ok1251); mpk-2(ok219)* animals with 60 Gy of IR and identified 784 genes whose transcripts were significantly increased more than two-fold and 123 genes whose transcripts were decreased more than two-fold in *kri-1(ok1251)* worms (Figure 4.1B; Table 7.4). This is reminiscent of changes observed in transcription factor mutants (Brunquell, et al., 2016), and indicates that transcription is regulated downstream of KRI-1. To determine if MPK-2/ERK5 is responsible for these transcriptional changes, I compared the transcriptomes of *kri-1(ok1251); mpk-2(ok219)* double mutant worms to *kri-1(ok1251)* animals (Figure 4.1A) and found that of these transcripts, 629 up-regulated, and 99 down-regulated transcripts return to wild type-like levels in the double mutants (Figure 4.1B; Table 7.5). Many of these genes are predicted to be involved in innate immunity, stress response, and neuropeptide signalling (Figure 4.1C).

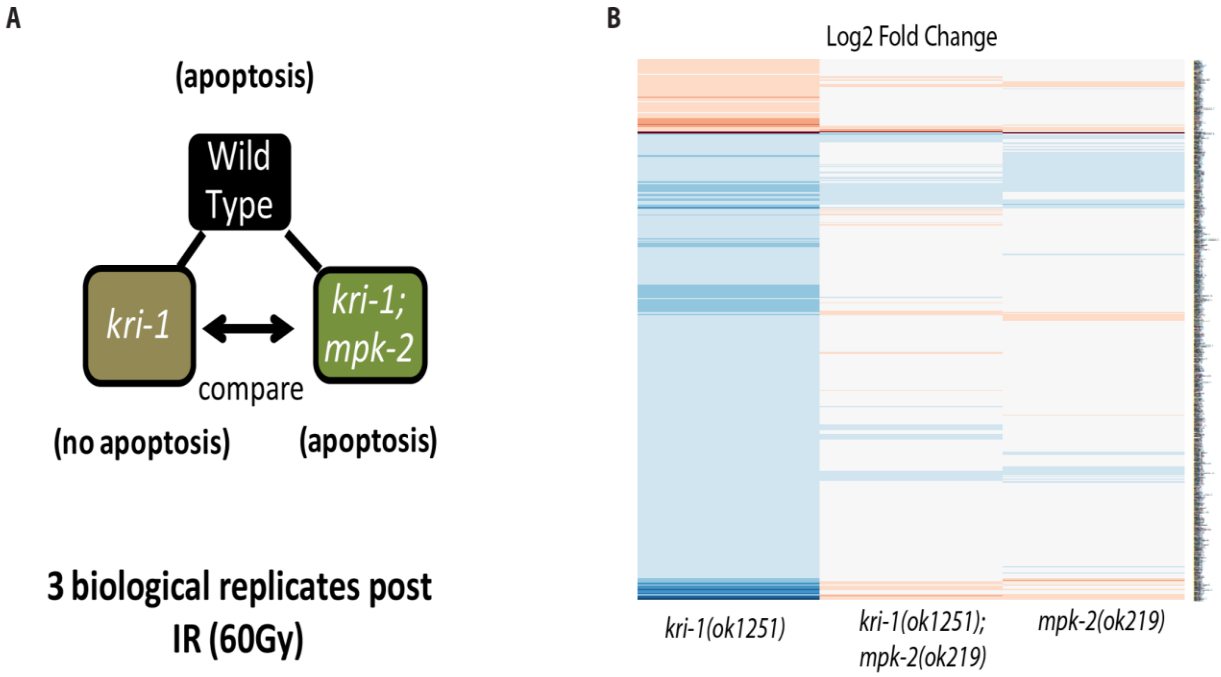
A
(apoptosis)
Wild Type
kri-1
kri-1; mpk-2
compare
(no apoptosis)
(apoptosis)
3 biological replicates post IR (60Gy)
B
Log2 Fold Change
kri-1(ok1251)
kri-1(ok1251); mpk-2(ok219)
mpk-2(ok219)

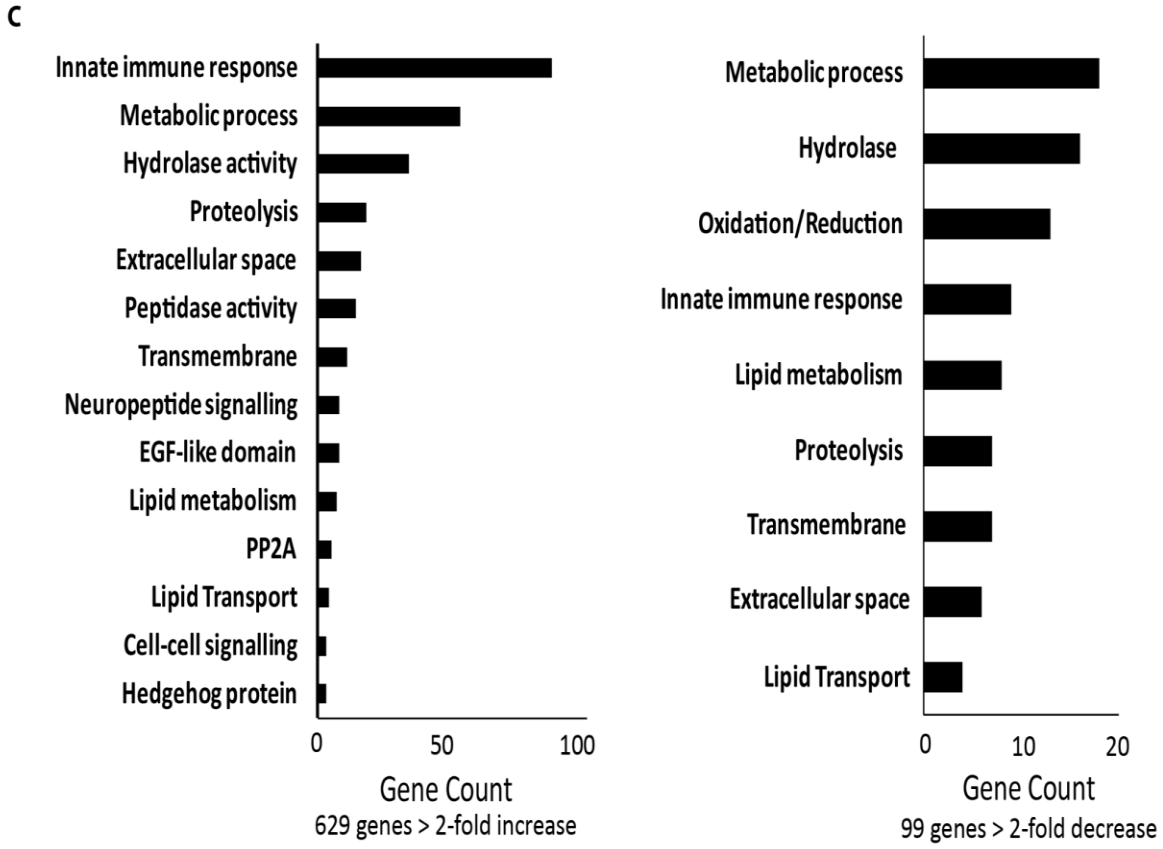
C
Innate immune response
Metabolic process
Hydrolase activity
Proteolysis
Extracellular space
Peptidase activity
Transmembrane
Neuropeptide signalling
EGF-like domain
Lipid metabolism
PP2A
Lipid Transport
Cell-cell signalling
Hedgehog protein
0
50
100
Gene Count
629 genes > 2-fold increase
Metabolic process
Hydrolase
Oxidation/Reduction
Innate immune response
Lipid metabolism
Proteolysis
Transmembrane
Extracellular space
Lipid Transport
0
10
20
Gene Count
99 genes > 2-fold decrease

Figure 4.1 KRI-1 regulates transcription through MPK-2/ERK5.
A) Schematic of worm strains irradiated (60Gy) and sent for mRNA sequencing in biological triplicate. B) Heat map depicting transcripts significantly altered in *kri-1(ok1251)* mutants compared to wild type animals, and how the relative expression of these genes changes in *kri-1(ok1251); mpk-2(ok219),* and *mpk-2(ok2189)* mutants. Transcript profiles represent the average expression of three biological replicates compared to wild type. Red represents genes down-regulated, and blue represents genes up-regulated compared to wild type. C) The program DAVID was used to group *kri-1(ok1251)* up- (left) or down-regulated (right) genes regulated by MPK-2/ERK5 into categories based on predicted or known function.

4.3 PHO-1 and ZIPT-2.3/SLC39 promote IR-induced apoptosis

Since many transcripts are regulated by MPK-2/ERK5 downstream of KRI-1, I conducted an RNA*i* screen of these genes to identify those that are required for IR-induced apoptosis. Using the RNA*i* library described earlier that covers 85% of the *C. elegans* genome, I knocked down 604/729 genes in *kri-1(ok1251)* mutants that were increased two-fold or greater, plus additional candidate genes increased between 1-2 fold in the absence of *kri-1* (Table 7.8). I also knocked down 87/99 genes in wild type animals that were decreased two-fold or more in *kri-1(ok1251)* mutants (Table 7.7). Knockdown of the up-regulated genes failed to restore apoptosis in *kri-1(ok1251)* mutants (data not shown), but RNA*i* targeting two genes in wild type worms suppressed IR-induced germ cell apoptosis to the same extent as ablating *kri-1* (Figure 4.2A). These genes are *pho-1,* which encodes an intestinal acid **pho**sphatase (Beh et al., 1991), and the SLC39 (**so**l**l**ute **c**arrier 39) family zinc transporter *zipt-2.3* (**Z**rt, **I**rt- like **p**rotein **t**ransporter**)** (Dietrich, et al., 2016). To confirm the *pho-1* and *zipt-2.3* RNA*i* results, I obtained strains containing a loss of function *pho-1* allele (*ca101ca102*) (Beh et al., 1991; Fukushige et al., 2005) and the *zipt-2.3(ok2094)* deletion that removes the second and third exons, and half of exon 4, resulting in an out-of-frame sequence (Figure 4.2B). These *pho-1(ca101ca102)* (Figure 4.2C) and *zipt-2.3(ok2094)* (Figure 4.2D) alleles conferred resistant to IR-induced apoptosis.

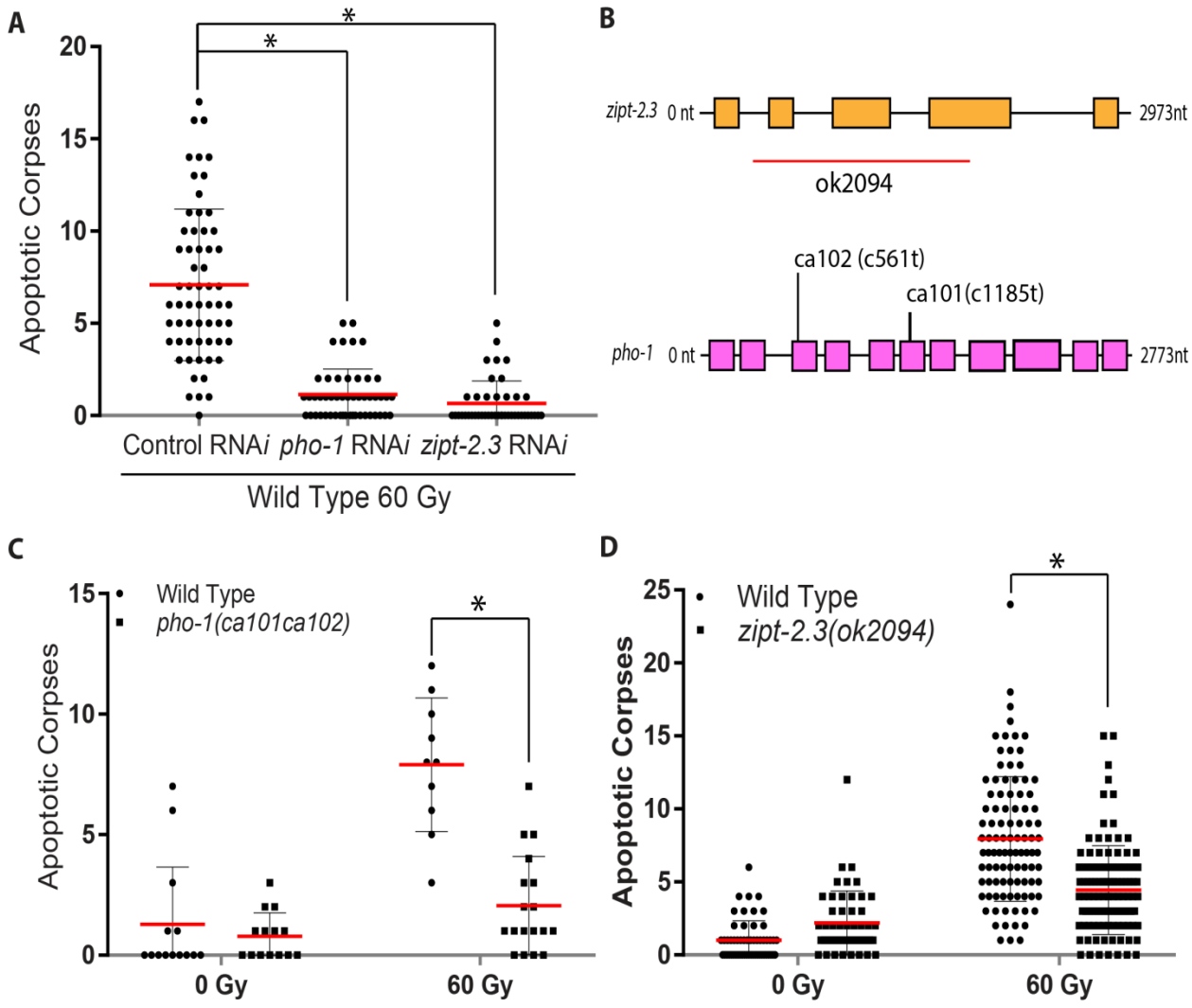

Figure 4.2 PHO-1 and ZIPT-2.3/SLC39 promote IR-induced apoptosis.
A) IR-induced germ cell apoptosis quantified in wild type animals after knockdown of *pho-1* and *zipt-2.3* by RNA*i*. B) The *zipt-2.3(ok2094)* allele consists of a complex re-arrangement including a 1561bp deletion in *zipt-2.3,* which removes the second, third, and half of the fourth exon. This deleted region is replaced by a 39bp insertion, resulting in an out-of-frame sequence. The *pho-1(ca101ca102)* allele consists of two point mutations. *(ca101)* results in D181N and *(ca102)* results in M70I substitutions in PHO-1. C) IR-induced germ cell apoptosis quantified in wild type, and *pho-1(ca101ca102)* animals. D) IR-induced germ cell apoptosis quantified in wild type, and *zipt-2.3(ok2094)* animals. Apoptotic corpses in (A, C & D) were quantified 24 hours post irradiation (60 Gy) or in the absence of radiation (0 Gy) (C & D), and the graphs represent three independent replicates (A), one experiment (C), and four independent replicates (D). Graph A represents at least 40 worms per strain, per condition. Graph C represents at least 15 worms per strain, per condition. Graph D represents at least 50 worms per strain, per condition. Red line is mean +/- standard deviation. *P<0.05, two-sided, unpaired t-test.

While PHO-1 and ZIPT-2.3/SLC39 promote IR-induced apoptosis, *pho-1(ca101ca102)* and *zipt-2.3(ok2094)* animals are not sensitive to starvation during L1 diapause (Figure 4.3) like *kri-1(ok1251)* mutants (Figure 3.12A). This is further evidence that the MPK-2/ERK5-KLF-3 cascade bifurcates to regulate survival during L1 diapause (Figure 3.13) and IR-induced apoptosis, downstream of KRI-1.

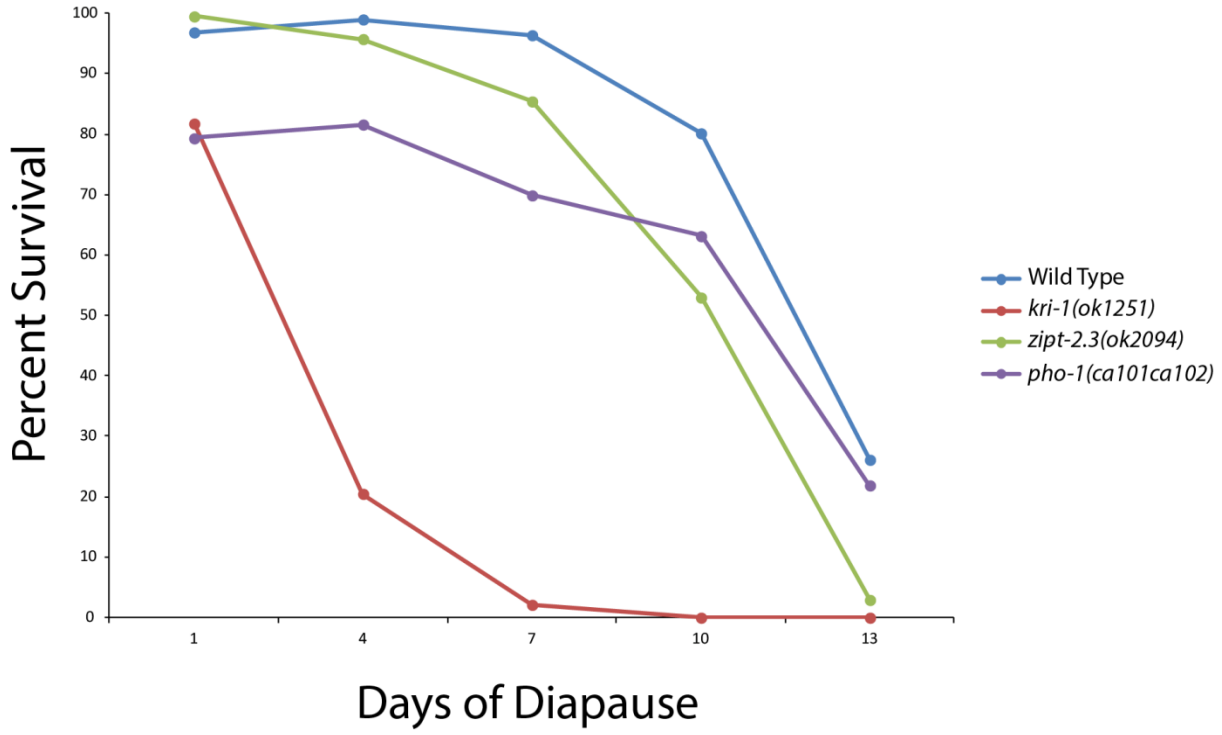

Figure 4.3 *zipt-2.3(ok2094)* and *pho-1(ca101ca102)* animals are not sensitive to starvation. Survival of wild type, *kri-1(ok1251), zipt-2.3(ok2094),* and *pho-1(ca101ca102)* L1 larvae in liquid buffer (M9) without food. Graph represents two technical replicates and 200 worms per strain.

I chose to continue my focus on ZIPT-2.3/SLC39 since zinc is known to regulate apoptosis (Ganju & Eastman, 2003; Perry et al., 1997), and ablation of other *C. elegans* zinc transporters have been shown to result in zinc storage defects (Roh, et al., 2012) where zinc diffuses throughout the animal (Roh et al., 2013). I confirmed by qPCR that *zipt-2.3* is downregulated in *kri-1(ok1251)* animals and increases in *kri-1(ok1251); mpk-2(ok219)* double mutants in the presence and absence of 60 Gy IR (Figure 4.4A). The levels of *zipt-2.3* were also restored in *kri-1(ok1251); klf-3(on34)* double mutants with and without radiation (Figure 4.4B), indicating that transcriptional regulation of *zipt-2.3* is KLF-3-dependent but independent of DNA damage. Interestingly, another zinc transporter gene, *K07G5*.5, is also downregulated in *kri-1(ok1251)* animals and is restored to wild type levels in *kri-1(ok1251); mpk-2(ok219)* double mutants (Table 7.4; Table 7.5), but knockdown of this gene in wild type worms did not suppress apoptosis (data not shown).

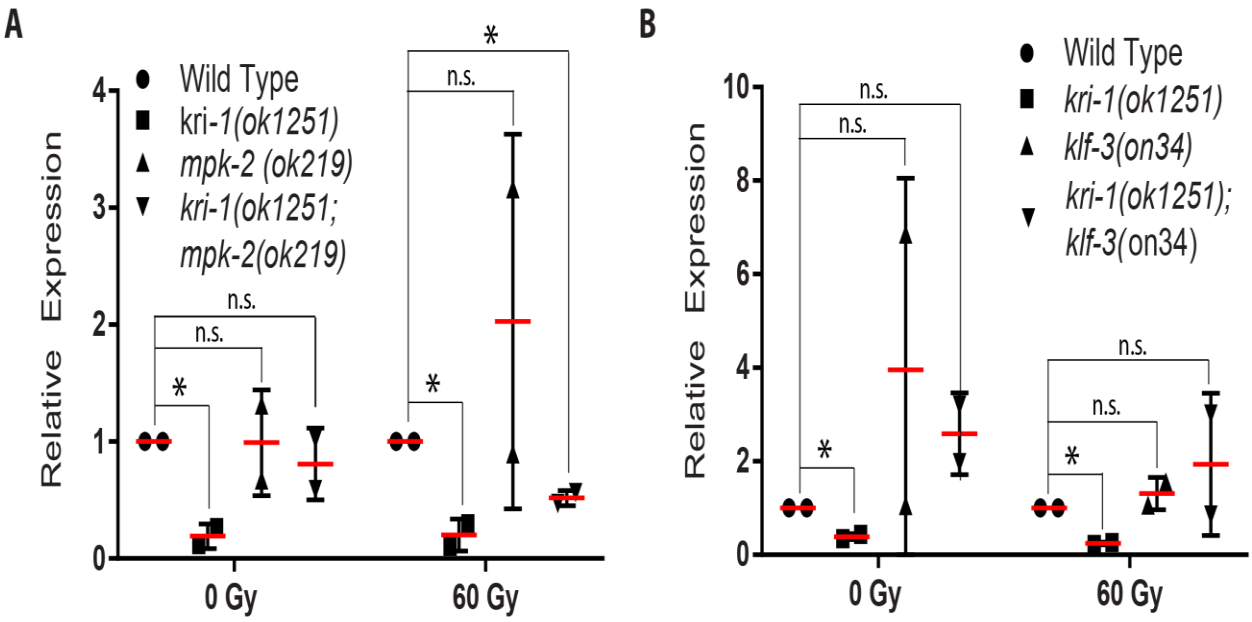

Figure 4.4 *zipt-2.3* transcription is regulated by MPK-2/ERK5 and KLF-3.
A) Relative expression of *zipt-2.3* in *kri-1(ok1251), mpk-2(ok219),* and *kri-1(ok1251); mpk-2(ok219)* animals compared to wild type, 5-6 hours post irradiation (60 Gy) or in the absence of radiation (0 Gy). B) Relative expression of *zipt-2.3* in *kri-1(ok1251), klf-3(on34),* and *kri-1(ok1251); klf-3(on34)* animals compared to wild type, 5-6 hours post irradiation (60 Gy) or in the absence of radiation (0 Gy). Graphs A & B represent two biological replicates. Red line is mean +/- standard deviation. *P<0.05, two-sided, unpaired t-test.

4.4 ZIPT-2.3/SLC39 is expressed in the intestine and promotes zinc storage

To determine the localization of ZIPT-2.3, I expressed a GFP translational fusion reporter consisting of *zipt-2.3* with a 5 kb promoter region in wild type animals. Three different array-containing lines were created, all expressing ZIPT-2.3::GFP throughout the intestine (Figure 4.5A). This expression pattern was later validated by a recent report finding that the *zipt-2.3* promoter drives GFP expression in the intestine (Dietrich, et al., 2017). Similar to other intestinal zinc transporters (Davis et al., 2009) ZIPT-2.3::GFP localizes to vesicular gut granules (Figure 4.5B), which are the main sites of zinc storage in the animal (Roh et al., 2012). To determine if ZIPT-2.3::GFP expression or localization is affected by loss of KRI-1, the ZIPT-2.3::GFP construct was crossed from a wild type background into *kri-1(ok1251)* mutants. While no change in ZIPT-2.3::GFP localization was observed, there was a strong reduction of expression in the absence of radiation and in irradiated animals (Figure 4.5C), consistent with the results from RNAseq and qPCR. Since ZIPT-2.3::GFP is expressed from a multi-copy array, I wondered if apoptosis is restored in the *kri-1(ok1251)* animals expressing this transgene. IR-induced apoptosis was not restored (Figure 4.5D), consistent with the strong suppression of ZIPT-2.3::GFP in *kri-1(ok1251)* mutants (Figure 4.5C). To circumvent the reduced expression of ZIPT-2.3::GFP in *kri-1(ok1251)* mutants, I attempted to express ZIPT-2.3::GFP from a 5 kb upstream region of the intestinal-specific *elt-2* gene in wild type and *kri-1(ok1251)* animals, but was not successful (data not shown). It is possible that I did not recover transgenic animals because expressing *zipt-2.3* from this intestinal promoter is toxic to the animal.

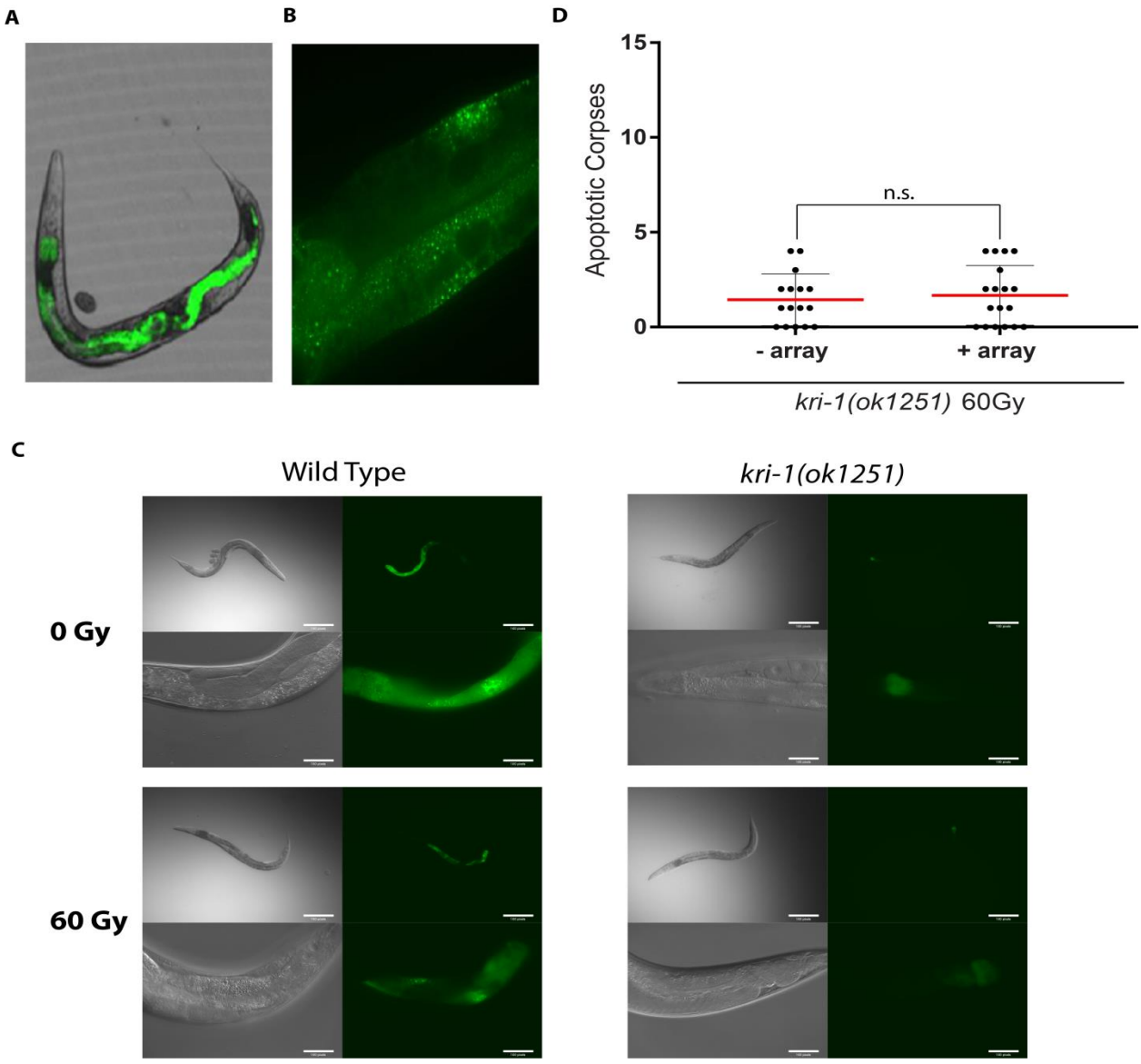

Figure 4.5 ZIPT-2.3/SLC39 localizes to intestinal gut granules

A) ZIPT-2.3::GFP is expressed in the intestine, under the control of a 5 kb *zipt-2.3* upstream element, in wild type animals. B) ZIPT-2.3::GFP localizes to vesicular gut granules in intestinal cells. Images in A & B are representative of three independent lines. C) Expression of ZIPT-2.3::GFP in wild type and *kri-1(ok1251)* animals in non-irradiated (0 Gy), and irradiated (60 Gy) conditions. Images are representative of three independent replicates and at least 15 worms per strain, per condition. D) IR-induced germ cell apoptosis quantified in *kri-1(ok1251)* mutants expressing P*zipt-2.3::zipt-2.3::gfp* (+ array) or siblings that have lost the array (- array). Apoptotic corpses were quantified 24 hours post irradiation (60 Gy) and represent one experiment. Graph D represents at least 15 worms per strain, per condition. Red line is mean +/- standard deviation. *P<0.05, two-sided, unpaired t-test.

To assess whether ZIPT-2.3/SLC39 regulates zinc levels and/or localization, I utilized the dye Fluozin-3, which detects stored zinc in gut granules (Roh et al., 2012). Incubating worms with this dye revealed that intestinal zinc storage is abrogated in *kri-1(ok1251)* animals but is restored to wild type levels in *kri-1(ok1251); mpk-2(ok219),* and *kri-1(ok1251); klf-3(on34)* double mutants (Figure 4.6A). As a control, I stained *zipt-2.3(ok2094)* animals, and *pgp-2(kx48)* (**p**-**g**lyco**p**rotein related-2) mutants which are defective in gut granule formation (Schroeder et al., 2007). Both of these strains had a reduction in stored zinc similar to *kri-1(ok1251)* mutants. Since intestinal zinc storage is lost in the absence of KRI-1, I wondered if the excess free zinc mislocalizes throughout the rest of the animal. To test this hypothesis, I utilized a second dye, Zinpyr-1, which detects zinc in the interstitial body cavity of the worm (Roh et al., 2013). Consistent with my hypothesis, I detected increased zinc throughout the pseudocoelom of *kri-1(ok1251)* mutants compared to wild type, *kri-1(ok1251)*; *mpk-2 (ok219),* and *kri-1(ok1251); klf-3(on34)* animals that store zinc in gut granules (Figure 4.6B; Figure 4.6A). As a positive control, I stained *ttm-1/SLC30(ok3505)* (**t**oxin-regulated **t**arget of **M**APK-1) mutants that have excess zinc in the pseudocoelom, and *cdf-1/SLC30(n2527)* (**c**ation **d**iffusion **f**acilitator family-1) animals as a negative control (Roh et al., 2013). Collectively, these results indicate that the KRI-1-MPK-2/ERK5-KLF-3 signalling cascade ensures proper storage of zinc in the intestine to prevent accumulation throughout the rest of the animal.

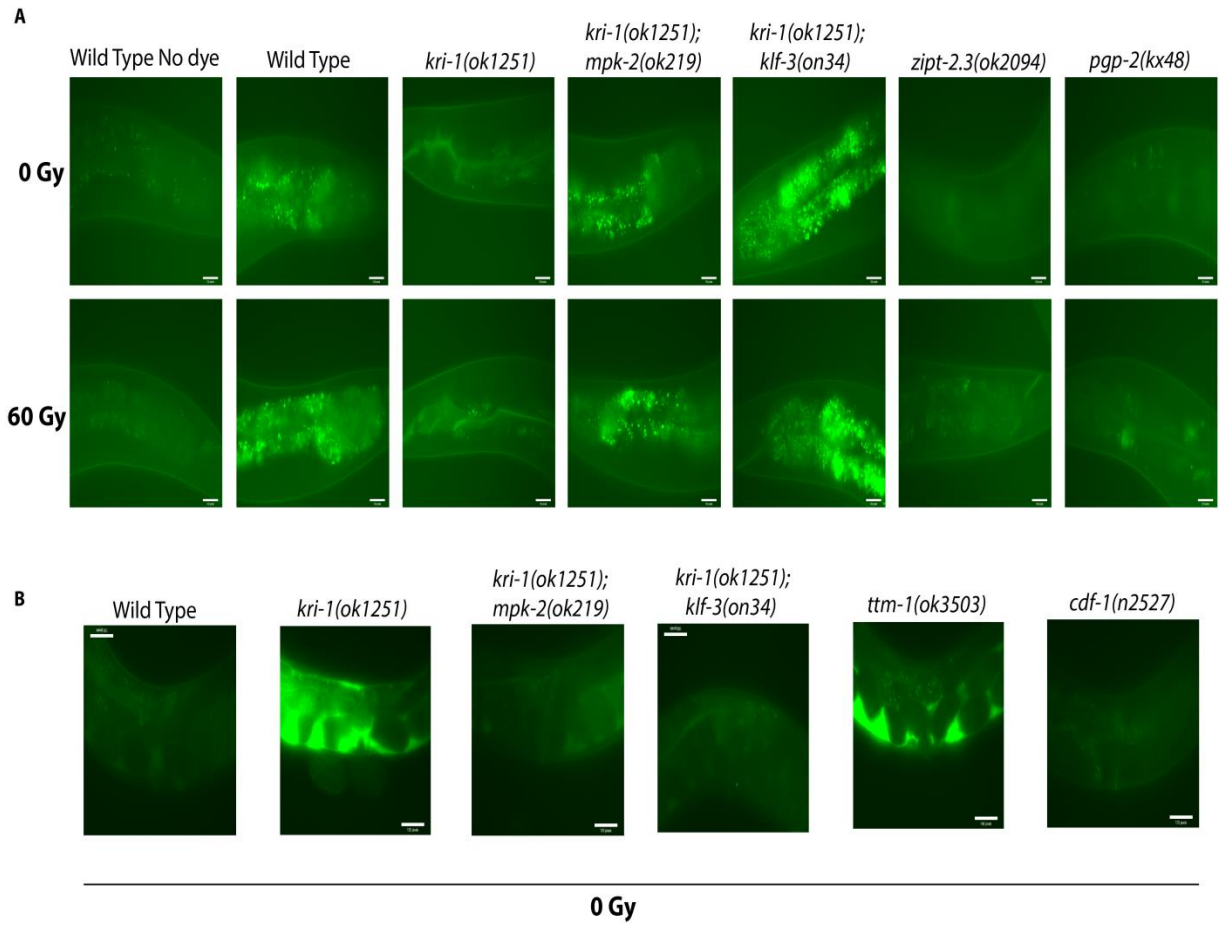

Figure 4.6 ZIPT-2.3/SLC39 promotes zinc storage.
A) Detection of stored intestinal zinc with Fluozin-3 in wild type, *kri-1(ok1251)*, *kri-1(ok1251); mpk-2(ok219)*, *kri-1(ok1251); klf-3(on34)*, *zipt-2.3(ok2094)*, and *pgp-2(kx48)* animals. Images are representative of three independent replicates and at least 15 worms per strain, per condition. B) Detection of interstitial zinc with Zinpyr-1 in wild type, *kri-1(ok1251)*, *kri-1(ok1251); mpk-2(ok219)*, *kri-1(ok1251); klf-3(on34)*, *ttm-1(ok3505)*, and *cdf-1(n2527)* animals. Images are representative of three independent replicates and at least 20 worms per strain, per condition.

Since *ttm-1(ok3503)* mutants have an increase in interstitial zinc, similar to *kri-1(ok1251)* animals, I wondered if they are also resistant to IR-induced apoptosis. Indeed, these animals have suppressed IR-induced apoptosis compared to wild type animals (Figure 4.7), suggesting that a mislocalization of zinc into the body cavity can suppress germ cell apoptosis. In the future, I would want to compare how the levels of apoptosis in *ttm-1(ok3503)* mutants compare to *kri-1(ok1251)* animals. Surprisingly, *cdf-1(n2527)* mutants which do not have an increase in

interstitial zinc, also have a significant reduction in IR-induced apoptosis compared to wild type animals (Figure 4.7). It is possible that in *cdf-1(n2527)* mutants, zinc mislocalizes to other tissues, or CDF-1 transports different molecules to regulate apoptosis.

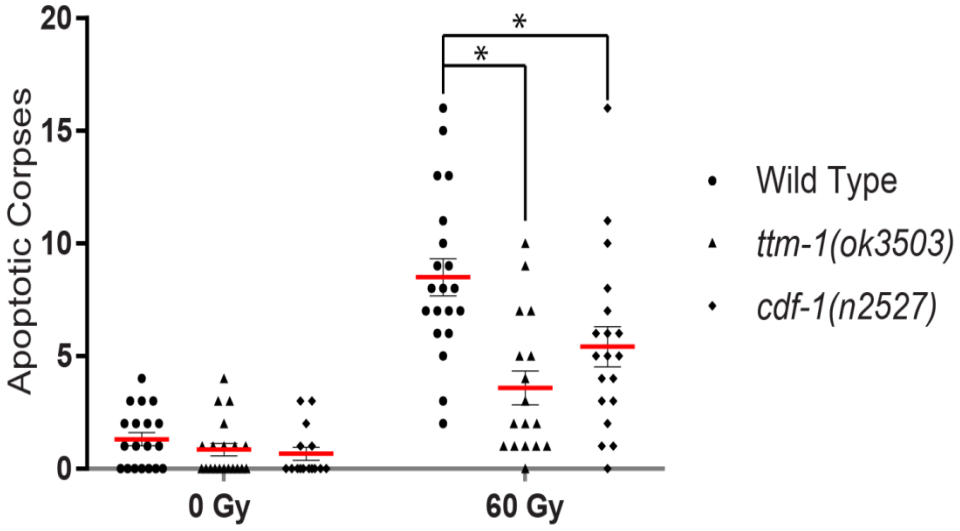

Figure 4.7 TTM-1 and CDF-1 regulate IR-induced apoptosis.
IR-induced germ cell apoptosis quantified in wild type, *ttm-1(ok3503),* and *cdf-1(n2527)* animals. Apoptotic corpses were quantified 24 hours post irradiation (60 Gy) or in the absence of radiation (0 Gy). The graph represents one experiment and at least 15 worms per strain, per condition. Red line is mean +/- standard deviation. *P<0.05, two-sided, unpaired t-test.

4.5 ZIPT-2.3/SLC39 promotes IR-induced apoptosis upstream of MPK-1/ERK1

To confirm that ZIPT-2.3/SLC39 regulates apoptosis downstream of MPK-2/ERK5 and KLF-3, I knocked down *zipt-2.3* in *kri-1(ok1251); mpk-2(ok219),* and *kri-1(ok1251); klf-3(on34)* double mutants and observed a similar suppression of IR-induced germ cell apoptosis as knocking down *zipt-2.3* in wild type animals (Figure 4.8A-B). This suggests that *zipt-2.3* functions downstream of *mpk-2/erk5* and *klf-3* to regulate IR-induced apoptosis.

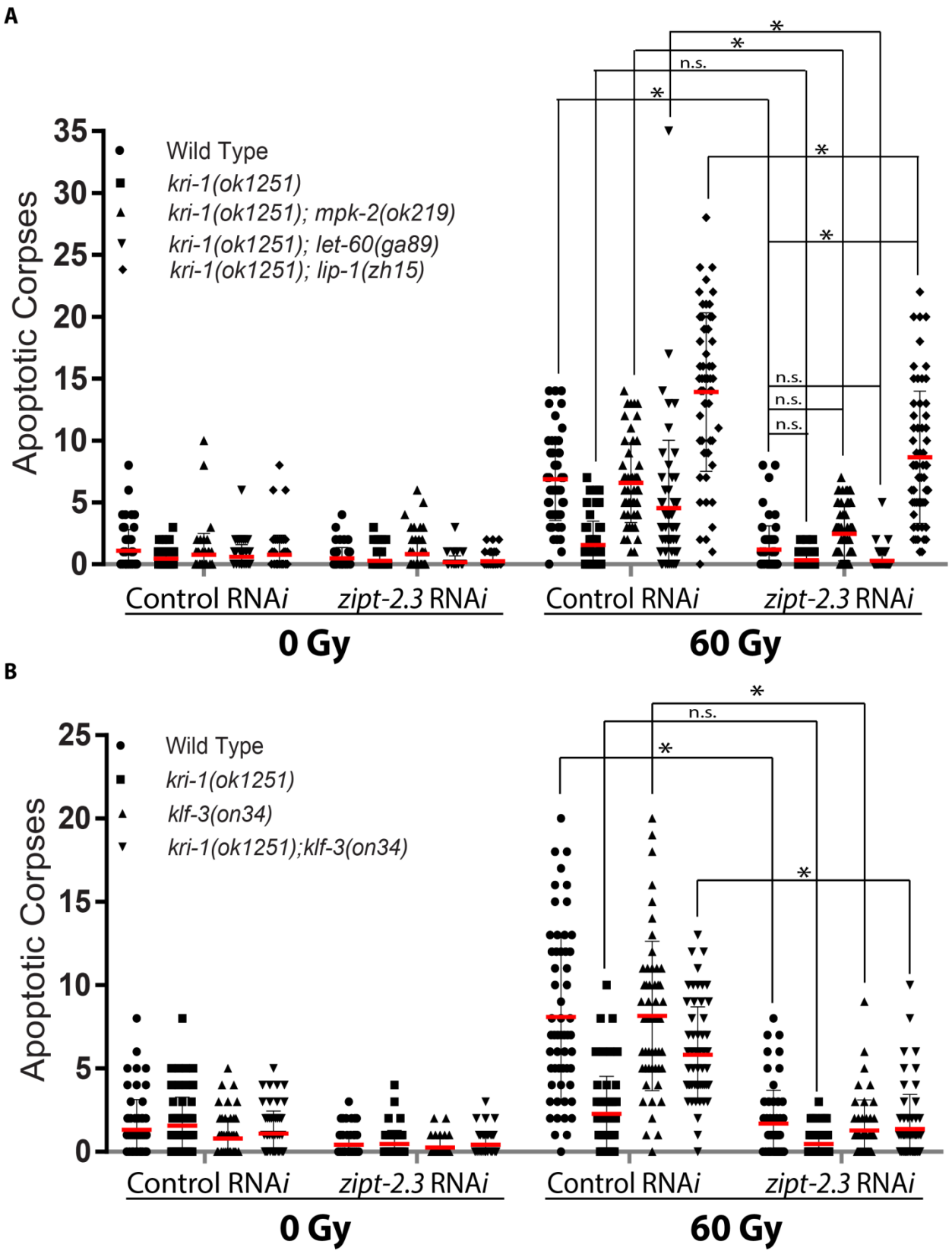
A
Apoptotic Corpses
35
30
25
20
15
10
5
0
Wild Type
kri-1(ok1251)
kri-1(ok1251); mpk-2(ok219)
kri-1(ok1251); let-60(ga89)
kri-1(ok1251); lip-1(zh15)
n.s.
n.s.
n.s.
n.s.
Control RNAi
zipt-2.3 RNAi
Control RNAi
zipt-2.3 RNAi
0 Gy
60 Gy
B
Apoptotic Corpses
25
20
15
10
5
0
Wild Type
kri-1(ok1251)
klf-3(on34)
kri-1(ok1251);klf-3(on34)
n.s.
Control RNAi
zipt-2.3 RNAi
Control RNAi
zipt-2.3 RNAi
0 Gy
60 Gy

Figure 4.8 ZIPT-2.3/SLC39 regulates apoptosis downstream of MPK-2/ERK5-KLF-3 and upstream of MPK-1/ERK1.
A) IR-induced germ cell apoptosis quantified in wild type, *kri-1(ok1251), kri-1(ok1251); mpk-2(ok219), kri-1(ok1251); let-60(ga89)* and *kri-1(ok1251); lip-1(zh15)* animals after knock-down of *zipt-2.3/slc39*. B) IR-induced germ cell apoptosis quantified in wild type, *kri-1(ok1251), klf-3(on34)*, and *kri-1(ok1251); klf-3(on34)* animals after knock-down of *zipt-2.3/slc39*. Apoptotic corpses in (A & B) were quantified 24 hours post irradiation (60 Gy) or in the absence of radiation (0 Gy) and the graphs represent three independent replicates. Graph A represents at least 55 worms per strain, per condition. Graph B represents at least 40 worms per strain, per condition. Red line is mean +/- standard deviation. *P<0.05, two-sided, unpaired t-test.

To determine if ZIPT-2.3/SLC39 regulates IR-induced germ cell apoptosis by promoting the activation of MPK-1/ERK1, downstream of KRI-1-MPK-2/ERK5, I immunostained germlines of wild type and *kri-1(ok1251); mpk-2(ok219)* double mutants for dp-MPK-1/ERK1 after knockdown of *zipt-2.3*. Knockdown of *zipt-2.3* by RNA*i* resulted in a reduction of IR-induced MPK-1/ERK1 activation in the pachytene region of the germline in wild type and *kri-1(ok1251); mpk-2(ok219)* animals compared to control RNA*i* (Figure 4.9). This result indicates that *zipt-2.3* promotes apoptosis by permitting the activation of MPK-1/ERK1 in the germline.

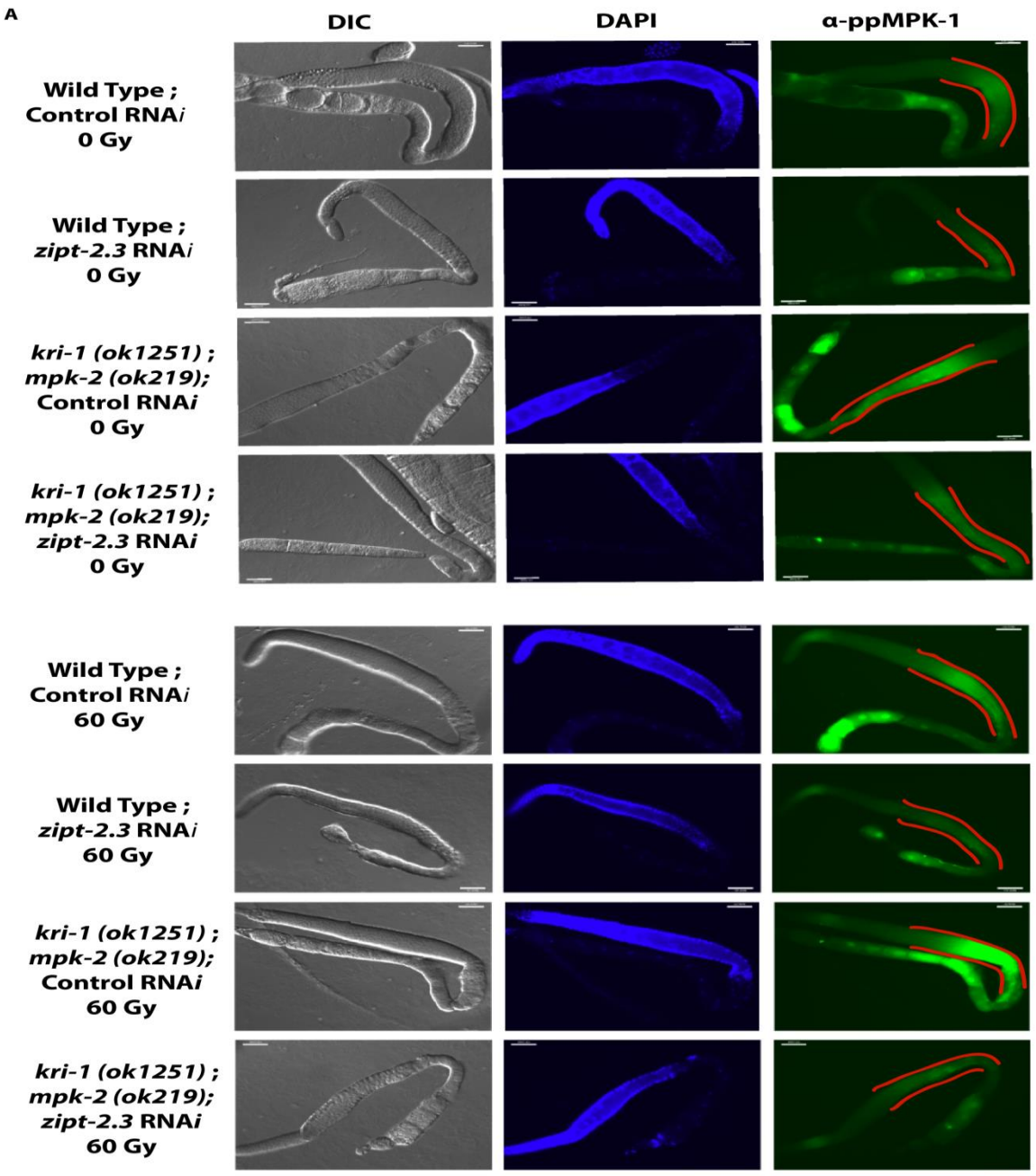

Figure 4.9 ZIPT-2.3/SLC39 regulates germline MPK-1/ERK1 activation.
Activated di-phosphorylated MPK-1/ERK1 in germlines of non-irradiated and irradiated (60 Gy) wild type; control RNA*i*, wild type; *zipt-2.3* RNA*i*, *kri-1(ok1251); mpk-2(ok219)*; control RNA*i*, and *kri-1(ok1251); mpk-2(ok219)*; *zipt-2.3* RNA*i* animals. Images are representative of two independent replicates and at least 20 worms per strain, per condition.

To determine where ZIPT-2.3/SLC39 intersects the MPK-1/MAPK pathway, I knocked down *zipt-2.3* in *kri-1(ok1251); let-60(ga89)* and *kri-1(ok1251); lip-1(zh15)* double mutants. Reduction of *zipt-2.3* abolished the partial restoration of apoptosis in *kri-1(ok1251); let-60(ga89)* animals but did not suppress the restored apoptosis in *kri-1(ok1251); lip-1(zh15)* mutants (Figure 4.8A). This indicates that ZIPT-2.3 regulates apoptosis downstream of *let-60/RAS* and upstream of *mpk-1/ERK1* (Figure 4.10A), similar to KRI-1 (Figure 3.9B).

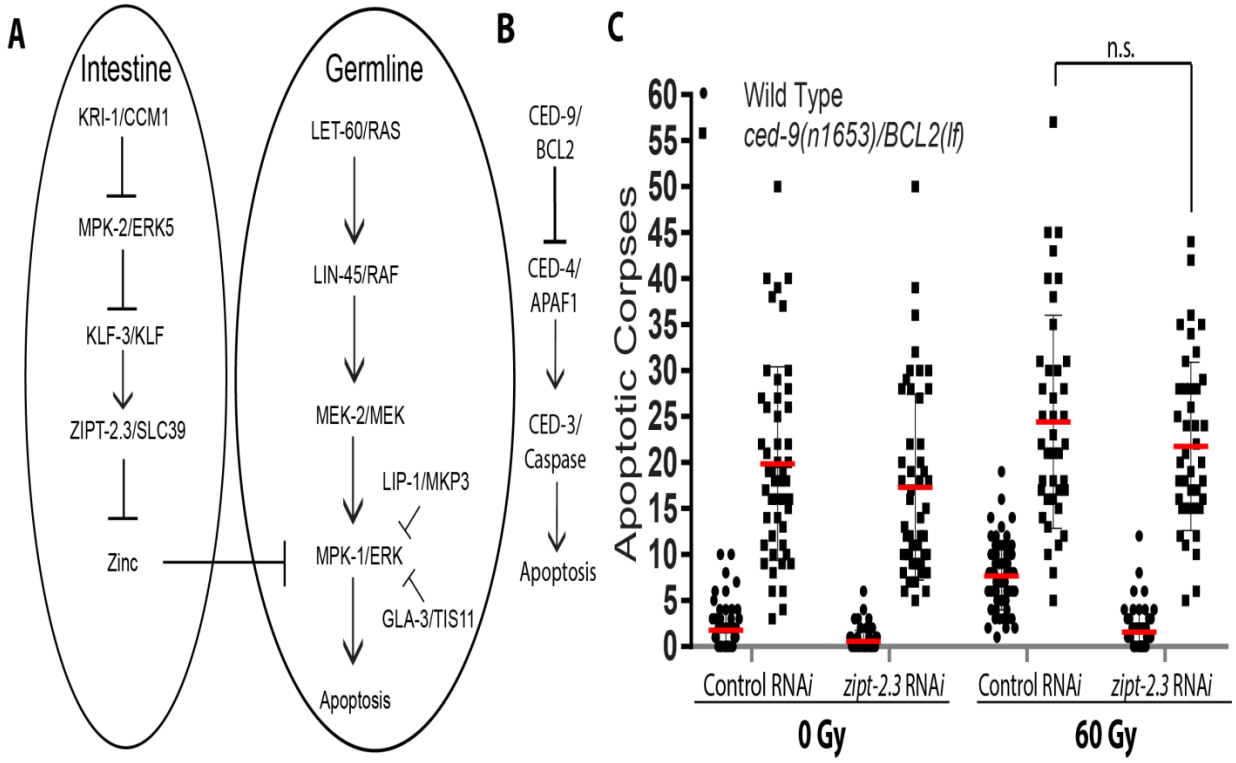

Figure 4.10 ZIPT-2.3/SLC39 regulates apoptosis upstream of MPK-1/ERK1 and independent of CED-3/Caspase.

A) Schematic of how intestinal ZIP-2.3/SLC39 regulates MPK-1/ERK1 in the germline. B) Schematic of the core apoptosis cascade. C) IR-induced germline apoptosis quantified in wild type and *ced-9(n1653)* animals after knock-down of *zipt-2.3/slc39*. Apoptotic corpses were quantified 24 hours post irradiation (60 Gy) or in the absence of radiation (0 Gy). The graph represents three independent replicates and at least 40 worms per strain, per condition. Red line is mean +/- standard deviation. *P<0.05, two-sided, unpaired t-test.

4.6 Zinc suppresses IR-induced apoptosis

My results thus far are consistent with a model whereby KR1-1 regulates ZIPT-2.3/SLC39 and promotes zinc storage to render the germline competent for apoptosis. To determine if zinc, itself, affects germ cell apoptosis, I added increasing concentrations of exogenous zinc to the worm growth media and raised wild type animals on this source. At 0.1mM, 0.2mM, and 0.5mM there was no effect, while 1mM zinc resulted in a significant inhibition of IR-induced germ cell apoptosis (Figure 4.11A-B). These wild type worms were otherwise able to grow normally from L1 to adult at all concentrations of zinc tested. At 2mM, zinc precipitated out of the growth media and was therefore not assessed. To determine if zinc inhibits IR-induced germ cell apoptosis regulated by the MPK-1/MAPK pathway, I grew *let-60(ga89)/RAS(gf)* and *lip-1(zh15)* animals on 1mM zinc. IR-induced apoptosis was suppressed in *let-60(ga89)/RAS* but not *lip-1(zh15)* mutants under these conditions (Figure 4.11B), indicating that zinc inhibits apoptosis downstream of LET-60/RAS but upstream of MPK-1/ERK1 (Figure 4.10A). Since exogenous zinc can suppress MPK-1/ERK1-induced apoptosis in the germline, it is possible that increased zinc in the body cavity of *kri-1(ok1251)* mutants (Figure 4.6B) is taken up into the germline, resulting in the inhibition of MPK-1/MAPK signalling and IR-induced apoptosis.

Since zinc has been shown to inhibit caspases (Perry et al., 1997), I wondered if this is an additional level of regulation in the germline. To test this hypothesis, I grew *ced-9(n1653)/BCL2(lf)* animals, which have enhanced caspase activation and apoptosis (Spector, et al., 1997) (Figure 4.10B), on 1mM zinc, but observed no effects (Figure 4.11B). This suggests that in the germline, zinc suppresses apoptosis by inhibiting the MPK-1/MAPK pathway, but not caspase activity. Consistently, knockdown of *zipt-2.3* does not suppress apoptosis in *ced-9(n1653)/BCL2(lf)* mutants (Figure 4.10C).

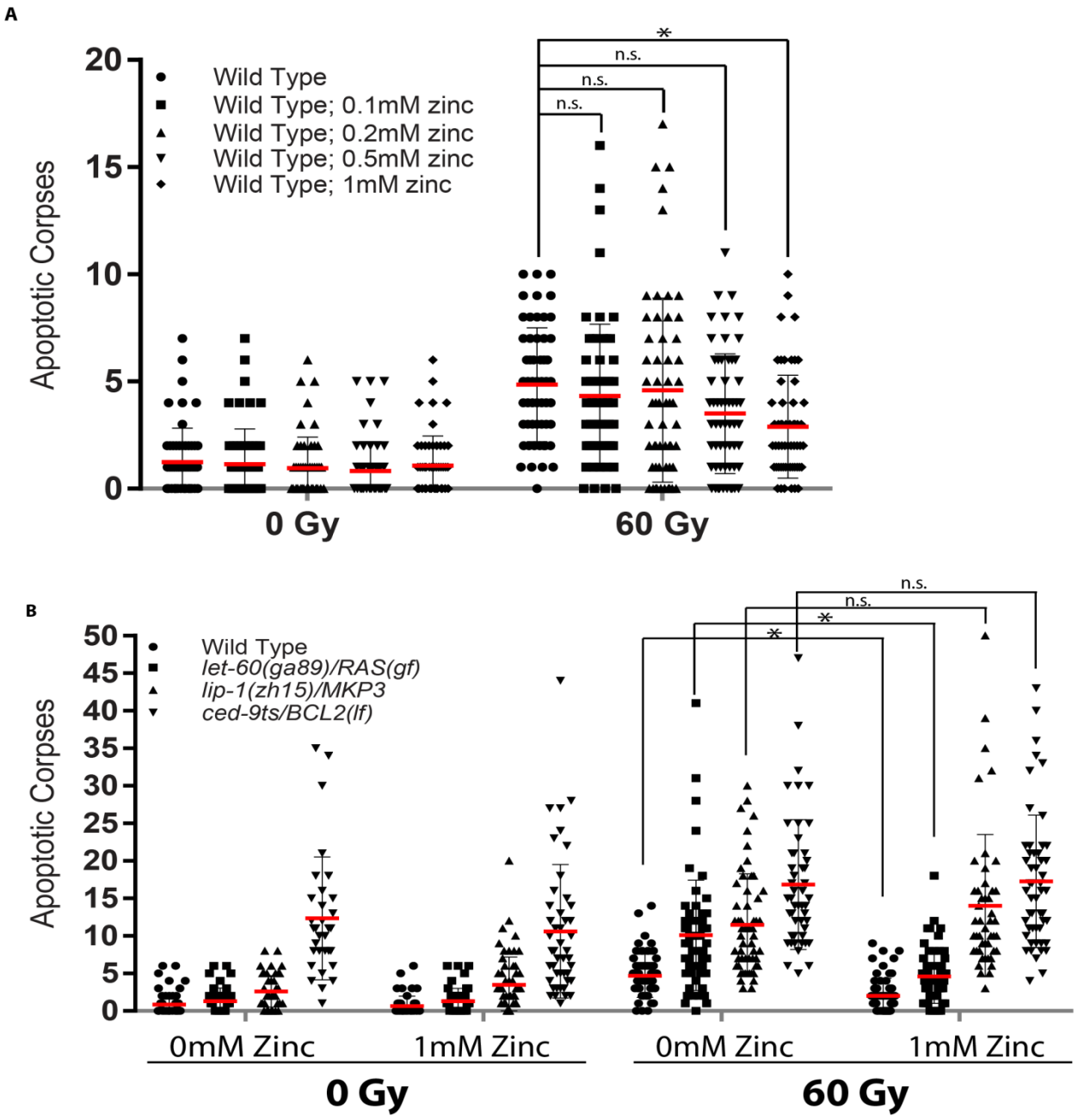

Figure 4.11 Zinc suppresses IR-induced apoptosis.

A) IR-induced germ cell apoptosis quantified in wild type worms grown on media supplemented with 0, 0.1, 0.2, 0.5, and 1 mM zinc. B) IR-induced germline apoptosis quantified in wild type, *let-60(ga89)/RAS(gf)*, *lip-1(zh15)* and *ced-9(n1653)/BLC2(lf)* animals grown on media supplemented with 1mM zinc. Apoptotic corpses in (A & B) were quantified 24 hours post irradiation (60 Gy) or in the absence of radiation (0 Gy) and represents three independent replicates. Graph A represents at least 55 worms per strain, per condition. Graph B represents at least 35 worms per strain, per condition. Red line is mean +/- standard deviation. *P<0.05, two-sided, unpaired t-test.

5 Discussion

5.1 A Conserved KRI-1/CCM1 Complex Regulates ERK5/MAPK and KLF-3 to Promote Transcription

5.1.1 The KRI-1/CCM1 complex regulates ERK5/MAPK

5.1.1.1 K07A9.3/CCM2 is the link between KRI-1 and ERK5/MAPK

To determine how the KRI-1 scaffold protein functions in the intestine to promote IR-induced germ cell death, I performed AP-MS, and identified the ICAP1 and CCM2 orthologues, Y45F10D.10 and K07A9.3 as binding partners of KRI-1 (Figure 3.19A). Since ICAP1 and CCM2 bind separate N-terminal NPxY/F motifs in mammalian KRIT1/CCM1 (Zawistowski et al., 2005) it is possible that both Y45F10D.10/ICAP1 and K07A9.3/CCM2 are required for IR-induced apoptosis (Figure 3.20), by functioning as part of a complex with KRI-1. Alternatively, Y45F10D.10/ICAP1 might function independently of K07A9.3/CCM2, through integrin signalling (Zhang, et al., 2001). Interestingly, *C. elegans* homologues of RAP1 and HEG1, which interact with the C-terminal FERM domain of mammalian KRIT1, were not identified as KRI-1 binding partners. This could be due to weaker conservation between the KRI-1 and KRIT-1/CCM1 C-terminal FERM domain (Mably et al., 2006), or as a result of RAP1, HEG1, and KRIT1/CCM1 interactions evolving more recently in vertebrates. Alternatively, their binding might be of lower affinity and not detectable with the protocol used in this study. While the KRI-1 binding protein F37C4.5 does not regulate apoptosis, its interaction with KRI-1 might be relevant for other biological processes, such as lifespan (Berman & Kenyon, 2006). Since the binding of Y45F10D.10/ICAP1 and K07A9.3/CCM2 to KRI-1 is not affected by radiation (Figure 3.19A), the KRI-1 complex does not likely respond to radiation *per se*, but rather maintains an environment whereby germ cells are licensed to undergo apoptosis.

In vertebrates, CCM2 was first identified as a scaffold for the MAP kinase kinase kinase, MEKK3, in response to osmotic stress (Uhlik et al., 2003). Recently, this interaction was shown to occur between the C-terminal Harmonin Homology (HH) domain of CCM2 and the N-terminal PB1 (**P**hox and **B**em1) domain of MEKK3 (Fisher et al., 2015a). While ERK5 was not known to be regulated downstream of vertebrate KRIT-1/CCM1 when I started this project, the

link was established subsequent to my *kri-1(ok1251)* suppressor screen that identified the ERK5/MAPK pathway (Zhou et al., 2015). In the mouse endothelium, over-activation of ERK5 results in the formation of CCM lesions (Zhou et al., 2016b), validating the use of *C. elegans* for identifying conserved CCM disease-relevant pathways. Given that auto-phosphorylation of MEKK3, and subsequent activation of ERK5 increases in the absence of CCM2 (Cullere, et al., 2015), it is likely that *C. elegans* KRI-1 also functions to suppress ERK5 signalling by attenuating Y106G6A.1/MEKK3 activation through K07A9.3/CCM2.

ERK5 was first named **B**ig **M**itogen **K**inase-1 (BMK1) due to its large C-terminal region which allows it to enter the nucleus and function as a transcriptional co-regulator (Nithianandarajah-Jones, et al., 2012). Complete loss of *Erk5* in mice results in embryonic lethality, with the most striking defects observed in the vasculature. Interestingly, ablation of *Erk5* specifically in the endothelium result in the death of adult animals due to excessive apoptosis (Hayashi et al., 2004), revealing the anti-apoptotic function of this kinase in the vasculature. In *C. elegans*, a canonical ERK5/MAPK pathway had not been identified until the work presented in this thesis. Previously, a MEKK3-like protein, DRL-1 (**d**ietary **r**estriction **l**ike-1) (Chamoli, et al., 2014), and an ERK5-like protein, SMA-5 (**sma**ll-5) (Watanabe, et al., 2005) were reported, but these two proteins regulate distinct biological processes and both are synthetic lethal with *kri-1* (data not shown). It is possible that two parallel ERK5/MAPK pathways exist in *C. elegans*, but it is unclear if *drl-1* and *sma-5* function in the same molecular pathway.

5.1.1.2 MPK-2/ERK5 regulates transcription through KLF-3

Since ERK5 is known to regulate transcription (Sohn, et al., 2005) by phosphorylating the MEF2C transcription factor (Drew, et al., 2012), I wondered if *C. elegans* MPK-2/ERK5 regulates apoptosis through MEF-2/MEF2. However, knockdown of *mef-2* did not restore apoptosis in *kri-1(ok1251)* mutants or suppress apoptosis in wild type and *kri-1(ok1251); mpk-2(ok219)* animals (Figure 3.16D). Therefore, since MPK-2/ERK5 regulates transcription downstream of KRI-1 (Figure 4.1), a different TF must be targeted. In vertebrates, over-activation of ERK5 results in increased levels of *KLF2* and *KLF4* (Renz et al., 2015; Shannon et al., 2012; Sunadome et al., 2011), which contributes to CCM disease (Zhou et al., 2016b). *C. elegans* contains three KLF transcription factors, *klf-1,-2,* and *-3* which are homologous to

"Group 2" KLFs including KLF2 and KLF4 (McConnell & Yang, 2010). While *klf-1* is up-regulated in *kri-1(ok1251)* animals and returns to wild type levels in *kri-1(ok1251); mpk-2(ok219)* double mutants (Table 7.4; Table 7.5), knockdown of *klf-1* beginning at the L1 stage in *kri-1(ok1251)* animals is synthetic lethal (data not shown). Ablation of *klf-1* from the L4 stage results in sick *kri-1(ok1251)* animals and no restoration of IR-induced germ cell apoptosis (Figure 3.17D).

Intriguingly, I identified a gain-of-function mutation in *klf-3* from my *kri-1(ok1251)* suppressor screen that restores IR-induced apoptosis (Figure 3.17). Despite the potential differences between *C. elegans* and vertebrate regulation of KLFs by ERK5, I hypothesize that the gain-of-function mutation in KLF-3 restores normal transcription in the absence of KRI-1. This is apparent from the ability of the *klf-3(on34)* protein product to restore expression of the *zipt-2.3/slc39* zinc transporter gene in *kri-1(ok1251)* animals (Figure 4.4B). Since KLF-3 is expressed in the *C. elegans* intestine (Zhang et al., 2009b) with KRI-1 and MPK-2/ERK5, it is likely that KLF-3 functions downstream of MPK-2/ERK5 to promote *zipt-2.3* expression (Figure 5.1). While many of the mis-regulated genes in *kri-1(ok1251)* animals do not regulate apoptosis (data not shown), they are identified to be part of functional categories such as innate immunity (Figure 4.1C). Therefore, it is possible that KRI-1-MPK-2/ERK5-KLF-3 also regulates additional processes such as lifespan (Berman & Kenyon, 2006) and survival during L1 diapause. Consistent with this hypothesis, both KLF-3 (Hsieh et al., 2017) and innate immunity factors (Yunger, et al., 2017) have recently been shown to promote lifespan extension in *C. elegans*.

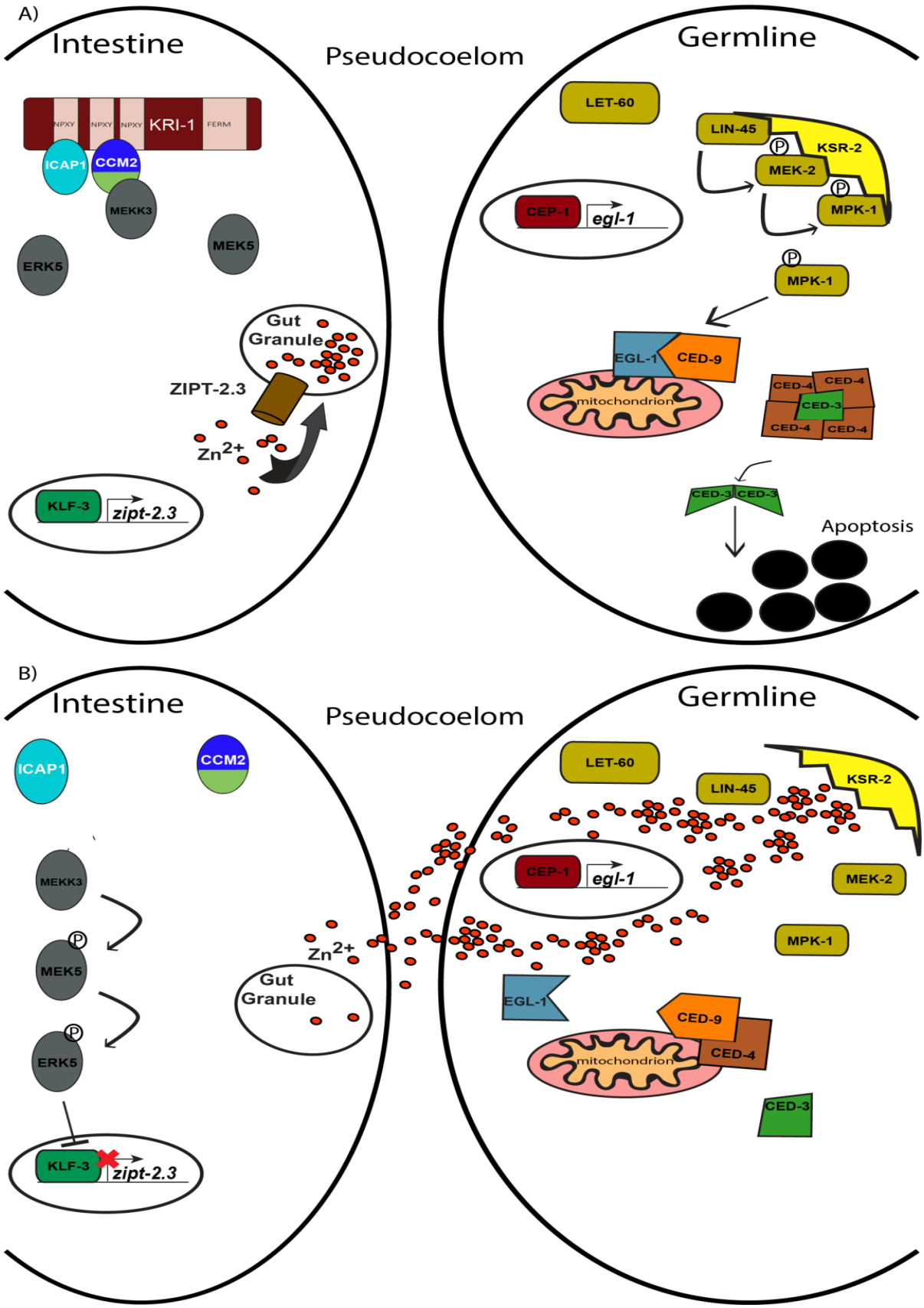
A)
Intestine
Pseudocoelom
Germline
NPXY
NPXY
NPXY
KRI-1
FERM
ICAP1
CCM2
MEKK3
MEK5
ERK5
Gut Granule
ZIPT-2.3
Zn2+
KLF-3
zipt-2.3
LET-60
LIN-45
KSR-2
MEK-2
MPK-1
CEP-1
egl-1
EGL-1
CED-9
mitochondrion
CED-4
CED-3
Apoptosis
B)
Intestine
Pseudocoelom
Germline
ICAP1
CCM2
MEKK3
MEK5
ERK5
Zn2+
Gut Granule
KLF-3
zipt-2.3
LET-60
LIN-45
KSR-2
CEP-1
egl-1
MEK-2
MPK-1
EGL-1
CED-9
CED-4
mitochondrion
CED-3

5.1 KRI-1 promotes apoptosis by regulating MPK-2/ERK5-KLF-3-ZIPT-2.3 and zinc storage.

A) The KRI-1-K07A9.3/CCM2-Y45F10D.10/ICAP1 complex prevents ERK5/MAPK signalling, likely through the binding and inhibition of Y106G6A.1/MEKK3. This allows KLF-3 to promote the expression of the *zipt-2.3/slc39* zinc transporter gene. ZIPT-2.3/SLC39 localizes to intestinal gut granules and promotes zinc storage in these vesicles. This permits IR-induced phosphorylation and activation of MPK-1/ERK1 in the germline and cell death. B) In the absence of KRI-1, MPK-2/ERK5 is active and suppresses KLF-3-mediated expression of *zipt-2.3*. Reduced levels of ZIPT-2.3 results in decreased stored zinc in the intestine and increased free zinc in the interstitial pseudocoelom. Under these circumstances, it is possible that zinc levels rise in the germline and inhibit MPK-1/MAPK signalling and apoptosis.

In the future, it would be interesting to conduct DNA binding assays to confirm that KLF-3 directly promotes the expression of *zipt-2.3*. KLFs are known to have a 5'-CACCC-3' DNA-binding consensus motif (McConnell & Yang, 2010). Since ZIPT-2.3::GFP under the control of a 5 kb upstream element has reduced expression in the absence of KRI-1 (Figure 4.5C), it is possible that KLF-3 binds directly to at least one of the nine 5'-CACCC-3' motifs in this 5kb region (Figure 5.2) to promote *zipt-2.3* expression. Additional studies might include targeted deletion of these motifs to determine if *zipt-2.3* expression becomes abrogated. Since KRI-1 promotes the expression of yolk genes (Goszczynski et al., 2016; Figure 3.1A) it is possible that KLF-3 is also functioning in this pathway to promote vitellogenin expression.

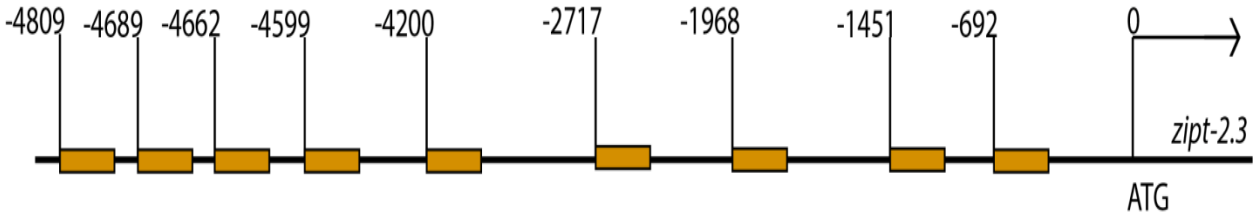

5.2 KLF-binding motifs in the promoter of *zipt-2.3/slc39*.

The location of nine KLF 5'-CACCC-3' binding motifs in the 5 kb *zipt-2.3* promoter.

5.1.1.3 ERK5 and apoptosis

My findings in *C. elegans* are consistent with the role for ERK5 as a negative regulator of apoptosis in vertebrates. In HeLa cells, ERK5 prevents apoptosis by activating MEF2C and inducing expression of the anti-apoptotic factor DDIAS (**D**NA **d**amage **i**nduced **a**poptosis **s**uppressor) (Im et al., 2016), and suppression of ERK5 induces pancreatic cell apoptosis in mice (Nam, et al., 2017). ERK5 is also over-expressed or constitutively active in cancers such as prostate (Mehta et al., 2003), breast (Montero et al., 2009), and cervical (Zheng et al., 2016), with increased ERK5 expression correlating with poor survival of colon cancer patients (Pereira et al., 2016). Inhibition of ERK5 in colon cancer cells resulted in increased caspase-3 activation and apoptosis after radiation (Pereira et al., 2016). In mice, ablation of ATM results in tumor formation in thymocytes, however deletion of *Erk5* in this tissue restored IR-induced apoptosis and improved animal survival (Granados-Jaén et al., 2016). Given that MPK-2/ERK5 inhibits zinc storage in *C. elegans*, it is possible that over-activation of ERK5 in these cancer cells prevents proper zinc storage, and a subsequent inability to undergo cell death. Since ERK5 also prevents cell death throughout the endothelium in mice (Hayashi et al., 2004), and over-expression prevents endothelial cell apoptosis (Vu et al., 2018) it is possible that reduced endothelial cell turn over contributes to the pathology of CCM disease.

5.2 KRI-1-Regulated Zinc Storage Permits IR-induced MPK-1/ERK1 Activation and Apoptosis

5.2.1 KRI-1 permits the activation of germline MPK-1/ERK1

Previously, it had been established that KRI-1 functions from the somatic tissue to regulate IR-induced germ cell apoptosis in parallel to CEP-1/p53 (Ito et al., 2010). Based on my results, I have demonstrated that KRI-1 is required specifically in the intestine (Figure 3.20C) for IR-induced activation of MPK-1/ERK1 in the germline (Figure 3.7) to promote germ cell apoptosis (Figure 3.8). While MPK-1/ERK1 is known to promote IR-induced apoptosis (Eberhard et al., 2013; Perrin et al., 2013; Rutkowski et al., 2011), it remains to be determined how this kinase engages the core apoptosis pathway. Since the expression of *egl-1/BH3-only* is induced normally after radiation in *kri-1(ok1251)* mutants (Ito et al., 2010), it is possible that MPK-1/ERK1 promotes the translation, or regulates post-translational modifications of EGL-1. In support of

the first hypothesis, I discovered that the EIF-3.D translation initiation complex subunit is required for the restored IR-induced apoptosis in *kri-1(ok1251);lip-1(zh15)* animals (Figure 3.11). Since EIF-3.D is a predicted germline target of MPK-1/ERK1 (Arur et al., 2009), it is possible that MPK-1 phosphorylates EIF-3.D to promote the translation of pro-apoptotic proteins such as EGL-1. In the future, it will be important to confirm this potential mode of regulation in response to radiation. Interestingly, another EIF-3 subunit, EIF-3.K, is also required for germ cell death in *C. elegans*. While complete loss of all other EIF-3 subunits results in germline sterility, *eif-3.k* null worms have intact germlines, revealing a pro-apoptotic role for EIF-3.K. Since EIF-3.K promotes apoptosis upstream of CED-3 (Huang et al., 2012), it is possible that EIF-3.K and EIF-3.D function together to promote the translation of apoptotic proteins, such as EGL-1. Since complete loss of the other EIF-3 complex subunits results in sterility (Huang et al., 2012), I predict that partial knockdown by RNA*i*, similar to *eif-3.d*, will expose the pro-apoptotic function of the entire complex. In mammals, ERK1/2 is known to regulate the phosphorylation of eIFs through RSK (**r**ibosomal **s**6 **k**inase) and MNK (**M**APK- **i**nteracting protein **k**inase) family kinases (Roux & Topisirovic, 2012). While knockdown of the RSK homologue, *rskn-1,* did not suppress apoptosis in *kri-1(ok1251); lip-1(zh15)* animals (Figure 3.10B) a second homologue, *rskn-2,* remains to be tested. In addition, *C. elegans* has one MNK kinase, MNK-1 (Okuyama et al., 2010), which might activate EIF-3.D in response to radiation. One way to confirm whether ELG-1 translation depends on EIF-3.D would be to create a single copy fluorescently tagged EGL-1 fusion protein that is expressed in the germline. If hypothetical EGL-1::GFP levels are reduced in *kri-1(ok1251)* mutants, restored in *kri-1(ok1251);lip-1(zh15)* animals, but again reduced upon ablation of *eif-3.d*, this would confirm that MPK-1/ERK1 and EIF-3.D are required for the translation of EGL-1 downstream of KRI-1.

It is also possible that MPK-1/ERK1 directly regulates EGL-1, however this is unlikely because EGL-1 does not have MPK-1/ERK1 docking sites or a phospho-recognition site (Arur et al., 2009). While phosphorylation of the BH3-only proteins NOXA (Lowman et al., 2010) and PUMA (Fricker, et al., 2010) destabilizes these proteins, BIM is stabilized by phosphorylation (Moujalled et al., 2011), and phospho-BID is required to promote apoptosis in response to mitotic arrest (Wang et al., 2014). Therefore, MPK-1/ERK1 might activate another kinase that phosphorylates and stabilizes EGL-1. Alternatively, since EGL-1 contains lysine residues, MPK-

1/ERK1 might phosphorylate and suppresses an E3-ligase that degrades EGL-1. However, such a factor would have to be a currently unidentified target of MPK-1/ERK1, since neither of the two E3 ligase targets of MPK-1/ERK1, HRD-1/SYVN1 and TOE-4 (**t**arget **o**f **E**RK kinase MPK-1), nor the deubiquitinating enzyme, TOE-3 had an effect on apoptosis in *kri-1(ok1251); lip-1(zh15)* animals (Figure 3.10B). Since NOXA levels in mammals increases upon proteosome inhibition (Fernendez et al., 2005), it is possible that NOXA is targeted by an E3 ligase for degradation, and that this mechanism of BH3-only regulation occurs in *C. elegans*.

5.2.2 Zinc inhibits germline MPK-1/ERK1 and apoptosis

5.2.2.1 Zinc is an important biological molecule

My work has revealed that KRI-1 promotes zinc storage in intestinal vesicles, allowing germline MPK-1/ERK1 to be activated. In the absence of KRI-1, free zinc leaks into the body cavity, and possibly the germline, inhibiting MAPK signalling required for IR-induced apoptosis. Zinc is an essential molecule that is estimated to bind approximately 3000 proteins, from enzymes to transcription factors (Maret, 2017). The binding of zinc to zinc-binding motifs can stabilize proteins, promote transcription factor DNA binding, and prevent protein complex formation (Maret, 2017). Zinc also inhibits enzymes that have cysteines in their active site, such as caspases (Eron et al., 2018), and phosphatases (Maret, 2013). Due to this wide of range of functions, it is not surprising that aberrant zinc levels can deregulate important processes such as apoptosis. This is evident from zinc deficiency and excess zinc causing disease (Plum, et al., 2010), and zinc transporters mis-expressed in many types of cancers (Bafaro, et al., 2017). As such, free zinc in the cell cytosol is carefully regulated and maintained at very low levels to prevent non-specific protein binding. Therefore, small changes in the levels of cellular zinc can have significant repercussions, highlighting the importance of cellular zinc storage. Two methods that are conserved from *C. elegans* to mammals include sequestration of zinc by **m**etallo**t**heonein-family proteins (MTs) (Zeitoun-Ghandour et al., 2010) and localization to vesicles (Roh, et al., 2012). Interestingly, MTs with sequestered zinc can be secreted by cells and imported from the extracellular space, providing a systematic way to transport zinc between tissues. Zinc transporters are also used to shuttle zinc into vesicles or across the plasma membrane for transport. Changes in cellular zinc levels are detected by transcription factors such

as MTF1 (**m**etal regulatory **t**ranscription **f**actor 1) in mammals or HIZR-1 (**Hi**gh **z**inc activated nuclear **r**eceptor-1) in *C. elegans* (Warnhoff et al., 2017). These TFs promote the expression of genes such as zinc transporters which can respond to changing concentrations by shuttling zinc in and out of vesicles or cells. In *C. elegans*, the intestine is main site of zinc storage, specifically, in vesicles known as gut granules (Roh, et al., 2012). Zinc regulation in the animal is important for lifespan (Kumar et al., 2016), vulva (Bruinsma, et al., 2002) and germline development (Hester, et al., 2017; Mendoza, et al., 2017). Increasing the levels of exogenous zinc, ablating zinc binding proteins (Shirasu et al., 1999) and also zinc transporters, prevents normal development and function of these tissues.

5.2.2.2 Zinc inhibits ERK1/MAPK signalling

The ERK-1/MAPK cascade is one of the pathways affected by aberrant zinc levels. High concentrations of zinc have been reported to inhibit phosphorylation of ERK1/2 in human T-cells (Hönscheid, et al., 2012), while decreased concentrations of zinc activates the pathway (Pang et al., 2012). Since the activation of MPK-1/ERK1 in the *C. elegans* germline is necessary for apoptosis downstream of KRI-1, I wondered if the failure to store intestinal zinc in *kri-1(ok1251)* animals might result in elevated zinc levels in the germline and suppression of MPK-1/ERK. During *C. elegans* vulva development, zinc and loss of zinc transporters have been shown to suppress the MPK-1/MAPK pathway downstream of LET-60/RAS (Bruinsma, et al., 2002), and upstream of MPK-1/ERK1 (Yoder, et al., 2004). Consistently, I found that knockdown of *zipt-2.3/slc39* and exogenous zinc both suppressed IR-induced germ cell apoptosis downstream of *let-60/RAS*, and upstream of *mpk-1/ERK1* (Figure 4.8A; Figure 4.11B). Since I detected interstitial zinc accumulation in the pseudocoelom of *kri-1(ok1251)* animals compared to wild type (Figure 4.6B) it is possible that zinc might leak into the germline to suppress MPK-1/MAPK signalling. Since zinc is suggested to inhibit RAF (Jirakulaporn & Muslin, 2004) and KSR (Yoder et al., 2004) in *C. elegans*, it is possible that zinc suppresses germline MPK-1/ERK1 activation at either of these steps of the pathway (Figure 5.1). However, the mechanism by which excess zinc exits intestinal cells, and enters the germline in *kri-1(ok1251)* animals remains to be determined.

Since MPK-1 is required for the progression through meiosis I (Church et al., 1995) and other germline processes (Arur et al., 2009; Lee et al., 2007b), defective zinc storage alters but does not completely abolish MPK-1/MAPK signalling, as *kri-1(ok1251)* animals do not have observable germline defects (Ito et al., 2010). It is possible that there are different thresholds of MPK-1/MAPK activity required for IR-induced apoptosis compared to other biological events mediated by MPK-1 (Figure 5.2). This is apparent by the suppression of hyper-activated apoptosis in *let-60(ga89)/RASgf* animals on exogenous zinc (Figure 4.11B), while no other germline defects were observed.

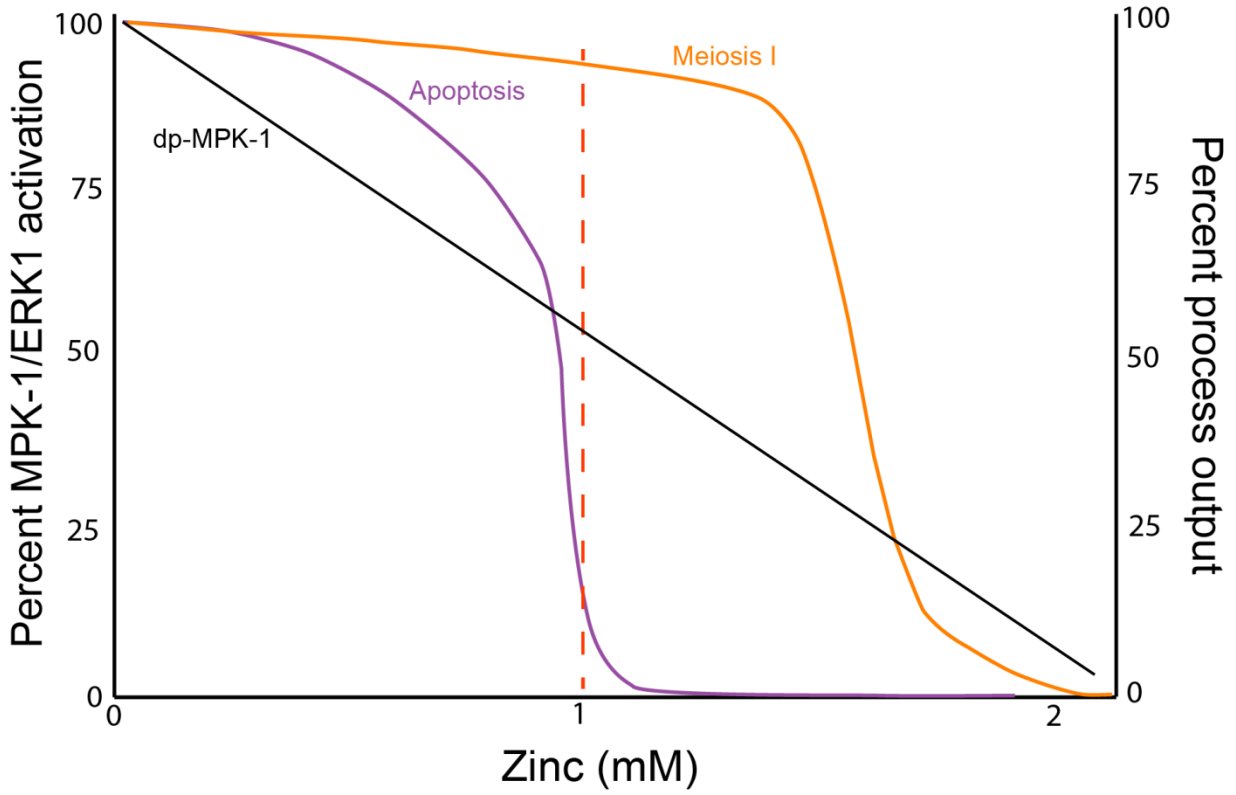

5.3 Unique MPK-1/ERK1 thresholds are required for different germline processes.
A threshold model of MPK-1/ERK1 signalling explains how *kri-1(ok1251)* mutants defective in zinc storage are resistant to IR-induced apoptosis yet do not have other observable germline defects. In this model, higher levels of activated MPK-1 are required for IR-induced apoptosis compared to other processes, such as meiotic cell cycle progression. This is consistent with the observation that supplementing *C. elegans* growth media with 1mM zinc suppresses IR-induced apoptosis without inhibiting other MPK-1-dependent germline processes.

5.2.2.3 Zinc and apoptosis

In addition to inhibiting the ERK1/MAPK pathway, zinc also prevents apoptosis in mammals by suppressing the function of the pro-apoptotic multi-BH domain proteins BAX and BAK (Ganju & Eastman, 2003), and caspases, such as Caspase-3 (Perry et al., 1997). Since I did not observe a suppression of apoptosis upon knockdown of *zipt-2.3/slc39* or increasing zinc in *ced-9(n1653)* animals with increased CED-3/Caspase activation (Spector, et al., 1997) (Figure 4.10C; Figure 4.11B), it is not likely that zinc inhibits caspases in *C. elegans* at the concentrations tested. In addition, BAX and BAK are not conserved in *C. elegans* (Dewson & Kluck, 2009), indicating that zinc must be suppressing IR-induced germ cell death by inhibiting another pathway, such as MPK-1/MAPK. Interestingly, reduced zinc levels in cultured hippocampal neurons increases ERK1/MAPK activation and apoptosis, while co-addition of zinc mitigates these observations (Pang et al., 2012). Furthermore, prolonged treatment with zinc in neuroblastoma cells inhibits ERK1/2 activation and suppresses apoptosis (An, et al., 2005). These results suggest that, at least in some contexts, the zinc-induced suppression of MPK-1/ERK1 and apoptosis I observe in the *C. elegans* germline is conserved in mammals. Zinc is also known to alter mitochondrial function (Dineley, et al., 2003). Since mitochondria are critical for apoptosis, it would be interesting to assess mitochondrial dynamics in the germlines of *kri-1(ok1251)* mutants, and if potential morphology defects can be prevented by restoring intestinal zinc storage. Altered mitochondrial morphology might weaken EGL-1/BH3-only binding to CED-9/BCL2 or prevent CED-9/BCL2 from releasing CED-4/APAF1 to form the apoptosome. Alternatively, zinc might interfere with mitochondrial fragmentation, which contributes to apoptosis in *C. elegans* (Jagasia, et al., 2005). Finally, zinc inhibits TRKA signalling in mammalian neurons (Ross et al., 1997). Since TRKA promotes cell death in conjunction with CCM2 (Harel et al., 2009), it would be interesting to determine if the *C. elegans* TRK-1 receptor promotes germ cell death, and if this is abrogated by the loss of KRI-1-K07A9.3/CCM2-mediated zinc storage.

5.2.3 KRI-1 regulates intestinal zinc storage to permit apoptosis

5.2.3.1 Zinc transporters regulate zinc storage

The inhibition of MPK-1/ERK1 and apoptosis by zinc in the absence of KRI-1 indicates the importance of proper zinc storage. Since two mechanisms to sequester zinc include binding to

MTs and transport into storage vesicles by zinc transporters, it was likely that KRI-1 was involved in at least one of these processes. My studies revealed that the zinc transporter gene *zipt-2.3* is downregulated in the absence of KRI-1 (Table 7.4; Figure 4.4). Coincidentally, while I was characterizing *zipt-2.3*, a study was published describing the transcriptional regulation of *zipt-2.3* in the intestine in response to zinc stress (Dietrich, et al., 2017). This is consistent with my observations that ZIPT-2.3 localizes to intestinal gut granules (Figure 4.5B). In eukaryotes, there are two classes of zinc transporters (Gaither & Eide, 2001). The SLC39 or "ZIP" family has 14 members in humans and *C. elegans*, including ZIPT-2.3, while the SLC30 or "ZnT" family has 10 members in humans, and 14 in *C. elegans* (Bafaro et al., 2017; Dietrich et al., 2016). Since crystal structures of zinc transporters have been ill-defined, it is unclear if zinc transport occurs by primary or secondary active transport, or by diffusion (Hojyo & Fukada, 2016). In general, SLC39 family members have eight transmembrane domains and transport zinc into the cytosol from intracellular organelles or from outside the cell, while SLC30 family members have six transmembrane domains transport zinc out of the cytosol (Hojyo & Fukada, 2016) (Figure 5.3). Since I observed a decrease of stored zinc in the vesicular gut granules of *kri-1(ok1251)* and *zipt-2.3(ok2094)* mutants (Figure 4.6A), ZIPT-2.3/SLC39 must be an exception to this rule. My results demonstrate that ZIPT-2.3 is important for the storage of intestinal zinc in vesicular gut granules, suggesting that it transports zinc from the cytosol into these vesicles.

It is surprising that ablation of a single zinc transporter, such as *zipt-2.3,* can suppress apoptosis, given that zinc-responsive transcription factors control the expression of multiple zinc transporters in response to changing zinc levels. This reveals the distinct role of ZIPT-2.3 in the fine-tuning of MAPK signalling in the context of a broader zinc homeostasis network. In addition to *zipt-2.*3, RNAseq revealed that a second zinc transporter, *K07G5.5*, was decreased more than 2-fold in *kri-1(ok1251)* animals (Table 7.4). While ablation of this gene does not suppress IR-induced apoptosis in wild type animals (data not shown), it is possible that *K07G5.5* levels are reduced in the absence of KRI-1 as a response to decreased zinc storage, or that it affects another cellular process not examined in this study. In the future, it would be interesting to ablate *K07G5.5* in *kri-1(ok1251)* mutants to determine if apoptosis sensitivity can be restored. Since zinc transporters can also regulate ions such as copper (Antala & Dempski, 2012), it is possible that the minor MPK-1/ERK1-indepdent role I observed for ZIPT-2.3 (Figure 4.8A)

might be due to altered copper localization. In support of this hypothesis, there is some data to suggest that copper regulates germ cell apoptosis in *C. elegans* (Wang, et al., 2009).

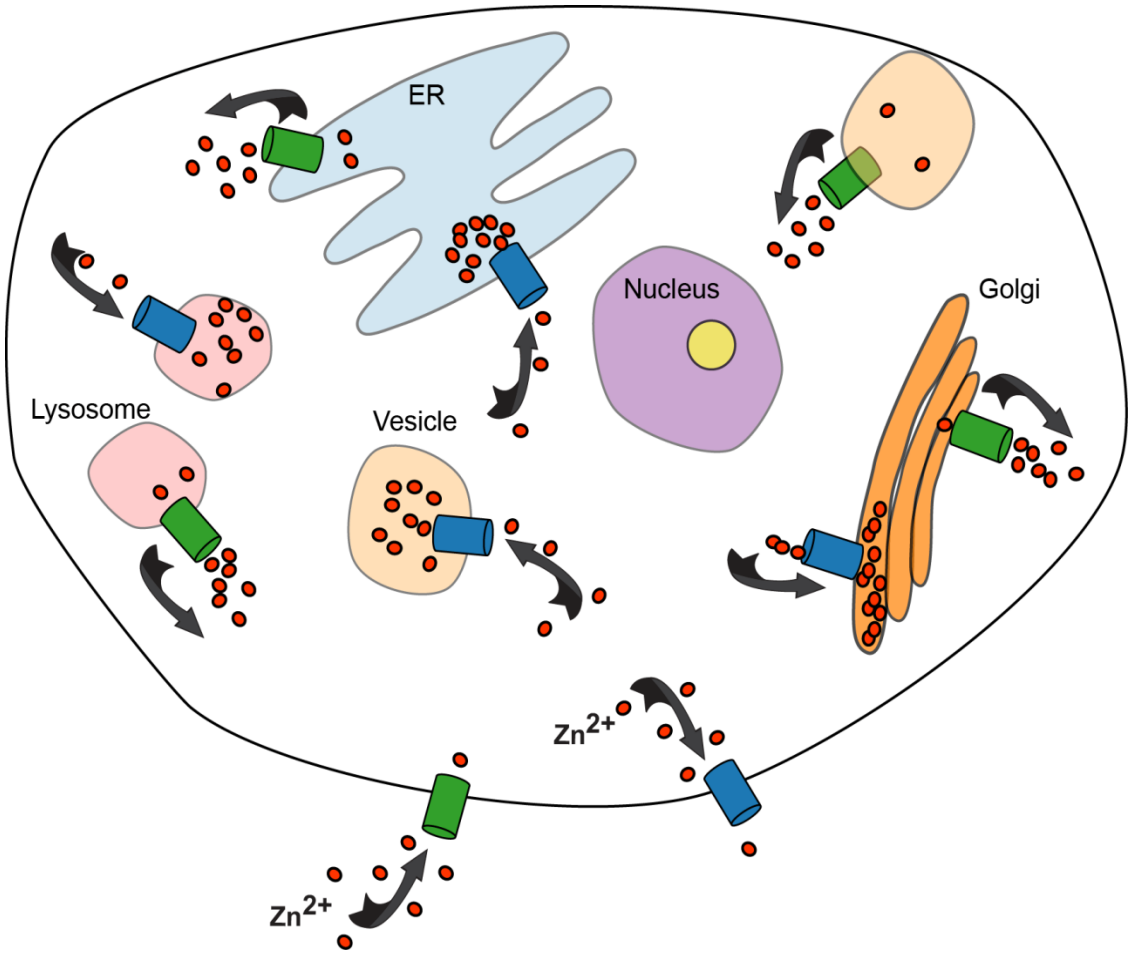

5.4 Zinc transporters and cellular zinc homeostasis.
SLC39 (ZIP) and SLC30 (ZnT) family zinc transporters are expressed in multiple cell types and organelles to regulate cellular zinc levels. Canonically, SLC39 zinc transporters (green) increase cytoplasmic zinc by import from outside the cell, or through the release of stored zinc from intracellular vesicles. Conversely, SLC30 zinc transporters (blue) decrease cytoplasmic zinc by exporting it out of the cell or promoting zinc storage in vesicles and organelles.

5.2.3.2 Zinc transporter localization

While the precise subcellular localization of many mammalian zinc transporters are not well established, these proteins have been found to associate with the plasma membrane (SLC30A1,

SLC39A1), Golgi (SLC30A7, SLC39A9), lysosomes (SLC30A10), vesicles (SLC30A6), and endoplasmic reticulum (SLC39A7) (Baltaci & Yuce, 2018) (Figure 5.4). Many of these transporters have overlapping expression patterns, while others are restricted to specific tissues (Baltaci & Yuce, 2018). *C. elegans* ZIPT-2.3 aligns most closely with SLC39A1-3 (Figure 5.5) but is functionally conserved with transporters that have vesicle expression and promote zinc storage. In *C. elegans* only six of 28 transporters have known localization. CDF-1/SLC30 is expressed at the basolateral membrane of intestinal cells and the plasma membrane of vulva cells to positively regulate the MPK-1/MAPK pathway (Bruinsma et al., 2002). SUR-7/SLC30 (**su**ppressor of let-60/**R**AS-7) localizes to the endoplasmic reticulum of somatic cells and is also a positive regulator of MPK-1/ERK1 (Yoder et al., 2004). Similar to ZIPT-2.3, CDF-2/SLC30 localizes to intestinal gut granules (Davis et al., 2009), and TTM-1/SLC30 is expressed in the apical membrane of intestinal cells (Roh et al., 2013). Since loss of TTM-1 and CDF-1 suppresses IR-induced apoptosis (Figure 4.7), it would be interesting to determine if other zinc transporters, including SUR-7, also regulate cell death. Finally, a report showing ZIPT-7.1 localization to the germline was published at the time of writing this thesis (Zhao et al. 2018). It would be intriguing to investigate if ZIPT-7.1 is required for transport of excess interstitial zinc into the germline, and specifically, if this occurs in the absence of KRI-1.

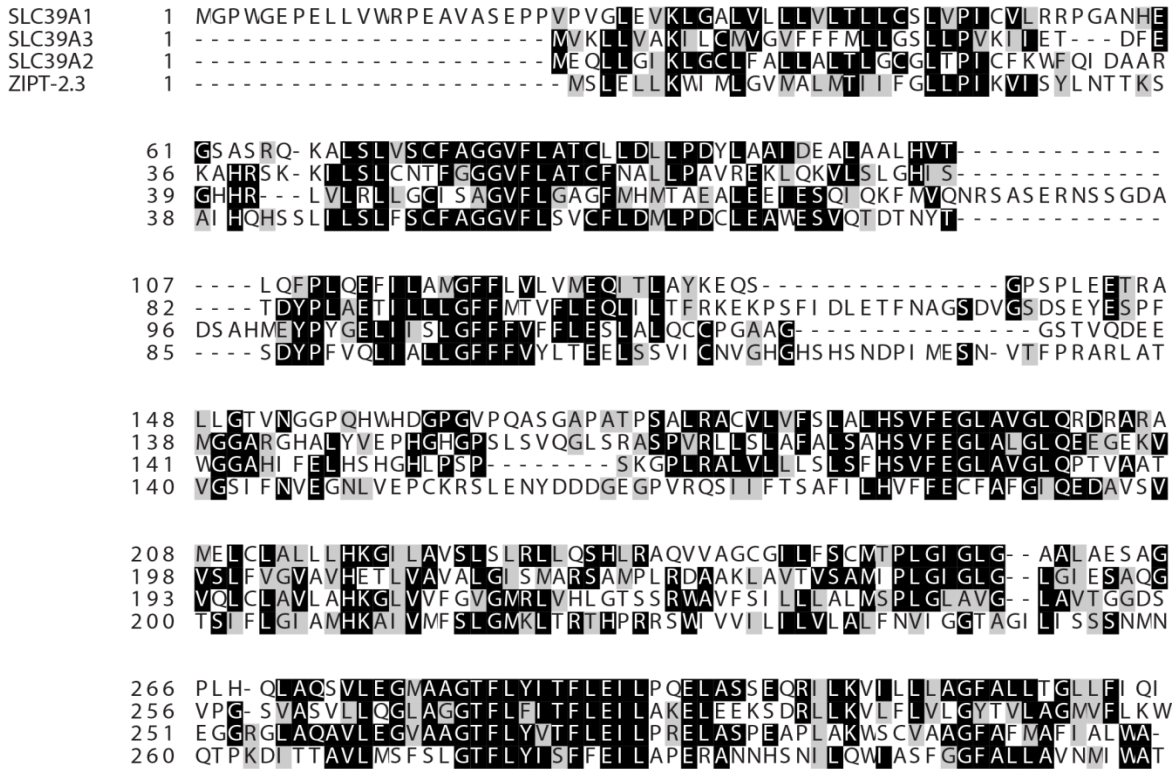

5.5 ZIPT-2.3 is most closely related to SLC39A1-3.
Alignment of *C. elegans* ZIPT-2.3 with human SLC39A1, SLC39A2, and SLC39A3 using ClustalW. Scores are 23.8 (SLC38A1), 23.9 (SLC39A2), and 23.2 (SLC39A3) and represent the number of identities divided by the length of the alignment as a percent. Black background represents identical amino acids, and grey background indicates strong similarity.

5.2.3.3 Zinc as a cell non-autonomous signalling molecule

The importance of proper zinc storage is also apparent in the context of cell non-autonomous signalling. For instance, free zinc can be released from glutamatergic neurons into the synapse resulting in Kainate (Fukushima, et al., 2003) and NMDA (***N*-methyl-D-aspartate**) receptor inhibition (Tóth, 2011). Therefore, zinc storage in these neurons is critical for proper signalling. In the mammalian intestine, zinc is secreted from paneth cells (Giblin et al., 2006), and SLC30A1 is expressed on the basolateral membrane to promote zinc secretion from enterocytes into the blood (Xiaoxi et al., 2010). Conversely, SLC39A5 imports zinc into the intestine from blood (Dufner-Beattie, et al., 2004). Thus, aberrant zinc secretion has the potential to impact multiple tissues and warrants the use of *C. elegans* to understand cell non-autonomous zinc signalling.

5.3 Implications for CCM disease

Since my work reveals the conservation of the CCM1 signalling cascade from nematodes to humans, I wondered if regulating zinc storage is a function of vertebrate KRIT1/CCM1, and if aberrant zinc localization is relevant to CCM disease. To answer these questions, I collaborated with Dr. Issam Awad's group in Chicago, IL, and Dr. Salim Abdelilah-Seyfried's team in Potsdam, Germany. The Awad group surveyed zinc transporter gene regulation in *Krit1/Ccm1*$^{-/-}$ mouse **B**rain **M**icrovascular **E**ndothelial **C**ells (BMECs) and patient CCM tissue, revealing mis-expression of several zinc transporters in both sample types. Intriguingly, a recent report described a role for endothelial-expressed SLC39A8 in regulating mouse myocardium development by promoting proper zinc localization (Lin et al., 2018). Since myocardium development is altered in a similar manner upon loss of CCM proteins in zebrafish (Renz et al., 2015; Zhou et al., 2015), and given that we found *Slc39a8* to be down-regulated in *Krit1/Ccm1* mouse BMECs (data not shown), it is possible that aberrant zinc regulation plays a role in the development of CCM disease. The Abdelilah-Seyfried lab assessed zebrafish vasculature to determine if zinc localization is altered in *krit1/ccm1* mutants. Zinc was detected in the **p**osterior **c**ardinal **v**ein (PCV) and **c**audal **v**ein (CV) of wild type animals, and this localization becomes completely abrogated in *krit1/ccm1* animals (data not shown). This demonstrates that zinc regulation is a conserved function for the CCM1 signalling complex and warrants further investigation into the role of zinc in the development of CCM lesions.

From RNA sequencing, I revealed many innate immunity genes up-regulated in *kri-1(ok1251)* animals (Figure 4.1C). This is intriguing since a recent study found that gram-negative bacteria and the gut microbiome signal through TLR4 (**T**oll-**l**ike **r**eceptor 4), which contributes to ERK5/MAPK activation in the absence of KRIT1/CCM1 (Tang et al., 2017). Since TLR4 activates the innate immune response (Takeda & Akira, 2005), it is possible that the sole Toll-like receptor in *C. elegans*, TOL-1 (Brandt & Ringstad, 2015), might regulate apoptotic signalling in conjunction with KRI-1. While no single innate immunity gene was identified from my RNA*i* screen, it is possible that many of these genes function together in the KRI-1-MPK-2/ERK5-KLF-3 cascade. Alternatively, the TOL-1/TLR receptor and innate immunity might be important for regulating other KRI-1-mediated processes, such as survival during L1 diapause, or life span extension (Berman & Kenyon, 2006).

6 Future Directions

6.1 Does K07A9.3/CCM2 physically interact with Y106G6A.1/MEKK3?

Based on my results and vertebrate models, I propose that KRI-1-K07A9.3/CCM2 binds to Y106G6A.1/MEKK3, preventing activation of the ERK5/MAPK pathway. In the future, it will be important to investigate if there is a physical association between K07A9.3/CCM2 and Y106G6A.1/MEKK3. **Co-i**mmuno**p**recipitation (Co-IP) experiments can determine if K07A9.3/CCM2 and Y106G6A.1/MEKK3 interact, which can be done with epitope-tagged proteins or antibodies generated to endogenous peptides. Since the C-terminal Harmonin Homology domain of CCM2 binds to the N-terminal PB1 region of MEKK3 (Fisher et al., 2015), recombinant K07A9.3/CCM2 and Y106G6A.1/MEKK3 proteins with deletions in these regions could be assessed for abrogated binding. Alternatively, point mutations could be made by site directed mutagenesis to identify key residues required for the interaction.

Another consideration is whether the interaction between K07A9.3/CCM2 and Y106G6A.1/MEKK3 is sufficient for the KRI-1- K07A9.3/CCM2 complex to sequester and prevent Y106G6A.1 from activating the ERK5/MAPK pathway. To determine this, Y106G6A.1 can be tagged with a fluorescent reporter, such as mCherry, and assessed if a significant ratio of Y106G6A.1 colocalizes with the KRI-1- K07A9.3/CCM2 complex. Since GFP::KRI-1 localizes to the apical membrane of intestinal cells (Berman & Kenyon, 2006), I hypothesize that most of Y106G6A.1::mCherry will also be present at this membrane. In the absence of KRI-1 or K07A9.3/CCM2, I predict that Y106G6A.1::mCherry will diffuse throughout the cytoplasm where it phosphorylates E02D9.1/MEK5 to activate the ERK5/MAPK pathway.

Since mammalian phospho-MEK5 (Hu et al., 2012) and phospho-ERK5 (Dorado et al., 2008) antibodies are commercially available, it will be useful to test them for cross-reactivity with *C. elegans* E02D9.1/MEK5 and MPK-2/ERK5. If so, these will be useful reagents to confirm whether phosphorylation of these kinases increases in the absence of KRI-1-K07A9.3/CCM2, and if this phosphorylation is dependent on Y106G6A.1/MEKK3.

6.2 Does MPK-2/ERK5 directly regulate KLF-3?

Since KLF transcription factors are regulated by vertebrate ERK5, I hypothesize that KLF-3 is downstream of MPK-2/ERK5 in the KRI-1 pathway. While I demonstrated that MPK-2/ERK5 regulates phospho-MPK-1/ERK1 in the germline, I did not do the same for KLF-3. In the future, it would be important to confirm that KLF-3 regulates the activation of germline MPK-1/ERK1 to promote apoptosis. A negative result would be surprising since MPK-2/ERK5 and KLF-3 both regulate intestinal zinc storage and apoptosis.

It also remains to be determined whether MPK-2/ERK5 regulates KLF-3 directly through phosphorylation, or indirectly. It would be useful to create a MPK-2/ERK5::mCherry translational fusion protein to determine if MPK-2/ERK5 colocalizes with KLF-3::GFP in the intestine (Zhang et al., 2009b). Since direct targets of MPK-2/ERK5 are unknown, proximity-based labeling such as the APX (**a**scorbate **p**ero**x**idase) method (Reinke, et al., 2017) could be employed to identify proteins that interact with MPK-2/ERK5. If KLF-3 is not identified, it is possible that one of the other MPK-2/ERK5-identified targets is involved in regulating KLF-3. For example, the kinase HIPK2 (**h**omeodomain-**i**nteracting **p**rotein **k**inase 2), is able to bind and phosphorylate mammalian KLF3, which reduces its ability to bind DNA and regulate transcription (Dewi et al., 2015). Since *C. elegans* contains a homologue of HIPK2, HPK-1, it is possible that HPK-1/HIPK2 is a target of MPK-2/ERK5, which would be revealed by proximity labeling.

Since KLF-3::GFP is expressed in the intestine (Zhang et al., 2009b), it would be beneficial to obtain this construct and determine if the ratio of cytoplasmic to nuclear localization changes in in the absence of KRI-1, and assess if proper distribution is restored in *kri-1(ok1251); mpk-2(ok219)* animals. This would indicate that KLF-3 is functioning downstream of MPK-2/ERK5. Finally, *in vitro* kinase assays with recombinant MPK-2/ERK5 and KLF-3 could determine if KLF-3 is phosphorylated by MPK-2/ERK5. If so, site directed mutagenesis of analogous mammalian KLF phospho-residues could potentially abrogate the ability of MPK-2/ERK5 to phosphorylate KLF-3.

6.3 How is zinc imported to inhibit germline MPK-1/ERK1?

Here, I propose a model whereby a failure to store intestinal zinc in the absence of KRI-1 results in an accumulation in the pseudocoelom, and increased zinc levels in the germline. While I have shown that exogenous zinc suppresses germ cell apoptosis (Figure 4.11) I need to prove that zinc levels are higher in *kri-1(ok1251)* mutant germlines compared to wild type animals. One possibility would be to isolate germlines and attempt zinc staining with either Fluozin-3 or Zinpyr-1. Since a protocol for this experiment has not been established, careful optimization will be required. Another method would be to collect a population of wild type and *kri-1(ok1251)* germlines in buffer, followed by permeabilization to release the zinc, and quantification using zinc-detection assays. This would be a more precise way to determine if levels of zinc increase in *kri-1(ok1251)* germlines.

If excess interstitial zinc does indeed enter the germline, it will be important to determine how import occurs. It is possible that entry is passive, by diffusion across the germline membrane, however, it is more likely that zinc uptake is active, through import by metallothioneins (MTs) or zinc transporters on the germline membrane. As mentioned previously, *C. elegans* has 28 zinc transporters, with five already known to be expressed in the soma (Dietrich et al., 2017; Dietrich, et al., 2016). This relatively small number of genes provides an opportunity to screen for germline zinc transporters using RNA*i* knockdown and CRISPR-Cas9 genome editing. Ideally, such a screen should identify genes that suppress IR-induced apoptosis in wild type animals or restore apoptosis in *kri-1(ok1251)* mutants, when ablated. The zinc transporters encoded by such genes would then be fluorescently tagged by single copy genome insertion to determine potential germline expression. As previously mentioned, a recent study identified the first *C. elegans* germline zinc transporter (Zhao et al. 2018). This transporter, ZIPT-7.1 is a good candidate for ablation in *kri-1(ok1251)* animals. In addition, *C. elegans* has two MTs (Zeitoun-Ghandour et al., 2010) which might transport interstitial zinc across the germline membrane. Knockdown of either *mtl-1* (**me**t**a**l**l**othionein-1) or *mlt-2* might restore apoptosis in *kri-1(ok1251)* mutants.

Finally, since I have demonstrated that zinc suppresses the MPK-1/MAPK pathway upstream of MPK-1/ERK1 (Figure 4.11B), it would be good to test at what step of the pathway inhibition occurs. For instance, is the phosphorylation of MEK-2/MEK in the germline abrogated in the absence of *zipt-2.3/slc39* or in the presence of excess zinc? Since mammalian phospho-MEK antibodies cross-react with *C. elegans* MEK-2 (Mizuno, et al., 2008), germline isolation and phospho-MEK immunostaining can be performed, similar to the dp-MPK-1/ERK1 experiments described in this thesis. If the phosphorylation of germline MEK-2 is not altered in *kri-1(ok1251)* mutants, then zinc does not inhibit the pathway at the level of LIN-45/RAF (Jirakulaporn & Muslin, 2004) or KSR (Yoder et al., 2004), as previously suggested. If this is the case, *in vitro* assays could be conducted to determine if zinc prevents the interaction between MEK-2/MEK and MPK-1/ERK1.

6.4 What does MPK-1/ERK1 target in the germline?

Since my RNA*i* screen of known MPK-1/ERK1 germline targets identified the EIF-3.D subunit as being required for IR-induced germ cell apoptosis, it would be ideal to follow up with this candidate to determine how the core apoptosis pathway is being regulated. Since it is possible that EIF-3.D is required for the translation of *egl-1/BH3-only*, it will be important to assess the levels of EGL-1 protein. This could be accomplished by creating an EGL-1 fusion construct with a tag that is recognized by a commercially available antibody. Additionally, germline targets of MPK-1/ERK1 could be identified by APX-based proximity labelling, as described for MPK-2/ERK5. For this experiment, I would create a strain that expresses MPK-1::APX under the control of a germline-specific promoter, since MPK-1/ERK1 is known to target different proteins in the soma compared to the germline (Sundaram, 2013). Profiles from non-irradiated and irradiated samples could be compared, followed by an RNA*i* screen to identify the targets that promote IR-induced apoptosis, and then confirmed with hypothetical phospho-antibodies. The identification of apoptosis-relevant MPK-1/ERK1 targets would aid in the elucidation of how this kinase promotes apoptosis in response to radiation.

6.5 How does PHO-1 regulate apoptosis?

In addition to *zipt-2.3/slc39,* I identified the intestinal acid phosphatase gene, *pho-1,* as a transcriptional target of KRI-1-MPK-2/ERK5 that is required for IR-induced apoptosis (Figure 4.2A). Acid phosphatases often function in lysosomes to promote the degradation of proteins, however, *pho-1* in the intestine is not restricted to lysosomes (Beh, et al., 1991). Surprisingly, *pho-1* was found to be required in the intestine but not the germline to promote embryogenesis (Fukushige, et al., 2005). This suggests that a product or pathway downstream of PHO-1 is signalling cell non-autonomously to the germline. It is possible that this same signal is required to promote IR-induced germ cell apoptosis. Alternatively, the absence of PHO-1 could result in metabolic changes (Fukushige et al., 2005), which render the germline incompetent to carry out normal processes such as cell death. Since targets of PHO-1 have not been identified (Beh et al., 1991), it is tempting to speculate that PHO-1 might inhibit the MPK-2/ERK5 pathway as part of a regulatory feedback loop downstream of KRI-1. In this case, the absence of the PHO-1 phosphatase would result in increased activation of MPK-2/ERK5 and suppression of germ cell apoptosis. It would be interesting to compare the phospho-status of E02D9.1/MEK5 and MPK-2/ERK5 in wild type and *pho-1(ca101ca102)* animals to determine if PHO-1 suppresses this pathway. If MPK-2/ERK5 is not regulated by PHO-1, the phospho-proteomes of wild type and *pho-1(ca101ca102)* animals could be compared to identify potential targets of this phosphatase.

6.6 How does KRI-1 regulate starvation stress during L1 diapause?

Since neither ZIPT-2.3 nor PHO-1 regulate survival during L1 diapause (Figure 4.3), KRI-1-MPK-2/ERK5-KLF-3 likely regulates this process through other genes that are transcriptionally regulated (Figure 4.1), but not involved in IR-induced apoptosis. Such genes could be identified in the future by screening available mutant strains for survival defects during L1 diapause.

7 Appendix

7.1 VEGF Signalling Promotes IR-induced Apoptosis

Given my interest in cell non-autonomous regulation of apoptosis, I wondered if other major cell signalling pathways in the soma can promote MPK-1/ERK1 activation and IR-induced germ cell death. One candidate is the *C. elegans* VEGF (**v**ascular **e**ndothelial **g**rowth **f**actor) homologue, PVF-1 (**P**DGF/**V**EGF growth **f**actor related-1), which is expressed in body wall muscles (Dalpe, et al., 2013). VEGF signalling has been shown to activate mammalian ERK1/2 to promote apoptosis (Narasimhan, et al., 2009), and CCM proteins regulate VEGF signalling (DiStefano, et al., 2014; He et al., 2010), providing a potential link between *C. elegans* PVF-1/VEGF and KRI-1. To test whether PVF-1 regulates germline MPK-1 and IR-induced germ cell apoptosis, I obtained *pvf-1(ev763)* mutants that have a predicted null deletion in *pvf-1/VEGF* (Dalpe, et al., 2013; Tarsitano, et al., 2006), and found that these animals have reduced germline dp-MPK-1 (Figure 7.1A) and IR-induced germ cell apoptosis (Figure 7.1B-C). Since knockdown of *ced-9/BCL2* by RNA*i* restores IR-induced apoptosis in *pvf-1(ev763)* mutants, the core apoptosis pathway is intact in these animals (Figure 7.1B). I have also confirmed that PVF-1 does not regulate engulfment (data not shown). To determine if PVF-1 is functioning in the KRI-1-MPK-2/ERK5 pathway, I created *kri-1(ok1251); mpk-2(ok219); pvf-1(ev763)* triple mutants and found that they have suppressed IR-induced apoptosis, in contrast to *kri-1(ok1251); mpk-2(ok1251)* animals (Figure 7.1C) This result suggests that PVF-1 is functioning downstream or independent of KRI-1-MPK-2/ERK5. Transcription of *pvf-1/vegf* is not regulated by KRI-1-MPK-2/ERK5 (Table 7.4) suggesting that PVF-1 is not downstream of this cascade. However, it is possible that secretion or translation of PVF-1 is regulated by KRI-1, which can be addressed by creating a fluorescently tagged protein. To assess whether PVF-1 might function through any of the four *C. elegans* VEGF receptors, VER-1,2,3,4 (**VE**GF **r**eceptor family-1,2,3,4) (Popovici, et al., 2002), I obtained strains with deletions in each of these genes (Dalpe et al., 2013), and observed resistance to IR-induced apoptosis (Figure 7.1D) It is possible that all four receptors function downstream of PVF-1/VEGF (Dalpe et al., 2013). Finally, I have completed mRNA sequencing of *pvf-1(ev763)* animals post 60 Gy IR, in biological triplicate, which has revealed genes that are mis-regulated compared to wild type animals (Figure 7.1E).

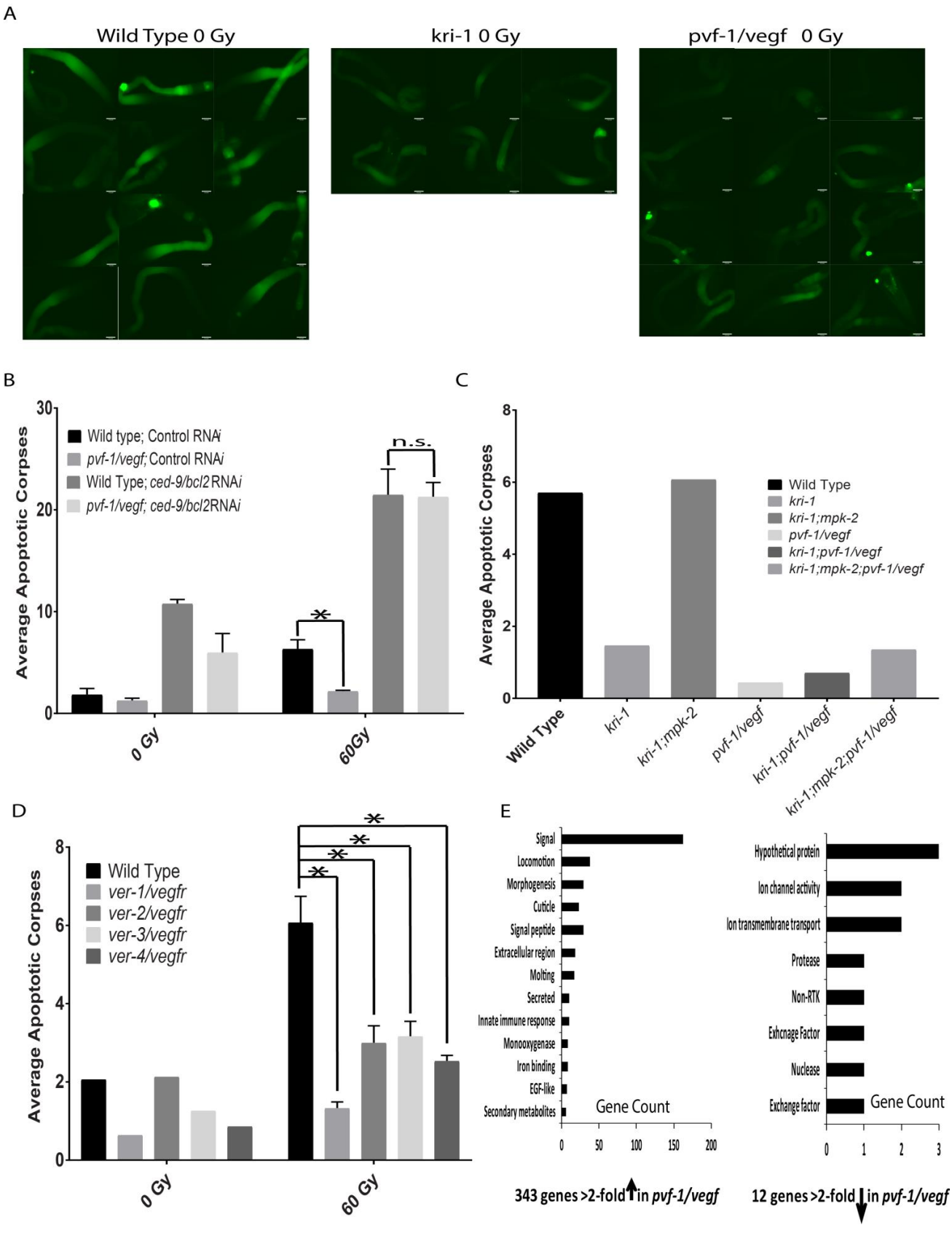
A
Wild Type 0 Gy
kri-1 0 Gy
pvf-1/vegf 0 Gy
B
Average Apoptotic Corpses
Wild type; Control RNAi
pvf-1/vegf; Control RNAi
Wild Type; ced-9/bcl2 RNAi
pvf-1/vegf; ced-9/bcl2RNAi
n.s.
0 Gy
60Gy
C
Average Apoptotic Corpses
Wild Type
kri-1
kri-1;mpk-2
pvf-1/vegf
kri-1;pvf-1/vegf
kri-1;mpk-2;pvf-1/vegf
D
Average Apoptotic Corpses
Wild Type
ver-1/vegfr
ver-2/vegfr
ver-3/vegfr
ver-4/vegfr
0 Gy
60 Gy
E
Signal
Locomotion
Morphogenesis
Cuticle
Signal peptide
Extracellular region
Molting
Secreted
Innate immune response
Monooxygenase
Iron binding
EGF-like
Secondary metabolites
Gene Count
343 genes >2-fold in pvf-1/vegf
Hypothetical protein
Ion channel activity
Ion transmembrane transport
Protease
Non-RTK
Exhcnage Factor
Nuclease
Exchange factor
Gene Count
12 genes >2-fold in pvf-1/vegf

Figure 7.1. VEGF signalling promotes IR-induced apoptosis. A) Activated di-phosphorylated MPK-1/ERK1 in germlines of non-irradiated wild type, *kri-1(ok1251),* and *pvf-1(ev763)* animals. Germlines were isolated 24hrs past the fourth larval stage. B) IR-induced germ cell apoptosis quantified in wild type; control RNA*i*, *pvf-1(ev763);* control RNA*i*, wild type; *ced-9* RNA*i*, and *pvf-1(ev763); ced-9* RNA*i* animals. C) IR-induced germ cell apoptosis quantified in wild type, *kri-1(ok1251), kri-1(ok1251); mpk-2(ok219), pvf-1(ev763), kri-1(ok1251); pvf-1(ev763),* and *kri-1(ok1251); mpk-2(ok219); pvf-1(ev763)* animals. D) IR-induced germ cell apoptosis quantified in wild type, *ver-1, ver-2, ver-3,* and *ver-4* animals. Apoptotic corpses in (B-D) were quantified 24 hours post irradiation (60 Gy) or in the absence of radiation (0 Gy) (B & D). Graph B represents two independent replicates, and at least 30 worms per strain, per condition. Graph C represents one experiment, and at least 15 worms per strain, per condition. The 60Gy condition in Graph D represents three independent replicates, and at least 45 worms per strain, per condition, while the 0 Gy condition represents one experiment and at least 15 worms per strain, per condition. Bars represent mean +/- standard deviation. *P<0.05, two-sided, unpaired t-test. E) 343 genes were found to be up-regulated more than two-fold in *pvf-1(ev763)* mutants, while only 12 genes were down-regulated more than two-fold, compared to wild type animals. The program DAVID was used to group these genes into categories based on predicted or known function.

7.2 Significant P-values

Table 7.1 Significant P-values

Figure	Condition	P-value
Figure 3.1B		0.00287
Figure 3.1D		2.15896E-06
Figure 3.2		0.046768
Figure 3.3	*kri-1(ok1251) rho-1* RNA*i* 0Gy and 60Gy	0.000972
Figure 3.3	Wild type and *kri-1(ok1251) rho-1* RNA*i* 60Gy	0.004127
Figure 3.5		0.008909
Figure 3.8A		4.39551E-05
Figure 3.8B		0.000112
Figure 3.9A	*let-60(ga89)* and *kri-1(ok1251); let-60(ga89)* 60Gy	0.004483

Figure 3.9A	*kri-1(ok1251)* and *kri-1(ok1251); let-60(ga89)* 60Gy	0.040321
Figure 3.10B	*kri-1(ok1251);lip-1(zh15)* control and *eif-3.d* RNA*i* 60Gy	0.000146
Figure 3.10B	*kri-1(ok1251);lip-1(zh15)* control and *zim-2* RNA*i* 60Gy	0.016716987
Figure 3.10B	*kri-1(ok1251);lip-1(zh15)* control and *pac-1* RNA*i* 60Gy	0.027058935
Figure 3.16A	*kri-1(ok1251)* control and *Y106G6A.1* RNA*i* 60Gy	0.000984
Figure 3.16A	*kri-1(ok1251)* control and *E02D9.1* RNA*i* 60Gy	0.002229
Figure 3.16A	*kri-1(ok1251)* control and *mpk-2* RNA*i* 60Gy	0.001379
Figure 3.16C		0.007662
Figure 3.17A		6.38083E-21
Figure 3.17B		7.61793E-11
Figure 3.17C		0.036709
Figure 3.18B		0.001376
Figure 3.18C		0.032326
Figure 3.20A	Wild type control and *kri-1* RNA*i* 60Gy	0.000133
Figure 3.20A	Wild type control and *K07A9.3* RNA*i* 60Gy	0.028177
Figure 3.20A	Wild type control and *Y45F10D.10* RNA*i* 60Gy	0.024217
Figure 3.20C	*sid-1(qt9)* control and *kri-1* RNA*i* 60Gy	0.002461
Figure 3.20C	*sid-1(qt9)* control and *K07A9.3* RNA*i* 60Gy	0.012892
Figure 3.20C	*sid-1(qt9)* control and *Y45F10D.10* RNA*i* 60Gy	0.011138
Figure 4.2A	Wild type control and *pho-1* RNA*i* 60Gy	0.010128
Figure 4.2A	Wild type control and *zipt-2.3* RNA*i* 60Gy	0.007312
Figure 4.2C		9.08454E-07
Figure 4.2D		0.004378
Figure 4.4A	Wild type and *kri-1(ok1251) zipt-2.3* expression 0 Gy	0.008111

Figure 4.4A	Wild type and *kri-1(ok1251) zipt-2.3* expression 60 Gy	0.014308
Figure 4.4A	Wild type and *kri-1(ok1251);mpk-2(ok219) zipt-2.3* expression 60 Gy	0.008961
Figure 4.4B	Wild type and *kri-1(ok1251) zipt-2.3* expression 0 Gy	0.004933
Figure 4.4B	Wild type and *kri-1(ok1251) zipt-2.3* expression 60 Gy	0.000695
Figure 4.7	Wild type control and *ttm-1(ok3503)* 60Gy	0.000107
Figure 4.7	Wild type control and *cdf-1(n2527)* 60Gy	0.01505
Figure 4.8A	Wild type control and *zipt-2.3* RNA*i* 60Gy	0.002713
Figure 4.8A	*kri-1(ok1251);mpk-2(ok219)* control and *zipt-2.3* RNA*i* 60Gy	0.00121
Figure 4.8A	*kri-1(ok1251);let-60(ga89)* control and *zipt-2.3* RNA*i* 60Gy	0.005697
Figure 4.8A	*kri-1(ok1251);lip-1(zh15)* control and *zipt-2.3* RNA*i* 60Gy	0.016154
Figure 4.8A	Wild type and *kri-1(ok1251);lip-1(zh15)* on *zipt-2.3* RNA*i* 60Gy	0.000504
Figure 4.8B	Wild type control and *zipt-2.3* RNA*i* 60Gy	0.000222
Figure 4.8B	*klf-3(on34)* control and *zipt-2.3* RNA*i* 60Gy	0.000388
Figure 4.8B	*kri-1(ok1251);klf-3(on34)* control and *zipt-2.3* RNA*i* 60Gy	0.003116
Figure 4.11A	Wild type on 0mM and 1mM zinc 60Gy	0.01471
Figure 4.11B	Wild type on 0mM and 1mM zinc 60Gy	0.045706
Figure 4.11B	*let-60(ga89)* on 0mM and 1mM zinc 60Gy	0.006032

7.3 AP-MS Spectral Counts

Table 7.2 AP-MS spectral counts

	KRI-1 0Gy				KRI-1 60Gy				
Prey	**Spectral Counts 3 replicates**	**Average Spectral Count**	**Saint Score**	**Bayesian false discovery rate (BFDR)**	**Spectral Counts 3 replicates**	**Average Spectral Count**	**Saint Score**	**BFDR**	**Control Counts (12 sets)**
HSP-17	N/A	N/A			87|16|54	52.33	0.67	0.04	5|3|12|8|6|12|0|0|0|0|0|0
F37C4.5	49|25|40	38	1	0	56|26|30	37.33	1	0	0|0|0|0|0|0|0|0|0|0|0|0
Y45F10D.10	65|24|15	34.67	1	0	66|26|19	37	1	0	0|0|0|0|0|0|0|0|0|0|0|0
K07A9.3	35|28|39	34	1	0	35|27|34	32	1	0	0|0|0|0|0|0|0|0|0|0|0|0
HIP-1	3|11|4	6	0.82	0.02	7|3|6	5.33	0.86	0	1|0|0|1|0|0|0|0|0|0|0|0

7.4 AP-MS Normalized Spectral Counts

Table 7.3 AP-MS normalized spectral counts

Protein Name	Average Spectral Counts 0 Gy	Average Spectral Counts 60 Gy	Protein Mass (kDa)	Normalized Spectral Counts 0 Gy	Normalized Spectral Counts 60 Gy
HSP-17	0	52.33	17.6	0	2.97
F37C4.5	38	37.33	61.4	0.62	0.61
Y45F10D.10	34.67	37	17.5	1.98	2.11
K07A9.3	34	32	28.7	1.18	1.11
HIP-1	6	5.33	44.7	0.13	0.12

7.5 RNAseq: Significant genes *kri-1(ok1251)*

Table 7.4 RNAseq: significant genes *kri-1(ok1251)*

Gene Name	Locus	Wild Type FPKM	*kri-1 (ok1251)* FPKM	log2 Fold Change	P value	Q value
F33E11.7	V:318953-319050	134.751	0	N/A	0.00135	0.018306
R74.11	III:4190496-4190640	15.8862	0	N/A	0.00315	0.035708
Y102A5C.36	V:16926926-16927447	20.8543	0	N/A	5.00E-05	0.001092
Y102A5C.5, Y102A5C.6	V:16928327-16930098	19.2112	0.142083	-7.07907	0.0001	0.002025
fat-7	V:7145655-7159188	40.7604	1.18615	-5.10281	5.00E-05	0.001092
cpt-3	III:2082818-2088272	1.19123	0.056302	-4.40312	0.00285	0.033288
sdz-24	II:658668-659867	1.99773	0.099809	-4.32305	0.0003	0.005333

vit-3	X:3567396-3572566	570.126	31.3001	-4.18704	5.00E-05	0.001092
ilys-5	X:6516306-6536845	1147.26	63.9787	-4.16445	5.00E-05	0.001092
clec-166	IV:1247385-1251517	3.3104	0.189025	-4.13035	5.00E-05	0.001092
clec-218	V:8307969-8310878	10.4379	0.621689	-4.0695	5.00E-05	0.001092
Y45G12C.1	V:2565683-2570743	2.02835	0.127168	-3.9955	0.0007	0.010705
clec-10	II:402659-404235	9.84056	0.648144	-3.92435	5.00E-05	0.001092
pud-3	V:2324509-2327262	12.1165	0.820443	-3.88443	5.00E-05	0.001092
clec-52	IV:8167162-8168774	7.51704	0.540548	-3.79767	5.00E-05	0.001092
K11G9.3	V:6669822-6672038	1.89146	0.152798	-3.62981	5.00E-05	0.001092
lipl-3	V:521675-524218	1.83124	0.15288	-3.58235	0.00015	0.002918
vit-1	X:7727900-7733308	998.293	86.2405	-3.53303	5.00E-05	0.001092
pud-4	V:2324509-2327262	8.53458	0.751687	-3.50512	0.00125	0.017212
lys-4	IV:11621442-11623124	452.457	42.5484	-3.4106	5.00E-05	0.001092
scl-2	IV:13057677-13059092	96.6659	11.2278	-3.10594	5.00E-05	0.001092
cyp-25A1	III:3832599-3834589	14.5353	1.71009	-3.08742	5.00E-05	0.001092
E02H4.7	X:14256270-14257422	15.8473	1.88689	-3.07016	5.00E-05	0.001092
C42D4.2	IV:7180543-7182993	3.57514	0.441387	-3.01788	5.00E-05	0.001092
F40H7.12	II:3687790-3688691	3.89267	0.54699	-2.83117	5.00E-05	0.001092
cpr-5	V:1132596-1133993	209.494	30.5915	-2.77571	5.00E-05	0.001092
C30G12.2	II:7290372-7291943	20.0043	3.13807	-2.67236	5.00E-05	0.001092
unc-49	III:10520675-10532706	51.7403	8.22361	-2.65344	5.00E-05	0.001092
T16G1.6	V:12935535-12937187	2.42504	0.389375	-2.63878	5.00E-05	0.001092
F14D7.6	V:14301420-14306871	12.5242	2.06768	-2.59863	5.00E-05	0.001092

col-43	V:8049743-8050893	2.31478	0.38878	-2.57385	5.00E-05	0.001092
F26C11.1	II:9895544-9897339	1.72391	0.304792	-2.49979	5.00E-05	0.001092
E01G6.3	X:12241715-12244652	1.61192	0.30654	-2.39464	5.00E-05	0.001092
lipl-2	V:9791570-9793391	2.28603	0.439611	-2.37854	5.00E-05	0.001092
oac-20	V:15978715-15982854	2.63898	0.529232	-2.31801	0.0001	0.002025
lys-6	IV:11626909-11627947	10.8793	2.40455	-2.17775	5.00E-05	0.001092
dod-23	II:8398159-8399160	401.759	91.9407	-2.12755	5.00E-05	0.001092
W03D8.8	I:2791688-2794895	3.10215	0.715458	-2.11633	5.00E-05	0.001092
ugt-30	V:15121728-15125214	1.59063	0.389376	-2.03036	0.00015	0.002918
ugt-53	V:2849351-2852031	8.36722	2.13186	-1.97264	5.00E-05	0.001092
spp-17	I:1016404-1017180	1994.66	512.742	-1.95984	5.00E-05	0.001092
ZK550.2	IV:17245597-17249749	8.70729	2.2399	-1.95879	5.00E-05	0.001092
gst-10	V:2561689-2564708	27.4036	7.18711	-1.93088	5.00E-05	0.001092
ugt-6	V:12795480-12798154	3.92724	1.04558	-1.90922	5.00E-05	0.001092
ZK228.4	V:18462803-18465320	21.4393	5.71503	-1.90742	5.00E-05	0.001092
Y69A2AR.12	IV:2568467-2572317	1.10391	0.298239	-1.88808	0.00015	0.002918
cpr-1	V:11975514-11976759	489.475	134.27	-1.8661	5.00E-05	0.001092
B0507.8	V:8760686-8763194	1.03214	0.291031	-1.8264	0.00145	0.01944
T01D3.6	V:13716848-13720402	34.2641	9.83019	-1.80141	5.00E-05	0.001092
lys-10	IV:8332825-8333559	8.25238	2.4306	-1.7635	0.00025	0.004581
oac-54	II:9158107-9159874	3.20931	0.955743	-1.74757	5.00E-05	0.001092
ugt-43	IV:10464658-10467240	1.67932	0.501183	-1.74447	0.0003	0.005333
F55E10.6	X:8344699-8346359	11.4683	3.5012	-1.71173	5.00E-05	0.001092

M04C9.4	I:9355071-9357079	1.45824	0.445295	-1.71139	0.0004	0.006764
lys-7	V:3481418-3482600	225.51	69.2924	-1.70242	5.00E-05	0.001092
tsp-10	II:6718534-6723951	7.05617	2.16942	-1.70158	0.00025	0.004581
daao-1	IV:2614199-2617192	5.26879	1.64582	-1.67867	5.00E-05	0.001092
F38A1.9,clec-165	IV:1244246-1246957	2.19778	0.703275	-1.64389	0.0042	0.044827
col-165	X:4353617-4354811	4.6168	1.48269	-1.63868	0.00035	0.006018
fat-5	V:17723779-17730381	18.0972	5.81929	-1.63685	5.00E-05	0.001092
dhs-26	X:3360684-3362493	4.8737	1.56796	-1.63613	5.00E-05	0.001092
ifc-1	V:2881392-2883754	9.74499	3.25161	-1.58351	5.00E-05	0.001092
Y116F11A.6	V:19727480-19727922	15.6174	5.26003	-1.57001	0.00075	0.011348
ZK673.1	II:10443326-10445156	30.5756	10.3189	-1.56709	0.0003	0.005333
ZC266.1	V:4694969-4700289	7.51959	2.58204	-1.54214	5.00E-05	0.001092
C44C1.5	X:975525-978445	30.9054	10.6209	-1.54096	5.00E-05	0.001092
cyp-35A5	V:3936373-3938496	1.96413	0.675882	-1.53905	0.0002	0.003787
F14E5.1	II:8417662-8419754	1.52344	0.537521	-1.50294	0.00125	0.017212
unc-103	III:4115322-4147279	6.31044	2.23592	-1.49687	5.00E-05	0.001092
vit-5	X:3403470-3408605	1423.23	508.141	-1.48587	5.00E-05	0.001092
ZK1240.5	II:2316162-2318124	1.2984	0.467098	-1.47494	0.00255	0.030847
asp-8	V:3024218-3027933	2.60003	0.936791	-1.47273	0.00025	0.004581
ttr-44	V:13523529-13530744	39.9006	14.4225	-1.46809	5.00E-05	0.001092
gba-4	IV:5344590-5350929	34.5309	12.6992	-1.44315	5.00E-05	0.001092
pqn-73	II:8540719-8545452	1.40537	0.518399	-1.43882	0.0001	0.002025
clec-26	V:16848633-16850196	1.89045	0.699508	-1.43432	0.0013	0.017798
cyp-14A2	X:13267604-13269697	0.878041	0.325279	-1.43261	0.0039	0.042453

C10C5.4	IV:9378602-9380450	20.5355	7.77336	-1.40151	5.00E-05	0.001092
T05E12.3	V:17076864-17077978	14.2426	5.41869	-1.39419	5.00E-05	0.001092
dhs-25	X:1486492-1494356	96.5948	37.8343	-1.35225	5.00E-05	0.001092
spp-4	X:7318274-7318776	73.8469	29.1765	-1.33973	5.00E-05	0.001092
cutl-28	IV:684496-688339	0.74655	0.295414	-1.3375	0.0034	0.037998
cyp-35C1	V:13896656-13898488	11.6888	4.65523	-1.3282	5.00E-05	0.001092
clec-170	IV:1266865-1274371	2.71861	1.08649	-1.3232	0.00045	0.007424
C08B6.2	V:10105711-10107392	1.33014	0.535851	-1.31168	0.00255	0.030847
F31D4.8	V:20866752-20868429	9.71249	3.94172	-1.30101	0.00035	0.006018
asns-2	X:8748430-8750969	17.3013	7.02723	-1.29985	5.00E-05	0.001092
lipl-5	V:385736-388090	215.89	89.1547	-1.27591	5.00E-05	0.001092
F23F12.13	III:6495676-6498177	1.65172	0.684851	-1.27011	0.00115	0.016068
irg-2	V:4042403-4043600	2.32599	0.970106	-1.26163	0.00455	0.047775
dhs-23	V:15381096-15382305	4.11585	1.71907	-1.25956	0.00115	0.016068
C33G8.3	V:7007300-7008339	10.8717	4.54484	-1.25828	0.00155	0.020606
F09B12.3	X:15095334-15097954	26.7354	11.1949	-1.25592	5.00E-05	0.001092
ptr-22	V:18919233-18931381	1.07063	0.45168	-1.24509	0.00115	0.016068
F22H10.6	X:16689319-16690860	49.8727	21.4671	-1.21613	5.00E-05	0.001092
F31F4.1	V:684088-686289	3.60945	1.55475	-1.21509	0.0017	0.022267
K07G5.5	I:7170025-7172189	6.61891	2.86318	-1.20898	0.00035	0.006018
F32A5.3	II:7232852-7238349	27.8117	12.0753	-1.20363	5.00E-05	0.001092
Y54G9A.4 (*zipt-2.3*)	II:13713018-13715872	4.03322	1.76528	-1.19204	0.00195	0.024679
ZK822.1	IV:11918109-11922128	1.10491	0.485696	-1.1858	0.00225	0.027688

fpn-1.2	V:1462012-1464777	3.10506	1.38549	-1.16422	0.00105	0.014995
F42A10.7	III:6177914-6178702	20.6649	9.2947	-1.1527	5.00E-05	0.001092
frm-7	V:12302483-12306972	68.1039	30.6418	-1.15224	5.00E-05	0.001092
F22F7.8	V:2120683-2121942	52.1072	23.709	-1.13605	0.00115	0.016068
pcp-3	IV:9155078-9159019	19.9207	9.10909	-1.12889	5.00E-05	0.001092
T16G1.7	V:12932940-12935052	3.31843	1.52174	-1.12478	0.0017	0.022267
daf-36	V:10222306-10225722	15.3007	7.03819	-1.12032	5.00E-05	0.001092
clec-265	X:3031722-3033203	18.5804	8.56301	-1.11759	5.00E-05	0.001092
nhr-114	V:4175886-4191515	118.816	54.9412	-1.11278	0.0015	0.020016
Y113G7B.12	V:20208683-20212451	2.29027	1.06421	-1.10573	0.0002	0.003787
aqp-1	II:7232852-7238349	27.0157	12.5681	-1.10403	0.00455	0.047775
clec-65	II:12901293-12903335	107.096	49.8531	-1.10315	5.00E-05	0.001092
R09E10.5	IV:10295407-10302310	1.76283	0.821287	-1.10193	0.00045	0.007424
odc-1	V:6898540-6900223	22.057	10.4445	-1.07849	5.00E-05	0.001092
oac-6	V:16302747-16306156	3.41632	1.62043	-1.07606	0.00045	0.007424
C46F2.1	X:8078062-8080253	5.45809	2.59553	-1.07237	0.0018	0.023277
T16G12.1,T16G12.7	III:10038532-10049859	6.85023	3.28238	-1.06141	5.00E-05	0.001092
pho-1	II:5231423-5235926	33.8303	16.3236	-1.05135	5.00E-05	0.001092
C53A3.2	V:5762333-5763846	3.91101	1.8997	-1.04177	0.0022	0.027238
clec-8	II:12575690-12577722	3.87109	1.89511	-1.03046	0.00235	0.028745
R10E8.6	V:18258995-18266364	1.22623	0.606877	-1.01475	0.0016	0.021211
Y32F6B.1	V:10478589-10484740	7.89739	3.90912	-1.01453	0.00085	0.012567
lea-1	V:10011870-10031094	473.029	234.225	-1.01403	5.00E-05	0.001092

T28H10.3	V:12513020-12517205	90.511	181.936	1.00727	5.00E-05	0.001092
T19H12.3	V:4885696-4886809	21.3087	42.8359	1.00738	0.0005	0.00809
srx-134,ttr-21	V:13853833-13856476	2.81752	5.67031	1.009	0.0008	0.011965
sph-1	IV:8130566-8133692	16.7217	33.7005	1.01105	0.0029	0.033789
M60.2	X:8242055-8247882	47.4304	95.8764	1.01536	5.00E-05	0.001092
C26B9.5	X:5329454-5332339	33.7403	68.261	1.01659	5.00E-05	0.001092
C27D6.12	II:5171909-5177996	33.8469	68.5218	1.01754	0.00375	0.04123
ugt-44	IV:10469762-10471890	21.7003	44.071	1.02211	5.00E-05	0.001092
pqn-31	V:9109602-9111019	5.16159	10.4946	1.02376	0.0002	0.003787
qua-1	II:8198802-8204005	0.8155	1.65856	1.02418	0.00075	0.011348
F22E12.1,Y32F6A.5	V:10446533-10457347	110.911	225.665	1.02478	5.00E-05	0.001092
ZK1320.2	II:9657875-9659002	125.208	255.132	1.02691	5.00E-05	0.001092
nlp-8	I:7800459-7801822	6.18341	12.6234	1.02963	0.0006	0.00946
linc-8	II:2501837-2503802	7.05403	14.4083	1.03038	0.00015	0.002918
pgp-1	IV:12591695-12599169	3.31506	6.77463	1.03111	5.00E-05	0.001092
fipr-1	V:12358646-12363691	32.3359	66.1363	1.03231	0.0007	0.010705
cyp-33E2	IV:8612391-8614647	4.61324	9.43834	1.03275	5.00E-05	0.001092
-	III:6628270-6631527	2.51309	5.14236	1.03297	5.00E-05	0.001092
tag-290	V:11613306-11614876	6.44563	13.2053	1.03473	0.0004	0.006764
W02D9.10	I:12551537-12552370	18.8536	38.6325	1.03498	5.00E-05	0.001092
C18A11.1	X:8069504-8070289	14.6828	30.0925	1.03528	0.0004	0.006764
F09E10.14,tts-1	X:1504130-1504998	767.703	1575.42	1.03712	5.00E-05	0.001092

flp-26	X:7029135-7029639	11.1329	22.8562	1.03775	0.00225	0.027688
fbxa-190	X:1372011-1374630	1.29638	2.67038	1.04255	0.0034	0.037998
F57C2.4	II:14525311-14526033	367.05	756.545	1.04345	5.00E-05	0.001092
aqp-7	X:3025061-3026971	63.8638	131.843	1.04575	5.00E-05	0.001092
nlp-33	V:11147343-11147810	64.7125	133.867	1.04869	5.00E-05	0.001092
B0302.5	X:17193297-17195118	23.4619	48.615	1.05108	5.00E-05	0.001092
C45G9.13	III:5042425-5044674	5.19271	10.7701	1.05247	0.0035	0.038932
F42G4.5	II:13073492-13076225	10.9296	22.6827	1.05335	5.00E-05	0.001092
F22B8.7	V:16095223-16097320	11.7581	24.4053	1.05353	5.00E-05	0.001092
col-167	X:6323296-6324517	1.50226	3.12159	1.05515	0.0046	0.048193
ugt-2	V:10398809-10401313	3.78757	7.88755	1.0583	0.0001	0.002025
F47B10.5	X:10889080-10890526	10.6314	22.15	1.05897	0.00115	0.016068
ram-2	II:11015587-11016842	9.15592	19.0833	1.05954	5.00E-05	0.001092
F55F3.2	X:13760289-13763993	6.68261	13.9329	1.06001	5.00E-05	0.001092
M02D8.6	X:8731273-8731911	8.07174	16.8333	1.06037	0.0007	0.010705
mpst-3	V:14895646-14899019	17.9158	37.4195	1.06256	5.00E-05	0.001092
tat-2	IV:4827853-4846893	1.30241	2.72512	1.06513	0.0002	0.003787
C18H7.11	IV:596890-601695	2.67584	5.60338	1.06631	0.00065	0.010148
C45G9.6,klp-6	III:5030928-5040402	21.4182	44.9897	1.07076	5.00E-05	0.001092
F07C6.2	IV:12791170-12791808	4.6766	9.845	1.07393	0.00425	0.045158
pqm-1	II:11142750-11152600	16.1136	33.9661	1.07582	5.00E-05	0.001092
ZC196.5	V:8729457-8732789	2.30101	4.85213	1.07635	0.00025	0.004581
C14H10.3	X:10220645-10228142	9.64371	20.3554	1.07775	5.00E-05	0.001092
ZC443.4	V:12816920-12819545	2.38258	5.0305	1.07818	0.0003	0.005333

F59C6.14	I:10526601-10530094	8.47315	17.8971	1.07876	0.0039	0.042453
T23B12.11	V:8455395-8457606	9.36489	19.8035	1.08043	0.0009	0.013143
C11E4.7	X:9617246-9619093	4.8418	10.2401	1.08061	0.00025	0.004581
scd-2	V:6633268-6639658	0.479564	1.01431	1.0807	0.00165	0.021692
ttr-23	V:10589091-10589958	4.18024	8.84583	1.08141	0.00215	0.026712
nlp-24	V:11616282-11618266	69.4983	147.184	1.08257	5.00E-05	0.001092
Y43C5A.3	IV:10274035-10275411	17.1132	36.3086	1.0852	5.00E-05	0.001092
F10D7.2	X:17359769-17368642	5.72825	12.1572	1.08564	5.00E-05	0.001092
Y75B8A.28	III:12319107-12323868	6.20244	13.1777	1.08719	5.00E-05	0.001092
nlp-3	X:13177853-13178454	12.2159	25.9844	1.08889	0.00035	0.006018
F11A5.9	V:16214889-16218605	32.4226	69.2636	1.0951	5.00E-05	0.001092
T05E12.6	V:17084997-17090023	144.828	309.633	1.09622	5.00E-05	0.001092
K02E11.7	V:14253487-14254320	5.89823	12.6182	1.09715	0.00255	0.030847
C24B5.4	V:9191616-9197309	4.05427	8.6769	1.09774	0.00075	0.011348
nspc-10	X:12343613-12344043	89.2842	191.193	1.09855	5.00E-05	0.001092
col-124	IV:10214983-10232552	390.926	837.873	1.09984	0.0014	0.018912
F53A9.6	X:8713462-8713952	26.3561	56.6002	1.10267	5.00E-05	0.001092
K02E2.6	V:20380579-20382036	9.11086	19.5728	1.10319	0.00105	0.014995
ugt-54	IV:10761639-10764424	1.81071	3.90031	1.10704	0.001	0.01447
T05B11.4	V:7751897-7754139	4.43619	9.57222	1.10953	5.00E-05	0.001092
T11F9.12	V:11493555-11496548	10.9334	23.5921	1.10956	5.00E-05	0.001092
clec-84	IV:2842473-2845595	28.7404	62.0692	1.1108	5.00E-05	0.001092

F22H10.2	X:16678487-16679823	32.6704	70.5602	1.11087	0.0005	0.00809
best-24	III:7898980-7904476	4.7264	10.2385	1.11519	5.00E-05	0.001092
F47B8.2	V:14315853-14316624	11.8722	25.7355	1.11617	0.0001	0.002025
lips-16	II:12610312-12612357	1.38615	3.01794	1.12248	0.00415	0.044394
nspc-9	X:12342954-12343355	90.2662	196.724	1.12391	5.00E-05	0.001092
B0205.12	I:10730466-10730712	253.75	553.568	1.12535	0.0009	0.013143
T01G5.8	V:15116267-15116595	83.9522	183.849	1.13088	0.0007	0.010705
clec-205	V:1760892-1765301	3.69449	8.10066	1.13266	5.00E-05	0.001092
B0344.1	X:1597050-1597835	3.0633	6.71672	1.13267	0.0019	0.024197
drr-1	II:13495048-13495896	18.561	40.7914	1.13599	5.00E-05	0.001092
Y34F4.2	III:1010534-1011374	10.3995	22.9155	1.13981	0.00075	0.011348
daf-28	V:19815444-19816219	10.4547	23.0648	1.14154	0.0029	0.033789
M110.10	II:8214062-8214467	9.76296	21.5418	1.14175	0.0021	0.026205
K02E11.6	V:14250626-14251508	2.98545	6.5992	1.14434	0.0026	0.030952
C34D10.2	X:8014247-8031616	13.4927	29.8381	1.14498	5.00E-05	0.001092
D2096.1	IV:8396502-8397958	30.3144	67.0643	1.14554	0.0012	0.016653
sek-4	X:5375069-5376994	3.83488	8.4899	1.14656	0.0001	0.002025
F36D1.7	I:11263147-11263661	9.19526	20.3648	1.14712	0.00105	0.014995
C31H5.4	I:9042273-9042599	114.129	252.907	1.14794	5.00E-05	0.001092
C44B11.6	III:3152735-3153472	12.0683	26.8083	1.15146	0.00055	0.008779
F19G12.9	X:1419582-1420181	18.2602	40.5795	1.15205	0.0026	0.030952
F56F10.1	X:872516-875951	39.892	88.6845	1.15258	5.00E-05	0.001092
sox-4	X:3505439-3506391	6.23827	13.9336	1.15935	5.00E-05	0.001092
T03F6.10	III:13377530-13378339	5.4568	12.1943	1.16008	0.00365	0.04038

F13D12.6	II:11725223-11759311	141.721	316.862	1.16081	0.00105	0.014995
W04B5.1	III:2428193-2429434	2.65705	5.98195	1.17079	0.004	0.043244
lact-3	II:10652351-10657801	20.103	45.2669	1.17105	5.00E-05	0.001092
K02E11.4	V:14247523-14248075	8.66328	19.5103	1.17125	0.0015	0.020016
fipr-2	V:12363753-12369537	42.8135	96.5227	1.1728	0.0001	0.002025
F23D12.7	X:14448223-14453846	178.467	402.931	1.17488	0.00255	0.030847
F53A9.7	X:8716533-8716999	14.6087	32.9882	1.17512	0.0003	0.005333
Y38C1AA.6,cutl-24	IV:162630-169980	2.2013	4.97581	1.17658	0.00145	0.01944
mlc-6	X:14245731-14246611	4.40721	9.96557	1.17709	0.00435	0.045946
C05D12.3	II:11424759-11430599	18.9285	42.8628	1.17917	5.00E-05	0.001092
C16B8.3	X:3968035-3968637	73.4921	166.493	1.1798	5.00E-05	0.001092
nep-14	X:8375287-8377304	1.65419	3.75348	1.1821	0.0003	0.005333
C02E7.6	V:4919206-4919581	39.4196	89.5538	1.18384	0.00025	0.004581
pho-9	III:2757167-2760816	5.81578	13.2431	1.1872	5.00E-05	0.001092
ZK856.18,ZK856.5	V:10184726-10190131	5.82238	13.2786	1.18942	5.00E-05	0.001092
nhr-162	V:6990147-6991863	0.929093	2.11982	1.19005	0.003	0.034475
Y51A2D.14	V:18582627-18582952	711.261	1623.58	1.19073	5.00E-05	0.001092
bre-1,nstp-1	IV:8984812-8990501	32.3873	74.0304	1.19269	5.00E-05	0.001092
T12B5.15	III:954294-954652	106.352	243.406	1.19451	5.00E-05	0.001092
fut-1	II:8756290-8758723	6.03664	13.8369	1.1967	5.00E-05	0.001092
nspc-18	X:14527170-14527582	37.2224	85.3256	1.19681	5.00E-05	0.001092
F25E5.8	V:7435412-7436962	36.8435	84.5704	1.19874	5.00E-05	0.001092
folt-2	V:2872464-2875600	241.213	553.852	1.19919	5.00E-05	0.001092

F32H5.1	V:13346277-13358037	31.3876	72.3528	1.20485	5.00E-05	0.001092
F19F10.3	V:7552154-7552679	9.64248	22.2426	1.20585	0.00075	0.011348
T23F4.2	II:1163574-1165486	5.17849	11.9487	1.20625	5.00E-05	0.001092
K08D8.5	IV:12910644-12912136	20.9021	48.2529	1.20697	5.00E-05	0.001092
pmp-1	II:6880700-6883754	13.915	32.1457	1.20798	5.00E-05	0.001092
C25F9.14	V:19436598-19437217	5.43532	12.5602	1.20842	0.0011	0.015507
Y7A9C.1	IV:16294153-16298479	1.14247	2.64324	1.21015	0.00085	0.012567
flp-32	X:15433786-15434970	5.51267	12.7589	1.21068	0.00195	0.024679
Y32F6A.4,tag-314	V:10426632-10433604	20.5635	47.8165	1.21742	5.00E-05	0.001092
maf-1,mgl-2	I:10382745-10391395	2.32963	5.42493	1.2195	0.00145	0.01944
R13A5.10	III:7582111-7583047	2.99479	6.97749	1.22025	0.00415	0.044394
clec-223	V:11273147-11278159	10.7518	25.1469	1.22581	5.00E-05	0.001092
D1005.4,acly-1	X:1484856-1486260	6.56022	15.3848	1.22969	0.00285	0.033288
aagr-2	II:4914493-4925248	91.0352	214.394	1.23577	5.00E-05	0.001092
K08D9.9	V:3236486-3236711	316.925	747.078	1.23712	0.00035	0.006018
hsp-16.2	V:1804333-1804971	19.7176	46.4965	1.23764	5.00E-05	0.001092
T24C4.4	III:872621-873531	6.88915	16.2501	1.23805	0.0005	0.00809
C27H5.2	II:7155630-7160938	4.68433	11.0757	1.24149	5.00E-05	0.001092
F10A3.17	V:16158670-16159781	11.4453	27.0938	1.24321	5.00E-05	0.001092
F52H2.3	X:2540066-2541073	3.70262	8.76709	1.24355	0.001	0.01447
nhr-112	V:16722060-16723844	1.20378	2.85919	1.24803	0.0009	0.013143
swt-6	V:13954276-13958323	12.4729	29.6323	1.24838	5.00E-05	0.001092

T10H10.2	X:2294749-2298194	3.55207	8.4463	1.24966	5.00E-05	0.001092
fmo-2	IV:10682523-10684385	2.03056	4.83311	1.25108	0.0006	0.00946
F55H12.2	I:8867797-8868300	19.3034	45.9688	1.2518	5.00E-05	0.001092
nspc-20	X:14529784-14530209	52.6421	125.936	1.25841	5.00E-05	0.001092
trx-3	IV:4487058-4488998	4.36867	10.4641	1.26019	0.0003	0.005333
ZC239.14	II:3221124-3222010	1.91646	4.62381	1.27064	0.00165	0.021692
gfi-1	V:6392535-6399921	24.5813	59.7375	1.28107	5.00E-05	0.001092
C08A9.11	X:17083161-17083742	6.03435	14.6996	1.28451	0.00105	0.014995
fbxa-60	III:944769-946293	15.6851	38.3463	1.28969	5.00E-05	0.001092
C27A2.12	II:5056227-5058113	0.646708	1.58969	1.29756	0.0019	0.024197
C55A6.7	V:11519334-11520484	2.86371	7.04969	1.29968	0.0001	0.002025
clec-41	V:13134964-13138086	65.5716	161.447	1.29992	5.00E-05	0.001092
C18A11.2	X:8067687-8068095	9.38942	23.1467	1.3017	0.00475	0.049329
nhr-178	V:1603931-1607846	0.525397	1.29908	1.30601	0.00335	0.037616
mltn-1	II:13139478-13145310	1.39386	3.44737	1.30641	5.00E-05	0.001092
T09F5.12	V:15164748-15166350	3.62566	9.00966	1.31323	5.00E-05	0.001092
C10G8.4	V:5311934-5312316	786.662	1956.37	1.31437	5.00E-05	0.001092
K09C6.9	V:853463-855076	5.86766	14.6187	1.31696	0.0001	0.002025
ttr-29	V:12906129-12906746	3.3398	8.3281	1.31823	0.0019	0.024197
grl-7	V:11344816-11347012	1.07026	2.66936	1.31854	0.00225	0.027688
Y94H6A.10	IV:2709899-2710670	40.7338	101.782	1.32118	5.00E-05	0.001092
zip-5	V:13264545-13269863	7.67661	19.1824	1.32124	5.00E-05	0.001092
lgc-1,nhr-57	V:4131899-4138825	3.68201	9.21934	1.32417	5.00E-05	0.001092
lips-5	IV:11768637-	1.08474	2.72297	1.32783	0.0006	0.00946

	11773742					
col-159	V:13198229-13199315	16.414	41.2696	1.33015	5.00E-05	0.001092
F09E10.1	X:1502879-1503219	78.2563	196.98	1.33177	5.00E-05	0.001092
Y22D7AR.10	III:1701709-1702436	708.139	1783.26	1.33241	5.00E-05	0.001092
aqp-4,marc-1	V:9737591-9740870	13.7676	34.709	1.33403	5.00E-05	0.001092
Y41C4A.11	III:11719899-11723602	11.7641	29.7207	1.33708	5.00E-05	0.001092
C28C12.11	IV:8474098-8475280	0.744913	1.88551	1.33981	0.0036	0.03992
F54D5.3	II:11571644-11573028	304.961	772.156	1.34027	5.00E-05	0.001092
rrn-2.1	I:15064300-15064453	4250.48	10764.1	1.34054	5.00E-05	0.001092
sid-2	III:13674880-13686445	11.8227	29.9553	1.34125	5.00E-05	0.001092
Y41C4A.8	III:11706968-11708820	6.27967	15.9474	1.34456	5.00E-05	0.001092
nlp-26	V:19613527-19614521	46.2846	117.673	1.34618	5.00E-05	0.001092
fbxa-162	II:1607868-1609014	1.35889	3.45874	1.34782	0.00185	0.023816
C50F7.5	IV:7726717-7727951	13.9494	35.5692	1.35042	5.00E-05	0.001092
F18E3.11	V:7413436-7413840	44.6808	114.353	1.35577	5.00E-05	0.001092
Y69A2AL.2	IV:2482256-2484112	68.0284	174.226	1.35676	5.00E-05	0.001092
far-7	II:319792-321107	11.8555	30.3792	1.35752	5.00E-05	0.001092
ctb-1	MtDNA:4503-5676	1342.37	3439.85	1.35756	5.00E-05	0.001092
fbxa-24	II:3816960-3818238	2.60167	6.69288	1.36319	5.00E-05	0.001092
C44C1.6	X:969072-970270	1.54117	3.96515	1.36335	0.0044	0.046371
ZK1010.5	III:12984498-12987502	0.221608	0.570655	1.36461	0.00465	0.04861
wrt-6	X:3480250-3483661	0.337429	0.869855	1.36619	0.00405	0.043718
tbb-6	V:12261803-12263845	4.45942	11.4996	1.36665	5.00E-05	0.001092

ZC21.3	III:8525039-8528652	5.1489	13.287	1.36768	5.00E-05	0.001092
nspc-13	X:12357507-12357919	46.8893	121.144	1.36939	5.00E-05	0.001092
W02B12.12	II:11476754-11479161	0.519491	1.34216	1.36939	0.003	0.034475
Y34F4.4	III:1023227-1026249	3.39179	8.7845	1.37291	0.0008	0.011965
F31E9.11	V:17315590-17315954	24.0295	62.313	1.37472	5.00E-05	0.001092
C25F9.11	V:19432440-19433158	1.90572	4.95877	1.37964	0.0021	0.026205
nspe-1	II:12620547-12620885	19.6461	51.1345	1.38005	0.00035	0.006018
C18A3.10	II:5714923-5716250	6.31294	16.4349	1.38038	0.0006	0.00946
nlt-1	II:9991144-10001142	140.51	366.292	1.38232	5.00E-05	0.001092
F59E11.5	V:8995100-8996405	4.19732	10.9453	1.38277	5.00E-05	0.001092
cebp-1	X:1452694-1454000	9.21421	24.0316	1.383	5.00E-05	0.001092
nspc-17	X:14524757-14525181	20.818	54.7587	1.39526	5.00E-05	0.001092
F38B2.6	X:11280621-11281236	3.64249	9.58373	1.39566	0.00035	0.006018
F08G2.5	II:13832852-13833631	4.15998	10.9519	1.39653	0.0001	0.002025
ttm-5	I:14688671-14700349	6.41334	16.8938	1.39734	5.00E-05	0.001092
abu-12	X:450444-457648	0.235101	0.619776	1.39847	0.00165	0.021692
F28B12.1	II:5942988-5943963	1.57904	4.16568	1.3995	0.0019	0.024197
F56D6.16	IV:3898477-3899806	6.46652	17.1314	1.40558	0.0001	0.002025
abt-4	V:323776-330727	8.01147	21.2521	1.40747	5.00E-05	0.001092
F53A9.9	X:8720221-8720758	3.64978	9.6841	1.40781	0.0005	0.00809
R02D5.3	V:14483159-14484682	4.1552	11.0416	1.40996	5.00E-05	0.001092
F32A11.3	II:13151459-13153386	1.06241	2.82365	1.41022	0.00045	0.007424
poml-3	I:4145311-4147136	4.77683	12.7264	1.4137	5.00E-05	0.001092
R12E2.15	I:4148831-4149429	14.0228	37.4501	1.41719	0.0042	0.044827

Y39B6A.41	V:18970499-18977978	1.56423	4.19632	1.42367	5.00E-05	0.001092
Y60A3A.16	V:19921696-19922594	5.27694	14.165	1.42456	5.00E-05	0.001092
C18H9.6	II:6700657-6701625	33.0722	88.8122	1.42514	5.00E-05	0.001092
F47B8.4	V:14323531-14324631	1.6993	4.56883	1.42688	0.0018	0.023277
Y105C5A.25	IV:15860220-15861442	0.517285	1.39094	1.42703	0.00395	0.042899
M199.9	IV:15127490-15127791	15.233	40.9653	1.4272	0.0046	0.048193
Y75B8A.11	III:12186410-12190116	11.5465	31.0815	1.4286	0.0026	0.030952
T02C12.5	III:4026611-4028129	4.61093	12.4188	1.42939	0.00385	0.042037
cyp-13A6	II:9800760-9802721	0.375405	1.01163	1.43017	0.00215	0.026712
F41H10.1	IV:5382908-5383864	1.09067	2.9406	1.43089	0.0026	0.030952
T24F1.5	II:11319106-11319760	13.5868	36.691	1.43322	5.00E-05	0.001092
F26D11.12,F26D11.13	V:7953353-7955343	5.65175	15.3178	1.43844	0.00045	0.007424
ncx-9	V:4991504-4995064	0.302348	0.820048	1.4395	0.0028	0.032893
clec-204	V:1757185-1760306	2.11542	5.74669	1.44178	5.00E-05	0.001092
nhr-168	V:13331114-13333871	1.8211	4.96052	1.44568	5.00E-05	0.001092
C25H3.18	II:5689430-5690000	90.158	246.412	1.45055	0.0005	0.00809
C50F4.1	V:9526732-9529250	33.2106	90.8237	1.45142	5.00E-05	0.001092
K10G4.3	V:17262758-17265345	0.694015	1.90403	1.45602	0.0007	0.010705
K12C11.6	I:1337019-1338120	17.0546	46.7939	1.45616	5.00E-05	0.001092
C41G7.8	I:9522577-9532831	6.50581	17.8825	1.45875	0.0002	0.003787
Y39B6A.29	V:19020486-19024765	0.56179	1.54515	1.45965	0.00065	0.010148
Y67D8C.23	IV:3051755-3052358	5.15925	14.2082	1.46149	0.0001	0.002025

C48B4.1	III:9586612-9592192	16.8114	46.3383	1.46277	5.00E-05	0.001092
ugt-16	V:12825025-12827432	3.90043	10.7618	1.46421	5.00E-05	0.001092
pcp-1	III:7758729-7761273	18.0284	49.7715	1.46505	5.00E-05	0.001092
B0205.13	I:10727750-10728795	6.28876	17.4246	1.47027	0.00025	0.004581
tsp-2	III:8236916-8237893	3.83826	10.6439	1.4715	0.00015	0.002918
ceh-62	II:10805393-10809992	3.16345	8.78442	1.47345	5.00E-05	0.001092
F30A10.13	I:9478466-9479091	37.8806	105.293	1.47487	5.00E-05	0.001092
fbxa-31	III:1269578-1271428	1.51953	4.22899	1.47669	0.0002	0.003787
T15B7.10	V:6810420-6813247	0.335601	0.935645	1.47921	0.0013	0.017798
frpr-9	V:10992098-10994817	0.298755	0.834759	1.4824	0.0018	0.023277
gst-9	II:4891579-4893574	1.98249	5.54264	1.48326	0.00115	0.016068
T19D12.4	II:6631153-6643117	15.8778	44.4241	1.48433	5.00E-05	0.001092
F59C6.16	I:10506999-10515506	185.838	520.521	1.48591	0.0002	0.003787
ftn-1	V:7545973-7548012	2.01885	5.67911	1.49213	0.0007	0.010705
Y53F4B.45	II:15037988-15048907	18.9874	53.5704	1.49639	0.0022	0.027238
glct-6	IV:3774134-3794046	6.43361	18.1574	1.49686	5.00E-05	0.001092
C54D10.13,srh-25	V:12431367-12433817	3.77044	10.6445	1.4973	0.0001	0.002025
T09E11.11	I:12343903-12345702	1.69588	4.78962	1.49787	0.0007	0.010705
skr-3	V:16121779-16122641	38.378	108.901	1.50467	5.00E-05	0.001092
dmsr-16	V:6807830-6809062	0.56571	1.60615	1.50547	0.0038	0.041683
cyp-33C7	V:2250544-2252524	3.00211	8.53224	1.50695	5.00E-05	0.001092
srp-7	V:8179130-8183442	163.134	464.476	1.50955	5.00E-05	0.001092
asp-12	V:8269253-8272058	44.9923	128.291	1.51167	5.00E-05	0.001092
aagr-1	IV:8366538-8375372	20.179	57.542	1.51176	5.00E-05	0.001092

B0252.8	II:6916155-6916967	19.7238	56.2566	1.51209	5.00E-05	0.001092
Y66A7A.7	III:11628385-11631014	6.90655	19.7357	1.51477	0.0006	0.00946
C36C9.10	X:1681751-1681886	1440.53	4117.97	1.51533	5.00E-05	0.001092
T02B5.1	V:14163249-14166730	0.696303	2.00358	1.52479	0.00035	0.006018
col-142	V:6831162-6832254	21.83	62.865	1.52595	5.00E-05	0.001092
F25F2.1	III:4508861-4512127	0.330555	0.956107	1.53228	0.00145	0.01944
F44G3.2	V:16103893-16106140	1.16428	3.37005	1.53333	0.00015	0.002918
C05D11.5,nas-4	III:6410035-6414993	9.17557	26.5608	1.53343	5.00E-05	0.001092
F52G3.6	X:16943322-16943517	250.07	724.424	1.5345	5.00E-05	0.001092
glt-5	II:9706495-9708885	1.60666	4.66474	1.53773	5.00E-05	0.001092
C32D5.18	II:6343053-6345925	3403.61	9925.53	1.54408	0.00035	0.006018
col-147	V:9632270-9633337	2.91268	8.49939	1.54501	5.00E-05	0.001092
ZK1320.13	II:9680797-9683058	58.2822	170.451	1.54823	5.00E-05	0.001092
comt-3	V:2057628-2066851	9.79909	28.6588	1.54826	0.0041	0.044091
ZK287.9	V:9679402-9680243	15.6558	45.8016	1.5487	5.00E-05	0.001092
H23N18.5	V:4911763-4912383	4.6056	13.5324	1.55496	0.00305	0.034908
C02B8.12	X:8120409-8123220	0.600142	1.77436	1.56392	0.00115	0.016068
K04A8.1	V:6566335-6570882	8.90088	26.4357	1.57047	5.00E-05	0.001092
M04D5.3	I:11339777-11341611	8.32515	24.7521	1.57201	5.00E-05	0.001092
clec-63	II:12895637-12897462	663.591	1976.33	1.57446	5.00E-05	0.001092
ZK354.2	IV:5313481-5315525	0.375183	1.11766	1.57482	0.00205	0.025716
Y106G6D.3	I:10112083-10114198	0.261524	0.780003	1.57654	0.003	0.034475
W03D2.13,W03D2.6	IV:4056515-4058550	20.2694	60.5612	1.57909	0.0001	0.002025

hex-2	V:5654448-5658687	11.7143	35.0063	1.57934	5.00E-05	0.001092
rmd-3	II:11338449-11339599	0.819206	2.45065	1.58086	0.00205	0.025716
klf-1	III:2874817-2880728	6.72045	20.1176	1.58183	5.00E-05	0.001092
nspc-19	X:14528716-14529074	37.9027	113.664	1.5844	5.00E-05	0.001092
C12D12.1	X:3499252-3505267	48.8412	147.102	1.59065	5.00E-05	0.001092
Y51A2D.21	V:18571832-18572949	5.70817	17.2054	1.59176	0.00015	0.002918
B0238.12	V:5267821-5268823	1.79025	5.398	1.59227	0.0002	0.003787
C04E6.7	V:5893316-5895209	3.55165	10.7591	1.599	5.00E-05	0.001092
M7.8	IV:11093962-11095003	3.96167	12.0239	1.60172	5.00E-05	0.001092
mlk-1	V:5053618-5064806	5.39476	16.3885	1.60306	5.00E-05	0.001092
grl-16	I:572176-575119	2.48844	7.57231	1.60549	5.00E-05	0.001092
C45G9.12	III:5070430-5071597	11.949	36.5092	1.61137	0.0004	0.006764
R12E2.7	I:4153956-4154550	5.79944	17.7505	1.61387	0.0001	0.002025
-	III:1006730-1007139	10.0258	30.7926	1.61886	0.0001	0.002025
F02E11.7	II:3267662-3271502	2.29722	7.07539	1.62292	0.00305	0.034908
F49C12.15	IV:9324441-9327532	0.843289	2.59949	1.62413	5.00E-05	0.001092
Y17D7B.7	V:18780489-18782605	11.3061	34.9065	1.6264	5.00E-05	0.001092
F46A8.7	I:11237049-11238340	2.91228	9.04543	1.63504	5.00E-05	0.001092
nspc-16	X:14523574-14523997	22.4772	69.8165	1.63511	5.00E-05	0.001092
W10C8.6	I:2858598-2859847	20.3965	63.376	1.63561	0.00025	0.004581
F23A7.1	X:16217391-16217666	9.81017	30.5232	1.63755	0.00085	0.012567
F13H8.1	II:6283385-6284727	2.06701	6.45926	1.64382	0.00135	0.018306
ift-74	II:6679544-6682971	0.277689	0.869234	1.64628	0.00055	0.008779
sul-3	X:7827084-7834535	0.670635	2.09942	1.64639	5.00E-05	0.001092

clec-225	V:13133749-13134858	2.93849	9.20465	1.64729	0.00015	0.002918
C31B8.7	V:2900447-2903310	1.94447	6.09577	1.64843	5.00E-05	0.001092
clec-150	III:1002706-1006247	186.771	588.636	1.6561	5.00E-05	0.001092
F14H12.3	X:4344250-4345650	6.48856	20.4922	1.6591	5.00E-05	0.001092
smz-1	IV:12455116-12456200	1.14556	3.62403	1.66154	5.00E-05	0.001092
K10C2.7	X:6443054-6443441	10.8057	34.2442	1.66406	0.0001	0.002025
Y54G11A.4	II:14292823-14296055	0.813141	2.57697	1.6641	5.00E-05	0.001092
H34I24.2	III:2842043-2845197	80.8044	256.784	1.66805	5.00E-05	0.001092
nlp-42	V:18903771-18906201	5.77578	18.4088	1.67231	0.0001	0.002025
C38H2.2	III:10381772-10385256	11.5898	37.1888	1.68201	5.00E-05	0.001092
clec-62	II:12893063-12895098	37.2336	119.499	1.68232	5.00E-05	0.001092
W02B12.1	II:11449019-11453004	16.0985	51.701	1.68326	0.0003	0.005333
slc-17.9	X:9761488-9764922	0.840223	2.69877	1.68346	5.00E-05	0.001092
T28B4.4	X:6597917-6598866	1.34084	4.32366	1.68912	0.0002	0.003787
F58F12.4	II:6386766-6388242	2.50576	8.08587	1.69016	5.00E-05	0.001092
col-92	III:10982165-10983253	1.31489	4.25367	1.69376	5.00E-05	0.001092
ZK593.11	IV:10909914-10913079	103.296	334.638	1.69582	0.0048	0.04974
cyp-33C8	V:3800775-3803454	3.46488	11.2566	1.6999	5.00E-05	0.001092
K05F1.1	II:5801381-5805477	1.00848	3.2852	1.7038	0.00035	0.006018
skr-4	V:19924223-19925030	25.9351	84.4943	1.70395	5.00E-05	0.001092
Y106G6H.13	I:10471213-10471959	1.31573	4.29379	1.70639	0.0035	0.038932
gale-1	I:12975183-12978781	118.882	388.104	1.70691	5.00E-05	0.001092

T23F2.3	X:5511994-5512336	96.4752	315.412	1.709	5.00E-05	0.001092
C04G2.8,egl-38	IV:10106632-10111577	2.30911	7.57956	1.71478	5.00E-05	0.001092
glb-28	X:15314983-15317223	0.614904	2.02151	1.717	0.0038	0.041683
C01B10.6	IV:6640160-6645352	108.866	358.067	1.71768	5.00E-05	0.001092
cth-1	V:16100654-16102744	19.6197	64.5551	1.71823	5.00E-05	0.001092
Y40C7B.4	X:17256234-17256780	1.12912	3.72602	1.72243	0.00385	0.042037
F54E2.1	V:2810426-2811985	67.4522	223.04	1.72536	5.00E-05	0.001092
Y9C9A.8	IV:4930364-4932217	1.23096	4.09853	1.73533	5.00E-05	0.001092
W02G9.4	V:2666865-2670229	12.5432	41.8853	1.73954	5.00E-05	0.001092
F46G10.1	X:13310049-13311812	67.3356	224.855	1.73955	5.00E-05	0.001092
T21C9.9	V:10590550-10592579	0.311875	1.05023	1.75166	0.001	0.01447
C54F6.5	V:7529113-7529426	16.317	54.9578	1.75195	0.0015	0.020016
frk-1	IV:10043182-10045703	0.211531	0.713986	1.75503	0.0017	0.022267
col-129	IV:12108670-12110258	17.7908	60.0983	1.7562	5.00E-05	0.001092
K02E2.11	V:20383361-20384404	11.4556	38.9368	1.76507	5.00E-05	0.001092
F35F10.1	V:3316359-3318027	3.58553	12.1917	1.76564	5.00E-05	0.001092
R08E5.3	V:3772057-3776136	13.2476	45.184	1.77008	5.00E-05	0.001092
LLC1.2	IV:14456906-14464098	154.393	527.075	1.7714	5.00E-05	0.001092
-	III:1976846-1976895	19561.4	66928.5	1.77461	0.00475	0.049329
F56C9.7	III:7311296-7315251	147.476	504.774	1.77515	5.00E-05	0.001092
his-11	II:13821777-13822314	1.04381	3.57467	1.77595	0.00165	0.021692
lgc-21	X:14064314-14067984	0.464087	1.59002	1.77658	0.00015	0.002918

M28.10	II:10647515-10648676	94.1229	322.482	1.7766	5.00E-05	0.001092
T25C12.3	X:11491094-11499999	85.4446	293.456	1.78008	5.00E-05	0.001092
K01H12.4	IV:9713219-9714886	0.322367	1.10793	1.7811	0.0031	0.035282
W03F9.4	V:147525-152104	1.63235	5.61044	1.78117	5.00E-05	0.001092
F39G3.5	V:4722619-4724565	7.41982	25.5051	1.78133	5.00E-05	0.001092
F35H8.4	II:9559524-9559944	2.8995	9.97718	1.78283	0.004	0.043244
-	II:13475966-13476375	1.64698	5.67135	1.78387	0.0034	0.037998
arf-1.1	IV:7634831-7641858	2.77923	9.58119	1.78552	0.0028	0.032893
F09C8.1	X:16159647-16163548	19.8994	68.7698	1.78905	5.00E-05	0.001092
sod-3	X:17087881-17094223	2.14085	7.3987	1.78909	0.0001	0.002025
nspd-3	IV:5162742-5163074	3.93342	13.5968	1.78941	0.0012	0.016653
grd-6	V:9221889-9224349	0.339931	1.1788	1.79401	0.00045	0.007424
T05F1.8	I:9642343-9643794	0.226081	0.784464	1.79487	0.00395	0.042899
ttm-2	II:4763193-4770013	5.38855	18.7027	1.79528	5.00E-05	0.001092
B0205.10	I:10708362-10710375	0.364025	1.26469	1.79668	0.00035	0.006018
C09D4.3	I:5488339-5490626	0.203589	0.709513	1.80117	0.0033	0.037201
B0416.2	X:9299170-9300131	2.7724	9.66808	1.8021	5.00E-05	0.001092
msp-49	II:5194331-5194792	2.43319	8.48739	1.80247	0.0003	0.005333
K09E9.4	X:15628603-15630416	19.8228	69.2971	1.80564	0.00195	0.024679
spe-46	I:9056293-9057822	0.319741	1.11807	1.80604	0.00385	0.042037
F53B6.4	I:8947333-8954394	1.32179	4.62812	1.80794	0.00055	0.008779
K05F1.10	II:5801381-5805477	12.9573	45.4116	1.8093	5.00E-05	0.001092
C54C6.7	III:3545578-3546419	2.77424	9.72776	1.81002	5.00E-05	0.001092
spp-23	I:1018834-1019219	61.4803	215.689	1.81075	5.00E-05	0.001092

twk-28	X:4271164-4279212	0.785261	2.75756	1.81215	0.00305	0.034908
tsp-1	III:8237994-8239423	3.46055	12.1662	1.8138	5.00E-05	0.001092
C39B5.5	III:2208269-2211296	1.95401	6.89208	1.8185	5.00E-05	0.001092
B0563.5	X:9146115-9147555	1.4104	4.97818	1.81951	0.0014	0.018912
T25D10.4	II:6407536-6410281	5.2392	18.4966	1.81985	5.00E-05	0.001092
catp-4	II:14593523-14597640	0.211797	0.747946	1.82025	5.00E-05	0.001092
Y51H7C.13	II:1463265-1467367	1.78379	6.30653	1.8219	5.00E-05	0.001092
LLC1.121	IV:14446554-14447620	0.42335	1.50128	1.82627	0.00185	0.023816
F36D3.4	V:16516474-16517704	0.391473	1.38936	1.82743	0.00195	0.024679
glc-1	V:16219608-16221916	8.59833	30.5355	1.82836	5.00E-05	0.001092
kel-10	III:10098472-10101584	0.196047	0.696814	1.82957	0.00105	0.014995
F23H12.5	V:12358646-12363691	0.489075	1.74005	1.831	0.0028	0.032893
cpr-3	V:15296833-15298676	15.5351	55.2983	1.8317	5.00E-05	0.001092
msp-40	II:4825379-4825845	2.90742	10.4049	1.83946	0.00035	0.006018
ZK384.4	V:18736636-18737894	14.2936	51.2325	1.84169	5.00E-05	0.001092
F09G8.5	III:8254974-8257666	1.57233	5.63906	1.84255	5.00E-05	0.001092
C02E7.7	V:4918153-4918585	22.1752	79.6615	1.84494	5.00E-05	0.001092
col-97	III:12987671-12993704	3.40671	12.2483	1.84613	5.00E-05	0.001092
C27D8.2	IV:12712769-12714755	0.229357	0.829772	1.85512	0.00205	0.025716
xtr-1	X:11850767-11853729	1.05138	3.80796	1.85673	0.00015	0.002918
pqn-60	V:504038-504616	3.21385	11.6645	1.85974	5.00E-05	0.001092
R10E9.2	III:3962727-3964098	0.929915	3.3886	1.86552	0.0001	0.002025

F19B2.5	V:20162623-20164587	29.5816	107.822	1.86588	5.00E-05	0.001092
asp-14,fah-1	X:6444184-6448999	97.5968	356.538	1.86915	5.00E-05	0.001092
Y69E1A.2	IV:10949816-10951133	0.912658	3.34179	1.87247	5.00E-05	0.001092
col-139	V:4652381-4653986	16.612	60.8798	1.87373	5.00E-05	0.001092
F52B11.5	IV:14101989-14103155	2.50928	9.20783	1.87559	5.00E-05	0.001092
smz-2	I:6872596-6873755	0.616855	2.26451	1.87619	0.00025	0.004581
lec-11	IV:6588189-6590205	9.97339	36.6383	1.87719	5.00E-05	0.001092
T05A7.6	II:4668643-4671790	0.182577	0.672013	1.87998	0.00055	0.008779
Y50E8A.1	V:14726906-14727240	14.0363	51.7303	1.88185	0.00015	0.002918
F08G5.6	IV:12435826-12438274	3.74102	13.7903	1.88215	5.00E-05	0.001092
R09H10.5	IV:10621715-10628841	29.681	109.455	1.88273	5.00E-05	0.001092
F11E6.6	IV:17464554-17465927	0.674725	2.50073	1.88998	0.0011	0.015507
mul-1	IV:4121341-4123069	10.0273	37.2074	1.89166	5.00E-05	0.001092
ugt-36	V:7167008-7169205	0.33706	1.25667	1.89853	0.0002	0.003787
hrg-2	V:12409368-12410513	1.45027	5.41736	1.90127	5.00E-05	0.001092
W03D8.9	I:2784616-2786068	0.480484	1.79778	1.90366	0.00035	0.006018
C39B10.1	X:10454308-10463580	0.240415	0.905459	1.91312	0.00265	0.031442
nhr-21	II:7339204-7349476	4.80689	18.1534	1.91706	5.00E-05	0.001092
F09A5.2	X:13135106-13139777	0.557227	2.1067	1.91865	5.00E-05	0.001092
fil-1	V:14993908-14995201	1.1208	4.23836	1.91897	5.00E-05	0.001092
pqn-94	V:20278652-20279861	34.6236	131.645	1.92682	5.00E-05	0.001092
mtl-1	V:6691368-6691863	55.2233	210.116	1.92784	5.00E-05	0.001092

B0507.6	V:8746157-8750193	0.193104	0.73557	1.92948	0.00025	0.004581
Y38F1A.8	II:12997985-13000853	2.60429	9.93764	1.93201	5.00E-05	0.001092
F35B3.4	X:17019622-17020805	0.591397	2.26085	1.93467	0.0011	0.015507
C23H4.2	X:12219678-12222813	0.633677	2.42699	1.93735	5.00E-05	0.001092
T13F2.9	IV:9768056-9768984	1.00351	3.85221	1.94063	0.00015	0.002918
C49G7.12	V:4038820-4039934	0.647383	2.49944	1.94891	0.00035	0.006018
clec-73	IV:3953934-3956206	0.244678	0.945694	1.95049	0.0005	0.00809
spe-11	I:5330575-5332175	0.452818	1.75092	1.95111	0.0009	0.013143
Y69E1A.1	IV:10947231-10948896	0.618633	2.39281	1.95155	0.0001	0.002025
wrt-4	X:15752257-15757269	0.271567	1.0563	1.95964	0.0006	0.00946
fbxa-143	V:16125810-16127497	0.582757	2.26828	1.96063	0.0002	0.003787
C49C3.4	IV:17320794-17328663	40.824	159.009	1.96162	5.00E-05	0.001092
C33F10.11	II:4834158-4834834	0.698808	2.72213	1.96177	0.0009	0.013143
msp-76	IV:9688981-9689436	3.76322	14.6798	1.96379	5.00E-05	0.001092
dyla-1	X:16841104-16842975	0.407609	1.59091	1.9646	0.0018	0.023277
F07C6.6	IV:12792794-12793274	1.48498	5.79621	1.96467	0.00105	0.014995
Y37E11B.10	IV:3603548-3606466	0.283358	1.10637	1.96513	0.0001	0.002025
C05E7.2	X:12938696-12940711	0.556733	2.17846	1.96825	0.00085	0.012567
poml-4	II:1540927-1542718	0.376941	1.47495	1.96826	0.00035	0.006018
msp-38	IV:10143311-10143775	1.13878	4.46216	1.97026	0.0041	0.044091
lbp-8	V:13890699-13891362	1.72805	6.77222	1.97048	5.00E-05	0.001092
K10D3.6	I:7116096-7116706	9.95522	39.0484	1.97174	5.00E-05	0.001092

Y41E3.460	IV:15059460-15059685	19.1762	75.2771	1.97289	0.0003	0.005333
F53C11.1	V:13775750-13777771	11.7548	46.2536	1.97631	5.00E-05	0.001092
Y53F4B.48	II:15165890-15166028	104.849	412.65	1.97661	0.00255	0.030847
linc-1	I:13652523-13652727	71.8949	283.892	1.98138	0.0011	0.015507
Y34F4.1	III:1020969-1021876	27.8585	110.299	1.98523	5.00E-05	0.001092
msp-36	IV:10095399-10095851	2.24621	8.89931	1.9862	0.0001	0.002025
C39H7.1	IV:5631738-5633370	0.543978	2.15701	1.98741	0.0001	0.002025
T06A1.5	V:1927222-1931376	9.03934	35.9151	1.9903	5.00E-05	0.001092
T28H11.7	IV:5015280-5016273	0.503788	2.00511	1.99279	0.00385	0.042037
Y22D7AL.15	III:1658247-1659863	41.8996	167.243	1.99693	5.00E-05	0.001092
C28C12.4	IV:8487496-8488423	1.91523	7.74216	2.01522	5.00E-05	0.001092
C04G2.9	IV:10112890-10114231	1.54446	6.28387	2.02456	5.00E-05	0.001092
F21H7.5	V:16237538-16238821	0.841139	3.42878	2.02728	5.00E-05	0.001092
K10D11.5	IV:12989684-12991804	5.92632	24.1605	2.02744	5.00E-05	0.001092
msp-142	II:5797892-5798339	1.6601	6.77366	2.02867	0.00055	0.008779
gln-2	III:9943239-9944761	0.327591	1.33885	2.03103	0.0007	0.010705
T22F3.10	V:3606817-3610927	0.289363	1.18692	2.03627	0.00035	0.006018
col-38	II:8568032-8569088	4.10901	16.8948	2.03972	5.00E-05	0.001092
col-125	IV:11225504-11226519	5.30849	21.8641	2.04219	5.00E-05	0.001092
col-109	IV:1817044-1820253	1.3128	5.40713	2.04222	5.00E-05	0.001092
Y36E3A.2	V:15426198-15426846	0.996245	4.10518	2.04287	0.0033	0.037201
sss-2	V:14346007-14346997	0.589597	2.43469	2.04594	5.00E-05	0.001092

R08E3.1,R08E3.2	X:4822653-4853065	40.0078	166.954	2.0611	5.00E-05	0.001092
F20D6.6	V:8159940-8161600	0.236636	0.989673	2.06428	0.0035	0.038932
F54C9.3	II:8566519-8566857	293.936	1235.32	2.07131	5.00E-05	0.001092
Y116A8B.4	IV:17223778-17224987	14.416	60.7163	2.07441	5.00E-05	0.001092
F26B1.8	I:6329535-6330183	1.50874	6.38859	2.08215	5.00E-05	0.001092
T08B6.2	IV:4894369-4897043	0.25025	1.06703	2.09216	0.00235	0.028745
F52H3.6	II:10026593-10027924	0.295122	1.2655	2.10032	0.00185	0.023816
T22E5.7,igcm-2	X:6379473-6391591	0.969063	4.17033	2.1055	0.0018	0.023277
T27E7.1	IV:14519758-14521000	0.701186	3.03183	2.11232	5.00E-05	0.001092
E03H12.5	IV:4977095-4978073	0.758945	3.28716	2.11477	0.00015	0.002918
clec-64	II:12898289-12900403	0.265044	1.1487	2.1157	0.00115	0.016068
ssq-3	IV:7111631-7112861	0.329839	1.43256	2.11876	0.00045	0.007424
ssq-4	IV:5016480-5017762	1.16287	5.05514	2.12006	5.00E-05	0.001092
R07E5.15	III:4401457-4402505	0.3032	1.32442	2.12702	0.004	0.043244
C27D8.1	IV:12717882-12719390	0.375189	1.6407	2.12862	0.0005	0.00809
Y38E10A.17	II:12632585-12634787	0.40589	1.77575	2.12927	5.00E-05	0.001092
T06A1.1	V:1923123-1925565	0.459552	2.01092	2.12956	5.00E-05	0.001092
F14H3.12	V:16074112-16075321	10.8854	47.6803	2.131	5.00E-05	0.001092
C04F12.7	I:9695707-9696762	1.02722	4.50435	2.13257	0.00015	0.002918
cht-4	III:1653730-1657480	0.371848	1.63056	2.13258	0.00025	0.004581
T16A9.5	V:14213590-14215089	0.46376	2.03673	2.13481	0.00015	0.002918
F29G6.1	X:11501109-11509430	0.138651	0.610735	2.13908	0.0002	0.003787

ant-1.4	IV:8459221-8460277	0.279105	1.23237	2.14255	0.0039	0.042453
col-157	V:11484053-11484998	0.513282	2.26837	2.14383	0.0003	0.005333
ZK6.11	V:415712-417706	201.938	893.511	2.14557	5.00E-05	0.001092
C29F9.3,C29F9.4	III:120491-127862	21.2013	94.1757	2.1512	5.00E-05	0.001092
scav-6	I:7354490-7357173	6.09486	27.1324	2.15435	5.00E-05	0.001092
ssq-2	IV:4996141-4997553	0.886799	3.95067	2.15542	5.00E-05	0.001092
col-71	II:3500072-3502449	2.94326	13.155	2.16013	5.00E-05	0.001092
gipc-2	IV:10026410-10027665	1.72865	7.7279	2.16043	5.00E-05	0.001092
gipc-1	III:4870777-4872049	1.05505	4.74484	2.16905	5.00E-05	0.001092
F02E11.2	II:3262828-3264283	5.44224	24.554	2.17369	0.00155	0.020606
cdr-4	V:12407363-12408592	29.7299	134.177	2.17415	5.00E-05	0.001092
B0348.2	V:45462-46923	2.87837	13.034	2.17896	0.00255	0.030847
K06G5.1	X:14214938-14219089	177.255	803.143	2.17983	5.00E-05	0.001092
F13A7.1	V:16376238-16377925	0.247999	1.12697	2.18404	0.0025	0.030423
oac-5	V:16292708-16295600	0.227823	1.03538	2.18417	5.00E-05	0.001092
T25D10.1	II:6403480-6405034	5.21127	23.8795	2.19607	5.00E-05	0.001092
col-81	II:11012394-11013779	9.63085	44.2097	2.19863	5.00E-05	0.001092
D1086.17	V:14067855-14071214	0.517305	2.38285	2.2036	0.0005	0.00809
F19C7.1	IV:4605785-4609679	193.265	891.281	2.2053	5.00E-05	0.001092
T23B3.5	I:6705547-6706378	0.923349	4.26281	2.20686	5.00E-05	0.001092
ZK1025.3	I:11460779-11463068	0.517602	2.39252	2.20861	5.00E-05	0.001092
Y55F3AM.11	IV:1038668-1043218	4.01482	18.5581	2.20864	5.00E-05	0.001092
T20D3.2	IV:9328009-9330855	338.155	1568.17	2.21333	5.00E-05	0.001092

C34F11.5	II:5195894-5199259	0.124447	0.577871	2.21521	0.0003	0.005333
C17H1.7	I:13136466-13138521	0.334794	1.55578	2.21629	0.00035	0.006018
slcf-2	X:3393863-3397468	0.67743	3.15965	2.22162	5.00E-05	0.001092
rol-8	II:7544105-7545332	1.29391	6.03626	2.22192	5.00E-05	0.001092
clec-79	IV:3973348-3975935	0.133613	0.624571	2.2248	0.0025	0.030423
grl-5	V:4412746-4414626	0.630445	2.94712	2.22486	0.00045	0.007424
msp-51	IV:5294921-5295375	1.38903	6.49546	2.22535	0.0009	0.013143
C39H7.4	IV:5611089-5614608	14.6447	68.8022	2.23208	5.00E-05	0.001092
spin-3	X:13130262-13134208	1.8748	8.81687	2.23353	5.00E-05	0.001092
col-145	V:9162050-9163005	0.831813	3.91535	2.23481	5.00E-05	0.001092
T21D12.14	IV:287307-288116	1.05744	4.98708	2.23762	0.0026	0.030952
Y47H10A.5	I:12095480-12097939	5.38856	25.6236	2.2495	5.00E-05	0.001092
C36H8.1	IV:12743038-12744738	0.24352	1.15913	2.25093	0.00085	0.012567
C38C3.3	V:1495672-1497942	0.260616	1.24123	2.25177	0.0025	0.030423
Y69A2AR.19	IV:2488819-2494145	0.110571	0.526827	2.25236	5.00E-05	0.001092
F40F4.6	X:3235767-3243624	106.769	510.816	2.25831	5.00E-05	0.001092
F38E9.6	X:16437744-16440363	17.2904	82.828	2.26015	5.00E-05	0.001092
C17H12.3	IV:6793914-6795629	0.241853	1.1587	2.26031	0.00105	0.014995
msp-45	II:5155435-5157625	3.1663	15.2515	2.26808	0.0001	0.002025
fbxa-59	III:940779-943502	6.65135	32.4695	2.28737	5.00E-05	0.001092
col-130	IV:12425216-12432539	1.48665	7.31815	2.29941	0.00135	0.018306
linc-17	II:3596225-3596812	1.88792	9.35161	2.30841	0.0007	0.010705
col-17	II:4866435-4867574	1.5082	7.47197	2.30866	5.00E-05	0.001092

col-104	IV:1353678-1355305	2.13808	10.618	2.31213	5.00E-05	0.001092
acs-2	V:15567393-15569889	16.0007	79.5953	2.31455	5.00E-05	0.001092
F19C7.5,F19C7.6,F28E10.5	IV:4594131-4596811	1.16667	5.80756	2.31553	0.00105	0.014995
dpy-4	IV:14981555-14996316	3.78702	18.8913	2.31859	5.00E-05	0.001092
ZK945.7	II:10107473-10108438	0.445368	2.22569	2.32118	0.00045	0.007424
C55A6.11	V:11520584-11521554	0.422528	2.11204	2.32152	0.0019	0.024197
C17H12.12	IV:6795926-6798692	0.185153	0.926256	2.3227	0.00025	0.004581
sqt-2	II:23327-24457	1.16494	5.83823	2.32527	5.00E-05	0.001092
-	IV:2710947-2711235	4.46066	22.4041	2.32843	0.00055	0.008779
ZK1290.14	II:7554091-7554844	5.79464	29.1192	2.32918	5.00E-05	0.001092
msp-3	II:4785860-4786315	1.09695	5.53093	2.33402	0.0008	0.011965
T15B7.17	V:6813699-6814961	0.456554	2.30456	2.33563	0.0011	0.015507
F27C8.5	IV:9589791-9592526	0.105323	0.531689	2.33576	0.00265	0.031442
K08C9.2	I:11486895-11488446	0.515241	2.60135	2.33594	0.00035	0.006018
hsp-17	V:8383921-8385927	49.9695	252.557	2.33749	5.00E-05	0.001092
M04C3.2	V:19445874-19448901	0.541889	2.75884	2.348	5.00E-05	0.001092
C39H7.2	IV:5611089-5614608	2.61086	13.2994	2.34877	0.0011	0.015507
cyp-13A5	II:9798275-9800363	4.91943	25.0817	2.35007	5.00E-05	0.001092
rol-6	II:8733049-8734314	0.846394	4.32487	2.35326	5.00E-05	0.001092
C33F10.1	II:4835028-4835717	1.53627	7.89908	2.36226	5.00E-05	0.001092
Y34B4A.6	X:5248472-5255071	178.775	919.403	2.36256	5.00E-05	0.001092
Y43F8A.2	V:19371567-19376583	0.22442	1.15422	2.36265	5.00E-05	0.001092
dpy-13	IV:4235613-4236706	3.76449	19.3937	2.36506	5.00E-05	0.001092

R07B7.6	V:12072876-12074986	3.94033	20.4778	2.37767	5.00E-05	0.001092
ZK938.1	II:9829417-9830754	0.499568	2.60302	2.38143	5.00E-05	0.001092
C07A12.2	X:4544875-4545418	17.4567	91.1377	2.38426	0.00175	0.022776
clec-173	IV:3266202-3267675	17.4972	91.4817	2.38636	5.00E-05	0.001092
F55G11.8	IV:12962807-12964624	5.49194	28.8888	2.39512	5.00E-05	0.001092
clec-186	IV:12866115-12869083	60.2138	316.809	2.39545	5.00E-05	0.001092
oac-31	V:1538352-1541824	0.569329	3.00011	2.39768	5.00E-05	0.001092
Y73B6BL.35	IV:6409558-6413563	9.9152	52.3102	2.39938	5.00E-05	0.001092
col-138	IV:17176437-17189806	2.98742	15.7897	2.40201	0.00015	0.002918
col-88	III:41060-42018	1.3292	7.03088	2.40315	5.00E-05	0.001092
fbxa-53	X:1716432-1718568	1.02187	5.40609	2.40338	5.00E-05	0.001092
F35E12.4	V:13731196-13733387	1.16242	6.16499	2.40697	5.00E-05	0.001092
F33H12.7	II:2586076-2586911	5.91154	31.4363	2.41082	5.00E-05	0.001092
Y34B4A.9	X:5255193-5256858	133.668	711.8	2.41282	5.00E-05	0.001092
ZK265.3	I:8242105-8243571	0.30594	1.63248	2.41574	0.00035	0.006018
decr-1.1	II:2353314-2354375	0.906398	4.83691	2.41587	0.00105	0.014995
T08B6.4	IV:4905680-4908489	0.2604	1.3929	2.41929	5.00E-05	0.001092
nspd-4	II:4842563-4842907	1.10325	5.93017	2.42631	0.00305	0.034908
B0462.5	V:18322214-18323327	1.77479	9.55867	2.42916	5.00E-05	0.001092
F36H1.12	IV:11052815-11053634	0.815559	4.39491	2.42997	0.0031	0.035282
ctc-2	MtDNA:9648-10401	1708.89	9210.08	2.43015	5.00E-05	0.001092
fbxa-30	III:1274513-1275588	0.536272	2.91906	2.44447	0.00025	0.004581

col-77	II:8358227-8359378	3.7057	20.1756	2.44479	5.00E-05	0.001092
gsp-3	I:4709316-4710708	0.464939	2.53306	2.44577	5.00E-05	0.001092
W01B6.2	IV:10073434-10075116	0.187297	1.02473	2.45185	0.00345	0.038496
C10G11.8	I:6271980-6273768	0.650505	3.56338	2.45361	5.00E-05	0.001092
ZC412.10	V:14875952-14876819	166.092	910.171	2.45415	0.0017	0.022267
C14C10.1	V:12588427-12589621	0.435216	2.38773	2.45584	5.00E-05	0.001092
col-73	II:4872097-4873127	3.22452	17.8205	2.46639	5.00E-05	0.001092
Y43C5A.2	IV:10269882-10272698	65.8645	365.222	2.4712	5.00E-05	0.001092
nspa-5	V:14878323-14878502	31.9	177.854	2.47907	0.0006	0.00946
C50F4.9	V:9523168-9524201	3.68533	20.6063	2.48322	5.00E-05	0.001092
C05B5.2	III:9999818-10000516	0.635991	3.57133	2.48938	0.00015	0.002918
T10E9.4	I:6525048-6528689	0.339165	1.92271	2.50308	5.00E-05	0.001092
col-180	X:11711310-11712280	0.732916	4.16266	2.50578	5.00E-05	0.001092
linc-71	II:3509947-3510110	29.1685	165.87	2.50757	0.0003	0.005333
col-60	I:7105318-7106924	1.14481	6.52035	2.50984	5.00E-05	0.001092
R03G8.3	X:13091130-13094424	1.97614	11.2614	2.51062	5.00E-05	0.001092
sodh-1	V:11888235-11889650	52.2673	299.417	2.51818	5.00E-05	0.001092
F54B8.4	V:15816463-15817143	5.02504	28.8223	2.51998	5.00E-05	0.001092
irg-1	V:3523586-3524575	1.1113	6.40137	2.52614	5.00E-05	0.001092
msp-57	IV:5062542-5062997	1.46016	8.41964	2.52763	0.0001	0.002025
T24B8.5	II:9082681-9083142	128.224	740.505	2.52984	5.00E-05	0.001092
R09E10.2	IV:10317556-10318299	1.57351	9.11858	2.53482	5.00E-05	0.001092
msp-152	II:4932992-4933449	1.0117	5.87794	2.53853	0.00205	0.025716

F58E6.5	V:9753424-9754578	0.313213	1.82785	2.54493	0.00025	0.004581
C30F2.3	X:16076776-16085768	0.485581	2.85732	2.55688	5.00E-05	0.001092
alg-4	III:9887210-9891437	0.147559	0.871335	2.56193	5.00E-05	0.001092
F17E9.5	IV:8345817-8346546	2.03892	12.071	2.56566	5.00E-05	0.001092
B0379.7	I:10072581-10074387	0.17643	1.05417	2.57894	0.0005	0.00809
npr-8	X:7377301-7388400	0.46764	2.79883	2.58135	5.00E-05	0.001092
alg-3	IV:11704250-11708242	0.154721	0.926118	2.58153	5.00E-05	0.001092
msd-4	III:4868333-4868769	2.61954	15.6988	2.58326	5.00E-05	0.001092
col-176	X:10077612-10078738	0.291149	1.75617	2.59261	0.0001	0.002025
msp-59	IV:5312689-5313146	1.22545	7.43999	2.60199	0.00055	0.008779
msp-78	IV:9770029-9770456	2.16593	13.1935	2.60677	5.00E-05	0.001092
C03C11.1	I:10014730-10015497	0.228359	1.39152	2.60728	0.00165	0.021692
dpy-5	I:5432157-5433054	3.74839	22.9786	2.61595	5.00E-05	0.001092
ZK180.6	IV:4520180-4524937	0.501252	3.09072	2.62434	5.00E-05	0.001092
F49F1.7	IV:4123524-4125757	4.66839	28.7892	2.62453	5.00E-05	0.001092
ZK353.4	III:8388459-8389639	0.145312	0.901496	2.63317	0.00165	0.021692
cav-2	V:13557159-13559922	0.944798	5.87062	2.63543	5.00E-05	0.001092
F07A5.2	I:7352443-7353707	0.713372	4.44395	2.63912	5.00E-05	0.001092
F38H4.4	IV:11848249-11850221	0.099327	0.620994	2.64432	0.00435	0.045946
col-49	I:3137187-3138446	1.51032	9.46793	2.6482	5.00E-05	0.001092
F08H9.2	V:14460625-14461134	1.11494	7.07246	2.66524	0.0003	0.005333
C54F6.12	V:7536865-7537970	0.318552	2.02276	2.66673	0.0026	0.030952
Y51H4A.25	IV:16731218-16743088	6.13746	39.0787	2.67067	5.00E-05	0.001092

fbxa-88	V:16142007-16143116	0.361232	2.30252	2.67222	0.00015	0.002918
col-161	V:13317031-13318010	1.03642	6.71714	2.69623	5.00E-05	0.001092
K04H4.5	III:9360268-9361331	0.296706	1.92431	2.69724	0.00075	0.011348
C34H4.1,C34H4.2	IV:1545245-1567716	18.2758	119.506	2.70907	5.00E-05	0.001092
F27C1.1	I:5433906-5443026	0.912684	6.01044	2.71928	0.00315	0.035708
C16D9.4	V:8240930-8242900	3.59693	23.7114	2.72075	5.00E-05	0.001092
C49C8.5	IV:8648664-8653677	34.7316	229.383	2.72344	5.00E-05	0.001092
F49F1.1,ubc-1	IV:4103019-4119221	56.7124	378.029	2.73676	5.00E-05	0.001092
T27A3.4	I:6098976-6099726	0.877762	5.89466	2.74751	5.00E-05	0.001092
clc-1	X:11047414-11049232	55.0636	372.229	2.75702	5.00E-05	0.001092
bli-6	IV:6377093-6378195	2.54214	17.2945	2.7662	5.00E-05	0.001092
sqt-1	II:11336690-11337835	0.966856	6.58856	2.76859	5.00E-05	0.001092
ZK484.5	I:6087368-6087764	4.83886	33.1021	2.77418	5.00E-05	0.001092
acs-10	V:14146508-14148784	0.099479	0.682033	2.77739	0.0016	0.021211
C15C6.2	I:12203799-12205809	0.642301	4.40917	2.77918	5.00E-05	0.001092
nas-5	I:9886199-9888216	1.46714	10.0721	2.77929	5.00E-05	0.001092
Y59E9AL.6	IV:5224895-5225769	0.691605	4.75728	2.78212	5.00E-05	0.001092
F55G11.2	IV:12967447-12969289	2.41492	16.6191	2.7828	5.00E-05	0.001092
fut-6	II:4647599-4655934	2.99834	20.6468	2.78368	5.00E-05	0.001092
acdh-8	II:5794506-5796274	0.187296	1.29015	2.78415	0.0003	0.005333
R09H10.7	IV:10621192-10621691	17.0059	117.887	2.79329	5.00E-05	0.001092
Y38C1AA.7	IV:158966-159831	1.86223	13.0001	2.80342	5.00E-05	0.001092
nspd-1	I:6097495-6097837	3.85287	27.17	2.81801	5.00E-05	0.001092

sss-1	IV:9892738-9893749	0.564981	4.00445	2.82533	5.00E-05	0.001092
Y47D7A.15	V:4431682-4433187	0.877726	6.25887	2.83406	5.00E-05	0.001092
gska-3	I:8749615-8751369	0.14294	1.0198	2.8348	0.0015	0.020016
VZK822L.2	IV:11912026-11913245	3.72857	26.7113	2.84075	5.00E-05	0.001092
C01G10.17	V:15090756-15091119	3.29313	23.7106	2.848	0.00045	0.007424
F41C3.1	II:4752387-4752942	2.57529	18.5574	2.84919	5.00E-05	0.001092
K02E11.10	V:14239923-14241151	0.322658	2.32996	2.85222	5.00E-05	0.001092
F49C12.6,F49C12.7	IV:9307330-9312927	19.3184	140.01	2.85748	5.00E-05	0.001092
ZC15.11	V:20278112-20278412	4.39529	31.8797	2.85861	5.00E-05	0.001092
-	II:3816620-3816795	45.5268	331.518	2.8643	5.00E-05	0.001092
fbxa-105	V:7390526-7392087	2.56488	18.8401	2.87684	5.00E-05	0.001092
cdr-2	V:12414621-12415711	9.73457	71.64	2.87958	5.00E-05	0.001092
F57B1.1	V:13193932-13195648	0.249947	1.84283	2.88222	0.00015	0.002918
F22B8.4	V:16083997-16088417	0.475941	3.55641	2.90157	5.00E-05	0.001092
Y18H1A.10	I:680413-686599	0.235535	1.76579	2.9063	5.00E-05	0.001092
dod-22	IV:12965386-12967376	6.10223	46.2048	2.92063	5.00E-05	0.001092
aman-3	I:5324510-5330212	2.2942	17.4205	2.92472	5.00E-05	0.001092
fbxa-128	III:11136801-11138894	1.50009	11.4347	2.9303	5.00E-05	0.001092
F22E5.6	II:2649869-2650899	0.203836	1.55884	2.935	0.0038	0.041683
Y57G7A.6	II:1281973-1285585	0.086252	0.661313	2.9387	0.0005	0.00809
msp-50	II:5199762-5200222	1.56057	11.9987	2.94273	5.00E-05	0.001092
col-63	I:8243692-8244961	0.934999	7.24472	2.95389	5.00E-05	0.001092

T06F4.1,T06F4.3	X:4056827-4081045	4.21279	33.0974	2.97387	5.00E-05	0.001092
T22B3.3	IV:11703181-11703785	0.308722	2.43418	2.97905	0.00475	0.049329
F46A8.13	I:11237049-11238340	86.9592	689.832	2.98783	0.0011	0.015507
clec-80,clec-81	IV:2823745-2828092	8.99415	71.6301	2.99351	5.00E-05	0.001092
K10D11.6	IV:12986718-12989433	1.95455	15.7523	3.01065	5.00E-05	0.001092
C49C3.9	IV:17339655-17342314	11.853	95.8566	3.01563	5.00E-05	0.001092
Y69H2.9	V:18701555-18706254	2.11997	17.2021	3.02047	0.00425	0.045158
E04D5.4	II:10440285-10442515	4.79153	38.9605	3.02345	5.00E-05	0.001092
valv-1	IV:7424495-7445365	25.406	207.581	3.03044	5.00E-05	0.001092
msp-64	II:5809923-5810342	1.46848	12.0324	3.03452	0.00025	0.004581
F15B9.6	V:13014143-13016654	1.08226	8.86785	3.03454	5.00E-05	0.001092
F01D5.2	II:13998496-13998956	5.25545	43.0832	3.03524	5.00E-05	0.001092
mlt-11	V:20667210-20678613	3.23286	26.5315	3.03682	5.00E-05	0.001092
F08B4.8	IV:8677602-8678019	1.99747	16.5561	3.05112	5.00E-05	0.001092
F01D5.3	II:13999157-14000065	17.2983	145.163	3.06897	5.00E-05	0.001092
C30G7.3	V:14942132-14945668	0.153516	1.28956	3.07042	0.00375	0.04123
T04F8.7	X:11677508-11680930	4.67043	39.5842	3.0833	5.00E-05	0.001092
C06B8.2	V:15471334-15478655	3.09037	26.5343	3.10201	5.00E-05	0.001092
col-12	V:10423906-10425092	0.483438	4.26841	3.14229	5.00E-05	0.001092
acs-18	IV:10310790-10313670	0.069976	0.621982	3.15194	0.004	0.043244
F42A9.7	IV:8616058-8617079	0.092288	0.835385	3.17822	0.00435	0.045946

col-175	X:9233641-9234616	1.06442	9.63848	3.17874	5.00E-05	0.001092
Y71G12B.2	I:1816149-1818509	0.28386	2.57301	3.1802	5.00E-05	0.001092
nspd-7	IV:10268661-10269228	6.07438	55.381	3.18858	5.00E-05	0.001092
C32E8.4	I:3783834-3784435	0.832619	7.61873	3.19382	0.0022	0.027238
C32H11.4	IV:12921287-12923292	6.0802	56.4664	3.2152	5.00E-05	0.001092
col-162	V:13441966-13443402	0.558012	5.21783	3.22508	5.00E-05	0.001092
col-133	IV:14098334-14099352	1.7074	15.9972	3.22795	5.00E-05	0.001092
best-1	IV:13107656-13111503	1.56102	14.6582	3.23115	0.00385	0.042037
nspd-2	IV:9844028-9844337	5.2336	49.464	3.2405	5.00E-05	0.001092
Y40D12A.2	III:6592520-6620121	20.2951	191.897	3.24113	0.0013	0.017798
col-13	V:10420889-10421892	0.150661	1.42588	3.24248	0.0028	0.032893
M04C3.5	V:19449774-19451078	5.84137	57.2609	3.29317	5.00E-05	0.001092
K10C2.14	X:6439893-6440559	0.849524	8.34895	3.29687	0.00175	0.022776
H43E16.1	II:6674267-6679363	1.23423	12.1415	3.29827	5.00E-05	0.001092
C54D2.1	X:7842631-7845557	0.130638	1.30602	3.32153	0.00035	0.006018
dod-19	V:411778-414760	117.172	1172.16	3.32246	5.00E-05	0.001092
ZK1290.10	II:7549334-7553906	0.321891	3.22216	3.32338	5.00E-05	0.001092
Y40H4A.2	V:14583305-14585436	0.069499	0.696249	3.32453	0.00335	0.037616
F01D5.5	II:14001683-14002300	9.8555	99.7401	3.33917	5.00E-05	0.001092
Y71G12B.32	I:1813908-1816061	0.363694	3.85229	3.40492	5.00E-05	0.001092
ttr-22	V:12241429-12241912	0.563115	6.04542	3.42434	0.0027	0.031982
F35E12.6	V:13734041-13736247	53.1864	594.984	3.48372	5.00E-05	0.001092

C34D4.3	IV:7153661-7154198	0.532889	6.05518	3.50626	0.00215	0.026712
ech-9	IV:10233319-10235329	2.72622	31.0392	3.50911	5.00E-05	0.001092
col-146	V:9629942-9631011	0.228168	2.62563	3.5245	0.0005	0.00809
F35E12.8	V:13749184-13751921	4.99376	57.6666	3.52954	5.00E-05	0.001092
F46C5.1	II:8820198-8821200	3.11159	36.3578	3.54654	5.00E-05	0.001092
K12H6.9	II:2824413-2824946	0.307901	3.61767	3.55453	0.00295	0.03412
C07E3.3	II:10353632-10357518	3.36646	40.6009	3.59221	5.00E-05	0.001092
Y18H1A.1	I:688285-691267	0.042442	0.513231	3.59603	0.0027	0.031982
ugt-18	V:12820264-12822758	1.73824	22.1178	3.6695	5.00E-05	0.001092
gst-38	V:15915167-15916079	1.44758	18.9763	3.71249	5.00E-05	0.001092
oac-57	IV:12304297-12307820	13.044	173.664	3.73484	5.00E-05	0.001092
srj-29	V:16075658-16077387	0.294363	3.95723	3.74882	5.00E-05	0.001092
F49F1.5	IV:4119460-4120398	1.46688	20.6239	3.8135	5.00E-05	0.001092
rnh-1.3	I:9710087-9710767	11.0668	162.519	3.8763	5.00E-05	0.001092
oac-58	IV:12308178-12311773	0.41502	6.09677	3.87679	5.00E-05	0.001092
C14C6.5	V:536627-537418	92.6835	1368.3	3.88393	5.00E-05	0.001092
F25A2.1	V:1179603-1181548	1.10014	16.3205	3.89093	5.00E-05	0.001092
F13B6.1	IV:7456747-7458035	0.625258	9.33242	3.89973	5.00E-05	0.001092
mpk-2	II:5104117-5108901	2.25244	33.6414	3.90068	5.00E-05	0.001092
Y37H2A.13	V:18142848-18143543	0.506332	7.79911	3.94515	0.0004	0.006764
F48G7.5,F48G7.8	V:622055-627650	0.467413	7.26759	3.95871	5.00E-05	0.001092
clec-172	IV:1515527-1516627	0.484657	7.59839	3.97066	0.0003	0.005333

Y38H6C.8	V:20514765-20515706	0.445409	7.03123	3.98058	0.00045	0.007424
oac-57	IV:12304297-12307820	41.8476	666.37	3.99311	5.00E-05	0.001092
D2062.6	II:2619441-2619747	0.871041	14.8226	4.08891	0.0026	0.030952
Y18H1A.11	I:680413-686599	0.54377	9.28601	4.09399	5.00E-05	0.001092
clec-70	IV:3932732-3936238	0.647549	11.2294	4.11615	5.00E-05	0.001092
K10D11.3	IV:12982119-12986088	0.936218	16.2867	4.12071	5.00E-05	0.001092
C08E8.4	V:18371845-18373531	5.50931	98.3006	4.15726	5.00E-05	0.001092
clec-85	IV:2854345-2855456	82.1429	1633.1	4.31333	5.00E-05	0.001092
srx-12	IV:1046031-1049506	0.146088	2.96897	4.34505	0.0026	0.030952
K06A9.1	X:1547504-1560558	1.45053	29.9818	4.36943	5.00E-05	0.001092
dod-17	IV:12976292-12978344	4.97469	107.227	4.42992	5.00E-05	0.001092
K08D8.4	IV:12893575-12909998	5.95764	132.631	4.47653	5.00E-05	0.001092
C17H12.6	IV:6820994-6822506	1.62657	37.1073	4.5118	5.00E-05	0.001092
C30F2.4	X:16075060-16075668	10.8953	267.436	4.61742	0.0001	0.002025
T22F3.11	V:3612172-3614551	2.0698	50.8999	4.6201	5.00E-05	0.001092
M28.8	II:10628268-10633217	4.04028	100.679	4.63916	5.00E-05	0.001092
F01D5.1	II:13996953-13997596	8.9412	225.996	4.65969	5.00E-05	0.001092
dod-20	V:422497-424166	0.252297	6.39	4.66262	5.00E-05	0.001092
C06E1.7	III:8591238-8593092	0.543695	13.9817	4.6846	5.00E-05	0.001092
comt-2	V:16493654-16494449	1.23058	35.9984	4.87052	5.00E-05	0.001092
Y41D4B.15,hpo-6	IV:1545245-1567716	15.9244	470.126	4.88374	5.00E-05	0.001092
clec-125	II:3516007-3518898	0.234699	7.08165	4.9152	5.00E-05	0.001092

Y54G2A.49	IV:2851692-2853261	6.17508	192.428	4.96172	5.00E-05	0.001092
oac-18	V:16288787-16292154	0.058934	1.93807	5.03938	0.0026	0.030952
Y47H9C.1	I:11830984-11833166	1.21987	43.6254	5.16037	5.00E-05	0.001092
clec-86	X:7139900-7143641	7.05194	257.214	5.18881	5.00E-05	0.001092
C01G10.5	V:15089101-15089499	2.47114	94.7041	5.26018	0.0026	0.030952
clec-72	IV:3944815-3947364	1.03061	39.534	5.26152	5.00E-05	0.001092
-	II:13663795-13667855	0.044162	1.82256	5.36703	5.00E-05	0.001092
M01H9.7	IV:4464436-4465466	1.08457	48.2155	5.4743	5.00E-05	0.001092
Y37H2A.14	V:18143737-18144721	8.58294	397.922	5.53487	5.00E-05	0.001092
F44G3.10	V:16138760-16139627	0.527271	25.0432	5.56973	5.00E-05	0.001092
dod-24	IV:12940141-12941368	33.6565	1718.84	5.67441	5.00E-05	0.001092
Y39G8B.9	II:13981351-13981786	3.25625	171.9	5.72222	5.00E-05	0.001092
F09C12.2	II:5110028-5112232	0.054438	2.9627	5.76616	0.0026	0.030952
F20G2.5	V:13771507-13773700	0.472415	29.2909	5.95425	5.00E-05	0.001092
C32H11.1	IV:12912789-12914969	0.218548	19.8945	6.50827	5.00E-05	0.001092
H02F09.2,H02F09.3	X:1568668-1574110	0.728134	72.6242	6.6401	5.00E-05	0.001092
dct-17	V:13727760-13730776	10.3817	1171.73	6.81845	5.00E-05	0.001092
B0024.4	V:10297398-10298982	2.31407	265.014	6.83949	5.00E-05	0.001092
clec-17	I:12430028-12431474	0.177454	20.4435	6.84805	5.00E-05	0.001092
clec-42	V:18191442-18194262	0.165497	25.4238	7.26323	5.00E-05	0.001092
F55G11.4	IV:12973635-12975597	29.2943	5507.62	7.55466	5.00E-05	0.001092
clec-60	II:10480101-10481846	0.272176	51.2837	7.55782	5.00E-05	0.001092

clec-71	IV:3937463-3939924	0.532444	178.869	8.39205	5.00E-05	0.001092
F35E12.5	V:13737006-13738471	3.5881	1692.17	8.88144	5.00E-05	0.001092
C32H11.9	IV:12935050-12936271	0.14385	105.614	9.52002	0.0012	0.016653
Y53G8AM.5	III:3256729-3258395	0.288702	411.71	10.4778	0.0011	0.015507
dod-21	IV:12936737-12937948	0.064343	114.415	10.7962	0.0026	0.030952
fipr-16	III:8590832-8590982	0	214.008	N/A	5.00E-05	0.001092
-	X:3387109-3387290	0	108.773	N/A	5.00E-05	0.001092
Y57E12B.11	V:6949568-6949854	0	49.4078	N/A	5.00E-05	0.001092
F46B3.1	V:20596008-20597244	0	29.3339	N/A	5.00E-05	0.001092
Y46C8AL.11	IV:3943302-3943744	0	15.5845	N/A	5.00E-05	0.001092
B0294.3	X:1892186-1893272	0	14.4938	N/A	0.003	0.034475
F14F8.8	V:16671621-16672186	0	12.0395	N/A	5.00E-05	0.001092
Y37H2A.11	V:18141460-18142577	0	11.9199	N/A	5.00E-05	0.001092
fipr-6	V:10231267-10231536	0	8.19549	N/A	0.00375	0.04123

7.6 RNAseq: Significant genes *kri-1(ok1251); mpk-2(ok219)*

Table 7.5 RNAseq: Significant genes *kri-1(ok1251); mpk-2(ok219)*

Gene Name	Locus	Wild Type FPKM	*kri-1 (ok1251); mpk-2 (ok219)* FPKM	log2 Fold Change	P value	Q value
dct-17	V:13727760-13730776	10.0887	0.60505	-4.05954	5.00E-05	0.005765

K02G10.15	X:4680978-4682718	9.06842	0.70032	-3.69477	5.00E-05	0.005765
Y69A2AR.12	IV:2568467-2572317	1.0743	0.089071	-3.5923	0.00015	0.014538
unc-49	III:10520675-10532706	50.0222	5.58	-3.16423	5.00E-05	0.005765
dod-24	IV:12940141-12941368	32.7341	4.0197	-3.02564	5.00E-05	0.005765
cnc-6	III:1763523-1764901	6.54708	0.971181	-2.75304	0.00065	0.039517
asm-3	IV:520209-523757	0.704495	0.120621	-2.54611	0.0004	0.030056
ora-1	IV:7977835-7979014	3.60817	0.630518	-2.51666	0.0002	0.018322
Y41D4B.26	IV:1631950-1633257	3.11491	0.5882	-2.40481	0.0006	0.037854
K12B6.11	V:6288907-6289656	7.34276	1.39969	-2.39121	0.00065	0.039517
H02F09.2,H02F09.3	X:1568668-1574110	0.70618	0.135973	-2.37672	0.00025	0.021998
hch-1	X:14696411-14699977	5.92976	1.29304	-2.19721	5.00E-05	0.005765
ces-2	I:14961500-14965355	5.29438	1.16773	-2.18075	5.00E-05	0.005765
cutl-2	II:9721763-9724526	1.75265	0.441032	-1.99058	0.00045	0.032186
dod-22	IV:12965386-12967376	5.94226	1.54225	-1.94598	5.00E-05	0.005765
fbxb-88	II:4826506-4827872	1.58945	0.424703	-1.904	0.00075	0.043238
C08F1.10	II:1785261-1786277	6.13003	1.71734	-1.83572	5.00E-05	0.005765
F40H7.12	II:3687790-3688691	3.76923	1.06508	-1.8233	0.00015	0.014538

cutl-28	IV:684496-688339	0.726496	0.210467	-1.78736	0.00085	0.047568
lipl-3	V:521675-524218	1.77547	0.518575	-1.77558	0.0006	0.037854
C09F9.2	II:14705515-14718225	2.9194	0.85317	-1.77477	5.00E-05	0.005765
dpy-3	X:2144601-2145647	3.8187	1.11972	-1.76994	0.0004	0.030056
C26F1.1	V:7785418-7787711	7.14913	2.10582	-1.76339	0.0009	0.048538
dpy-14	I:6843594-6845136	47.1943	14.0496	-1.74808	5.00E-05	0.005765
arrd-1	II:627512-628668	8.05337	2.44426	-1.7202	5.00E-05	0.005765
pqn-73	II:8540719-8545452	1.36671	0.415271	-1.71858	0.0002	0.018322
T02E9.5	V:11342230-11344735	19.9825	6.2315	-1.68109	5.00E-05	0.005765
egl-46	V:6679328-6681573	3.51284	1.10137	-1.67334	0.0004	0.030056
dod-17	IV:12976292-12978344	4.83303	1.53981	-1.65017	5.00E-05	0.005765
cyp-37B1	V:16278190-16280614	2.3822	0.774659	-1.62066	0.0004	0.030056
dsl-3	IV:1610418-1612915	4.02756	1.31397	-1.61597	0.0003	0.025078
T19C4.1	V:11149706-11151319	1.94676	0.636233	-1.61345	0.00055	0.03606
his-24	X:14490005-14491111	93.1653	30.5934	-1.60657	5.00E-05	0.005765
clec-266	X:6617440-6627975	50.0224	16.4914	-1.60086	5.00E-05	0.005765
F08G2.5	II:13832852-13833631	4.02727	1.32943	-1.59899	0.0007	0.041245
F46E10.2	V:6520434-6521086	13.9983	4.65366	-1.58881	5.00E-05	0.005765
lpr-4	X:11065132-11066811	2.70363	0.899411	-1.58784	0.00055	0.03606

F55G11.4	IV:12973635-12975597	28.4445	9.56082	-1.57294	5.00E-05	0.005765
unc-103	III:4115322-4147279	6.16419	2.07702	-1.5694	5.00E-05	0.005765
Y110A2AL.4	II:2839303-2840386	8.91506	3.07374	-1.53625	0.00015	0.014538
lpr-3	X:11057371-11059794	4.72028	1.63167	-1.53252	5.00E-05	0.005765
clec-85	IV:2854345-2855456	79.6064	28.0159	-1.50664	5.00E-05	0.005765
dpy-17	III:5107329-5108589	47.0138	16.612	-1.50086	5.00E-05	0.005765
R09E10.5	IV:10295407-10302310	1.71629	0.608246	-1.49657	0.00015	0.014538
noah-1	I:5874418-5878961	11.2674	4.00485	-1.49233	5.00E-05	0.005765
H42K12.3	X:1311604-1316636	2.26258	0.812881	-1.47685	0.00035	0.0277
T01D3.3	V:13704495-13711090	1.10701	0.39809	-1.4755	0.0004	0.030056
F55G11.2	IV:12967447-12969289	2.34867	0.862138	-1.44585	0.0007	0.041245
Y7A9D.1	IV:16381375-16382211	9.0653	3.33692	-1.44184	0.00045	0.032186
fbxc-51	II:868813-871700	8.06036	2.9837	-1.43374	5.00E-05	0.005765
fbxb-37	II:2091742-2093853	2.45609	0.913147	-1.42744	0.00075	0.043238
hil-7	IV:6646033-6646939	33.2829	12.399	-1.42456	0.00055	0.03606
cht-1	X:3397607-3400343	22.278	8.41223	-1.40506	5.00E-05	0.005765
wrt-10	II:7533299-7534514	6.63733	2.51698	-1.39891	0.0004	0.030056

mul-1	IV:4121341-4123069	9.74287	3.69867	-1.39734	5.00E-05	0.005765
noah-2	IV:14091253-14096624	12.633	4.83335	-1.3861	0.0004	0.030056
Y82E9BR.1	III:1458438-1466732	1.4687	0.563643	-1.38168	0.00065	0.039517
tba-7	III:11366751-11371775	15.9654	6.14856	-1.37663	0.00055	0.03606
Y71A12B.11	I:13978429-13980148	9.0251	3.49017	-1.37065	0.00015	0.014538
igcm-1	X:845729-851507	1.15833	0.451973	-1.35773	0.00015	0.014538
F30H5.3	III:505236-512175	0.887711	0.346543	-1.35706	0.0006	0.037854
sqt-3	V:12352993-12354314	45.0553	17.5901	-1.35693	5.00E-05	0.005765
ZK970.7	II:10310399-10316219	6.26364	2.44884	-1.3549	0.00045	0.032186
ham-1	IV:12542033-12545724	4.00982	1.59115	-1.33347	0.0002	0.018322
dpy-7,glb-16	X:7536459-7540131	4.60984	1.83758	-1.32691	0.0006	0.037854
jmjc-1	I:3631089-3636485	4.9734	2.00067	-1.31375	0.00015	0.014538
R193.2	X:1128982-1151343	14.7076	5.94038	-1.30794	0.00035	0.0277
clec-67	IV:3922164-3925045	7.36444	2.98096	-1.3048	5.00E-05	0.005765
cav-1	IV:9771153-9773474	104.413	42.3785	-1.30089	5.00E-05	0.005765
M153.2	X:12150079-12154089	3.7844	1.54235	-1.29493	0.0003	0.025078
zag-1	IV:3855842-3861499	1.89737	0.784026	-1.27503	0.00075	0.043238

cec-8	III:429299-431752	5.06981	2.12656	-1.25341	5.00E-05	0.005765
ptr-4	X:6060756-6065986	2.08453	0.874523	-1.25316	0.00025	0.021998
bath-47	II:1601788-1604618	2.43604	1.02767	-1.24516	0.0009	0.048538
C35E7.5	I:10823357-10829015	11.5194	4.89183	-1.23562	5.00E-05	0.005765
B0507.3	V:8768908-8770876	3.19051	1.35929	-1.23093	0.0009	0.048538
Y41C4A.11	III:11719899-11723602	11.3747	4.8902	-1.21786	5.00E-05	0.005765
pat-9	X:16536836-16540195	2.74826	1.19039	-1.20708	0.0005	0.034472
hbl-1	X:5822149-5827758	6.32128	2.74929	-1.20116	5.00E-05	0.005765
cfz-2	V:3441500-3444877	2.83472	1.23563	-1.19796	0.00065	0.039517
frm-7	V:12302483-12306972	65.9712	29.1074	-1.18045	5.00E-05	0.005765
Y41D4B.15,hpo-6	IV:1545245-1567716	15.4442	6.82258	-1.17867	0.00055	0.03606
pha-4	V:20752935-20760303	4.36874	1.94186	-1.16978	0.00015	0.014538
nhr-25	X:13008492-13013961	2.18094	0.969797	-1.1692	0.00065	0.039517
dod-19	V:411778-414760	113.568	50.5331	-1.16826	5.00E-05	0.005765
ttr-50	IV:11640144-11641015	66.4085	29.6795	-1.1619	5.00E-05	0.005765
mnp-1	III:4356538-4364966	4.29701	1.9262	-1.15758	5.00E-05	0.005765
F55G11.8	IV:12962807-12964624	5.33921	2.47782	-1.10756	0.0007	0.041245

slc-17.5	V:8282374-8284885	3.97304	1.84839	-1.10398	0.0003	0.025078
F53B3.5	X:2872743-2879619	14.1148	6.74226	-1.06591	5.00E-05	0.005765
aman-3	I:5324510-5330212	2.22647	1.06584	-1.06277	0.0006	0.037854
ceh-43	III:4445463-4449943	7.34827	3.54074	-1.05335	0.00045	0.032186
F33E2.5	I:12591114-12598923	11.8008	5.72133	-1.04446	0.0006	0.037854
ncam-1	X:692977-710007	4.28998	2.09839	-1.03169	0.00025	0.021998
K08D8.5	IV:12910644-12912136	20.292	9.99472	-1.02167	5.00E-05	0.005765
cth-1	V:16100654-16102744	19.1106	9.5426	-1.00192	5.00E-05	0.005765
F42A10.7	III:6177914-6178702	20.17	10.0967	-0.99832	0.0003	0.025078
C17H12.8	IV:6818605-6820643	181.012	91.244	-0.98828	5.00E-05	0.005765
hmg-11	II:4672797-4673747	51.0794	25.8897	-0.98036	0.0001	0.010963
odc-1	V:6898540-6900223	21.4473	10.8992	-0.97658	5.00E-05	0.005765
dsl-2	IV:1202646-1204970	9.27638	4.75706	-0.96349	0.0009	0.048538
fat-5	V:17723779-17730381	17.5678	9.02077	-0.96161	5.00E-05	0.005765
hil-3	X:8159153-8160086	26.339	13.6032	-0.95325	0.0001	0.010963
C44C11.6,sop-2	II:12339943-12352459	20.633	10.6921	-0.94841	5.00E-05	0.005765
aagr-1	IV:8366538-8375372	19.6106	10.2156	-0.94087	5.00E-05	0.005765
lea-1	V:10011870-10031094	458.873	240.917	-0.92956	5.00E-05	0.005765

ZC190.4	V:8650432-8673545	3.62092	1.90637	-0.92553	0.0006	0.037854
T19B10.2	V:11221301-11226011	37.3776	19.7229	-0.9223	0.00015	0.014538
F53F1.4	V:13411076-13411714	68.17	36.1023	-0.91705	5.00E-05	0.005765
sepa-1	I:13298223-13300715	6.76051	3.58844	-0.91378	0.00035	0.0277
K07C11.7	V:8206866-8213968	59.8179	31.8118	-0.91102	5.00E-05	0.005765
eef-1A.2	X:7823651-7826072	319.21	172.103	-0.89124	5.00E-05	0.005765
sto-1	X:7562836-7564812	12.3749	6.67343	-0.89092	0.00035	0.0277
C33G3.4	X:14071183-14076295	3.78899	2.04674	-0.88848	0.0009	0.048538
T09B4.5	I:6154074-6157400	28.2628	15.3923	-0.87669	5.00E-05	0.005765
T06A1.5	V:1927222-1931376	8.78914	4.84301	-0.85982	0.00045	0.032186
arrd-13	II:13758413-13761227	61.5979	34.1485	-0.85106	5.00E-05	0.005765
aqp-2	II:9258912-9262002	60.8366	33.7553	-0.84983	5.00E-05	0.005765
H34I24.2	III:2842043-2845197	78.4068	44.2068	-0.82671	5.00E-05	0.005765
ZK6.11	V:415712-417706	195.738	111.186	-0.81594	5.00E-05	0.005765
F35E12.6	V:13734041-13736247	51.5603	29.4032	-0.81029	5.00E-05	0.005765
haf-9	I:6081781-6085962	15.8608	9.23226	-0.78071	5.00E-05	0.005765
hpo-15	V:5505295-5513830	33.773	19.911	-0.76231	0.0002	0.018322
cpr-3	V:15296833-15298676	15.0722	8.88818	-0.76194	0.0004	0.030056
F13C5.2	X:593959-596299	17.6153	10.3995	-0.76032	0.0002	0.018322

M28.10	II:10647515-10648676	91.3476	54.2182	-0.75259	5.00E-05	0.005765
lam-3	I:10608465-10621428	3.63304	2.15991	-0.7502	5.00E-05	0.005765
D1086.3	V:14092862-14093986	32.2701	19.4075	-0.73359	0.0008	0.045532
K06G5.1	X:14214938-14219089	171.89	105.779	-0.70044	5.00E-05	0.005765
F57F4.4	V:6401368-6408783	39.8245	24.7436	-0.6866	5.00E-05	0.005765
clec-63	II:12895637-12897462	644.02	407.082	-0.66179	5.00E-05	0.005765
acs-1	V:6524988-6533075	77.234	48.8928	-0.65961	5.00E-05	0.005765
W01C8.5	X:5692371-5697308	20.3538	12.9333	-0.65421	0.00085	0.047568
clec-65	II:12901293-12903335	103.95	66.1607	-0.65184	5.00E-05	0.005765
clec-186	IV:12866115-12869083	58.43	37.2484	-0.64953	0.00015	0.014538
asns-2	X:8748430-8750969	16.8159	10.8388	-0.63362	0.0006	0.037854
C30F12.2	I:6967665-6970190	31.4015	20.8474	-0.59097	0.0005	0.034472
R06C1.4	I:11930724-11931762	335.065	223.655	-0.58316	0.00015	0.014538
C05D12.3	II:11424759-11430599	18.4048	12.3392	-0.57684	0.00035	0.0277
Y54F10AM.8	III:2503447-2507972	34.7095	23.744	-0.54777	0.0004	0.030056
clec-50	V:19752400-19755363	265.37	181.578	-0.54742	5.00E-05	0.005765
C49C3.4	IV:17320794-17328663	39.6084	27.2704	-0.53847	0.00035	0.0277
C12D12.1	X:3499252-3505267	47.3902	32.7778	-0.53187	0.0002	0.018322

fard-1	X:2933360-2937742	43.9827	30.5446	-0.52602	0.0005	0.034472
hsp-43	X:6233144-6235954	58.5206	40.717	-0.52331	0.00075	0.043238
dod-23	II:8398159-8399160	389.822	274.784	-0.50452	5.00E-05	0.005765
K07E3.4	X:8080871-8084018	43.84	31.0242	-0.49885	0.00075	0.043238
clec-150	III:1002706-1006247	181.192	128.616	-0.49446	0.00015	0.014538
gale-1	I:12975183-12978781	115.335	83.0508	-0.47376	0.0005	0.034472
iff-2	II:8559392-8561352	215.261	155.096	-0.47293	0.0007	0.041245
lys-1	V:10277826-10279127	318.68	231.237	-0.46274	0.00045	0.032186
T20D3.2	IV:9328009-9330855	327.991	238.972	-0.45681	0.00055	0.03606
vit-3	X:3567396-3572566	552.653	402.891	-0.45599	0.00015	0.014538
F19C7.1	IV:4605785-4609679	187.399	136.946	-0.45251	0.0008	0.045532
nep-17	II:13507818-13516481	66.8942	48.9721	-0.44992	0.0002	0.018322
rps-29	III:794299-795077	5541.12	7344.08	0.406406	0.00085	0.047568
emb-9	III:9336876-9344447	30.882	41.1864	0.415402	0.00065	0.039517
W01D2.1	II:14815517-14840005	4124.32	5513.96	0.418932	0.0009	0.048538
let-2	X:16380592-16389382	45.7933	61.8308	0.43319	0.00055	0.03606
tnt-2	X:8721554-8723552	142.17	192.029	0.4337	0.0005	0.034472
col-178,col-179	X:11199454-11203990	760.896	1031.59	0.439102	0.0003	0.025078
lys-4	IV:11621442-	438.019	598.691	0.450819	0.00035	0.0277

	11623124					
upb-1	II:6288412-6290097	74.8699	102.798	0.457354	0.0008	0.045532
cpr-4	V:6614673-6615845	440.829	612.096	0.473539	0.00025	0.021998
F57F5.1	V:12003027-12004600	673.364	937.893	0.478038	0.00015	0.014538
col-80	II:10695053-10714299	599.982	836.21	0.478945	0.00065	0.039517
T25F10.6	V:6765559-6768788	165.457	235.443	0.508919	5.00E-05	0.005765
Y57G11B.5	IV:14574823-14576581	206.028	294.816	0.516975	0.0001	0.010963
F23D12.11	X:14423404-14424749	379.597	544.328	0.520008	0.00065	0.039517
mlc-3	III:5565024-5567384	296.368	426.577	0.525415	0.00035	0.0277
F32D8.11,F32D8.12	V:10887870-10891030	46.2498	67.2798	0.540726	0.00055	0.03606
rpl-39	V:7774515-7776086	14004.8	20491.5	0.549101	5.00E-05	0.005765
unc-15	I:7376603-7383197	105.142	154.763	0.557716	5.00E-05	0.005765
col-19	X:406451-425631	483.154	711.768	0.558923	0.00015	0.014538
pat-10	I:5018769-5020166	977.686	1481.12	0.599242	5.00E-05	0.005765
col-8	III:7019582-7020600	520.215	790.393	0.603464	5.00E-05	0.005765
C10G8.4	V:5311934-5312316	763.737	1166.73	0.611327	5.00E-05	0.005765
F09G8.7	III:8267946-8268357	258.635	400.263	0.630033	0.0009	0.048538
col-20	II:4869606-4870791	757.368	1185.76	0.646749	5.00E-05	0.005765

act-4	X:4960552-4969359	350.705	550.037	0.649272	5.00E-05	0.005765
myo-3	V:12226815-12234343	8.07289	12.6779	0.651153	5.00E-05	0.005765
spp-2	X:7315994-7316773	87.7502	138.266	0.655977	0.0007	0.041245
col-135	IV:15129661-15131786	14.7248	23.3063	0.662471	0.0002	0.018322
col-93	III:10984554-10985608	276.231	441.104	0.675244	5.00E-05	0.005765
Y69H2.14	V:18638476-18639591	170.067	274.115	0.688678	5.00E-05	0.005765
T13F3.6	V:16270215-16271221	109.656	177.605	0.695693	5.00E-05	0.005765
F23A7.8	X:16213372-16213599	2786.98	4524.04	0.69891	5.00E-05	0.005765
F11E6.3	IV:17470509-17472025	123.137	199.982	0.699611	5.00E-05	0.005765
col-103	IV:762377-763678	138.017	226.202	0.712766	5.00E-05	0.005765
F15E6.4	IV:4291461-4292109	235.073	389.237	0.727539	0.00045	0.032186
C35A5.3	V:10497058-10501477	18.6386	31.0015	0.734039	5.00E-05	0.005765
C49F5.7	X:11994783-11995839	172.428	293.54	0.767558	5.00E-05	0.005765
asp-12	V:8269253-8272058	43.5706	74.5138	0.774153	5.00E-05	0.005765
act-1	V:11079166-11082497	94.5725	164.9	0.802097	5.00E-05	0.005765
Y94H6A.10	IV:2709899-2710670	39.5329	68.9716	0.802947	5.00E-05	0.005765
hsp-16.41	V:1805232-1805875	23.8922	41.6938	0.80329	0.00055	0.03606

col-159	V:13198229-13199315	15.9472	28.1661	0.820659	0.0001	0.010963
spp-4	X:7318274-7318776	71.7004	127.457	0.829955	5.00E-05	0.005765
unc-89	I:4035743-4090961	4.06307	7.29362	0.844064	0.0001	0.010963
tbx-32	X:1654434-1657792	1512.66	2727.36	0.850417	0.0007	0.041245
col-98	III:13018934-13020231	94.4747	172.142	0.865597	5.00E-05	0.005765
Y10G11A.90	IV:16417117-16417416	156.176	286.789	0.876821	5.00E-05	0.005765
acdh-2,ins-13	II:5544584-5547577	19.1963	35.3569	0.881159	5.00E-05	0.005765
unc-43	IV:10324264-10350217	50.0581	93.7679	0.905491	5.00E-05	0.005765
unc-54	I:14855898-14863540	80.2372	151.885	0.920634	5.00E-05	0.005765
col-139	V:4652381-4653986	16.171	30.903	0.934334	5.00E-05	0.005765
nlp-24	V:11616282-11618266	67.5044	129.47	0.939569	5.00E-05	0.005765
T12B5.15	III:954294-954652	103.123	199.211	0.949929	0.00025	0.021998
poml-3	I:4145311-4147136	4.63355	9.07622	0.969974	0.0005	0.034472
C10C5.3	IV:9374764-9376492	7.78461	15.3683	0.981262	5.00E-05	0.005765
Y105C5B.5	IV:15899923-15901225	286.809	566.703	0.982502	5.00E-05	0.005765
asp-8	V:3024218-3027933	2.52152	5.00826	0.990018	0.0009	0.048538
col-129	IV:12108670-	17.3404	34.6454	0.998522	5.00E-05	0.005765

	12110258					
acs-2	V:15567393-15569889	15.4689	31.0902	1.00709	5.00E-05	0.005765
F18E3.11	V:7413436-7413840	43.3159	89.7717	1.05136	5.00E-05	0.005765
col-142	V:6831162-6832254	21.1918	45.3168	1.09654	5.00E-05	0.005765
hsp-16.2	V:1804333-1804971	19.119	41.6981	1.12497	5.00E-05	0.005765
B0205.12	I:10730466-10730712	247.01	554.439	1.16646	0.00035	0.0277
F52G3.6	X:16943322-16943517	243.625	559.892	1.20049	0.0003	0.025078
nlp-33	V:11147343-11147810	62.856	146.179	1.21762	5.00E-05	0.005765
col-81	II:11012394-11013779	9.37574	21.9271	1.22571	5.00E-05	0.005765
F55H12.2	I:8867797-8868300	18.6994	45.9264	1.29634	5.00E-05	0.005765
rrn-2.1	I:15064300-15064453	4144.01	10373	1.32373	5.00E-05	0.005765
F52D2.14,linc-6	X:1982709-1982935	406.209	1017.34	1.32451	0.00055	0.03606
Y51A2D.21	V:18571832-18572949	5.54425	14.1474	1.35148	0.0009	0.048538
C10C5.5	IV:9381420-9383115	2.67552	7.1781	1.42378	5.00E-05	0.005765
Y38C1AA.1	IV:208188-217393	67.165	186.896	1.47646	5.00E-05	0.005765
-	III:5092685-5093154	6.49714	18.7426	1.52844	5.00E-05	0.005765
-	III:5092009-5092382	9.89529	29.8967	1.59517	5.00E-05	0.005765
C32D5.18	II:6343053-6345925	3316.75	10674.4	1.68632	5.00E-05	0.005765
F19F10.13	V:7567998-7568735	1.20117	4.30436	1.84136	0.00015	0.014538

linc-1	I:13652523-13652727	69.9373	320.846	2.19775	0.0007	0.041245
F59C6.16	I:10506999-10515506	180.106	835.884	2.21446	5.00E-05	0.005765
R03G8.4	X:13101305-13104205	0.126784	0.685841	2.43551	0.0005	0.034472
ctb-1	MtDNA:4503-5676	1303.44	7117.91	2.44913	5.00E-05	0.005765
-	III:1976846-1976895	19052.9	108289	2.5068	0.0003	0.025078
C33A12.3	IV:9510751-9513002	65.7578	391.759	2.57473	5.00E-05	0.005765
linc-71	II:3509947-3510110	28.1628	206.112	2.87156	0.0001	0.010963
mlt-11	V:20667210-20678613	3.151	65.2278	4.37161	5.00E-05	0.005765
M01H9.7	IV:4464436-4465466	1.06015	27.1946	4.68098	0.0003	0.025078
Y54G2A.10	IV:2799693-2800984	7.33697	223.826	4.93105	5.00E-05	0.005765
nduo-2	MtDNA:3361-4328	56.1713	3799.88	6.07998	5.00E-05	0.005765
C16C8.19	II:3458500-3459056	0	0.854265	N/A	5.00E-05	0.005765
C24D10.49	IV:5157140-5157326	0	8.88414	N/A	0.00025	0.021998
M01D7.9	I:1851680-1852280	1.14844	0	N/A	0.00085	0.047568
M02G9.4	II:10317268-10317587	3.69787	0	N/A	0.00045	0.032186
Y102A5C.36	V:16926926-16927447	20.2452	0	N/A	5.00E-05	0.005765
Y113G7A.17,linc-70	V:20142572-20142859	4.33384	0	N/A	0.00045	0.032186

7.7 RNAseq: Significant genes *mpk-2(ok219)*

Table 7.6 RNAseq: Significant genes *mpk-2(ok219)*

Gene Name	Locus	Wild Type FPKM	*mpk-2 (ok219)* FPKM	log2 Fold Change	P value	Q value
T22F3.11	V:3612172-3614551	2.0414	0.20074	-3.34616	5.00E-05	0.003242
pud-3	V:2324509-2327262	11.9506	1.42096	-3.07213	5.00E-05	0.003242
unc-49	III:10520675-10532706	50.984	6.41311	-2.99095	5.00E-05	0.003242
dod-24	IV:12940141-12941368	33.1742	4.43657	-2.90255	5.00E-05	0.003242
dct-17	V:13727760-13730776	10.2316	1.56802	-2.70602	5.00E-05	0.003242
pud-4	V:2324509-2327262	8.41769	1.29182	-2.70402	0.00025	0.012688
cyp-37B1	V:16278190-16280614	2.43203	0.440715	-2.46424	5.00E-05	0.003242
cyp-14A3	X:13271876-13274218	0.719579	0.137179	-2.39109	0.0015	0.048862
cyp-34A2	V:15288981-15291107	2.63426	0.554496	-2.24815	5.00E-05	0.003242
mtl-1	V:6691368-6691863	54.4568	11.617	-2.22887	5.00E-05	0.003242
C50F7.5	IV:7726717-7727951	13.7559	3.29895	-2.05997	5.00E-05	0.003242
acs-2	V:15567393-15569889	15.7657	4.03852	-1.96489	5.00E-05	0.003242
lipl-3	V:521675-524218	1.80625	0.466602	-1.95273	5.00E-05	0.003242
ugt-18	V:12820264-12822758	1.71467	0.44606	-1.94262	5.00E-05	0.003242

lipl-2	V:9791570-9793391	2.25485	0.6007	-1.90831	5.00E-05	0.003242
C18H7.1	IV:615543-620930	1.02201	0.290282	-1.81588	0.00025	0.012688
ptr-22	V:18919233-18931381	1.05578	0.302315	-1.80419	5.00E-05	0.003242
scl-2	IV:13057677-13059092	95.3402	28.1724	-1.7588	5.00E-05	0.003242
unc-103	III:4115322-4147279	6.22481	1.84602	-1.75361	5.00E-05	0.003242
trx-3	IV:4487058-4488998	4.30654	1.31242	-1.7143	0.0002	0.010464
F09E10.14,tts-1	X:1504130-1504998	757.129	240.393	-1.65514	5.00E-05	0.003242
Y6E2A.4	V:15712205-15715644	1.26291	0.40304	-1.64775	0.0003	0.014519
F10D7.3	X:17371395-17374951	11.8323	3.83015	-1.62725	5.00E-05	0.003242
ora-1	IV:7977835-7979014	3.66812	1.19419	-1.619	0.0006	0.024126
F46C5.1	II:8820198-8821200	3.06842	1.01731	-1.59273	0.00075	0.028629
F45D3.4	V:12552210-12553229	105.863	35.2416	-1.58685	5.00E-05	0.003242
Y69A2AR.12	IV:2568467-2572317	1.08831	0.364694	-1.57733	0.00015	0.008229
dsl-6	IV:11396787-11398317	2.02342	0.680325	-1.5725	0.00085	0.031731
F55G11.4	IV:12973635-12975597	28.8688	10.1967	-1.50141	5.00E-05	0.003242
cutl-28	IV:684496-688339	0.736026	0.266945	-1.46321	0.00085	0.031731
F35E12.5	V:13737006-13738471	3.53486	1.29138	-1.45274	5.00E-05	0.003242

slc-17.9	X:9761488-9764922	0.82868	0.311771	-1.41033	0.00115	0.039754
slc-28.1	V:3463760-3466246	0.946296	0.361068	-1.39002	0.001	0.03604
K06A9.1	X:1547504-1560558	1.42948	0.551603	-1.37378	5.00E-05	0.003242
cyp-35A3	V:4022618-4024473	3.01805	1.19548	-1.33603	0.0004	0.017889
T16G1.7	V:12932940-12935052	3.2729	1.2989	-1.33328	5.00E-05	0.003242
cyp-32B1	V:2198054-2201415	2.19564	0.888546	-1.30512	0.0004	0.017889
F14D7.6	V:14301420-14306871	12.3538	5.0198	-1.29925	0.00065	0.025605
F15E6.3	IV:4292868-4299083	52.0372	21.3752	-1.2836	5.00E-05	0.003242
M153.2	X:12150079-12154089	3.82842	1.57848	-1.27822	0.0002	0.010464
T01D3.3	V:13704495-13711090	1.12238	0.483384	-1.21531	0.0005	0.021108
pqn-73	II:8540719-8545452	1.38562	0.601844	-1.20307	0.00035	0.016299
daao-1	IV:2614199-2617192	5.19399	2.29549	-1.17804	0.00015	0.008229
F42A10.7	III:6177914-6178702	20.3804	9.09991	-1.16326	5.00E-05	0.003242
F53A9.8	X:8718557-8718974	111.614	50.1308	-1.15475	5.00E-05	0.003242
F30H5.3	III:505236-512175	0.899618	0.404729	-1.15235	0.0005	0.021108
dod-22	IV:12965386-12967376	6.01679	2.72382	-1.14336	0.00025	0.012688
R09E10.5	IV:10295407-10302310	1.73829	0.792214	-1.13371	5.00E-05	0.003242
coel-1	X:4265881-4270486	5.13754	2.44635	-1.07045	0.00015	0.008229

cyp-34A4	V:3950026-3952068	3.83916	1.84724	-1.05542	0.00045	0.019359
T20B3.1	V:16815566-16821320	5.1138	2.53261	-1.01377	0.0002	0.010464
ZC443.3	V:12812290-12814122	13.2761	6.64216	-0.99911	5.00E-05	0.003242
K07E3.4	X:8080871-8084018	44.5636	22.3907	-0.99297	5.00E-05	0.003242
hbl-1	X:5822149-5827758	6.40104	3.27139	-0.9684	5.00E-05	0.003242
lys-7	V:3481418-3482600	222.234	113.999	-0.96307	5.00E-05	0.003242
C14C6.5	V:536627-537418	91.3409	47.0041	-0.95848	5.00E-05	0.003242
K04H4.2	III:9347713-9355480	1.93419	1.00078	-0.9506	0.00115	0.039754
arrd-13	II:13758413-13761227	62.5674	33.0878	-0.91911	5.00E-05	0.003242
C34C6.7	II:8707154-8708854	6.46781	3.43288	-0.91386	0.00145	0.047576
sodh-1	V:11888235-11889650	51.545	27.6606	-0.898	5.00E-05	0.003242
asah-1	I:12505097-12508064	20.0763	11.2041	-0.84146	5.00E-05	0.003242
dpy-14	I:6843594-6845136	47.7699	27.3034	-0.80702	5.00E-05	0.003242
clec-173	IV:3266202-3267675	17.2449	9.95156	-0.79318	0.00115	0.039754
F53B2.8	IV:12526246-12527339	38.7132	22.5452	-0.78	0.0006	0.024126
MTCE.33	MtDNA:10402-11354	45.5272	26.6781	-0.77107	5.00E-05	0.003242
T19D12.1	II:6666897-6673752	4.72281	2.7815	-0.76379	0.0001	0.005996
clec-85	IV:2854345-2855456	80.9374	47.8828	-0.7573	5.00E-05	0.003242
F11A5.9	V:16214889-16218605	31.9557	18.962	-0.75297	5.00E-05	0.003242

dpy-17	III:5107329-5108589	47.571	28.9401	-0.71701	0.0001	0.005996
MTCE.7	MtDNA:897-1593	84.201	51.3105	-0.71458	5.00E-05	0.003242
C34D10.2	X:8014247-8031616	13.3017	8.11175	-0.71353	0.0007	0.027102
acl-7	II:12811036-12816462	18.5359	11.5172	-0.68653	0.00025	0.012688
sqt-3	V:12352993-12354314	45.6034	29.8638	-0.61075	0.001	0.03604
aagr-1	IV:8366538-8375372	19.8935	13.1925	-0.59258	0.00035	0.016299
icl-1	V:724206-728103	133.121	88.5621	-0.58797	5.00E-05	0.003242
F35E12.6	V:13734041-13736247	52.412	35.4553	-0.5639	0.0008	0.030197
atg-2	X:6806598-6817632	7.65799	5.18093	-0.56376	0.0005	0.021108
dpy-22	X:9810230-9822273	7.80379	5.31451	-0.55424	0.001	0.03604
R09H10.5	IV:10621715-10628841	29.256	20.0528	-0.54493	0.0002	0.010464
smg-1	I:6900971-6913579	24.7513	17.2946	-0.51719	0.0004	0.017889
cpr-1	V:11975514-11976759	482.491	340.747	-0.5018	0.0005	0.021108
F28B4.3	X:3227488-3235408	35.6905	25.5266	-0.48354	0.00045	0.019359
gale-1	I:12975183-12978781	117.182	84.5823	-0.47033	0.00125	0.042667
ZC373.2	X:10057924-10058437	1745.42	2395.21	0.456581	0.00095	0.034793
tag-174	III:5081725-5083007	531.066	736.034	0.47088	0.00135	0.044948
act-4	X:4960552-4969359	355.932	495.236	0.476515	0.0006	0.024126
act-3	V:11071683-11074498	122.391	170.826	0.481025	0.00075	0.028629

rpl-41	II:11096570-11097204	5648.29	7893.12	0.482782	0.0011	0.038617
nduo-4	MtDNA:6505-7808	264.201	370.014	0.485942	0.0003	0.014519
cpn-3	I:3987890-3988702	278.941	393.093	0.494911	0.0006	0.024126
T08H10.1	V:4483467-4486531	79.4722	112.177	0.49726	0.00125	0.042667
lec-10	V:6488198-6489050	202.885	286.498	0.497867	0.0009	0.033231
rpl-43	II:14155279-14155686	5973.14	8438.21	0.498447	0.0002	0.010464
K12H4.5	III:8044480-8044911	344.014	488.124	0.50478	0.00125	0.042667
F26E4.6	I:9773169-9774012	932.309	1324.39	0.506445	0.00035	0.016299
alh-9	III:5856037-5859185	81.97	116.869	0.511725	0.0003	0.014519
H28G03.1	X:5216348-5219100	31.4339	44.8239	0.511948	0.00135	0.044948
lys-4	IV:11621442-11623124	445.892	635.851	0.511996	0.0004	0.017889
rps-21	III:7189140-7189631	3861.48	5531.16	0.518428	0.00015	0.008229
ttr-15	III:10337839-10343413	834.951	1199.57	0.522756	0.0002	0.010464
upb-1	II:6288412-6290097	76.0478	109.56	0.526741	0.00045	0.019359
ctb-1	MtDNA:4503-5676	1323.43	1909.41	0.52885	0.0003	0.014519
Y47G6A.22	I:3559916-3562851	60.3176	87.0406	0.529111	0.00135	0.044948
kbp-4	III:1080869-1081300	377.843	545.725	0.530389	0.0011	0.038617
csq-1	X:14684876-14688365	62.8851	90.8642	0.530995	0.00055	0.023003

K01G5.8	III:10740279-10740772	213.689	309.219	0.533113	0.0009	0.033231
Y82E9BR.3	III:1419195-1427226	4738.52	6861.74	0.534136	0.0014	0.046272
dim-1	X:8050469-8058220	49.7858	72.3955	0.540166	0.00065	0.025605
unc-54	I:14855898-14863540	81.5562	118.623	0.540523	0.0003	0.014519
lev-11	I:14620758-14631254	286.284	416.58	0.541148	0.0001	0.005996
C08F11.11	IV:13646734-13647658	1557.37	2278.1	0.548726	5.00E-05	0.003242
R02D3.1	IV:245120-251928	40.6806	59.5126	0.548854	0.0012	0.041377
col-143	V:6835634-6836700	880.042	1290.68	0.552485	0.00015	0.008229
aqp-7	X:3025061-3026971	62.9449	92.3336	0.552767	0.00015	0.008229
F53F10.3	I:3827207-3828143	210.786	309.79	0.55551	0.0006	0.024126
C48B6.10	I:6923075-6923690	369.466	543.418	0.556618	0.0006	0.024126
C18E9.4	II:8964237-8964901	331.06	486.937	0.556644	0.0004	0.017889
F29C4.2	IV:126730-127636	478.909	706.568	0.561076	5.00E-05	0.003242
W01D2.1	II:14815517-14840005	4178.88	6171.08	0.562406	5.00E-05	0.003242
tnt-2	X:8721554-8723552	144.37	213.74	0.566082	5.00E-05	0.003242
T25F10.6	V:6765559-6768788	167.911	249.438	0.570981	0.0001	0.005996
col-181	X:12104929-12106081	1197.03	1780.92	0.57317	0.0001	0.005996
unc-27	X:8789105-8790625	260.739	388.109	0.573854	5.00E-05	0.003242

rpl-38	V:15512165-15522020	10440.8	15546.3	0.574342	0.00035	0.016299
B0286.3	II:4368489-4372568	31.3141	46.7179	0.577163	0.0004	0.017889
F44E7.17	V:5777428-5777901	246.212	367.349	0.577249	0.0011	0.038617
C14B9.10	III:8130863-8132442	815.557	1216.97	0.577441	0.00015	0.008229
cpr-4	V:6614673-6615845	448.799	670.383	0.578915	0.00015	0.008229
tsfm-1	V:12270270-12271549	62.1941	92.931	0.579381	5.00E-05	0.003242
F57C2.4	II:14525311-14526033	361.798	540.946	0.580298	0.00085	0.031731
glrx-10	I:1049593-1050726	242.942	364.895	0.58687	0.00045	0.019359
F23D12.11	X:14423404-14424749	384.942	578.739	0.58827	0.0004	0.017889
rmo-1	II:13237404-13237908	232.364	349.571	0.5892	0.00115	0.039754
Y63D3A.7	I:14113635-14114091	301.071	453.21	0.590076	0.00065	0.025605
F44E5.1	II:11774143-11774559	1104.27	1663.63	0.591239	5.00E-05	0.003242
Y119D3B.21	III:1214951-1215287	1494.5	2252.05	0.591575	0.00015	0.008229
W01F3.2	V:20660367-20662031	49.4642	74.6606	0.593962	0.0003	0.014519
F49C12.11	IV:9319379-9321400	804.686	1214.59	0.593975	0.0009	0.033231
ZK512.4	III:9145324-9145976	215.854	327.511	0.601483	0.0014	0.046272
rps-29	III:794299-795077	5615.17	8549.91	0.60658	5.00E-05	0.003242
Y54G11A.17	II:14348891-14349406	121.354	186.067	0.616598	0.0003	0.014519
Y69A2AR.3	IV:2641309-2642116	391.627	601.098	0.618121	0.0002	0.010464

F31D4.9	V:20850832-20851917	305.052	468.44	0.61881	0.0001	0.005996
snr-5	III:7862069-7862576	612.557	946.117	0.627175	5.00E-05	0.003242
pat-10	I:5018769-5020166	992.248	1534.45	0.628945	5.00E-05	0.003242
unc-87	I:6760431-6767797	109.136	169.092	0.631685	5.00E-05	0.003242
C10C6.9	IV:11468394-11468900	94.1106	145.959	0.633134	0.0008	0.030197
col-184	X:13469387-13470471	644.627	1001.12	0.635082	5.00E-05	0.003242
trx-4	I:3317977-3318586	133.578	207.571	0.635928	0.0006	0.024126
act-1	V:11079166-11082497	95.9674	149.238	0.637002	5.00E-05	0.003242
rps-28	IV:1637873-1660011	7989.38	12430.1	0.637681	5.00E-05	0.003242
C30G12.2	II:7290372-7291943	19.7183	30.7255	0.639898	0.00075	0.028629
lbp-6	I:6724916-6729376	704.893	1099.09	0.640828	5.00E-05	0.003242
ZK1055.7	V:6602736-6605375	14.5645	22.7355	0.642491	0.00065	0.025605
lec-9	X:17600397-17621477	256.039	400.881	0.646809	0.00045	0.019359
bca-1	X:6201907-6204746	23.658	37.0923	0.648792	0.00045	0.019359
mct-3	X:13847744-13857324	18.5923	29.2062	0.651571	5.00E-05	0.003242
C14H10.1	X:10233744-10236944	14.7692	23.211	0.652213	0.0007	0.027102
ttr-42	X:2577741-2580568	161.137	253.573	0.654112	5.00E-05	0.003242
F38B6.4	X:6674868-6679851	10.8343	17.0659	0.655504	0.00015	0.008229
mlc-3	III:5565024-5567384	300.659	474.312	0.657706	5.00E-05	0.003242

col-106	IV:1459857-1460786	730.769	1155.25	0.660717	5.00E-05	0.003242
unc-43	IV:10324264-10350217	50.8539	80.8383	0.668681	0.00135	0.044948
H36L18.2	X:12652586-12653520	86.6859	138.165	0.672527	0.00015	0.008229
F08F3.4	V:5410993-5412981	49.7861	79.5259	0.675682	5.00E-05	0.003242
T07D3.9	II:898043-900930	26.0264	41.652	0.678412	0.0001	0.005996
Y45F10C.4	IV:13663398-13664191	72.6786	116.367	0.679082	0.00115	0.039754
C35B1.5	IV:4083587-4084209	187.818	301.101	0.680911	5.00E-05	0.003242
fat-7	V:7145655-7159188	40.1725	64.5425	0.684043	0.0004	0.017889
T04F8.8	X:11647445-11648196	127.238	204.496	0.68454	5.00E-05	0.003242
tba-4	II:10918705-10920184	39.8951	64.1936	0.686217	5.00E-05	0.003242
C10G8.4	V:5311934-5312316	775.269	1248.4	0.687315	5.00E-05	0.003242
fkb-3	V:7225368-7226314	20.4238	32.9197	0.6887	0.00095	0.034793
K09G1.1	V:9583595-9590523	50.3737	81.4334	0.692949	5.00E-05	0.003242
F09G8.7	III:8267946-8268357	262.294	425.216	0.69701	0.00015	0.008229
ugt-44	IV:10469762-10471890	21.3855	34.7854	0.701848	5.00E-05	0.003242
Y50D4B.3,Y50D4B.4	V:1092021-1099023	38.7184	63.0538	0.703563	5.00E-05	0.003242
F15E6.4	IV:4291461-4292109	239.093	391.571	0.711699	0.00035	0.016299

col-122	IV:9560786-9566605	1255.25	2059.01	0.713974	5.00E-05	0.003242
Y69E1A.5	IV:10956859-10957685	26.863	44.3355	0.72284	0.0006	0.024126
mrpl-36	III:9847623-9848116	296.122	489.583	0.72536	0.00015	0.008229
lys-2	V:10280309-10281470	193.398	320.48	0.72866	5.00E-05	0.003242
gst-13	II:9231496-9232341	48.0561	79.748	0.730731	5.00E-05	0.003242
F19H6.4	X:12365687-12367263	31.942	53.2133	0.73633	0.00015	0.008229
figl-1,hpo-18	V:4341426-4346919	1276.81	2127.57	0.736663	0.0001	0.005996
tag-18	X:3729293-3733457	62.6081	104.837	0.743728	5.00E-05	0.003242
atp-6,nduo-1	MtDNA:1762-3235	2225.75	3754.75	0.754425	5.00E-05	0.003242
T25B9.1	IV:10744780-10750153	9.74808	16.4739	0.756994	0.0004	0.017889
T12D8.10	III:13641792-13642327	145.341	245.693	0.757417	0.00035	0.016299
C32E8.9	I:3794552-3798053	22.7613	38.5578	0.760442	5.00E-05	0.003242
gpd-2,mai-1	X:3113433-3116538	128.434	218.273	0.765111	5.00E-05	0.003242
gpd-3	X:3112082-3113382	159.703	271.744	0.766861	5.00E-05	0.003242
mif-2	V:11976773-11978404	72.8665	124.134	0.768576	0.00145	0.047576
tyr-2	III:13744221-13747287	4.0905	6.97345	0.769594	0.0003	0.014519
mup-2	X:6408463-6410359	71.6643	122.181	0.769699	5.00E-05	0.003242

ttr-18	II:11485509-11486774	68.9628	117.594	0.769924	5.00E-05	0.003242
VF13D12L.3	II:11705988-11713610	95.9491	163.876	0.772261	5.00E-05	0.003242
Y55B1AL.2	III:576955-577567	228.871	391.529	0.774586	5.00E-05	0.003242
fmo-3	III:10694646-10698868	5.08151	8.70069	0.775873	0.0006	0.024126
C10C5.3	IV:9374764-9376492	7.92958	13.5936	0.77761	0.0009	0.033231
mxl-3	X:13349639-13350804	25.6757	44.0532	0.778847	0.0001	0.005996
pck-1	III:62886-66261	52.38	90.2031	0.784162	5.00E-05	0.003242
K01C8.1	II:8264660-8269914	50.9119	87.7508	0.78541	5.00E-05	0.003242
haao-1	V:9505688-9507114	17.3027	29.8801	0.788187	5.00E-05	0.003242
acdh-9	II:846866-848602	57.9204	100.097	0.789258	5.00E-05	0.003242
Y58A7A.1	V:5067576-5069665	14.4971	25.1062	0.792273	0.00105	0.037444
nhr-137	X:6661792-6669005	4.86703	8.44168	0.794488	0.00115	0.039754
nspc-13	X:12357507-12357919	46.2269	80.221	0.795249	0.00145	0.047576
C35B1.4	IV:4079804-4080946	175.58	305.278	0.79799	5.00E-05	0.003242
clec-97	I:11152713-11155369	22.1539	38.5276	0.798332	0.00045	0.019359
F17C8.7,F17C8.9	III:4734456-4737256	10.1141	17.5915	0.798501	0.00035	0.016299
W01B11.6	I:3287381-3294356	85.0461	148.038	0.799649	0.00015	0.008229
Y10G11A.90	IV:16417117-	158.391	276.109	0.801747	0.00035	0.016299

	16417416					
ZK909.6	I:14967298-14968540	22.4929	39.3518	0.80696	0.0015	0.048862
lbp-1	X:3259101-3259855	94.2635	166.033	0.816699	5.00E-05	0.003242
C54E4.5	IV:2146670-2149299	11.2201	19.8299	0.821597	0.00035	0.016299
ugt-12	V:4887172-4889616	20.7633	36.7228	0.822641	5.00E-05	0.003242
emb-1	III:5173436-5173811	266.613	471.626	0.822899	5.00E-05	0.003242
clec-5	III:4881913-4883578	14.2066	25.1402	0.823435	0.0001	0.005996
T23E7.2	X:17671022-17682294	19.9804	35.4722	0.828104	0.0015	0.048862
F44E7.5	V:5778817-5781015	44.4273	79.0944	0.832129	5.00E-05	0.003242
rpl-39	V:7774515-7776086	14179.9	25341.9	0.837676	5.00E-05	0.003242
T01B11.2	IV:8449348-8451771	27.087	48.4099	0.837702	5.00E-05	0.003242
cyp-34A8	V:3964778-3967871	8.94669	16.0501	0.843155	5.00E-05	0.003242
F55H12.2	I:8867797-8868300	19.0292	34.3482	0.852022	0.0011	0.038617
Y102A5C.5,Y102A5C.6	V:16928327-16930098	18.9341	34.4434	0.86324	0.0003	0.014519
tomm-7,ufm-1	III:7857304-7860192	859.894	1566.56	0.865367	0.00045	0.019359
F35H10.5	IV:8300777-8301099	247.853	451.992	0.866812	0.0005	0.021108
T12B3.2	IV:7376896-7378900	5.29252	9.71014	0.875538	0.0002	0.010464
Y38E10A.24	II:12679024-12679404	480.901	884.583	0.879257	5.00E-05	0.003242

R07E4.3	X:5953449-5953783	177.134	325.971	0.879905	5.00E-05	0.003242
cpg-9	IV:3067845-3069847	106.745	196.905	0.883331	5.00E-05	0.003242
M117.6	IV:11827396-11828121	18.3959	34.2132	0.895168	0.0007	0.027102
F11E6.3	IV:17470509-17472025	125.042	233.306	0.899806	5.00E-05	0.003242
nlp-33	V:11147343-11147810	63.7761	119.107	0.901165	0.0001	0.005996
cyp-25A3	III:3837540-3839477	2.66888	4.99601	0.904544	0.00085	0.031731
C35A5.3	V:10497058-10501477	18.967	35.7936	0.916215	5.00E-05	0.003242
F16B4.4	V:1594111-1594665	134.781	254.373	0.916332	5.00E-05	0.003242
grsp-4	V:7624951-7626462	30.7715	58.0856	0.916585	5.00E-05	0.003242
F54E2.1	V:2810426-2811985	66.4717	125.603	0.91806	5.00E-05	0.003242
F18E3.13	V:7416115-7416819	32.2453	60.9851	0.919366	0.00015	0.008229
col-119	IV:8974853-8984575	1826.2	3454.02	0.919431	5.00E-05	0.003242
Y71D11A.3	III:1116462-1142928	4.21991	7.98166	0.919476	0.0014	0.046272
aldo-1	III:13563334-13564990	49.2823	93.6345	0.925971	5.00E-05	0.003242
T21D12.12	IV:266152-268370	13.0197	24.7393	0.926113	0.0002	0.010464
B0035.18	IV:11320319-11320643	194.673	370.374	0.927929	5.00E-05	0.003242
Y38E10A.14	II:12623188-12623952	8.39238	16.0403	0.934549	0.00025	0.012688

T01C8.2	X:16786443-16787620	42.5682	81.7332	0.941146	0.00015	0.008229
F23A7.8	X:16213372-16213599	2821.59	5443.23	0.947957	5.00E-05	0.003242
cuc-1	III:7860465-7861004	167.166	323.091	0.95066	5.00E-05	0.003242
fbxa-72	V:674881-676753	19.5006	37.8201	0.955631	5.00E-05	0.003242
fipr-13	V:10064502-10064939	18.2789	35.5335	0.959005	0.00105	0.037444
ZK228.4	V:18462803-18465320	21.129	41.0819	0.959281	5.00E-05	0.003242
ugt-62	III:4537276-4540637	49.5926	96.5931	0.961795	5.00E-05	0.003242
C35D10.17	III:4867061-4867469	94.361	185.123	0.972219	5.00E-05	0.003242
ZK593.3	IV:10916614-10917692	45.5553	89.9201	0.981026	5.00E-05	0.003242
F35F10.1	V:3316359-3318027	3.53365	6.98548	0.983198	0.00105	0.037444
D1054.8	V:10784272-10785369	19.4966	38.6114	0.985809	5.00E-05	0.003242
F57B10.14	I:6548643-6554292	1049.47	2079.71	0.986713	0.0006	0.024126
tbx-32	X:1654434-1657792	1531.09	3039.31	0.98918	5.00E-05	0.003242
nhr-210	V:515786-519545	1.80118	3.57755	0.99003	0.00135	0.044948
K06A4.7	V:9489933-9491492	1964.49	3909.13	0.992696	5.00E-05	0.003242
Y34F4.2	III:1010534-1011374	10.2516	20.4537	0.996511	0.0007	0.027102
dgat-2	V:17660303-17666039	8.94584	17.8675	0.998049	5.00E-05	0.003242
cyp-29A3	V:59241-63509	1.62519	3.24599	0.998053	0.001	0.03604
gly-8	III:11624990-	13.7615	27.5151	0.999584	5.00E-05	0.003242

	11628238					
Y45F10B.13	IV:13549438-13561652	7.55505	15.1461	1.00344	0.0002	0.010464
gst-39	II:15171150-15171912	11.1977	22.4689	1.00473	0.0001	0.005996
col-80	II:10695053-10714299	609.02	1222.63	1.00543	5.00E-05	0.003242
C08F8.9	IV:11177285-11178597	491.688	988.874	1.00804	5.00E-05	0.003242
F53B3.6	X:2864290-2865683	2.30282	4.65172	1.01436	0.00095	0.034793
F42F12.3	X:12350587-12351746	15.826	32.1137	1.02089	5.00E-05	0.003242
T13F3.6	V:16270215-16271221	111.397	226.044	1.02089	5.00E-05	0.003242
R04A9.9	X:389516-390567	9.44483	19.1669	1.02102	0.001	0.03604
C49G7.10	V:4040408-4042004	6.78679	13.7919	1.02302	0.0002	0.010464
C55A6.4	V:11516443-11517885	4.05139	8.34093	1.04179	0.00015	0.008229
Y94H6A.10	IV:2709899-2710670	40.1622	83.063	1.04837	5.00E-05	0.003242
oig-2	II:13006606-13008163	67.8158	141.862	1.0648	5.00E-05	0.003242
F58G6.3	IV:9653534-9654227	38.5392	80.6514	1.06537	5.00E-05	0.003242
gst-24	II:13610442-13611342	6.98623	14.6255	1.0659	0.00025	0.012688
C37C3.1,C37C3.2	V:7854249-7859911	160.328	338.128	1.07654	5.00E-05	0.003242
col-96	III:11705712-11706644	9.90089	20.899	1.07781	5.00E-05	0.003242

K10C2.12	X:6420108-6420781	42.5649	90.0605	1.08123	0.00045	0.019359
catp-3	V:8076084-8079914	3.553	7.60066	1.09709	5.00E-05	0.003242
Y105C5B.5	IV:15899923-15901225	291.424	628.908	1.10973	5.00E-05	0.003242
F18E3.11	V:7413436-7413840	44.0076	95.2906	1.11458	5.00E-05	0.003242
W06H8.2	V:6206814-6208676	1.28118	2.77664	1.11587	0.00045	0.019359
grd-10	IV:3441090-3441788	5.61032	12.2489	1.1265	0.0008	0.030197
F52D2.14,linc-6	X:1982709-1982935	410.452	896.16	1.12654	0.0006	0.024126
ugt-61	V:4742426-4745378	5.11236	11.1968	1.13103	5.00E-05	0.003242
poml-3	I:4145311-4147136	4.70909	10.3421	1.13501	5.00E-05	0.003242
F19B2.5	V:20162623-20164587	29.1595	64.2271	1.13921	5.00E-05	0.003242
nlp-26	V:19613527-19614521	45.6014	100.648	1.14217	0.0001	0.005996
col-150	V:10293564-10294621	1.88534	4.16241	1.1426	0.00105	0.037444
Y51A2D.14	V:18582627-18582952	700.802	1547.31	1.14269	5.00E-05	0.003242
col-140	V:5835852-5836841	1530.33	3398.63	1.15111	5.00E-05	0.003242
lact-1	X:7258159-7260377	3.24275	7.20294	1.15137	0.00015	0.008229
Y102A5C.36	V:16926926-16927447	20.5483	46.1846	1.16839	5.00E-05	0.003242
grd-13	IV:3438311-3439502	4.08062	9.1722	1.16848	0.0004	0.017889
C36C9.10	X:1681751-1681886	1420.45	3202.88	1.17302	0.00025	0.012688

col-178,col-179	X:11199454-11203990	772.129	1748.9	1.17953	5.00E-05	0.003242
col-147	V:9632270-9633337	2.87197	6.51761	1.1823	0.0001	0.005996
rrn-3.1	I:15064837-15068355	586.23	1337.07	1.18953	5.00E-05	0.003242
Y39A3CL.3	III:1772508-1778312	1417.44	3233.5	1.18981	0.0001	0.005996
F22H10.2	X:16678487-16679823	32.1873	73.5218	1.19168	5.00E-05	0.003242
H04D03.6	III:10438077-10438880	38.843	89.1992	1.19938	0.0013	0.044151
nlp-24	V:11616282-11618266	68.4879	157.32	1.19978	5.00E-05	0.003242
F26D11.12,F26D11.13	V:7953353-7955343	5.5728	12.8334	1.20343	0.00075	0.028629
K08D9.9	V:3236486-3236711	312.375	723.625	1.21196	5.00E-05	0.003242
col-8	III:7019582-7020600	527.843	1223.38	1.2127	5.00E-05	0.003242
F42F12.4	X:12351977-12352977	21.7023	50.6952	1.224	5.00E-05	0.003242
F30A10.13	I:9478466-9479091	37.3344	87.6445	1.23116	5.00E-05	0.003242
T12B5.15	III:954294-954652	104.779	246.9	1.23659	5.00E-05	0.003242
col-160	V:13200979-13202189	386.144	910.399	1.23736	5.00E-05	0.003242
ugt-13	V:4908870-4911458	3.68416	8.70493	1.2405	5.00E-05	0.003242
kin-15	II:9431382-9433709	2.38277	5.65632	1.24723	5.00E-05	0.003242
F43D2.7	V:14638685-14640015	7.13083	16.9395	1.24825	0.00055	0.023003

cdr-4	V:12407363-12408592	29.308	70.0467	1.25702	5.00E-05	0.003242
K08D12.6	IV:1720789-1723069	71.7436	171.833	1.26008	5.00E-05	0.003242
gst-30	II:4933882-4935021	3.4419	8.26552	1.2639	0.00015	0.008229
R08E5.3	V:3772057-3776136	13.0608	31.6134	1.2753	5.00E-05	0.003242
grd-3	IV:3439654-3440456	65.6663	161.434	1.29772	5.00E-05	0.003242
B0416.7	X:9296944-9297950	5.39716	13.317	1.303	0.00125	0.042667
R09H10.7	IV:10621192-10621691	16.7648	41.3689	1.30311	0.0011	0.038617
col-93	III:10984554-10985608	280.468	692.663	1.30432	5.00E-05	0.003242
rrn-3.56	I:15060298-15061159	32.2051	79.9594	1.31198	5.00E-05	0.003242
sdz-8	V:11515085-11516178	2.20278	5.47124	1.31254	0.00015	0.008229
col-19	X:406451-425631	489.916	1248.29	1.34935	5.00E-05	0.003242
grd-5	V:8619031-8619869	82.8	211.294	1.35155	5.00E-05	0.003242
C45B2.1	X:6086123-6086569	127.639	330.488	1.37252	5.00E-05	0.003242
col-20	II:4869606-4870791	768.42	2018.42	1.39326	5.00E-05	0.003242
pqn-60	V:504038-504616	3.16628	8.36161	1.40099	0.00045	0.019359
F43H9.4	V:8026690-8028794	15.6336	41.325	1.40237	5.00E-05	0.003242
bli-6	IV:6377093-6378195	2.5065	6.71607	1.42194	5.00E-05	0.003242
fipr-21	X:10304506-10304948	80.1417	218.359	1.44608	5.00E-05	0.003242

gst-9	II:4891579-4893574	1.95378	5.38808	1.4635	0.0005	0.021108
msra-1	II:7359960-7364107	242.714	669.828	1.46453	5.00E-05	0.003242
Y69H2.14	V:18638476-18639591	172.576	480.118	1.47615	5.00E-05	0.003242
col-149	V:10289720-10292868	1.81939	5.13214	1.49611	0.0001	0.005996
col-180	X:11711310-11712280	0.722493	2.08043	1.52583	0.00065	0.025605
B0205.12	I:10730466-10730712	250.121	737.501	1.56002	5.00E-05	0.003242
gst-4	IV:10142161-10143101	19.8805	58.6726	1.56133	5.00E-05	0.003242
T07A5.1	III:10303409-10306145	0.594234	1.75629	1.56343	0.0008	0.030197
ugt-32	V:3841858-3844007	0.655818	1.97536	1.59075	0.0004	0.017889
gst-33	V:3467452-3468501	1.25352	3.77892	1.59198	0.0002	0.010464
amt-1	X:4571447-4573914	2.20387	6.6793	1.59966	5.00E-05	0.003242
C45B2.2	X:6084738-6085188	4.91032	14.9713	1.60831	0.0001	0.005996
acd-1	I:4103712-4108045	0.349354	1.06861	1.61297	0.0007	0.027102
col-92	III:10982165-10983253	1.29586	3.97442	1.61684	5.00E-05	0.003242
col-12	V:10423906-10425092	0.476697	1.4632	1.61798	0.00055	0.023003
DC2.5	V:210150-212713	3.39784	10.4886	1.62613	5.00E-05	0.003242
R13A5.10	III:7582111-7583047	2.95125	9.16362	1.63459	5.00E-05	0.003242

C45G9.12	III:5070430-5071597	11.7731	36.9629	1.65058	0.0003	0.014519
F41C3.1	II:4752387-4752942	2.53955	8.11009	1.67514	0.0011	0.038617
col-103	IV:762377-763678	140.026	448.166	1.67834	5.00E-05	0.003242
smz-2	I:6872596-6873755	0.607933	1.94903	1.68077	0.00065	0.025605
K04F1.9	V:1665251-1665949	3.76446	12.0754	1.68156	5.00E-05	0.003242
ZC196.2	V:8739436-8742259	0.454203	1.47734	1.70159	0.0013	0.044151
col-98	III:13018934-13020231	95.9277	317.088	1.72487	5.00E-05	0.003242
F23A7.1	X:16217391-16217666	9.67149	32.1643	1.73365	0.0004	0.017889
C32D5.18	II:6343053-6345925	3355.27	11159.7	1.7338	5.00E-05	0.003242
sod-3	X:17087881-17094223	2.10864	7.07388	1.74619	5.00E-05	0.003242
R05D8.7	V:2761821-2763179	1.46144	4.90898	1.74803	5.00E-05	0.003242
Y37H2A.14	V:18143737-18144721	8.45478	28.4533	1.75076	5.00E-05	0.003242
F09E10.1	X:1502879-1503219	77.1175	260.595	1.75668	5.00E-05	0.003242
comt-5	V:2052285-2053600	0.990811	3.35044	1.75767	0.00035	0.016299
F20G2.1	V:13752264-13753564	1.67757	5.72	1.76964	5.00E-05	0.003242
Y51A2D.21	V:18571832-18572949	5.62715	19.2267	1.77264	5.00E-05	0.003242
C08E8.10	V:18339119-18339907	5.19431	18.3849	1.82352	0.0003	0.014519
ugt-2	V:10398809-10401313	3.7336	13.3481	1.83799	5.00E-05	0.003242
F25H5.10	I:9158800-9158986	49.3545	176.537	1.83871	0.0006	0.024126

Y41E3.460	IV:15059460-15059685	18.9051	69.0923	1.86975	0.00035	0.016299
col-133	IV:14098334-14099352	1.68314	6.17875	1.87616	5.00E-05	0.003242
gst-12	II:13616684-13617937	2.02461	7.4419	1.87803	5.00E-05	0.003242
C06E4.3	IV:7260884-7262028	0.761733	2.80775	1.88206	0.0003	0.014519
D1054.9	V:10785795-10791234	0.259254	0.974559	1.91038	5.00E-05	0.003242
-	III:1976846-1976895	19281.2	72713.7	1.91503	0.00065	0.025605
C05E7.2	X:12938696-12940711	0.548519	2.12119	1.95126	0.0007	0.027102
col-124	IV:10214983-10232552	385.272	1504.67	1.9655	5.00E-05	0.003242
-	III:5092685-5093154	6.59028	25.917	1.97548	5.00E-05	0.003242
col-159	V:13198229-13199315	16.1754	63.6961	1.9774	5.00E-05	0.003242
col-139	V:4652381-4653986	16.3755	67.5342	2.04408	5.00E-05	0.003242
T19C9.8	V:17118153-17252309	3.88737	16.429	2.07938	5.00E-05	0.003242
-	III:5092009-5092382	10.0516	42.9954	2.09675	5.00E-05	0.003242
F33H12.7	II:2586076-2586911	5.82554	25.0326	2.10335	5.00E-05	0.003242
R08F11.4	V:3803856-3805527	1.55323	6.79969	2.1302	5.00E-05	0.003242
tba-9	X:3252962-3256176	0.83863	3.72138	2.14973	5.00E-05	0.003242
ugt-36	V:7167008-7169205	0.332277	1.47468	2.14994	5.00E-05	0.003242

col-129	IV:12108670-12110258	17.5418	79.2373	2.17538	5.00E-05	0.003242
F58G6.9	IV:9651425-9652484	21.0325	95.116	2.17707	5.00E-05	0.003242
Y53F4B.48	II:15165890-15166028	103.355	468.734	2.18116	0.00045	0.019359
cyp-13A8	II:9805626-9807532	0.199257	0.915301	2.19962	0.001	0.03604
cyp-14A1	X:13265080-13267338	1.33087	6.24269	2.2298	5.00E-05	0.003242
col-81	II:11012394-11013779	9.49487	46.5633	2.29398	5.00E-05	0.003242
hrg-2	V:12409368-12410513	1.42911	7.65757	2.42177	5.00E-05	0.003242
ugt-19	IV:6076689-6079945	3.29703	17.7575	2.42919	5.00E-05	0.003242
cyp-33C8	V:3800775-3803454	3.4152	18.6574	2.44971	5.00E-05	0.003242
decr-1.1	II:2353314-2354375	0.893472	4.89387	2.45348	0.00075	0.028629
cdr-2	V:12414621-12415711	9.59583	52.849	2.4614	5.00E-05	0.003242
F01E11.17	X:6979816-6983133	0.454231	2.60566	2.52015	5.00E-05	0.003242
C39B5.5	III:2208269-2211296	1.92672	11.122	2.5292	5.00E-05	0.003242
col-176	X:10077612-10078738	0.287031	1.70777	2.57283	0.0003	0.014519
col-142	V:6831162-6832254	21.5087	129.575	2.5908	5.00E-05	0.003242
rrn-2.1	I:15064300-15064453	4190.57	26312.9	2.65055	5.00E-05	0.003242
linc-21	IV:4242085-4242466	5.83639	46.6499	2.99873	5.00E-05	0.003242
tbb-6	V:12261803-12263845	4.39273	35.17	3.00115	5.00E-05	0.003242
Y49G5A.1	V:5286342-5287360	2.02723	17.6395	3.12122	5.00E-05	0.003242

B0205.14	I:10726917-10727351	4.76227	83.232	4.12742	0.00025	0.012688
F19F10.13	V:7567998-7568735	1.21993	25.0184	4.35812	5.00E-05	0.003242
nduo-2	MtDNA:3361-4328	57.1783	1377.99	4.59095	5.00E-05	0.003242
B0205.13	I:10727750-10728795	6.19918	173.693	4.80832	5.00E-05	0.003242
F16H6.4	V:18198720-18200754	0	0.531349	N/A	5.00E-05	0.003242
F15A8.4	X:4408138-4409063	0.753786	0	N/A	0.00135	0.044948
M02G9.4	II:10317268-10317587	3.73421	0	N/A	0.0006	0.024126
W07G4.1	V:13033528-13034164	1.5713	0	N/A	0.00135	0.044948
ZK402.2	X:1403743-1404117	0.599201	0	N/A	0.00135	0.044948

7.8 RNAseq-based RNA*i* screen: Genes knocked down in wild type animals

Table 7.7 RNAseq-based RNA*i* screen: Genes knocked down in wild type animals

Gene Name	RNA*i* library location	Wild Type animals on RNA*i*
C33G8.3	0	No
cpr-5	0	No
E02H4.7	0	No
F22F7.8	0	No
F33E11.7	0	No
ilys-5	0	No
nhr-114	0	No

R74.11	0	No
Y102A5C.5	0	No
Y102A5C.6	0	No
ZK228.4	0	No
ZK550.2	0	No
aqp-1	II-5D15	Yes
asp-8	V-2B04	Yes
B0507.8	V-15N20	Yes
C08B6.2	V-7C19	Yes
C10C5.4	IV-4H16	Yes
C30G12.2	II-5D23	Yes
C42D4.2	IV-3F09	Yes
C44C1.5	X-1A04	Yes
C46F2.1	X-8K09	Yes
C53A3.2	V-4M02	Yes
clec-10	II-1M19	Yes
clec-165	IV-1M18	Yes
clec-166	IV-1M08	Yes
clec-170	IV-9B17	Yes
clec-218	V-15L03	Yes
clec-26	V-11A20	Yes
clec-265	X-2E19	Yes
clec-52	IV-4K07	Yes
clec-8	II-8M14	Yes

col-165	X-2J17	Yes
col-43	V-5D16	Yes
cpt-3	IV-8D22	Yes
cyp-14A2	X-6A06	Yes
cyp-25A1	III-1L24	Yes
cyp-35A5	V-3K04	Yes
cyp-35C1	V-9M01	Yes
daf-36	V-14H02	Yes
dhs-23	V-10I01	Yes
dhs-25	X-1B01	Yes
dhs-26	X-2O21	Yes
E01G6.3	X-5H08	Yes
F09B12.3	X-7A21	Yes
F14E5.1	II-6K13	Yes
F22H10.6	X-7B13	Yes
F23F12.13	III-8G13	Yes
F26C11.1	II-7E09	Yes
F31D4.8	V-13A24	Yes
F31F4.1	V-15P03	Yes
F32A5.3	II-5D11	Yes
F38A1.9	IV-1M16	Yes
F55E10.6	X-4C22	Yes
fat-7	V-5K17	Yes
fpn-1.2	V-1N07	Yes

gba-4	IV-9E02	Yes
gst-10	V-2E02	Yes
ifc-1	V-2H17	Yes
irg-2	V-3B17	Yes
K07G5.5	I-3D13	Yes
K11G9.3	V-4J24	Yes
lipl-5	V-1I21	Yes
lys-10	IV-6O01	Yes
lys-4	IV-6M23	Yes
lys-6	IV-6M23	Yes
M04C9.4	I-4J19	Yes
oac-20	V-10J07	Yes
oac-54	II-6H09	Yes
oac-6	V-10L10	Yes
pcp-3	IV-4N21	Yes
pho-1	II-4E10	Yes
R10E8.6	V-14I13	Yes
sdz-24	II-1G16	Yes
spp-17	I-7F15	Yes
spp-4	X-3H10	Yes
T01D3.6	V-9C15	Yes
T05E12.3	V-15A18	Yes
T16G1.6	V-8J21	Yes
T16G12.1	III-5K16	Yes

T16G12.7	III-5M04	Yes
tsp-10	II-5M17	Yes
ttr-44	V-8N10	Yes
ugt-30	V-9L04	Yes
ugt-43	IV-5D19	Yes
ugt-53	V-2F09	Yes
ugt-6	V-14C16	Yes
vit-1	X-4A17	Yes
vit-5	X-2A12	Yes
W03D8.8	I-1K12	Yes
Y102A5C.36	V-15M24	Yes
Y113G7B.12	V-14J12	Yes
Y116F11A.6	V-12D24	Yes
Y32F6B.1	V-7C02	Yes
Y45G12C.1	V-16L10	Yes
ZC266.1	V-3F10	Yes
zipt-2.3	II-8H14	Yes
ZK1240.5	II-11G16	Yes
ZK673.1	II-7G16	Yes
ZK822.1	IV-9D05	Yes

7.9 RNAseq-based RNA*i* screen: Genes knocked down in *kri-1(ok1251)* mutants

Table 7.8 RNAseq-based RNA*i* screen: Genes knocked down in *kri-1(ok1251)* mutants

Gene Name	RNA*i* library location	*kri-1 (ok1251)* animals on RNA*i*
B0462.5	0	No
B0563.5	0	No
C02B8.12	0	No
C05D12.3	0	No
C07A12.2	0	No
C08A9.11	0	No
C18A3.10	0	No
C25H3.18	0	No
C27D6.12	0	No
C32D5.18	0	No
C34D4.3	0	No
C36C9.10	0	No
C41G7.8	0	No
C44C1.6	0	No
C45G9.13	0	No

C49G7.12	0	No
C54F6.5	0	No
clec-173	0	No
clec-84	0	No
col-167	0	No
ctc-2	0	No
D1086.17	0	No
dmsr-16	0	No
F08B4.8	0	No
F09E10.14	0	No
tts-1	0	No
F10A3.17	0	No
F13A7.1	0	No
F19G12.9	0	No
F23D12.7	0	No
F31E9.11	0	No
F35B3.4	0	No
F36H1.12	0	No
F38B2.6	0	No

F46A8.13	0	No
F52G3.6	0	No
F53A9.7	0	No
F56D6.16	0	No
F56F10.1	0	No
flp-32	0	No
H34I24.2	0	No
K02E2.11	0	No
K09E9.4	0	No
K10C2.14	0	No
K10D3.6	0	No
K12C11.6	0	No
linc-1	0	No
linc-17	0	No
linc-71	0	No
linc-8	0	No
lips-5	0	No
M01H9.7	0	No
M02D8.6	0	No

M04C3.5	0	No
M110.10	0	No
M199.9	0	No
mlc-6	0	No
nlp-42	0	No
oac-58	0	No
pqn-60	0	No
R09H10.7	0	No
skr-4	0	No
srx-12	0	No
T01G5.8	0	No
T02C12.5	0	No
T03F6.10	0	No
T09F5.12	0	No
T22F3.10	0	No
T23B12.11	0	No
ttr-23	0	No
VZK822L.2	0	No
W02B12.1	0	No

W02G9.4	0	No
W10C8.6	0	No
Y105C5A.25	0	No
Y17D7B.7	0	No
Y22D7AL.15	0	No
Y22D7AL.15	0	No
Y22D7AL.15	0	No
Y22D7AR.10	0	No
Y34B4A.6	0	No
Y34F4.1	0	No
Y36E3A.2	0	No
Y37H2A.13	0	No
Y37H2A.14	0	No
Y39B6A.29	0	No
Y40C7B.4	0	No
Y41E3.460	0	No
Y51A2D.21	0	No
Y51H4A.11	0	No
Y51H4A.25	0	No

Y53F4B.45	0	No
Y53F4B.48	0	No
Y54G2A.49	0	No
Y57E12B.11	0	No
Y60A3A.16	0	No
Y67D8C.23	0	No
Y69A2AL.2	0	No
Y71G12B.32	0	No
Y73B6BL.35	0	No
Y75B8A.11	0	No
ZC15.11	0	No
ZC412.10	0	No
ZK1320.13	0	No
ZK593.11	0	No
F28E10.5	0	No
maf-1	0	No
T06F4.3	0	No
T22E5.7	0	No
W03D2.13	0	No

C07E3.3	0	No
C11E4.7	0	No
C44B11.6	0	No
C45G9.6	0	No
clec-62	0	No
dod-20	0	No
dpy-5	0	No
F13D12.6	0	No
fbxa-128	0	No
K05F1.10	0	No
nlp-42	0	No
rnh-1.3	0	No
W03F9.4	0	No
Y18H1A.11	0	No
cutl-24	0	No
C54D10.13	0	No
aagr-1	IV-4C04	Yes
aagr-2	II-4I09	Yes
abt-4	V-1G17	Yes

abu-12	X-1C15	Yes
acdh-8	II-4L02	Yes
acs-10	V-14B06	Yes
acs-18	IV-5O14	Yes
adt-2	X-3N18	Yes
alg-3	IV-6A22	Yes
alg-4	III-5E16	Yes
aman-3	I-2I22	Yes
ant-1.4	IV-4E22	Yes
aqp-4	V-6F08	Yes
arf-1.1	IV-3H14	Yes
asp-14	X-3O08,	Yes
fah-1	X-3O10	Yes
B0024.4	V-7K17	Yes
B0205.10	I-9I-02	Yes
B0238.12	V-16D01	Yes
B0252.8	II-10P07	Yes
B0294.3	X-1L13, X-1L09	Yes
B0302.5	X-7P23	Yes

B0344.1	V-3D01	Yes
B0348.2	V-16F09	Yes
B0348.2	V-16F09	Yes
B0348.2	V-16F09	Yes
B0379.7	I-5E17	Yes
B0416.2	X-4N01	Yes
B0507.6	V-6A20	Yes
best-1	IV-7A11	Yes
best-24	III-4K19	Yes
bre-1	IV-4H17	Yes
nstp-1	IV-4H15	Yes
C01B10.6	IV-3E02	Yes
C01B10.6	IV-3E02	Yes
C01G10.17	V-9H24	Yes
C01G10.5	V-9J02	Yes
C02E7.6	V-3P02	Yes
C02E7.7	V-3P04	Yes
C03C11.1	I-5C07	Yes
C04E6.7	V-4B07	Yes

C04F12.7	I-4H18	Yes
C04G2.8	IV-5E06	Yes
egl-38	IV-5E04	Yes
C04G2.9	IV-5E08	Yes
C05B5.2	III-5I14	Yes
C05D11.5	III-3M02	Yes
nas-4	III-3M04	Yes
C06B8.2	V-10P17	Yes
C06E1.7	III-4H11	Yes
C08E8.4	V-12E17	Yes
C09D4.3	I-2B15	Yes
C10G11.8	I-3C01	Yes
C12D12.1	X-2C10	Yes
C14C10.1	V-8K22	Yes
C14C6.5	V-16K14	Yes
C14H10.3	X-5C19	Yes
C15C6.2	I-6G13	Yes
C16B8.3	X-2B11	Yes
C16D9.4	V-5L22	Yes

C17H1.7	I-6L21	Yes
C17H12.12	IV-3I04	Yes
C17H12.3	IV-3G12	Yes
C17H12.6	IV-3G18	Yes
C18A11.1	X-4I15	Yes
C18A11.2	X-4I17	Yes
C18H7.11	IV-9K20	Yes
C18H9.6	II-5M05	Yes
C23H4.2	X-5F18	Yes
C24B5.4	V-6B09	Yes
C25F9.11	V-12F03, V-12P21	Yes
C25F9.14	V-12H11	Yes
C26B9.5	X-8C19	Yes
C27A2.12	II-4O07	Yes
C27D8.1	IV-6B16	Yes
C27D8.2	IV-6B18	Yes
C27H5.2	II-5O14	Yes
C28C12.11	IV-4I02	Yes
C28C12.4	IV-4G12	Yes

C29F9.3	III-1C11	Yes
C29F9.4	III-1C13	Yes
C30F2.3	X-7G02	Yes
C30F2.4	X-7E22	Yes
C30G7.3	V-16L21	Yes
C31B8.7	V-2L03	Yes
C31H5.4	I-9K24	Yes
C32E8.4	I-1H23	Yes
C32H11.1	IV-6H20	Yes
C32H11.4	IV-6J02	Yes
C32H11.9	IV-6J12	Yes
C33F10.1	III-5I14	Yes
C33F10.11	III-5I14, II-4E01	Yes
C34D10.2	X-4I13	Yes
C34F11.5	II-4C20	Yes
C34H4.1	IV-1F03	Yes
C34H4.2	IV-1F05	Yes
C36H8.1	IV-6D12	Yes
C38C3.3	V-1P07	Yes

C38H2.2	III-5F21	Yes
C39B10.1	X-5I01	Yes
C39H7.1	IV-2L22	Yes
C39H7.2	I-5N15	Yes
C39H7.4	IV-2N02	Yes
klp-6	III-2J07	Yes
C48B4.1	III-5I07	Yes
C49C3.4	IV-8C10	Yes
C49C3.4	IV-8C10	Yes
C49C3.9	IV-8C20	Yes
C49C8.5	IV-4K14	Yes
C50F4.1	V-6L23	Yes
C50F4.9	V-6N15	Yes
C50F7.5	IV-9N09	Yes
C54C6.7	III-8O06	Yes
C54D2.1	X-4E11	Yes
C54F6.12	V-15K20	Yes
C55A6.11	V-15E19	Yes
C55A6.7	V-15A04	Yes

catp-4	II-9O21	Yes
cav-2	V-8N20	Yes
cebp-1	X-1O16	Yes
ceh-62	II-7D05	Yes
cht-4	III-9B07	Yes
clc-1	X-5G08	Yes
clec-125	II-3E02	Yes
clec-150	III-9C16	Yes
clec-17	I-6C22	Yes
clec-172	IV-9N03	Yes
clec-186	IV-6H02	Yes
clec-204	V-1L02	Yes
clec-205	V-1L04	Yes
clec-223	V-14G24	Yes
clec-225	V-8P15	Yes
clec-41	V-8P17	Yes
clec-42	V-11P18	Yes
clec-60	II-7G20	Yes
clec-63	II-8B17	Yes

clec-64	II-8B19	Yes
clec-70	IV-10C03	Yes
clec-71	IV-8H19, IV-8J01	Yes
clec-72	IV-8J01, IV-8J11, IV-8H19	Yes
clec-73	IV-2A19, IV-8J13	Yes
clec-79	IV-2A19	Yes
clec-80	IV-10F15	Yes
clec-85	IV-9J20	Yes
clec-86	X-3B14	Yes
comt-2	V-11E05	Yes
comt-3	V-2A19	Yes
cpr-3	V-10E03	Yes
cth-1	V-10P21	Yes
cyp-13A5	II-6P24	Yes
cyp-13A6	II-7A01	Yes
cyp-33C7	V-2K07	Yes
cyp-33E2	IV-4I22	Yes
D1005.4	X-8L02	Yes
acly-1	X-1O12	Yes

D2062.6	II-2L11	Yes
D2096.1	IV-4A24	Yes
daf-28	V-14E03	Yes
dct-17	V-9E05	Yes
dod-17	IV-6L18	Yes
dod-19	V-1K03	Yes
dod-21	IV-6J14	Yes
dod-22	IV-6L06	Yes
dod-24	IV-6J18	Yes
dpy-13	IV-2K17	Yes
dpy-4	IV-7L15	Yes
drd-2	X-2M01	Yes
drr-1	II-8B22	Yes
dyla-1	X-8E16	Yes
E03H12.5	IV-2H03	Yes
E04D5.4	II-7E14	Yes
ech-9	IV-5M06	Yes
F01D5.1	II-8P24	Yes
F01D5.2	II-9A01	Yes

F01D5.3	II-9A03	Yes
F01D5.5	II-9A05	Yes
F02E11.2	II-3G09	Yes
F02E11.7	II-3G09	Yes
F07A5.2	I-3L15	Yes
F07C6.2	IV-6D22	Yes
F07C6.6	IV-10F23	Yes
F08G2.5	II-8L14	Yes
F08G5.6	IV-6J15	Yes
F08H9.2	V-9D03	Yes
F09A5.2	X-6M11	Yes
F09C12.2	II-4O15, II-10F17	Yes
F09C8.1	X-8M08	Yes
F09G8.5	III-4K14	Yes
F10D7.2	X-7F04	Yes
F11A5.9	V-14B12	Yes
F11E6.6	IV-8I12	Yes
F13B6.1	IV-3P23	Yes
F13H8.1	II-11A09, II-4L03	Yes

F14F8.8	V-11M11	Yes
F14H12.3	X-2J21	Yes
F14H3.12	V-10P11	Yes
F15B9.6	V-14H14	Yes
F17E9.5	IV-4A08	Yes
F19C7.1	IV-2I02	Yes
F19C7.5	IV-2I10	Yes
F19C7.6	IV-2I12	Yes
F19F10.3	V-5B13	Yes
F20D6.6	V-5J12	Yes
F20G2.5	V-9E21	Yes
F21H7.5	V-10H20	Yes
F22B8.4	V-10P17	Yes
F22B8.7	V-10P23	Yes
F22E12.1	V-7A18	Yes
F22E5.6	II-2N09	Yes
F23A7.1	X-7G20	Yes
F23H12.5	V-8C18	Yes
F25A2.1	V-1J23	Yes

F25E5.8	V-5K22	Yes
F25F2.1	III-2C12	Yes
F26B1.8	I-3C07, I-3A05	Yes
F27C1.1	I-2O06	Yes
F27C8.5	IV-5A01	Yes
F28B12.1	II-10N07	Yes
F29G6.1	X-5D01	Yes
F32A11.3	II-8J19	Yes
F32H5.1	V-8F20	Yes
F35E12.4	V-9C23	Yes
F35E12.5	V-9E01	Yes
F35E12.6	V-9E03	Yes
F35E12.8	V-9E07	Yes
F35H8.4	II-6H16	Yes
F36D1.7	I-5L19	Yes
F36D3.4	V-11E17	Yes
F38E9.6	X-7M10	Yes
F38H4.4	IV-6E20	Yes
F39G3.5	V-16D09	Yes

F40F4.6	X-2M01	Yes
F40F8.7	II-7N05	Yes
F41H10.1	IV-2F14	Yes
F42A9.7	IV-4I20	Yes
F42G4.5	II-8H15	Yes
F44G3.10	V-10B18	Yes
F44G3.2	V-14H24	Yes
F46A8.7	I-5L01	Yes
F46B3.1	V-13K01	Yes
F46C5.1	II-11I02	Yes
F46G10.1	X-6C06	Yes
F47B10.5	X-5C10	Yes
F47B8.2	V-9M08	Yes
F47B8.4	V-9M12	Yes
F48G7.5	V-1G12	Yes
F48G7.8	V-1G18	Yes
F49C12.15	IV-4F14	Yes
F49C12.6	IV-4D20	Yes
F49C12.7	IV-4D22	Yes

F49F1.1	IV-2G03	Yes
ubc-1	IV-9N16	Yes
F49F1.5	IV-2G11	Yes
F49F1.7	IV-2G05	Yes
F52B11.5	IV-7M10	Yes
F52H2.3	X-1L24	Yes
F52H3.6	II-7I19	Yes
F53A9.6	X-4M16	Yes
F53A9.9	X-4M22	Yes
F53B6.4	I-4M20	Yes
F53C11.1	V-9E23	Yes
F54B8.4	V-15F07	Yes
F54C9.3	II-6A10	Yes
F54D5.3	II-7J24	Yes
F54E2.1	V-2D21	Yes
F55F3.2	X-6O18	Yes
F55G11.2	IV-6J24	Yes
F55G11.4	IV-10E09	Yes
F55G11.8	IV-6L12	Yes

F56C9.7	III-3N02	Yes
F57B1.1	V-8B12	Yes
F58E6.5	V-15F10	Yes
F58F12.4	II-11E11	Yes
F59C6.14	I-5C18	Yes
F59E11.5	V-6G06	Yes
far-7	II-1K15	Yes
fbxa-105	V-5G18	Yes
fbxa-143	V-14O20	Yes
fbxa-162	II-1N12	Yes
fbxa-190	X-1K10	Yes
fbxa-24	II-3D07	Yes
fbxa-30	III-1M02	Yes
fbxa-31	III-1M04	Yes
fbxa-53	X-1F23	Yes
fbxa-59	III-1I06	Yes
fbxa-60	III-1I08	Yes
fbxa-88	V-10B24	Yes
fil-1	V-9D18	Yes

fipr-1	V-8C18	Yes
fipr-16	III-4H09	Yes
fipr-2	V-16I20	Yes
fipr-6	V-7I11	Yes
flp-26	X-8H11	Yes
fmo-2	IV-5L03	Yes
folt-2	V-2J03	Yes
frk-1	IV-5A14	Yes
frpr-9	V-14I02	Yes
ftn-1	V-5B07	Yes
fut-1	II-10A15	Yes
fut-6	II-10J05	Yes
gale-1	I-6H23	Yes
gfi-1	V-16H05	Yes
gipc-1	III-2B17	Yes
gipc-2	IV-5O19	Yes
glb-28	X-7G01	Yes
glc-1	V-10H04	Yes
glct-6	IV-1N14	Yes

gln-2	III-5G08	Yes
glt-5	II-6N18	Yes
grd-6	V-6B13	Yes
grl-16	I-9K02	Yes
grl-5	V-14P01	Yes
grl-7	V-7B06	Yes
gska-3	I-4G16	Yes
gsp-3	I-2G09	Yes
gst-38	V-10F05	Yes
H02F09.2	X-1B21	Yes
H02F09.3	X-1B23	Yes
H23N18.5	V-3N14	Yes
H43E16.1	II-5K17	Yes
hex-2	V-4I06	Yes
his-11	II-8J16	Yes
hsp-17	V-6C07	Yes
ift-74	II-5M09	Yes
irg-1	V-15K17	Yes
K01H12.4	IV-5C23	Yes

K02E11.10	V-16L20	Yes
K02E11.4	V-9I08	Yes
K02E11.6	V-16J07	Yes
K02E11.7	V-9I14	Yes
K02E2.6	V-13A13	Yes
K04A8.1	V-4F10	Yes
K04H4.5	III-5A17	Yes
K05F1.1	II-10G21	Yes
K06A9.1	X-1B13	Yes
K06G5.1	X-6L07	Yes
K08C9.2	I-5B22	Yes
K08D8.4	IV-9B24	Yes
K08D8.5	IV-6H16	Yes
K09C6.9	V-16L02	Yes
K10C2.7	X-8H08	Yes
K10D11.3	IV-6L22	Yes
K10D11.5	IV-6N02	Yes
K10D11.6	IV-6N04	Yes
K10G4.3	V-11H03	Yes

K12H6.9	II-2H04	Yes
kel-10	III-5M16	Yes
klf-1	III-1J15	Yes
lact-3	II-7M24	Yes
lbp-8	V-9K17	Yes
lec-11	IV-3A16	Yes
lgc-1	V-3F01	Yes
nhr-57	V-3F03	Yes
lgc-21	X-6H03	Yes
lips-16	II-8O02	Yes
LLC1.121	IV-7D09	Yes
LLC1.2	IV-7D15	Yes
M04C3.2	V-12H15	Yes
M04D5.3	I-5N17	Yes
M28.10	II-10L04	Yes
M28.8	II-7O04	Yes
M60.2	X-4O17	Yes
M7.8	IV-5L04	Yes
mgl-2	I-5O07	Yes

mlk-1	V-4E01	Yes
mltn-1	II-10C18	Yes
mpst-3	V-9B14	Yes
msd-4	III-2D11	Yes
msp-142	II-4N04, II-4L10	Yes
msp-152	II-4I21	Yes
msp-3	II-4C05	Yes
msp-36	IV-5C22	Yes
msp-38	IV-5I06	Yes
msp-40	II-4C23	Yes
msp-45	II-4A10	Yes
msp-49	II-4C22	Yes
msp-50	II-4C18	Yes
msp-51	IV-2D14	Yes
msp-57	IV-2J23	Yes
msp-59	IV-2D24	Yes
msp-64	II-4N04	Yes
msp-76	IV-5C09	Yes
msp-78	IV-5G09	Yes

mtl-1	V-4L06	Yes
mul-1	IV-10B17	Yes
nas-4	III-3M04	Yes
nas-5	I-4N20	Yes
nas-5	I-4N20	Yes
ncx-9	V-4C03	Yes
nep-14	X-4E02	Yes
nhr-112	V-11O01	Yes
nhr-162	V-14C24	Yes
nhr-168	V-8F10	Yes
nhr-178	V-1D12	Yes
nhr-21	II-5F23	Yes
nlp-3	X-6M21	Yes
nlp-37	X-1B18	Yes
nlp-8	I-3H18	Yes
nlt-1	II-7G21	Yes
npr-8	X-3J02	Yes
nspa-5	V-9B04, V-9P21	Yes
nspc-16-20	X-6D04	Yes

nspc-9,10	X-5L18	Yes
nspd-1	I-2J08	Yes
nspd-2	IV-5I11	Yes
nspd-3	IV-2P03	Yes
nspd-4	II-4E07	Yes
nspd-7	IV-5M22	Yes
nspe-1	II-8O08	Yes
oac-18	V-10J24	Yes
oac-31	V-1B14	Yes
oac-5	V-10L02	Yes
oac-57	IV-6F09	Yes
pcp-1	III-4G05	Yes
pgp-1	IV-6P19	Yes
pho-9	III-9E07	Yes
pmp-1	II-5C20	Yes
poml-4	I-1D16	Yes
pqn-31	V-6O04	Yes
pqn-94	V-12P18	Yes
qua-1	II-6C21	Yes

R02D5.3	V-9D23	Yes
R03G8.3	X-6K17	Yes
R07B7.6	V-8I05	Yes
R07E5.15	III-2A04	Yes
R08E3.1	X-2H04	Yes
R08E3.1	X-2H04	Yes
R08E3.2	X-2H06	Yes
R08E3.2	X-2H06	Yes
R09E10.2	IV-9H22	Yes
R09H10.5	IV-5J13	Yes
R09H10.5	IV-5J13	Yes
R10E9.2	III-1P24	Yes
R12E2.15	I-1H10	Yes
R12E2.7	I-1F18	Yes
ram-2	II-7J09	Yes
rmd-3	II-7D02	Yes
rol-6	II-6I10	Yes
rol-8	II-5N07	Yes
scav-6	I-3L17	Yes

scd-2	V-4J10	Yes
sek-4	X-3C21	Yes
sid-2	III-6F12	Yes
skr-3	V-10B10	Yes
slc-17.9	X-4H04	Yes
slcf-2	X-2O23	Yes
smz-1	IV-6L03	Yes
sodh-1	V-8C03	Yes
sox-4	X-2C18	Yes
spe-11	I-2K10	Yes
spe-46	I-4B19, I-9C11	Yes
sph-1	IV-4I15	Yes
spin-3	X-6M09	Yes
spp-23	I-7F15	Yes
sqt-1	II-7B24	Yes
sqt-2	II-1A03	Yes
srh-25	V-8G16	Yes
srj-29	V-10P13	Yes
srp-7	V-14F18	Yes

srx-134	V-9I19	Yes
ttr-21	V-9I17	Yes
ssq-2	IV-2H23	Yes
ssq-3	IV-3B11	Yes
ssq-4	IV-2H15	Yes
sss-1	IV-5K13	Yes
sss-2	V-9O02	Yes
sul-3	X-4E15	Yes
swt-6	V-16F04	Yes
T02B5.1	V-9E18	Yes
T04F8.7	X-5H07	Yes
T05A7.6	II-3N16	Yes
T05B11.4	V-5L01	Yes
T05E12.6	V-11M24	Yes
T05F1.8	I-4F08	Yes
T06A1.1	V-14O12	Yes
T06A1.5	V-1N24	Yes
T06F4.1	X-2D05	Yes
T08B6.2	IV-2F05	Yes

T08B6.4	IV-2F09	Yes
T09E11.11	I-6A04	Yes
T10E9.4	I-3K23	Yes
T10H10.2	X-1F10	Yes
T11F9.12	V-7F22	Yes
T13F2.9	IV-5G05	Yes
T15B7.10	V-16D19	Yes
T15B7.17	V-16G22	Yes
T16A9.5	V-9I02	Yes
T19D12.4	II-5K03	Yes
T19H12.3	V-3L12	Yes
T20D3.2	IV-9M01	Yes
T21C9.9	V-7G14	Yes
T21D12.14	IV-9L06	Yes
T22B3.3	IV-6A24	Yes
igcm-2	X-8D11	Yes
T22F3.11	V-3A02	Yes
T23B3.5	I-3C14	Yes
T23F2.3	X-3G17	Yes

T23F4.2	II-1D04	Yes
T24B8.5	II-6F01	Yes
T24C4.4	III-1E14	Yes
T24F1.5 (nlp-51)	II-7B18	Yes
T25C12.3	X-5B23	Yes
T25C12.3	X-5B23	Yes
T25D10.1	II-5A03	Yes
T25D10.4	II-5A09	Yes
T27A3.4	I-2J16	Yes
T27E7.1	IV-7F05	Yes
T28B4.4	X-3D11	Yes
T28H10.3	V-8I24	Yes
T28H11.7	IV-2J03	Yes
tag-290	V-7L08	Yes
tat-2	IV-2D09	Yes
trx-3	IV-2E16	Yes
tsp-1	III-4K02	Yes
tsp-2	III-4K02, III-4I20	Yes
ttm-2	II-4A23	Yes

ttm-5	I-7C18	Yes
ttr-22	V-8O11	Yes
ttr-29	V-8J03	Yes
twk-28	X-2H23	Yes
ugt-16	V-8F17	Yes
ugt-18	V-8F15	Yes
ugt-54	IV-5N23	Yes
valv-1	IV-3P19	Yes
W01B6.2	IV-5C02	Yes
W02B12.12	II-7H10	Yes
W02D9.10	I-6I18	Yes
W03D2.6	IV-2E07	Yes
W03D8.9	I-1K14	Yes
W04B5.1	III-1F17	Yes
wrt-4	X-7O15	Yes
wrt-6	X-2C04	Yes
xtr-1	X-5L21	Yes
Y106G6D.3	I-5E23	Yes
Y106G6H.13	I-5A18	Yes

Y116A8B.4	IV-8M19	Yes
Y18H1A.1	I-7B17, I-7D03	Yes
Y18H1A.10	I-1D09, I-7D05	Yes
Y32F6A.4	V-7A04	Yes
tag-314	V-14H15	Yes
Y34B4A.9	X-8J11	Yes
Y34F4.4	III-8O03	Yes
Y37E11B.10	IV-1L16	Yes
Y37H2A.11	V-15M08	Yes
Y38C1AA.6	IV-9J16	Yes
Y38C1AA.7	IV-10F04	Yes
Y38E10A.17	II-8O16	Yes
Y38F1A.8	II-8F15	Yes
Y38H6C.8	V-13E13	Yes
Y39B6A.41	V-16C16	Yes
Y39G8B.9	II-8P16	Yes
Y40D12A.2	III-3D13	Yes
Y40H4A.2	V-9H11	Yes
Y41C4A.11	III-6E19	Yes

Y41C4A.11	III-6E19	Yes
Y41C4A.8	III-8M12	Yes
Y41D4B.15	IV-8H15	Yes
hpo-6	IV-8H13	Yes
Y43C5A.2	IV-5M24	Yes
Y43C5A.3	IV-5O02	Yes
Y43F8A.2	V-12D07	Yes
Y46C8AL.11	IV-8J01	Yes
Y47D7A.15	V-16L12	Yes
Y47H10A.5	I-6C21	Yes
Y47H9C.1	I-5N16	Yes
Y50E8A.1	V-14E08	Yes
Y51H7C.13	II-9P05	Yes
Y53G8AM.5	III-7O15	Yes
Y54G11A.4	II-9G21	Yes
Y55F3AM.11	IV-8N17	Yes
Y57G7A.6	II-1F16	Yes
Y59E9AL.6	I-4P21, IV-8B08	Yes
Y66A7A.7	IV-8L09	Yes

Y69A2AR.19	IV-8J14, IV-8J16, IV-8J18	Yes
Y69E1A.1	IV-5F10	Yes
Y69E1A.2	IV-5F12	Yes
Y69H2.9	V-12M21	Yes
Y71G12B.2	I-8O05, I-8O01	Yes
Y75B8A.28	III-6A20	Yes
Y7A9C.1	IV-7L02	Yes
Y9C9A.8	IV-9E03	Yes
ZC196.5	V-6A02	Yes
ZC21.3	III-4F11	Yes
ZC239.14	II-3E09	Yes
ZC443.4	V-15K14	Yes
zip-5	V-8D10	Yes
ZK1010.5	III-6B15	Yes
ZK1025.3	I-5B06	Yes
ZK1290.10	II-5N21	Yes
ZK1290.14	II-10P03	Yes
ZK1320.2	II-6L22	Yes
ZK180.6	IV-2G10	Yes

ZK265.3	I-4E09	Yes
ZK287.9	V-15G11	Yes
ZK353.4	III-4B07	Yes
ZK354.2	IV-2D08	Yes
ZK384.4	V-12O17	Yes
ZK484.5	I-2J02	Yes
ZK6.11	V-15I07	Yes
ZK856.18	V-7G09	Yes
ZK856.5	V-7G13	Yes
ZK938.1	II-7A17	Yes
ZK945.7	II-7K19	Yes

8 References

Aballay, A., & Ausubel, F. M. (2001). Programmed cell death mediated by ced-3 and ced-4 protects *Caenorhabditis elegans* from Salmonella typhimurium-mediated killing. *Proceedings of the National Academy of Sciences*. https://doi.org/10.1073/pnas.041613098

Abraham, M. C., Lu, Y., & Shaham, S. (2007). A Morphologically Conserved Nonapoptotic Program Promotes Linker Cell Death in *Caenorhabditis elegans*. *Developmental Cell*. https://doi.org/10.1016/j.devcel.2006.11.012

Ahmed, S., Alpi, a, Hengartner, M. O., & Gartner, a. (2001). *C. elegans* RAD-5/CLK-2 defines a new DNA damage checkpoint protein. *Current Biology*. https://doi.org/S0960-9822(01)00604-2

Akers, A., Al-Shahi Salman, R., A. Awad, I., Dahlem, K., Flemming, K., Hart, B., … Whitehead, K. (2017). Synopsis of Guidelines for the Clinical Management of Cerebral Cavernous Malformations: Consensus Recommendations Based on Systematic Literature Review by the Angioma Alliance Scientific Advisory Board Clinical Experts Panel. *Neurosurgery*, *80*(5), 665–680. https://doi.org/10.1093/neuros/nyx091

Akers, A. L., Johnson, E., Steinberg, G. K., Zabramski, J. M., & Marchuk, D. A. (2009). Biallelic somatic and germline mutations in cerebral cavernous malformations (CCMs): Evidence for a two-hit mechanism of CCM pathogenesis. *Human Molecular Genetics*. https://doi.org/10.1093/hmg/ddn430

Altun, Z. F., & Hall, D. H. (2006). Introduction to *C. elegans* anatomy - *Caenorhabditis elegans* as a genetic organism. *WormAtlas*. http://www.wormatlas.org/

Amelio, I., Melino, G., & Knight, R. A. (2011). Cell death pathology: Cross-talk with autophagy and its clinical implications. *Biochemical and Biophysical Research Communications*. https://doi.org/10.1016/j.bbrc.2011.09.080

Ames, K., Da Cunha, D. S., Gonzalez, B., Konta, M., Lin, F., Shechter, G., … Meléndez, A. (2017). A Non-Cell-Autonomous Role of BEC-1/BECN1/Beclin1 in Coordinating Cell-Cycle Progression and Stem Cell Proliferation during Germline Development. *Current Biology*. https://doi.org/10.1016/j.cub.2017.02.015

An, W.-L., Pei, J.-J., Nishimura, T., Winblad, B., & Cowburn, R. F. (2005). Zinc-induced anti-apoptotic effects in SH-SY5Y neuroblastoma cells via the extracellular signal-regulated kinase 1/2. *Brain Research. Molecular Brain Research*. https://doi.org/10.1016/j.molbrainres.2004.11.010

Antala, S., & Dempski, R. E. (2012). The human ZIP4 transporter has two distinct binding affinities and mediates transport of multiple transition metals. *Biochemistry*. https://doi.org/10.1021/bi201553p

Aroian, R. V, Koga, M., Mendel, J. E., Ohshima, Y., & Sternberg, P. W. (1990). The let-23 gene necessary for *Caenorhabditis elegans* vulval induction encodes a tyrosine kinase of the EGF receptor subfamily. *Nature*. https://doi.org/10.1038/348693a0

Arur, S., Ohmachi, M., Nayak, S., Hayes, M., Miranda, A., Hay, A., … Schedl, T. (2009). Multiple ERK substrates execute single biological processes in *Caenorhabditis elegans* germ-line development. *Proceedings of the National Academy of Sciences*. https://doi.org/10.1073/pnas.0812285106

Ashida, H., Mimuro, H., Ogawa, M., Kobayashi, T., Sanada, T., Kim, M., & Sasakawa, C. (2011). Cell death and infection: A double-edged sword for host and pathogen survival. *Journal of Cell Biology*. https://doi.org/10.1083/jcb.201108081

Austin, J., & Kimble, J. (1987). glp-1 Is required in the germ line for regulation of the decision between mitosis and meiosis in *C. elegans*. *Cell*. https://doi.org/10.1016/0092-8674(87)90128-0

Bafaro, E., Liu, Y., Xu, Y., & Dempski, R. E. (2017). The emerging role of zinc transporters in cellular homeostasis and cancer. *Signal Transduction and Targeted Therapy*. https://doi.org/10.1038/sigtrans.2017.29

Bailly, A. P., Freeman, A., Hall, J., Déclais, A. C., Alpi, A., Lilley, D. M. J., … Gartner, A. (2010). The *Caenorhabditis elegans* homolog of Gen1/Yen1 resolvases links DNA damage signaling to DNA double-strand break repair. *PLoS Genetics*. https://doi.org/10.1371/journal.pgen.1001025

Balklava, Z., Pant, S., Fares, H., & Grant, B. D. (2007). Genome-wide analysis identifies a general requirement for polarity proteins in endocytic traffic. *Nature Cell Biology*. https://doi.org/10.1038/ncb1627

Baltaci, A.K., & Yuce, K. (2018). Zinc Transporter Proteins. *Neurochem Res, 43(3), 517-530.* https:// doi: 10.1007/s11064-017-2454-y.

Baranoski, J. F., Kalani, M. Y. S., Przybylowski, C. J., & Zabramski, J. M. (2016). Cerebral Cavernous Malformations: Review of the Genetic and Protein–Protein Interactions Resulting in Disease Pathogenesis. *Frontiers in Surgery*. https://doi.org/10.3389/fsurg.2016.00060

Beh, C. T., Ferrari, D. C., Chung, M. A., & McGhee, J. D. (1991). An acid phosphatase as a biochemical marker for intestinal development in the nematode *Caenorhabditis elegans*. *Developmental Biology*, *147*(1), 133–143. https://doi.org/10.1016/S0012-1606(05)80013-2

Beitel, G. J., Clark, S. G., & Horvitz, H. R. (1990). *Caenorhabditis elegans* ras gene let-60 acts as a switch in the pathway of vulval induction. *Nature*. https://doi.org/10.1038/348503a0

Béraud-Dufour, S., Gautier, R., Albiges-Rizo, C., Chardin, P., & Faurobert, E. (2007). Krit 1 interactions with microtubules and membranes are regulated by Rap1 and integrin

cytoplasmic domain associated protein-1. *FEBS Journal*. https://doi.org/10.1111/j.1742-4658.2007.06068.x

Berman, J. R., & Kenyon, C. (2006). Germ-cell loss extends *C. elegans* life span through regulation of DAF-16 by kri-1 and lipophilic-hormone signaling. *Cell*, *124*(5), 1055–1068. https://doi.org/10.1016/j.cell.2006.01.039

Berthelet, J., & Dubrez, L. (2013). Regulation of Apoptosis by Inhibitors of Apoptosis (IAPs). *Cells*. https://doi.org/10.3390/cells2010163

Boag, P. R., Nakamura, A., & Blackwell, T. K. (2005). A conserved RNA-protein complex component involved in physiological germline apoptosis regulation in *C. elegans*. *Development. 132*(22), 4975–86. https://doi.org/10.1242/dev.02060

Bolger, A. M., Lohse, M., & Usadel, B. (2014). Trimmomatic: A flexible trimmer for Illumina sequence data. *Bioinformatics*. https://doi.org/10.1093/bioinformatics/btu170

Borikova, A. L., Dibble, C. F., Sciaky, N., Welch, C. M., Abell, A. N., Bencharit, S., & Johnson, G. L. (2010). Rho kinase inhibition rescues the endothelial cell cerebral cavernous malformation phenotype. *J Biol Chem*, *285*(16), 11760–11764. https://doi.org/10.1074/jbc.C109.097220

Borisenko, G. G., Matsura, T., Liu, S. X., Tyurin, V. A., Jianfei, J., Serinkan, F. B., & Kagan, V. E. (2003). Macrophage recognition of externalized phosphatidylserine and phagocytosis of apoptotic Jurkat cells - Existence of a threshold. *Archives of Biochemistry and Biophysics*. https://doi.org/10.1016/S0003-9861(03)00083-3

Boulday, G., Rudini, N., Maddaluno, L., Blécon, A., Arnould, M., Gaudric, A., … Tournier-Lasserve, E. (2011). Developmental timing of CCM2 loss influences cerebral cavernous malformations in mice. *The Journal of Experimental Medicine*. https://doi.org/10.1084/jem.20110571

Brandt, J. P., & Ringstad, N. (2015). Toll-like Receptor Signaling Promotes Development and Function of Sensory Neurons Required for a *C. elegans* Pathogen-Avoidance Behavior. *Current Biology*. https://doi.org/10.1016/j.cub.2015.07.037

Brenner, S. (1974). The genetics of *Caenorhabditis elegans*. *Genetics*, *77*(1), 71–94. Retrieved from http://www.ncbi.nlm.nih.gov/pubmed/4366476

Brown, J. M., & Attardi, L. D. (2005). The role of apoptosis in cancer development and treatment response. *Nature Reviews. Cancer*. https://doi.org/10.1038/nrc1560

Bruinsma, J. J., Jirakulaporn, T., Muslin, A. J., & Kornfeld, K. (2002). Zinc ions and cation diffusion facilitator proteins regulate ras-mediated signaling. *Developmental Cell*, *2*(5), 567–578. https://doi.org/10.1016/S1534-5807(02)00151-X

Brunquell, J., Morris, S., Lu, Y., Cheng, F., & Westerheide, S. D. (2016). The genome-wide role of HSF-1 in the regulation of gene expression in *Caenorhabditis elegans*. *BMC Genomics*,

17(1), 559. https://doi.org/10.1186/s12864-016-2837-5

Burns, A. R., Luciani, G. M., Musso, G., Bagg, R., Yeo, M., Zhang, Y., … Roy, P. J. (2015). *Caenorhabditis elegans* is a useful model for anthelmintic discovery. *Nature Communications*, *6*. https://doi.org/10.1038/ncomms8485

Byerly, L., Cassada, R. C., & Russell, R. L. (1976). The life cycle of the nematode *Caenorhabditis elegans*. *Developmental Biology*. https://doi.org/10.1016/0012-1606(76)90119-6

Cao, L., Quan, X. B., Zeng, W. J., Yang, X. O., & Wang, M. J. (2016). Mechanism of hepatocyte apoptosis. *Journal of Cell Death*. https://doi.org/10.4137/JCD.S39824

Chakraborty, S., Lambie, E. J., Bindu, S., Mikeladze-Dvali, T., & Conradt, B. (2015). Engulfment pathways promote programmed cell death by enhancing the unequal segregation of apoptotic potential. *Nature Communications*. https://doi.org/10.1038/ncomms10126

Chalfie, M., Tu, Y., Euskirchen, G., Ward, W. W., & Prasher, D. C. (1994). Green fluorescent protein as a marker for gene expression. *Science* . https://doi.org/10.1126/science.8303295

Chamoli, M., Singh, A., Malik, Y., & Mukhopadhyay, A. (2014). A novel kinase regulates dietary restriction-mediated longevity in *Caenorhabditis elegans*. *Aging Cell*, *13*(4), 641–655. https://doi.org/10.1111/acel.12218

Chang, C., Hopper, N. a, & Sternberg, P. W. (2000). *Caenorhabditis elegans* SOS-1 is necessary for multiple RAS-mediated developmental signals. *The EMBO Journal*. https://doi.org/10.1093/emboj/19.13.3283

Chen, D., Li, P. W. L., Goldstein, B. A., Cai, W., Thomas, E. L., Chen, F., … Kapahi, P. (2013a). Germline Signaling Mediates the Synergistically Prolonged Longevity Produced by Double Mutations in daf-2 and rsks-1 in *C.elegans*. *Cell Reports*. https://doi.org/10.1016/j.celrep.2013.11.018

Chen, F., Hersh, B. M., Conradt, B., Zhou, Z., Riemer, D., Gruenbaum, Y., & Horvitz, H. R. (2000). Translocation of *C. elegans* CED-4 to nuclear membranes during programmed cell death. *Science*. https://doi.org/10.1126/science.287.5457.1485

Chen, Y. Z., Mapes, J., Lee, E. S., Robert Skeen-Gaar, R., & Xue, D. (2013b). Caspase-mediated activation of *Caenorhabditis elegans* CED-8 promotes apoptosis and phosphatidylserine externalization. *Nature Communications*. https://doi.org/10.1038/ncomms3726

Chinnaiyan, A. M., O'Rourke, K., Tewari, M., & Dixit, V. M. (1995). FADD, a novel death domain-containing protein, interacts with the death domain of fas and initiates apoptosis. *Cell*. https://doi.org/10.1016/0092-8674(95)90071-3

Choi, H., Larsen, B., Lin, Z. Y., Breitkreutz, A., Mellacheruvu, D., Fermin, D., … Nesvizhskii, A. I. (2011). SAINT: Probabilistic scoring of affinity purificationg-mass spectrometry data. *Nature Methods*. https://doi.org/10.1038/nmeth.1541

Church, D. L., Guan, K. L., & Lambie, E. J. (1995). Three genes of the MAP kinase cascade, mek-2, mpk-1/sur-1 and let-60 ras, are required for meiotic cell cycle progression in *Caenorhabditis elegans*. *Development (Cambridge, England)*.

Clark, S. G., Stern, M. J., & Horvritz, H. R. (1992). *C. elegans* cell-signalling gene sem-5 encodes a protein with SH2 and SH3 domains. *Nature*. https://doi.org/10.1038/356340a0

Clejan, I., Boerckel, J., & Ahmed, S. (2006). Developmental modulation of nonhomologous end joining in *Caenorhabditis elegans*. *Genetics*. https://doi.org/10.1534/genetics.106.058628

Clem, R. J., & Miller, L. K. (1994). Control of programmed cell death by the baculovirus genes p35 and iap. *Molecular and Cellular Biology*. https://doi.org/10.1128/MCB.14.8.5212

Close, D. M., Nelson, W. H., & Bernhard, W. A. (2013). DNA damage by the direct effect of ionizing radiation: Products produced by two sequential one-electron oxidations. *Journal of Physical Chemistry A*. https://doi.org/10.1021/jp4084844

Cobb, J. P., Hotchkiss, R. S., Karl, I. E., & Buchman, T. G. (1996). Mechanisms of cell injury and death. *British Journal of Anaesthesia*. https://doi.org/10.1093/bja/77.1.3

Conradt, B., & Horvitz, H. R. (1998). The *C. elegans* protein EGL-1 is required for programmed cell death and interacts with the Bcl-2-like protein CED-9. *Cell*, *93*(4), 519–529. Retrieved from http://www.ncbi.nlm.nih.gov/pubmed/9604928

Conradt, B., & Horvitz, H. R. (1999). The TRA-1A sex determination protein of *C. elegans* regulates sexually dimorphic cell deaths by repressing the egl-1 cell death activator gene. *Cell*. https://doi.org/10.1016/S0092-8674(00)81961-3

Conradt, B., Wu, Y. C., & Xue, D. (2016). Programmed Cell Death During *Caenorhabditis elegans* Development. *Genetics*. https://doi.org/ 10.1534/genetics.115.186247.

Crose, L. E. S., Hilder, T. L., Sciaky, N., & Johnson, G. L. (2009). Cerebral cavernous malformation 2 protein promotes smad ubiquitin regulatory factor 1-mediated RhoA degradation inendothelial cells. *Journal of Biological Chemistry*. https://doi.org/10.1074/jbc.C900009200

Cullere, X., Plovie, E., Bennett, P. M., MacRae, C. A., & Mayadas, T. N. (2015). The cerebral cavernous malformation proteins CCM2L and CCM2 prevent the activation of the MAP kinase MEKK3. *Proceedings of the National Academy of Sciences*, *112*(46), 14284–14289. https://doi.org/10.1073/pnas.1510495112

Cuttano, R., Rudini, N., Bravi, L., Corada, M., Giampietro, C., Papa, E., … Dejana, E. (2015). KLF4 is a key determinant in the development and progression of cerebral cavernous

malformations. *EMBO Molecular Medicine*. https://doi.org/10.15252/emmm.201505433

Cutter, A. D. (2015). Caenorhabditis evolution in the wild. *BioEssays*. https://doi.org/10.1002/bies.201500053

Dalfó, D., Michaelson, D., & Hubbard, E. J. A. (2012). Sensory regulation of the *C. elegans* germline through TGF-β-dependent signaling in the niche. *Current Biology*. https://doi.org/10.1016/j.cub.2012.02.064

Dalpe, G., Tarsitano, M., Persico, M. G., Zheng, H., & Culotti, J. (2013). *C. elegans* PVF-1 inhibits permissive UNC-40 signalling through CED-10 GTPase to position the male ray 1 sensillum. *Development*. https://doi.org/10.1242/dev.095190

D' Amora D.R., Hu, Q., Pizzardi, M., & Kubiseski, T. (2018). BRAP-2 promotes DNA damage induced germline apoptosis in *C. elegans* through the regulation of SKN-1 and AKT-1. *Cell Death Differ, 25*(7), 1276-1288. https:// doi: 10.1038/s41418-017-0038-7.

Darland-Ransom, M., Wang, X., Sun, C. L., Mapes, J., Gengyo-Ando, K., Mitani, S., & Xue, D. (2008). Role of *C. elegans* TAT-1 protein in maintaining plasma membrane phosphatidylserine asymmetry. *Science*. https://doi.org/10.1126/science.1155847

Das, G., Shravage, B. V., & Baehrecke, E. H. (2012). Regulation and function of autophagy during cell survival and cell death. *Cold Spring Harbor Perspectives in Biology*. https://doi.org/10.1101/cshperspect.a008813

Datta, S. R., Dudek, H., Xu, T., Masters, S., Haian, F., Gotoh, Y., & Greenberg, M. E. (1997). Akt phosphorylation of BAD couples survival signals to the cell- intrinsic death machinery. *Cell*. https://doi.org/10.1016/S0092-8674(00)80405-5

Davis, D. E., Hyun, C. R., Deshmukh, K., Bruinsma, J. J., Schneider, D. L., Guthrie, J., … Kornfeld, K. (2009). The cation diffusion facilitator gene cdf-2 mediates zinc metabolism in *Caenorhabditis elegans*. *Genetics*, *182*(4), 1015–1033. https://doi.org/10.1534/genetics.109.103614

Dekkers, M. P. J., Nikoletopoulou, V., & Barde, Y. A. (2013). Death of developing neurons: New insights and implications for connectivity. *Journal of Cell Biology*. https://doi.org/10.1083/jcb.201306136

Del Peso, L., González-García, M., Page, C., Herrera, R., & Nuñez, G. (1997). Interleukin-3-induced phosphorylation of BAD through the protein kinase Akt. *Science*. https://doi.org/10.1126/science.278.5338.687

Del Peso, L., González, V. M., Inohara, N., Ellis, R. E., & Núñez, G. (2000). Disruption of the CED-9·CED-4 complex by EGL-1 is a critical: Step for programmed cell death in *Caenorhabditis elegans*. *Journal of Biological Chemistry*. https://doi.org/10.1074/jbc.M000858200

Del Peso, L., González, V. M., & Núnez, G. (1998). *Caenorhabditis elegans* EGL-1 disrupts the

interaction of CED-9 with CED- 4 and promotes CED-3 activation. *Journal of Biological Chemistry*. https://doi.org/10.1074/jbc.273.50.33495

Deng, X., Hofmann, E. R., Villanueva, A., Hobert, O., Capodieci, P., Veach, D. R., … Kolesnick, R. (2004). *Caenorhabditis elegans* ABL-1 antagonizes p53-mediated germline apoptosis after ionizing irradiation. *Nature Genetics*, *36*(8), 906–912. https://doi.org/10.1038/ng1396

Deng, X., Yin, X., Allan, R., Lu, D. D., Maurer, C. W., Haimovitz-Friedman, A., … Kolesnick, R. (2008). Ceramide biogenesis is required for radiation-induced apoptosis in the germ line of *C. elegans*. *Science*. https://doi.org/10.1126/science.1158111

Denier, C., Gasc, J. M., Chapon, F., Domenga, V., Lescoat, C., Joutel, A., & Tournier-Lasserve, E. (2002). Krit1/cerebral cavernous malformation 1 mRNA is preferentially expressed in neurons and epithelial cells in embryo and adult. *Mechanisms of Development*. https://doi.org/10.1016/S0925-4773(02)00209-5

Denver, D. R., Feinberg, S., Estes, S., Thomas, W. K., & Lynch, M. (2005). Mutation rates, spectra and hotspots in mismatch repair-deficient *Caenorhabditis elegans*. *Genetics*. https://doi.org/10.1534/genetics.104.038521

Depina, A. S., Iser, W. B., Park, S. S., Maudsley, S., Wilson, M. A., & Wolkow, C. A. (2011). Regulation of *Caenorhabditis elegans* vitellogenesis by DAF-2/IIS through separable transcriptional and posttranscriptional mechanisms. *BMC Physiology*. https://doi.org/10.1186/1472-6793-11-11

Derry, W. B., Putzke, A.P., & Rothman J.H. (2001). *Caenorhabditis elegans* p53: Role in Apoptosis, Meiosis, and Stress Resistance. *Science*, *294*(5542), 591–595. https://doi.org/10.1126/science.1065486

Derry, W. B., Bierings, R., van Iersel, M., Satkunendran, T., Reinke, V., & Rothman, J. H. (2007). Regulation of developmental rate and germ cell proliferation in *Caenorhabditis elegans* by the p53 gene network. *Cell Death and Differentiation*. https://doi.org/10.1038/sj.cdd.4402075

Dewi, V., Kwok, A., Lee, S., Lee, M. M., Tan, Y. M., Nicholas, H. R., … Crossley, M. (2015). Phosphorylation of Kruppel-like Factor 3 (KLF3/BKLF) and C-terminal Binding Protein 2 (CtBP2) by Homeodomain Interacting Protein Kinase 2 (HIPK2) Modulates KLF3 DNA Binding and Activity. *Journal of Biological Chemistry*. https://doi.org/10.1074/jbc.M115.638338

Dewson, G., & Kluck, R. M. (2009). Mechanisms by which Bak and Bax permeabilise mitochondria during apoptosis. *Journal of Cell Science*. https://doi.org/10.1242/jcs.038166

Dietrich, N., Schneider, D. L., & Kornfeld, K. (2017). A pathway for low zinc homeostasis that is conserved in animals and acts in parallel to the pathway for high zinc homeostasis. *Nucleic Acids Research*. https://doi.org/10.1093/nar/gkx762

Dietrich, N., Tan, C. H., Cubillas, C., Earley, B. J., & Kornfeld, K. (2016). Insights into zinc and cadmium biology in the nematode *Caenorhabditis elegans*. *Archives of Biochemistry and Biophysics*. https://doi.org/10.1016/j.abb.2016.05.021

Dineley, K. E., Votyakova, T. V., & Reynolds, I. J. (2003). Zinc inhibition of cellular energy production: Implications for mitochondria and neurodegeneration. *Journal of Neurochemistry*. https://doi.org/10.1046/j.1471-4159.2003.01678.x

DiStefano, P. V., Kuebel, J. M., Sarelius, I. H., & Glading, A. J. (2014). KRIT1 protein depletion modifies endothelial cell behavior via increased vascular endothelial growth factor (VEGF) Signaling. *Journal of Biological Chemistry*. https://doi.org/10.1074/jbc.M114.582304

Donat, S., Lourenco, M., Paolini, A., Otten, C., Renz, M., & Abdelilah-Seyfried, S. (2018). Heg1 and Ccm1/2 proteins control endocardial mechanosensitivity during zebrafish valvulogenesis. *Elife.* https://doi: 10.7554/eLife.28939.

Dorado, F., Velasco, S., Esparís-Ogando, A., Pericacho, M., Pandiella, A., Silva, J., … Rodríguez-Barbero, A. (2008). The mitogen-activated protein kinase Erk5 mediates human mesangial cell activation. *Nephrology, Dialysis, Transplantation : Official Publication of the European Dialysis and Transplant Association - European Renal Association*. https://doi.org/10.1093/ndt/gfn333

Dorstyn, L., Akey, C.W., & Kumar, S. (2018). New insights into apoptosome structure and function. *Cell Death Differ*, *25*(7), 1194-1208. https://doi: 10.1038/s41418-017-0025-z.

Dowen, R. H., Breen, P. C., Tullius, T., Conery, A. L., & Ruvkun, G. (2016). A microRNA program in the *C. elegans* hypodermis couples to intestinal mTORC2/PQM-1 signaling to modulate fat transport. *Genes and Development*. https://doi.org/10.1101/gad.283895.116

Draheim, K. M., Fisher, O. S., Boggon, T. J., & Calderwood, D. A. (2014). Cerebral cavernous malformation proteins at a glance. *Journal of Cell Science*. https://doi.org/10.1242/jcs.138388

Drew, B. A., Burow, M. E., & Beckman, B. S. (2012). MEK5/ERK5 pathway: The first fifteen years. *Biochimica et Biophysica Acta - Reviews on Cancer*. https://doi.org/10.1016/j.bbcan.2011.10.002

Du, C., Fang, M., Li, Y., Li, L., & Wang, X. (2000). Smac, a mitochondrial protein that promotes cytochrome c-dependent caspase activation by eliminating IAP inhibition. *Cell*. https://doi.org/10.1016/S0092-8674(00)00008-8

Dufner-Beattie, J., Kuo, Y. M., Gitschier, J., & Andrews, G. K. (2004). The adaptive response to dietary zinc in mice involves the differential cellular localization and zinc regulation of the zinc transporters ZIP4 and ZIP5. *Journal of Biological Chemistry*. https://doi.org/10.1074/jbc.M409962200

Eberhard, R., Stergiou, L., Hofmann, E. R., Hofmann, J., Haenni, S., Teo, Y., … Hengartner, M. O. (2013). Ribosome synthesis and MAPK activity modulate ionizing radiation-induced

germ cell apoptosis in *Caenorhabditis elegans*. *PLoS Genet*, *9*(11), e1003943. https://doi.org/10.1371/journal.pgen.1003943

Eisenmann, D. M., & Kim, S. K. (1997). Mechanism of activation of the *Caenorhabditis elegans* ras homologue let- 60 by a novel, temperature-sensitive, gain-of-function mutation. *Genetics*, *146*(2), 553–565.

Ellis, H. M., & Horvitz, H. R. (1986). Genetic control of programmed cell death in the nematode *C. elegans*. *Cell*. https://doi.org/10.1016/0092-8674(86)90004-8

Ellis, R. E., Jacobson, D. M., & Horvitz, H. R. (1991). Genes required for the engulfment of cell corpses during programmed cell death in *Caenorhabditis elegans*. *Genetics*.

Elmore, S. (2007). Apoptosis: a review of programmed cell death. *Toxicol Pathol*, *35*(4), 495–516. https://doi.org/10.1080/01926230701320337

Erdelyi, P., Borsos, E., Takacs-Vellai, K., Kovacs, T., Kovacs, A. L., Sigmond, T., … Vellai, T. (2011). Shared developmental roles and transcriptional control of autophagy and apoptosis in *Caenorhabditis elegans*. *Journal of Cell Science*. https://doi.org/10.1242/jcs.080192

Ermolaeva, M. A., Segref, A., Dakhovnik, A., Ou, H.-L., Schneider, J. I., Utermöhlen, O., … Schumacher, B. (2013). DNA damage in germ cells induces an innate immune response that triggers systemic stress resistance. *Nature*. https://doi.org/10.1038/nature12452

Eron, S.J., MacPherson, D.J., Dagbay, K.B., & Hardy, J.A. (2018). Multiple Mechanisms of Zinc-Mediated Inhibition for the Apoptotic Caspases-3, -6, -7, and -8. *ACS Chem Biol, 13(5),* 1279-1290. https:// doi: 10.1021/acschembio.8b00064.

Fanidi, A., Harrington, E. A., & Evan, G. I. (1992). Cooperative interaction between c-myc and bcl-2 proto-oncogenes. *Nature*. https://doi.org/10.1038/359554a0

Félix, M.-A., & Braendle, C. (2010). The natural history of *Caenorhabditis elegans*. *Current Biology*. https://doi.org/10.1016/j.cub.2010.09.050

Fernandez, Y., Verhaegen, M., Miller, T. P., Rush, J. L., Steiner, P., Opipari, A. W., … Soengas, M. S. (2005). Differential regulation of Noxa in normal melanocytes and melanoma cells by proteasome inhibition: Therapeutic implications. *Cancer Research*. https://doi.org/10.1158/0008-5472.CAN-05-0686

Fischer, A., Zalvide, J., Faurobert, E., Albiges-Rizo, C., & Tournier-Lasserve, E. (2013). Cerebral cavernous malformations: from CCM genes to endothelial cell homeostasis. *Trends Mol Med*, *19*(5), 302–308. https://doi.org/10.1016/j.molmed.2013.02.004

Fisher, O. S., Deng, H., Liu, D., Zhang, Y., Wei, R., Deng, Y., … Su, B. (2015). Structure and vascular function of MEKK3–cerebral cavernous malformations 2 complex. *Nature Communications*, *6*, 7937. https://doi.org/10.1038/ncomms8937

Fraser, A. G., James, C., Evan, G. I., & Hengartner, M. O. (1999). *Caenorhabditis elegans* inhibitor of apoptosis protein (IAP) homologue BIR-1 plays a conserved role in cytokinesis. *Current Biology*. https://doi.org/10.1016/S0960-9822(99)80137-7

Fricker, M., O'Prey, J., Tolkovsky, A. M., & Ryan, K. M. (2010). Phosphorylation of Puma modulates its apoptotic function by regulating protein stability. *Cell Death and Disease*. https://doi.org/10.1038/cddis.2010.38

Frischer, J. M., Pipp, I., Stavrou, I., Trattnig, S., Hainfellner, J. A., & Knosp, E. (2008). Cerebral cavernous malformations: Congruency of histopathological features with the current clinical definition. *Journal of Neurology, Neurosurgery and Psychiatry*. https://doi.org/10.1136/jnnp.2007.132316

Fukushige, T., Goszczynski, B., Yan, J., & McGhee, J. D. (2005). Transcriptional control and patterning of the pho-1 gene, an essential acid phosphatase expressed in the *C. elegans* intestine. *Developmental Biology*, *279*(2), 446–461. https://doi.org/10.1016/j.ydbio.2004.12.012

Fukushima, T., Shingai, R., Ogurusu, T., & Ichinose, M. (2003). Inhibition of willardiine-induced currents through rat GluR6/KA-2 kainate receptor channels by Zinc and other divalent cations. *Neuroscience Letters*. https://doi.org/10.1016/S0304-3940(03)00805-X

Fukuyama, M., Sakuma, K., Park, R., Kasuga, H., Nagaya, R., Atsumi, Y., … Katada, T. (2012). *C. elegans* AMPKs promote survival and arrest germline development during nutrient stress. *Biology Open*. https://doi.org/10.1242/bio.2012836

Gaither, L. A., & Eide, D. J. (2001). Eukaryotic zinc transporters and their regulation. *BioMetals*. https://doi.org/10.1023/A:1012988914300

Ganju, N., & Eastman, a. (2003). Zinc inhibits Bax and Bak activation and cytochrome c release induced by chemical inducers of apoptosis but not by death-receptor-initiated pathways. *Cell Death and Differentiation*, *10*(6), 652–61. https://doi.org/10.1038/sj.cdd.4401234

Gao, M. X., Liao, E. H., Yu, B., Wang, Y., Zhen, M., & Derry, W. B. (2008). The SCFFSN-1ubiquitin ligase controls germline apoptosis through CEP-1/p53 in *C. elegans*. *Cell Death and Differentiation*. https://doi.org/10.1038/cdd.2008.30

Garcia-Muse, T., & Boulton, S. J. (2005). Distinct modes of ATR activation after replication stress and DNA double-strand breaks in *Caenorhabditis elegans*. *The EMBO Journal*. https://doi.org/10.1038/sj.emboj.7600896

Gartner, A., Milstein, S., Ahmed, S., Hodgkin, J., & Hengartner, M. O. (2000). A conserved checkpoint pathway mediates DNA damage--induced apoptosis and cell cycle arrest in *C. elegans*. *Mol Cell*, *5*(3), 435–443. Retrieved from http://www.ncbi.nlm.nih.gov/pubmed/10882129

Giacinti, C., & Giordano, A. (2006). RB and cell cycle progression. *Oncogene*. https://doi.org/10.1038/sj.onc.1209615

Giblin, L. J., Chang, C. J., Bentley, A. F., Frederickson, C., Lippard, S. J., & Frederickson, C. J. (2006). Zinc-secreting Paneth cells studied by ZP fluorescence. *Journal of Histochemistry and Cytochemistry*. https://doi.org/10.1369/jhc.5A6724.2005

Gingras, A. R., Liu, J. J., & Ginsberg, M. H. (2012). Structural basis of the junctional anchorage of the cerebral cavernous malformations complex. *Journal of Cell Biology*. https://doi.org/10.1083/jcb.201205109

Golstein, P., & Kroemer, G. (2007). Cell death by necrosis: towards a molecular definition. *Trends in Biochemical Sciences*. https://doi.org/10.1016/j.tibs.2006.11.001

Goszczynski, B., Captan, V. V., Danielson, A. M., Lancaster, B. R., & McGhee, J. D. (2016). A 44 bp intestine-specific hermaphrodite-specific enhancer from the *C. elegans* vit-2 vitellogenin gene is directly regulated by ELT-2, MAB-3, FKH-9 and DAF-16 and indirectly regulated by the germline, by daf-2/insulin signaling and by the TGF-β/Sma/Mab pa. *Developmental Biology*. https://doi.org/10.1016/j.ydbio.2016.02.031

Goudreault, M., D'Ambrosio, L. M., Kean, M. J., Mullin, M. J., Larsen, B. G., Sanchez, A., … Gingras, A.-C. (2009). A PP2A Phosphatase High Density Interaction Network Identifies a Novel Striatin-interacting Phosphatase and Kinase Complex Linked to the Cerebral Cavernous Malformation 3 (CCM3) Protein. *Molecular & Cellular Proteomics*. https://doi.org/10.1074/mcp.M800266-MCP200

Granados-Jaén, A., Angulo-Ibáñez, M., Rovira-Clavé, X., Gamez, C. P. V., Soriano, F. X., Reina, M., & Espel, E. (2016). Absence of ERK5/MAPK7 delays tumorigenesis in <i>Atm</i>^{-/-} mice. *Oncotarget*. https://doi.org/10.18632/oncotarget.12908

Grant, B., & Hirsh, D. (1999). Receptor-mediated endocytosis in the *Caenorhabditis elegans* oocyte. *Mol Biol Cell*, *10*(12), 4311–4326. Retrieved from http://www.ncbi.nlm.nih.gov/pubmed/10588660

Greiss, S., Hall, J., Ahmed, S., & Gartner, A. (2008). *C. elegans* SIR-2.1 translocation is linked to a proapoptotic pathway parallel to cep-1/p53 during DNA damage-induced apoptosis. *Genes and Development*. https://doi.org/10.1101/gad.482608

Gumienny, T. L., Lambie, E., Hartwieg, E., Horvitz, H. R., & Hengartner, M. O. (1999). Genetic control of programmed cell death in the *Caenorhabditis elegans* hermaphrodite germline. *Development*, *126*(5), 1011–1022. Retrieved from http://www.ncbi.nlm.nih.gov/pubmed/9927601

Han, M., Aorian, R. V., & Sternberg, P. W. (1990). The let-60 locus controls the switch between vulval and nonvulval cell fates in *Caenorhabditis elegans*. *Genetics*, *126*(4), 899–913. https://doi.org/10.1038/348693a0

Han, M., Golden, A., Han, Y., & Sternberg, P. W. (1993). *C. elegans* lin-45 raf gene participates in let-60 ras-stimulated vulval differentiation. *Nature*. https://doi.org/10.1038/363133a0

Han, M., & Sternberg, P. W. (1990). let-60, a gene that specifies cell fates during *C. elegans* vulval induction, encodes a ras protein. *Cell*. https://doi.org/10.1016/0092-8674(90)90495-Z

Harada, H., Quearry, B., Ruiz-vela, A., & Korsmeyer, S. J. (2004). Survival factor-induced extracellular signal-regulated kinase phosphorylates BIM , inhibiting its association with BAX and proapoptotic activity. *Proc. Natl. Acad. Sci.* https://doi.org/10.1073/pnas.0406837101

Harel, L., Costa, B., Tcherpakov, M., Zapatka, M., Oberthuer, A., Hansford, L. M., … Fainzilber, M. (2009). CCM2 Mediates Death Signaling by the TrkA Receptor Tyrosine Kinase. *Neuron*, *63*(5), 585–591. https://doi.org/10.1016/j.neuron.2009.08.020

Hatzold, J., & Conradt, B. (2008). Control of apoptosis by asymmetric cell division. *PLoS Biology*. https://doi.org/10.1371/journal.pbio.0060084

Hayashi, M., Kim, S. W., Imanaka-Yoshida, K., Yoshida, T., Abel, E. D., Eliceiri, B., … Lee, J. D. (2004). Targeted deletion of BMK1/ERK5 in adult mice perturbs vascular integrity and leads to endothelial failure. *Journal of Clinical Investigation*, *113*(8), 1138–1148. https://doi.org/10.1172/JCI200419890

Hayashizaki, S., Iino, Y., & Yamamoto, M. (1998). Characterization of the *C. elegans* gap-2 gene encoding a novel Ras-GTPase activating protein and its possible role in larval development. *Genes to Cells : Devoted to Molecular & Cellular Mechanisms*. https://doi.org/10.1046/j.1365-2443.1998.00179.x

He, Y., Zhang, H., Yu, L., Gunel, M., Boggon, T. J., Chen, H., & Min, W. (2010). Stabilization of VEGFR2 signaling by cerebral cavernous malformation 3 is critical for vascular development. *Science Signaling*. https://doi.org/10.1126/scisignal.2000722

Hedgecock, E. M., Sulston, J. E., & Thomson, J. N. (1983). Mutations affecting programmed cell deaths in the nematode *Caenorhabditis elegans*. *Science*. https://doi.org/10.1126/science.6857247

Hengartner, M. O., Ellis, R., & Horvitz, H. R. (1992). *Caenorhabditis elegans* gene ced-9 protects cells from programmed cell death. *Nature*. https://doi.org/10.1038/356494a0

Hengartner, M. O., & Horvitz, H. R. (1994a). *C. elegans* cell survival gene ced-9 encodes a functional homolog of the mammalian proto-oncogene bcl-2. *Cell*, *76*(4), 665–676. Retrieved from http://www.ncbi.nlm.nih.gov/pubmed/7907274

Hengartner, M. O., & Horvitz, H. R. (1994b). Programmed cell death in *Caenorhabditis elegans*. *Curr Opin Genet Dev*.

Hester, J., Hanna-Rose, W., & Diaz, F. (2017). Zinc deficiency reduces fertility in *C. elegans* hermaphrodites and disrupts oogenesis and meiotic progression. *Comparative Biochemistry and Physiology Part - C: Toxicology and Pharmacology*. https://doi.org/10.1016/j.cbpc.2016.09.006

Hirose, T., Galvin, B. D., & Horvitz, H. R. (2010). Six and Eya promote apoptosis through direct transcriptional activation of the proapoptotic BH3-only gene egl-1 in *Caenorhabditis elegans*. *Proceedings of the National Academy of Sciences of the United States of America*. https://doi.org/10.1073/pnas.1010023107

Hirose, T., & Horvitz, H. R. (2013). An Sp1 transcription factor coordinates caspase-dependent and -independent apoptotic pathways. *Nature*. https://doi.org/10.1038/nature12329

Hockenbery, D., Nuñez, G., Milliman, C., Schreiber, R. D., & Korsmeyer, S. J. (1990). Bcl-2 is an inner mitochondrial membrane protein that blocks programmed cell death. *Nature*. https://doi.org/10.1038/348334a0

Hodgkin, J. (2005). Karyotype, ploidy, and gene dosage. *WormBook*. https://doi.org/10.1895/wormbook.1.3.1

Hoeppner, D. J., Hengartner, M. O., & Schnabel, R. (2001). Engulfment genes cooperate with ced-3 to promote cell death in *Caenorhabditis elegans*. *Nature*, *412*(6843), 202–206. https://doi.org/10.1038/35084103

Hofmann, E. R., Milstein, S., Boulton, S. J., Ye, M., Hofmann, J. J., Stergiou, L., … Hengartner, M. O. (2002). *Caenorhabditis elegans* HUS-1 is a DNA damage checkpoint protein required for genome stability and EGL-1-mediated apoptosis. *Curr Biol*, *12*(22), 1908–1918. https://doi.org/S0960982202012629 [pii]

Hogan, B. M., Bussmann, J., Wolburg, H., & Schulte-Merker, S. (2008). ccm1 cell autonomously regulates endothelial cellular morphogenesis and vascular tubulogenesis in zebrafish. *Human Molecular Genetics*. https://doi.org/10.1093/hmg/ddn142

Hojyo, S., & Fukada, T. (2016). Zinc transporters and signaling in physiology and pathogenesis. *Archives of Biochemistry and Biophysics*. https://doi.org/10.1016/j.abb.2016.06.020

Hönscheid, A., Dubben, S., Rink, L., & Haase, H. (2012). Zinc differentially regulates mitogen-activated protein kinases in human T cells. *The Journal of Nutritional Biochemistry*. https://doi.org/10.1016/j.jnutbio.2010.10.007

Howard, R. M., & Sundaram, M. V. (2002). *C. elegans* EOR-1/PLZF and EOR-2 positively regulate Ras and Wnt signaling and function redundantly with LIN-25 and the SUR-2 mediator component. *Genes and Development*. https://doi.org/10.1101/gad.998402

Hsieh, P. N., Zhou, G., Yuan, Y., Zhang, R., Prosdocimo, D. A., Sangwung, P., … Jain, M. K. (2017). A conserved KLF-autophagy pathway modulates nematode lifespan and mammalian age-associated vascular dysfunction. *Nature Communications*, *8*(1). https://doi.org/10.1038/s41467-017-00899-5

Hu, B., Ren, D., Su, D., Lin, H., Xian, Z., Wan, X., … Wang, J. (2012). Expression of the phosphorylated MEK5 protein is associated with TNM staging of colorectal cancer. *BMC Cancer*. https://doi.org/10.1186/1471-2407-12-127

Hua, C., Zorn, S., Jensen, J., Coupland, R., Ko, H., Wright, J., & Bakhshi, A. (1988). Consequences of the t(14;18) chromosomal translocation in follicular lymphoma: deregulated expression of a chimeric and mutated BCL-2 gene. *Oncogene Res*.

Huang, C. Y., Chen, J. Y., Wu, S. C., Tan, C. H., Tzeng, R. Y., Lu, P. J., … Wu, Y. C. (2012). *C. elegans* EIF-3.K promotes programmed cell death through CED-3 caspase. *PLoS ONE*. https://doi.org/10.1371/journal.pone.0036584

Hubbard, E. J. A. (2007). *Caenorhabditis elegans* germ line: a model for stem cell biology. *Developmental Dynamics*. https://doi.org/10.1002/dvdy.21335

Im, J. Y., Yoon, S. H., Kim, B. K., Ban, H. S., Won, K. J., Chung, K. S., … Won, M. (2016). DNA damage induced apoptosis suppressor (DDIAS) is upregulated via ERK5/MEF2B signaling and promotes β-catenin-mediated invasion. *Biochimica et Biophysica Acta - Gene Regulatory Mechanisms*, *1859*(11), 1449–1458. https://doi.org/10.1016/j.bbagrm.2016.07.003

Ito, S., Greiss, S., Gartner, A., & Derry, W. B. (2010). Cell-nonautonomous regulation of *C. elegans* germ cell death by kri-1. *Curr Biol*, *20*(4), 333–338. https://doi.org/10.1016/j.cub.2009.12.032

Itoh, N., Yonehara, S., Ishii, A., Yonehara, M., Mizushima, S. I., Sameshima, M., … Nagata, S. (1991). The polypeptide encoded by the cDNA for human cell surface antigen Fas can mediate apoptosis. *Cell*. https://doi.org/10.1016/0092-8674(91)90614-5

Jacobs, D., Beitel, G. J., Clark, S. G., Horvitz, H. R., & Kornfeld, K. (1998). Gain-of-function mutations in the *Caenorhabditis elegans* lin-1 ETS gene identify a C-terminal regulatory domain phosphorylated by ERK MAP kinase. *Genetics*.

Jagasia, R., Grote, P., Westermann, B., & Conradt, B. (2005). DRP-1-mediated mitochondrial fragmentation during EGL-1-induced cell death in *C. elegans*. *Nature*. https://doi.org/10.1038/nature03316

Jiang, H. S., & Wu, Y. C. (2014). LIN-3/EGF Promotes the Programmed Cell Death of Specific Cells in *Caenorhabditis elegans* by Transcriptional Activation of the Pro-apoptotic Gene egl-1. *PLoS Genetics*. https://doi.org/10.1371/journal.pgen.1004513

Jirakulaporn, T., & Muslin, A. J. (2004). Cation diffusion facilitator proteins modulate Raf-1 activity. *Journal of Biological Chemistry*, *279*(26), 27807–27815. https://doi.org/10.1074/jbc.M401210200

Johnsen, H. L., & Horvitz, H. R. (2016). Both the apoptotic suicide pathway and phagocytosis are required for a programmed cell death in *Caenorhabditis elegans*. *BMC Biology*. https://doi.org/10.1186/s12915-016-0262-5

Johnson, T. E., Mitchell, D. H., Kline, S., Kemal, R., & Foy, J. (1984). Arresting development arrests aging in the nematode *Caenorhabditis elegans*. *Mechanisms of Ageing and Development*, *28*(1), 23–40. https://doi.org/10.1016/0047-6374(84)90150-7

Jung, C. H., Ro, S. H., Cao, J., Otto, N. M., & Kim, D. H. (2010). MTOR regulation of autophagy. *FEBS Letters*. https://doi.org/10.1016/j.febslet.2010.01.017

Kamath, R. S., & Ahringer, J. (2003). Genome-wide RNAi screening in *Caenorhabditis elegans*. *Methods*, *30*(4), 313–321. https://doi.org/10.1016/S1046-2023(03)00050-1

Kelly, W. G., Xu, S., Montgomery, M. K., & Fire, A. (1997). Distinct requirements for somatic and germline expression of a generally expressed *Caenorhabditis elegans* gene. *Genetics*, *146*(1), 227–238.

Kerr, J. F., Wyllie, A. H., & Currie, A. R. (1972). 29-Apoptosis: a basic biological phenomenon with wide-ranging implications in tissue kinetics. *British Journal of Cancer*. https://doi.org/10.1111/j.1365-2796.2005.01570.x

Kessner, D., Chambers, M., Burke, R., Agus, D., & Mallick, P. (2008). ProteoWizard: Open source software for rapid proteomics tools development. *Bioinformatics*. https://doi.org/10.1093/bioinformatics/btn323

Kim, Y. S., Morgan, M. J., Choksi, S., & Liu, Z. gang. (2007). TNF-Induced Activation of the Nox1 NADPH Oxidase and Its Role in the Induction of Necrotic Cell Death. *Molecular Cell*. https://doi.org/10.1016/j.molcel.2007.04.021

Kimble, J., & Hirsh, D. (1979). The postembryonic cell lineages of the hermaphrodite and male gonads in *Caenorhabditis elegans*. *Developmental Biology*. https://doi.org/10.1016/0012-1606(79)90035-6

Kinchen, J. M., Cabello, J., Kilngele, D., Wong, K., Felchtinger, R., Schnabel, H., Schnabel, R., & Hengartner, M. O. (2005). Two pathways converge at CED-10 to mediate actin rearrangement and corpse removal in *C. elegans*. *Nature*. https://doi.org/10.1038/nature03263

Kinet, M. J., Malin, J. A., Abraham, M. C., Blum, E. S., Silverman, M. R., Lu, Y., & Shaham, S. (2016). HSF-1 activates the ubiquitin proteasome system to promote non-apoptotic developmental cell death in *C. elegans*. *ELife*. https://doi.org/10.7554/eLife.12821

Klöditz, K., Chen, Y. Z., Xue, D., & Fadeel, B. (2017). Programmed cell clearance: From nematodes to humans. *Biochemical and Biophysical Research Communications*. https://doi.org/10.1016/j.bbrc.2016.12.005

Kornfeld, K., Hom, D. B., & Horvitz, H. R. (1995). The ksr-1 gene encodes a novel protein kinase involved in ras-mediated signaling in *C. elegans*. *Cell*. https://doi.org/10.1016/0092-8674(95)90206-6

Kritikou, E. A., Milstein, S., Vidalain, P. O., Lettre, G., Bogan, E., Doukoumetzidis, K., Gray, P., Chappell T.J., Vidal, M., & Hengartner, M. O. (2006). *C. elegans* GLA-3 is a novel component of the MAP kinase MPK-1 signaling pathway required for germ cell survival.

Genes Dev, *20*(16), 2279–2292. https://doi.org/10.1101/gad.384506

Kumar, J., Barhydt, T., Awasthi, A., Lithgow, G. J., Killilea, D. W., & Kapahi, P. (2016). Zinc levels modulate lifespan through multiple longevity pathways in *Caenorhabditis elegans*. *PLoS ONE*. https://doi.org/10.1371/journal.pone.0153513

L.Omonosova, E., & C.Hinnadurai, G. (2008). BH3-only proteins in apoptosis and beyond: An overview. *Oncogene*. https://doi.org/10.1038/onc.2009.39

Lackner, M. R., Kornfeld, K., Miller, L. M., Robert Horvitz, H., & Kim, S. K. (1994). A MAP kinase homolog, mpk-1, is involved in ras-mediated induction of vulval cell fates in *Caenorhabditis elegans*. *Genes and Development*. https://doi.org/10.1101/gad.8.2.160

Lans, H., & Vermeulen, W. (2011). Nucleotide Excision Repair in *Caenorhabditis elegans*. *Molecular Biology International*. https://doi.org/10.4061/2011/542795

Lascarez-Lagunas, L. I., Silva-Garcia, C. G., Dinkova, T. D., & Navarro, R. E. (2014). LIN-35/Rb Causes Starvation-Induced Germ Cell Apoptosis via CED-9/Bcl2 Downregulation in *Caenorhabditis elegans*. *Molecular and Cellular Biology*. https://doi.org/10.1128/MCB.01532-13

Lee, M. H., Hook, B., Pan, G., Kershner, A. M., Merritt, C., Seydoux, G., … Kimble, J. (2007a). Conserved regulation of MAP kinase expression by PUF RNA-binding proteins. *PLoS Genetics*. https://doi.org/10.1371/journal.pgen.0030233

Lee, M. H., Ohmachi, M., Arur, S., Nayak, S., Francis, R., Church, D., … Schedl, T. (2007b). Multiple functions and dynamic activation of MPK-1 extracellular signal-regulated kinase signaling in *Caenorhabditis elegans* germline development. *Genetics*, *177*(4), 2039–2062. https://doi.org/10.1534/genetics.107.081356

Lei, K., & Davis, R. J. (2003). JNK phosphorylation of Bim-related members of the Bcl2 family induces Bax-dependent apoptosis. *Proceedings of the National Academy of Sciences*. https://doi.org/10.1073/pnas.0438011100

Lemmens, B. B. L. G., & Tijsterman, M. (2011). DNA double-strand break repair in *Caenorhabditis elegans*. *Chromosoma*. https://doi.org/10.1007/s00412-010-0296-3

Levi-Ferber, M., Salzberg, Y., Safra, M., Haviv-Chesner, A., Bülow, H. E., & Henis-Korenblit, S. (2014). It's All in Your Mind: Determining Germ Cell Fate by Neuronal IRE-1 in *C. elegans*. *PLoS Genetics*, *10*(10). https://doi.org/10.1371/journal.pgen.1004747

Li, H., & Durbin, R. (2009). Fast and accurate short read alignment with Burrows-Wheeler transform. *Bioinformatics*. https://doi.org/10.1093/bioinformatics/btp324

Li, H., Zhu, H., Xu, C. J., & Yuan, J. (1998). Cleavage of BID by caspase 8 mediates the mitochondrial damage in the Fas pathway of apoptosis. *Cell*. https://doi.org/10.1016/S0092-8674(00)81590-1

Li, J., & Yuan, J. (2008). Caspases in apoptosis and beyond. *Oncogene*. https://doi.org/10.1038/onc.2008.297

Li, L. Y., Luo, X., & Wang, X. (2001). Endonuclease G is an apoptotic DNase when released from mitochondria. *Nature*. https://doi.org/10.1038/35083620

Li, P., Nijhawan, D., Budihardjo, I., Srinivasula, S. M., Ahmad, M., Alnemri, E. S., & Wang, X. (1997). Cytochrome c and dATP-dependent formation of Apaf-1/caspase-9 complex initiates an apoptotic protease cascade. *Cell*. https://doi.org/10.1016/S0092-8674(00)80434-1

Li, X., Johnson, R. W., Park, D., Chin-Sang, I., & Chamberlin, H. M. (2012). Somatic gonad sheath cells and Eph receptor signaling promote germ-cell death in *C. elegans*. *Cell Death Differ*, *19*(6), 1080–1089. https://doi.org/10.1038/cdd.2011.192

Libina, N., Berman, J. R., & Kenyon, C. (2003). Tissue-Specific Activities of *C. elegans* DAF-16 in the Regulation of Lifespan. *Cell*. https://doi.org/10.1016/S0092-8674(03)00889-4

Lin, K., Hsin, H., Libina, N., & Kenyon, C. (2001). Regulation of the *Caenorhabditis elegans* longevity protein DAF-16 by insulin/IGF-1 and germline signaling. *Nature Genetics*. https://doi.org/10.1038/88850

Lin, W., Li, D., Cheng, L., Li, L., Liu, F., Hand, N. J., … Rader, D. J. (2018). Zinc transporter Slc39a8 is essential for cardiac ventricular compaction. *Journal of Clinical Investigation*, *128*(2), 826–833. https://doi.org/10.1172/JCI96993

Liu, G., Zhang, J., Larsen, B., Stark, C., Breitkreutz, A., Lin, Z. Y., … Gingras, A. C. (2010). ProHits: Integrated software for mass spectrometry-based interaction proteomics. *Nature Biotechnology*. https://doi.org/10.1038/nbt1010-1015

Liu, H. (2006). Direct regulation of egl-1 and of programmed cell death by the Hox protein MAB-5 and by CEH-20, a *C. elegans* homolog of Pbx1. *Development*. https://doi.org/10.1242/dev.02234

Liu, H., Rigamonti, D., Badr, A., & Zhang, J. (2011). Ccm1 regulates microvascular morphogenesis during angiogenesis. *Journal of Vascular Research*. https://doi.org/10.1159/000316851

Liu, W., Draheim, K. M., Zhang, R., Calderwood, D. A., & Boggon, T. J. (2013). Mechanism for KRIT1 Release of ICAP1-Mediated Suppression of Integrin Activation. *Molecular Cell*. https://doi.org/10.1016/j.molcel.2012.12.005

Lopez-Ramirez, M. A., Fonseca, G., Zeineddine, H. A., Girard, R., Moore, T., Pham, A., … Ginsberg, M. H. (2017). Thrombospondin1 (TSP1) replacement prevents cerebral cavernous malformations. *The Journal of Experimental Medicine*, jem.20171178. https://doi.org/10.1084/jem.20171178

Lopez, A. L., Chen, J., Joo, H. J., Drake, M., Shidate, M., Kseib, C., & Arur, S. (2013). DAF-2

and ERK Couple Nutrient Availability to Meiotic Progression during *Caenorhabditis elegans* Oogenesis. *Developmental Cell*. https://doi.org/10.1016/j.devcel.2013.09.008

Louvi, A., Chen, L., Two, A. M., Zhang, H., Min, W., & Günel, M. (2011). Loss of cerebral cavernous malformation 3 (Ccm3) in neuroglia leads to CCM and vascular pathology. *Proceedings of the National Academy of Sciences of the United States of America*. https://doi.org/10.1073/pnas.1012617108

Lowenstein, E. J., Daly, R. J., Batzer, A. G., Li, W., Margolis, B., Lammers, R., … Schlessinger, J. (1992). The SH2 and SH3 domain-containing protein GRB2 links receptor tyrosine kinases to ras signaling. *Cell*. https://doi.org/10.1016/0092-8674(92)90167-B

Lowman, X. H., McDonnell, M. A., Kosloske, A., Odumade, O. A., Jenness, C., Karim, C. B., … Kelekar, A. (2010). The Proapoptotic Function of Noxa in Human Leukemia Cells Is Regulated by the Kinase Cdk5 and by Glucose. *Molecular Cell*. https://doi.org/10.1016/j.molcel.2010.11.035

Luke, C. J., Pak, S. C., Askew, Y. S., Naviglia, T. L., Askew, D. J., Nobar, S. M., … Silverman, G. A. (2007). An Intracellular Serpin Regulates Necrosis by Inhibiting the Induction and Sequelae of Lysosomal Injury. *Cell*. https://doi.org/10.1016/j.cell.2007.07.013

Mably, J. D., Chuang, L. P., Serluca, F. C., Mohideen, M.-A. P. K., Chen, J.-N., & Fishman, M. C. (2006). Santa and Valentine Pattern Concentric Growth of Cardiac Myocardium in the Zebrafish. *Development (Cambridge, England)*. https://doi.org/10.1242/dev.02469

Maddaluno, L., Rudini, N., Cuttano, R., Bravi, L., Giampietro, C., Corada, M., … Dejana, E. (2013). EndMT contributes to the onset and progression of cerebral cavernous malformations. *Nature*. https://doi.org/10.1038/nature12207

Malin, J. A., Kinet, M. J., Abraham, M. C., Blum, E. S., & Shaham, S. (2016). Transcriptional control of non-apoptotic developmental cell death in *C. elegans*. *Cell Death and Differentiation*. https://doi.org/10.1038/cdd.2016.77

Maret, W. (2013). Inhibitory zinc sites in enzymes. *BioMetals*. https://doi.org/10.1007/s10534-013-9613-7

Maret, W. (2017). Zinc in cellular regulation: The nature and significance of "zinc signals." *International Journal of Molecular Sciences*. https://doi.org/10.3390/ijms18112285

Martin, S. J., Finucane, D. M., Amarante-Mendes, G. P., O'Brien, G. A., & Green, D. R. (1996). Phosphatidylserine externalization during CD95-induced apoptosis of cells and cytoplasts requires ICE/CED-3 protease activity. *Journal of Biological Chemistry*. https://doi.org/10.1074/jbc.271.46.28753

Maurer, C. W., Chiorazzi, M., & Shaham, S. (2007). Timing of the onset of a developmental cell death is controlled by transcriptional induction of the *C. elegans* ced-3 caspase-encoding gene. *Development (Cambridge, England)*. https://doi.org/10.1242/dev.02818

McConnell, B. B., & Yang, V. W. (2010). Mammalian Krüppel-like factors in health and diseases. *Physiological Reviews*, *90*(4), 1337–81. https://doi.org/10.1152/physrev.00058.2009

McDonald, D. A., Shenkar, R., Shi, C., Stockton, R. A., Akers, A. L., Kucherlapati, M. H., … Marchuk, D. A. (2011). A novel mouse model of cerebral cavernous malformations based on the two-hit mutation hypothesis recapitulates the human disease. *Hum Mol Genet*, *20*(2), 211–222. https://doi.org/10.1093/hmg/ddq433

Medema, J. P., Scaffidi, C., Kischkel, F. C., Shevchenko, A., Mann, M., Krammer, P. H., & Peter, M. E. (1997). FLICE is activated by association with the CD95 death-inducing signaling complex (DISC). *EMBO Journal*. https://doi.org/10.1093/emboj/16.10.2794

Mehta, P. B., Jenkins, B. L., McCarthy, L., Thilak, L., Robson, C. N., Neal, D. E., & Leung, H. Y. (2003). MEK5 overexpression is associated with metastatic prostate cancer, and stimulates proliferation, MMP-9 expression and invasion. *Oncogene*. https://doi.org/10.1038/sj.onc.1206154

Meléndez, A., Tallóczy, Z., Seaman, M., Eskelinen, E. L., Hall, D. H., & Levine, B. (2003). Autophagy genes are essential for dauer development and life-span extension in *C. elegans*. *Science*. https://doi.org/10.1126/science.1087782

Meley, D., Bauvy, C., Houben-Weerts, J. H. P. M., Dubbelhuis, P. F., Helmond, M. T. J., Codogno, P., & Meijer, A. J. (2006). AMP-activated protein kinase and the regulation of autophagic proteolysis. *The Journal of Biological Chemistry*. https://doi.org/10.1074/jbc.M605488200

Mendoza, A. D., Woodruff, T. K., Wignall, S. M., & O'Halloran, T. V. (2017). Zinc availability during germline development impacts embryo viability in *Caenorhabditis elegans*. *Comparative Biochemistry and Physiology Part - C: Toxicology and Pharmacology*. https://doi.org/10.1016/j.cbpc.2016.09.007

Minnerly, J., Zhang, J., Parker, T., Kaul, T., & Jia, K. (2017). The cell non-autonomous function of ATG-18 is essential for neuroendocrine regulation of *Caenorhabditis elegans* lifespan. *PLoS Genetics*. https://doi.org/10.1371/journal.pgen.1006764

Miura, M., Zhu, H., Rotello, R., Hartwieg, E. A., & Yuan, J. (1993). Induction of apoptosis in fibroblasts by IL-1 beta-converting enzyme, a mammalian homolog of the *C. elegans* cell death gene ced-3. *Cell*, *75*(4), 653–660. Retrieved from http://www.ncbi.nlm.nih.gov/pubmed/8242741

Mizuno, T., Fujiki, K., Sasakawa, A., Hisamoto, N., & Matsumoto, K. (2008). Role of the *Caenorhabditis elegans* Shc adaptor protein in the c-Jun N-terminal kinase signaling pathway. *Molecular and Cellular Biology*. https://doi.org/10.1128/MCB.00938-08

Moll, U. M., & Petrenko, O. (2003). The MDM2-p53 interaction. *Molecular Cancer Research : MCR*. https://doi.org/10.1016/s0092-8674(00)81871-1

Montero, J. C., Ocaña, A., Abad, M., Ortiz-Ruiz, M. J., Pandiella, A., & Esparís-Ogando, A. (2009). Expression of Erk5 in early stage breast cancer and association with disease free survival identifies this kinase as a potential therapeutic target. *PloS One*. https://doi.org/10.1371/journal.pone.0005565

Morthorst, T. H., & Olsen, a. (2013). Cell-nonautonomous inhibition of radiation-induced apoptosis by dynein light chain 1 in *Caenorhabditis elegans*. *Cell Death & Disease*. https://doi.org/10.1038/cddis.2013.319

Moser, S. C., Von Elsner, S., Büssing, I., Alpi, A., Schnabel, R., & Gartner, A. (2009). Functional dissection of *Caenorhabditis elegans* CLK-2/TEL2 cell cycle defects during Embryogenesis and germline development. *PLoS Genetics*. https://doi.org/10.1371/journal.pgen.1000451

Moujalled, D., Weston, R., Anderton, H., Ninnis, R., Goel, P., Coley, A., … Puthalakath, H. (2011). Cyclic-AMP-dependent protein kinase A regulates apoptosis by stabilizing the BH3-only protein Bim. *EMBO Reports*. https://doi.org/10.1038/embor.2010.190

Muzio, M., Chinnaiyan, A. M., Kischkel, F. C., O'Rourke, K., Shevchenko, A., Ni, J., … Dixit, V. M. (1996). FLICE, a novel FADD-homologous ICE/CED-3-like protease, is recruited to the CD95 (Fas/APO-1) death-inducing signaling complex. *Cell*. https://doi.org/10.1016/S0092-8674(00)81266-0

Nagata, S., & Tanaka, M. (2017). Programmed cell death and the immune system. *Nature Reviews Immunology*. https://doi.org/10.1038/nri.2016.153

Nakano, K., & Vousden, K. H. (2001). PUMA, a novel proapoptotic gene, is induced by p53. *Molecular Cell*. https://doi.org/10.1016/S1097-2765(01)00214-3

Nam, D.-H., Han, J.-H., Lim, J. H., Park, K. M., & Woo, C.-H. (2017). CHOP Deficiency Ameliorates ERK5 Inhibition-Mediated Exacerbation of Streptozotocin-Induced Hyperglycemia and Pancreatic β-Cell Apoptosis. *Molecules and Cells*. https://doi.org/10.14348/molcells.2017.2296

Narasimhan, P., Liu, J., Song, Y. S., Massengale, J. L., & Chan, P. H. (2009). VEGF stimulates the ERK 1/2 signaling pathway and apoptosis in cerebral endothelial cells after ischemic conditions. *Stroke*. https://doi.org/10.1161/STROKEAHA.108.534644

Navarro, R. E., Shim, E. Y., Kohara, Y., Singson, A., & Blackwell, T. K. (2001). cgh-1, a conserved predicted RNA helicase required for gametogenesis and protection from physiological germline apoptosis in *C. elegans*. *Development (Cambridge, England)*.

Nehme, R., & Conradt, B. (2008). egl-1: A key activator of apoptotic cell death in *C. elegans*. *Oncogene*. https://doi.org/10.1038/onc.2009.41

Nehme, R., Grote, P., Tomasi, T., Löser, S., Holzkamp, H., Schnabel, R., & Conradt, B. (2010). Transcriptional upregulation of both egl-1 BH3-only and ced-3 caspase is required for the death of the male-specific CEM neurons. *Cell Death and Differentiation*.

https://doi.org/10.1038/cdd.2010.3

Nithianandarajah-Jones, G. N., Wilm, B., Goldring, C. E., Muller, J., & Cross, M. J. (2012). ERK5: structure, regulation and function. *Cell Signal*, *24*(11), 2187–2196. https://doi.org/10.1016/j.cellsig.2012.07.007

Oda, E., Ohki, R., Murasawa, H., Nemoto, J., Shibue, T., Yamashita, T., … Tanaka, N. (2000). Noxa, a BH3-only member of the Bcl-2 family and candidate mediator of p53-induced apoptosis. *Science*. https://doi.org/10.1126/science.288.5468.1053

Oh, K. H., & Kim, H. (2013). Reduced IGF signaling prevents muscle cell death in a *Caenorhabditis elegans* model of muscular dystrophy. *Proceedings of the National Academy of Sciences*. https://doi.org/10.1073/pnas.1308866110

Ohmachi, M., Rocheleau, C. E., Church, D., Lambie, E., Schedl, T., & Sundaram, M. V. (2002). *C. elegans* ksr-1 and ksr-2 have both unique and redundant functions and are required for MPK-1 ERK phosphorylation. *Current Biology*. https://doi.org/10.1016/S0960-9822(02)00690-5

Okuyama, T., Inoue, H., Ookuma, S., Satoh, T., Kano, K., Honjoh, S., … Nishida, E. (2010). The ERK-MAPK pathway regulates longevity through SKN-1 and insulin-like signaling in *Caenorhabditis elegans*. *Journal of Biological Chemistry*. https://doi.org/10.1074/jbc.M110.146274

Ou, H. Der, Löhr, F., Vogel, V., Mäntele, W., & Dötsch, V. (2007). Structural evolution of C-terminal domains in the p53 family. *The EMBO Journal*. https://doi.org/10.1038/sj.emboj.7601764

Paix, A., Folkmann, A., Rasoloson, D., & Seydoux, G. (2015). High Efficiency, Homology-Directed Genome Editing in *Caenorhabditis elegans* Using CRISPR-Cas9 Ribonucleoprotein Complexes. *Genetics*, *201*(1), 47–54. https://doi.org/10.1534/genetics.115.179382

Pang, W., Lu, H., Hu, Y. D., Yang, H. P., Leng, X., & Jiang, Y. G. (2012). Depletion of intracellular zinc induced apoptosis in cultured hippocampal neurons through Raf/MEK/ERK pathways. *Nutr Neurosci*. https://doi.org/10.1179/1476830511Y.0000000031

Pazdernik, N., & Schedl, T. (2013). Introduction to germ cell development in *Caenorhabditis elegans*. *Advances in Experimental Medicine and Biology*. https://doi.org/10.1007/978-1-4614-4015-4-1

Peden, E., Kimberly, E., Gengyo-Ando, K., Mitani, S., & Xue, D. (2007). Control of sex-specific apoptosis in *C. elegans* by the BarH homeodomain protein CEH-30 and the transcriptional repressor UNC-37/Groucho. *Genes and Development*. https://doi.org/10.1101/gad.1607807

Pereira, D. M., Simões, A. E. S., Gomes, S. E., Castro, R. E., Carvalho, T., Rodrigues, C. M. P., & Borralho, P. M. (2016). MEK5/ERK5 signaling inhibition increases colon cancer cell

sensitivity to 5-fluorouracil through a p53-dependent mechanism. *Oncotarget*. https://doi.org/10.18632/oncotarget.9107

Perrin, A. J., Gunda, M., Yu, B., Yen, K., Ito, S., Forster, S., … Derry, W. B. (2013). Noncanonical control of *C. elegans* germline apoptosis by the insulin/IGF-1 and Ras/MAPK signaling pathways. *Cell Death Differ*, *20*(1), 97–107. https://doi.org/10.1038/cdd.2012.101

Perry, D. K., Smyth, M. J., Stennicke, H. R., Salvesen, G. S., Duriez, P., Poirier, G. G., & Hannun, Y. A. (1997). Zinc is a potent inhibitor of the apoptotic protease, caspase-3: A novel target for zinc in the inhibition of apoptosis. *Journal of Biological Chemistry*, *272*(30), 18530–18533. https://doi.org/10.1074/jbc.272.30.18530

Peschiaroli, A., Scialpi, F., Bernassola, F., Pagano, M., & Melino, G. (2009). The F-box protein FBXO45 promotes the proteasome-dependent degradation of p73. *Oncogene*. https://doi.org/10.1038/onc.2009.177

Pitti, R. M., Marsters, S. A., Ruppert, S., Donahue, C. J., Moore, A., & Ashkenazi, A. (1996). Induction of apoptosis by Apo-2 ligand, a new member of the tumor necrosis factor cytokine family. *Journal of Biological Chemistry*. https://doi.org/10.1074/jbc.271.22.12687

Plum, L. M., Rink, L., & Hajo, H. (2010). The essential toxin: Impact of zinc on human health. *International Journal of Environmental Research and Public Health*. https://doi.org/10.3390/ijerph7041342

Plummer, N. W., Gallione, C. J., Srinivasan, S., Zawistowski, J. S., Louis, D. N., & Marchuk, D. A. (2004). Loss of p53 sensitizes mice with a mutation in Ccm1 (KRIT1) to development of cerebral vascular malformations. *American Journal of Pathology*. https://doi.org/10.1016/S0002-9440(10)63409-8

Plummer, N. W., Squire, T. L., Srinivasan, S., Huang, E., Zawistowski, J. S., Matsunami, H., … Marchuk, D. a. (2006). Neuronal expression of the Ccm2 gene in a new mouse model of cerebral cavernous malformations. *Mammalian Genome : Official Journal of the International Mammalian Genome Society*. https://doi.org/10.1007/s00335-005-0098-8

Popovici, C., Isnardon, D., Birnbaum, D., & Roubin, R. (2002). *Caenorhabditis elegans* receptors related to mammalian vascular endothelial growth factor receptors are expressed in neural cells. *Neuroscience Letters*. https://doi.org/10.1016/S0304-3940(02)00595-5

Quevedo, C., Kaplan, D. R., & Derry, W. B. (2007). AKT-1 Regulates DNA-Damage-Induced Germline Apoptosis in *C. elegans*. *Current Biology*. https://doi.org/10.1016/j.cub.2006.12.038

Ravichandran, K. S. (2011). Beginnings of a Good Apoptotic Meal: The Find-Me and Eat-Me Signaling Pathways. *Immunity*. https://doi.org/10.1016/j.immuni.2011.09.004

Reddien, P. W., Cameron, S., & Horvitz, H. R. (2001). Phagocytosis promotes programmed cell death in *C. elegans*. *Nature*. https://doi.org/10.1038/35084096

Reed, J. C. (2008). Bcl-2-family proteins and hematologic malignancies: History and future prospects. *Blood*. https://doi.org/10.1182/blood-2007-08-110114

Reinke, A. W., Mak, R., Troemel, E. R., & Ben, E. J. (2017). In vivo mapping of tissue- and subcellular-specific proteomes in *Caenorhabditis elegans*. *Science Advances*. https://doi.org/10.1126/sciadv.1602426

Reinke, V., Smith, H. E., Nance, J., Wang, J., Van Doren, C., Begley, R., … Kim, S. K. (2000). A global profile of germline gene expression in *C. elegans*. *Molecular Cell*. https://doi.org/10.1016/S1097-2765(00)00059-9

Renehan, A. G., Booth, C., & Potten, C. S. (2001). What is apoptosis, and why is it important? *BMJ (Clinical Research Ed.)*. https://doi.org/10.1136/bmj.322.7301.1536

Renz, M., Otten, C., Faurobert, E., Rudolph, F., Zhu, Y., Boulday, G., … Abdelilah-Seyfried, S. (2015). Regulation of β1 Integrin-Klf2-Mediated Angiogenesis by CCM Proteins. *Developmental Cell*, *32*(2), 181–190. https://doi.org/10.1016/j.devcel.2014.12.016

Richards, D. M., & Endres, R. G. (2014). The mechanism of phagocytosis: Two stages of engulfment. *Biophysical Journal*. https://doi.org/10.1016/j.bpj.2014.07.070

Roh, H. C., Collier, S., Deshmukh, K., Guthrie, J., Robertson, J. D., & Kornfeld, K. (2013). ttm-1 Encodes CDF Transporters That Excrete Zinc from Intestinal Cells of *C. elegans* and Act in a Parallel Negative Feedback Circuit That Promotes Homeostasis. *PLoS Genetics*, *9*(5). https://doi.org/10.1371/journal.pgen.1003522

Roh, H. C., Collier, S., Guthrie, J., Robertson, J. D., & Kornfeld, K. (2012). Lysosome-related organelles in intestinal cells are a zinc storage site in *C. elegans*. *Cell Metabolism*, *15*(1), 88–99. https://doi.org/10.1016/j.cmet.2011.12.003

Ross, A. J., Li, M., Yu, B., Gao, M. X., & Derry, W. B. (2011). The EEL-1 ubiquitin ligase promotes DNA damage-induced germ cell apoptosis in *C. elegans*. *Cell Death and Differentiation*. https://doi.org/10.1038/cdd.2010.180

Ross, G. M., Shamovsky, I. L., Lawrance, G., Solc, M., Dostaler, S. M., Jimmo, S. L., … Riopelle, R. J. (1997). Zinc alters conformation and inhibits biological activities of nerve growth factor and related neurotrophins. *Nature Medicine*. https://doi.org/10.1038/nm0897-872

Roux, P. P., & Topisirovic, I. (2012). Regulation of mRNA translation by signaling pathways. *Cold Spring Harbor Perspectives in Biology*. https://doi.org/10.1101/cshperspect.a012252

Rutkowski, R., Dickinson, R., Stewart, G., Craig, A., Schimpl, M., Keyse, S. M., & Gartner, A. (2011). Regulation of *Caenorhabditis elegans* p53/CEP-1-dependent germ cell apoptosis by Ras/MAPK signaling. *PLoS Genet*, *7*(8), e1002238. https://doi.org/10.1371/journal.pgen.1002238

Salinas, L. S., Maldonado, E., & Navarro, R. E. (2006). Stress-induced germ cell apoptosis by a

p53 independent pathway in *Caenorhabditis elegans*. *Cell Death and Differentiation*. https://doi.org/10.1038/sj.cdd.4401976

Samara, C., Syntichaki, P., & Tavernarakis, N. (2008). Autophagy is required for necrotic cell death in *Caenorhabditis elegans*. *Cell Death and Differentiation*. https://doi.org/10.1038/sj.cdd.4402231

Sato, K., Norris, A., Sato, M., & Grant, B. D. (2014). *C. elegans* as a model for membrane traffic. *WormBook : The Online Review of C. elegans Biology*. https://doi.org/10.1895/wormbook.1.77.2

Schenk, R. L., Strasser, A., & Dewson, G. (2017). BCL-2: Long and winding path from discovery to therapeutic target. *Biochemical and Biophysical Research Communications*. https://doi.org/10.1016/j.bbrc.2016.10.100

Schertel, C., & Conradt, B. (2007). *C. elegans* orthologs of components of the RB tumor suppressor complex have distinct pro-apoptotic functions. *Development*, *134*(20), 3691–3701. https://doi.org/10.1242/dev.004606

Schneider, P., Thome, M., Burns, K., Bodmer, J. L., Hofmann, K., Kataoka, T., … Tschopp, J. (1997). TRAIL receptors 1 (DR4) and 2 (DR5) signal FADD-dependent apoptosis and activate NF-κB. *Immunity*. https://doi.org/10.1016/S1074-7613(00)80401-X

Schouest, K. R., Kurasawa, Y., Furuta, T., Hisamoto, N., Matsumoto, K., & Schumacher, J. M. (2009). The germinal center kinase GCK-1 is a negative regulator of MAP kinase activation and apoptosis in the *C. elegans* germline. *PLoS ONE*. https://doi.org/10.1371/journal.pone.0007450

Schroeder, L. K., Kremer, S., Kramer, M. J., Currie, E., Kwan, E., Watts, J. L., … Hermann, G. J. (2007). Function of the *Caenorhabditis elegans* ABC Transporter PGP-2 in the Biogenesis of a Lysosome-related Fat Storage Organelle. *Molecular Biology of the Cell*, *18*(3), 995–1008. https://doi.org/10.1091/mbc.E06-08-0685

Schumacher, B., Hanazawa, M., Lee, M. H., Nayak, S., Volkmann, K., Hofmann, R., … Gartner, A. (2005a). Translational repression of *C. elegans* p53 by GLD-1 regulates DNA damage-induced apoptosis. *Cell*. https://doi.org/10.1016/j.cell.2004.12.009

Schumacher, B., Hofmann, K., Boulton, S., & Gartner, A. (2001). The *C. elegans* homolog of the p53 tumor suppressor is required for DNA damage-induced apoptosis. *Current Biology : CB*, *11*(21), 1722–7. https://doi.org/11696333

Schumacher, B., Schertel, C., Wittenburg, N., Tuck, S., Mitani, S., Gartner, A., … Shaham, S. (2005b). *C. elegans* ced-13 can promote apoptosis and is induced in response to DNA damage. *Cell Death and Differentiation*. https://doi.org/10.1038/sj.cdd.4401539

Seker, A., Pricola, K. L., Guclu, B., Ozturk, A. K., Louvi, A., & Gunel, M. (2006). CCM2 expression parallels that of CCM1. *Stroke*. https://doi.org/10.1161/01.STR.0000198835.49387.25

Sendoel, A., Kohler, I., Fellmann, C., Lowe, S. W., & Hengartner, M. O. (2010). HIF-1 antagonizes p53-mediated apoptosis through a secreted neuronal tyrosinase. *Nature*, *465*(7298), 577–583. https://doi.org/10.1038/nature09141

Sendoel, A., Maida, S., Zheng, X., Teo, Y., Stergiou, L., Rossi, C. A., … Hengartner, M. O. (2014). DEPDC1/LET-99 participates in an evolutionarily conserved pathway for anti-tubulin drug-induced apoptosis. *Nature Cell Biology*. https://doi.org/10.1038/ncb3010

Serebriiskii, I., Estojak, J., Sonoda, G., Testa, J. R., & Golemis, E. a. (1997). Association of Krev-1/rap1a with Krit1, a novel ankyrin repeat-containing protein encoded by a gene mapping to 7q21-22. *Oncogene*, *15*(9), 1043–1049. https://doi.org/10.1038/sj.onc.1201268

Shannon, L. A., McBurney, T. M., Wells, M. A., Roth, M. E., Calloway, P. A., Bill, C. A., … Vines, C. M. (2012). CCR7/CCL19 controls expression of EDG-1 in T cells. *Journal of Biological Chemistry*. https://doi.org/10.1074/jbc.M111.310045

Shaye, D. D., & Greenwald, I. (2011). Ortholist: A compendium of *C. elegans* genes with human orthologs. *PLoS ONE*. https://doi.org/10.1371/journal.pone.0020085

Shemesh, N., Shai, N., & Ben-Zvi, A. (2013). Germline stem cell arrest inhibits the collapse of somatic proteostasis early in *Caenorhabditis elegans* adulthood. *Aging Cell*. https://doi.org/10.1111/acel.12110

Shenkar, R., Shi, C., Austin, C., Moore, T., Lightle, R., Cao, Y., … Awad, I. A. (2017). RhoA kinase inhibition with fasudil versus simvastatin in murine models of cerebral cavernous malformations. *Stroke*. https://doi.org/10.1161/STROKEAHA.116.015013

Sherrard, R., Luehr, S., Holzkamp, H., Mcjunkin, K., Memar, N., & Conradt, B. (2017). miRNAs cooperate in apoptosis regulation during *C . elegans* development. *Genes and Development*, 1–14. https://doi.org/10.1101/gad.288555.116.

Shirasu, K., Lahaye, T., Tan, M. W., Zhou, F., Azevedo, C., & Schulze-Lefert, P. (1999). A novel class of eukaryotic zinc-binding proteins is required for disease resistance signaling in barley and development in *C. elegans*. *Cell*. https://doi.org/10.1016/S0092-8674(00)81522-6

Shteynberg, D., Deutsch, E. W., Lam, H., Eng, J. K., Sun, Z., Tasman, N., … Nesvizhskii, A. I. (2011). iProphet: Multi-level Integrative Analysis of Shotgun Proteomic Data Improves Peptide and Protein Identification Rates and Error Estimates. *Molecular & Cellular Proteomics*. https://doi.org/10.1074/mcp.M111.007690

Sieburth, D. S., Sun, Q., & Han, M. (1998). Sur-8, a conserved Ras-binding protein with leucine-rich repeats, positively regulates Ras-mediated signaling in *C. elegans*. *Cell*. https://doi.org/10.1016/S0092-8674(00)81227-1

Sohn, S. J., Li, D., Lee, L. K., & Winoto, A. (2005). Transcriptional regulation of tissue-specific genes by the ERK5 mitogen-activated protein kinase. *Mol Cell Biol*, *25*(19), 8553–8566. https://doi.org/10.1128/MCB.25.19.8553-8566.2005

Spanier, B., Rubio-Aliaga, I., Hu, H., & Daniel, H. (2010). Altered signalling from germline to intestine pushes daf-2;pept-1 *Caenorhabditis elegans* into extreme longevity. *Aging Cell*. https://doi.org/10.1111/j.1474-9726.2010.00591.x

Spector, M. S., Desnoyers, S., Hoeppner, D. J., & Hengartner, M. O. (1997). Interaction between the *C. elegans* cell-death regulators CED-9 and CED- 4. *Nature*, *385*(6617), 653–656. https://doi.org/10.1038/385653a0

Stergiou, L., Doukoumetzidis, K., Sendoel, A., & Hengartner, M. O. (2007). The nucleotide excision repair pathway is required for UV-C-induced apoptosis in *Caenorhabditis elegans*. *Cell Death and Differentiation*. https://doi.org/10.1038/sj.cdd.4402115

Stergiou, L., & Hengartner, M. O. (2004). Death and more: DNA damage response pathways in the nematode *C. elegans*. *Cell Death Differ*, *11*(1), 21–28. https://doi.org/10.1038/sj.cdd.4401340

Stiegler, A. L., Zhang, R., Liu, W., & Boggon, T. J. (2014). Structural determinants for binding of sorting nexin 17 (SNX17) to the cytoplasmic adaptor protein Krev interaction trapped 1 (KRIT1). *Journal of Biological Chemistry*. https://doi.org/10.1074/jbc.M114.584011

Stinchcomb, D. T., Shaw, J. E., Carr, S. H., & Hirsh, D. (1985). Extrachromosomal DNA transformation of *Caenorhabditis elegans*. *Molecular and Cellular Biology*, *5*(12), 3484–96. https://doi.org/10.1128/MCB.5.12.3484.Updated

Stockton, R. A., Shenkar, R., Awad, I. A., & Ginsberg, M. H. (2010). Cerebral cavernous malformations proteins inhibit Rho kinase to stabilize vascular integrity. *J Exp Med*, *207*(4), 881–896. https://doi.org/10.1084/jem.20091258

Sulston, J. E., & Horvitz, H. R. (1977). Post-embryonic cell lineages of the nematode, *Caenorhabditis elegans*. *Developmental Biology*. https://doi.org/10.1016/0012-1606(77)90158-0

Sulston, J. E., Schierenberg, E., White, J. G., & Thomson, J. N. (1983). The embryonic cell lineage of the nematode *Caenorhabditis elegans*. *Dev Biol*, *100*(1), 64–119. Retrieved from http://www.ncbi.nlm.nih.gov/pubmed/6684600

Sunadome, K., Yamamoto, T., Ebisuya, M., Kondoh, K., Sehara-Fujisawa, A., & Nishida, E. (2011). ERK5 Regulates Muscle Cell Fusion through Klf Transcription Factors. *Developmental Cell*, *20*(2), 192–205. https://doi.org/10.1016/j.devcel.2010.12.005

Sundaram, M., & Han, M. (1995). The *C. elegans* ksr-1 gene encodes a novel raf-related kinase involved in Ras-mediated signal transduction. *Cell*. https://doi.org/10.1016/0092-8674(95)90205-8

Sundaram, M. V. (2013). Canonical RTK-Ras-ERK signaling and related alternative pathways. *WormBook*. https://doi.org/10.1895/wormbook.1.80.2

Susin, S. a, Lorenzo, H. K., Zamzami, N., Marzo, I., Snow, B. E., Brothers, G. M., … Kroemer, G. (1999). Molecular characterization of mitochondrial apoptosis-inducing factor. *Nature*. https://doi.org/10.1038/17135

Suzanne, M., & Steller, H. (2013). Shaping organisms with apoptosis. *Cell Death and Differentiation*. https://doi.org/10.1038/cdd.2013.11

Suzuki, J., Denning, D. P., Imanishi, E., Horvitz, H. R., & Nagata, S. (2013). Xk-related protein 8 and CED-8 promote phosphatidylserine exposure in apoptotic cells. *Science*. https://doi.org/10.1126/science.1236758

Suzuki, Y., Imai, Y., Nakayama, H., Takahashi, K., Takio, K., & Takahashi, R. (2001a). A serine protease, HtrA2, is released from the mitochondria and interacts with XIAP, inducing cell death. *Molecular Cell*. https://doi.org/10.1016/S1097-2765(01)00341-0

Suzuki, Y., Nakabayashi, Y., & Takahashi, R. (2001b). Ubiquitin-protein ligase activity of X-linked inhibitor of apoptosis protein promotes proteasomal degradation of caspase-3 and enhances its anti-apoptotic effect in Fas-induced cell death. *Proceedings of the National Academy of Sciences*. https://doi.org/10.1073/pnas.161506698

Takacs-Vellai, K., Vellai, T., Puoti, A., Passannante, M., Wicky, C., Streit, A., … Müller, F. (2005). Inactivation of the autophagy Gene bec-1 triggers apoptotic cell death in *C. elegans*. *Current Biology*. https://doi.org/10.1016/j.cub.2005.07.035

Takeda, K., & Akira, S. (2005). Toll-like receptors in innate immunity. *International Immunology*. https://doi.org/10.1093/intimm/dxh186

Tang, A. T., Choi, J. P., Kotzin, J. J., Yang, Y., Hong, C. C., Hobson, N., … Kahn, M. L. (2017). Endothelial TLR4 and the microbiome drive cerebral cavernous malformations. *Nature*. https://doi.org/10.1038/nature22075

Tarsitano, M., De Falco, S., Colonna, V., McGhee, J. D., & Persico, M. G. (2006). The *C. elegans* pvf-1 gene encodes a PDGF/VEGF-like factor able to bind mammalian VEGF receptors and to induce angiogenesis. *The FASEB Journal : Official Publication of the Federation of American Societies for Experimental Biology*. https://doi.org/10.1096/fj.05-4147com

Teo, G., Liu, G., Zhang, J., Nesvizhskii, A. I., Gingras, A. C., & Choi, H. (2014). SAINTexpress: Improvements and additional features in Significance Analysis of INTeractome software. *Journal of Proteomics*. https://doi.org/10.1016/j.jprot.2013.10.023

The C. elegans Sequencing Consortium. (1998). Genome Sequence of the Nematode *Caenorhabditis elegans*: A Platform for Investigating Biology. *Science*. https://doi.org/10.1126/science.282.5396.2012

Thellmann, M., Hatzold, J., & Conradt, B. (2003). The Snail-like CES-1 protein of *C. elegans* can block the expression of the BH3-only cell-death activator gene egl-1 by antagonizing the function of bHLH proteins. *Development (Cambridge, England)*. https://doi.org/10.1242/dev.00597

Tiensuu, T., Larsen, M. K., Vernersson, E., & Tuck, S. (2005). lin-1 has both positive and negative functions in specifying multiple cell fates induced by Ras/MAP kinase signaling in *C. elegans*. *Developmental Biology*. https://doi.org/10.1016/j.ydbio.2005.08.007

Tóth, K. (2011). Zinc in Neurotransmission. *Annual Review of Nutrition*. https://doi.org/10.1146/annurev-nutr-072610-145218

Toth, M. L., Simon, P., Kovacs, A. L., & Vellai, T. (2007). Influence of autophagy genes on ion-channel-dependent neuronal degeneration in *Caenorhabditis elegans*. *Journal of Cell Science*. https://doi.org/10.1242/jcs.03401

Trapnell, C., Roberts, A., Goff, L., Pertea, G., Kim, D., Kelley, D. R., … Pachter, L. (2012). Differential gene and transcript expression analysis of RNA-seq experiments with TopHat and Cufflinks. *Nature Protocols*. https://doi.org/10.1038/nprot.2012.016

Tsujimoto, Y., Finger, L. R., Yunis, J., Nowell, P. C., & Croce, C. M. (1984). Cloning of the chromosome breakpoint of neoplastic B cells with the t(14;18) chromosome translocation. *Science*. https://doi.org/10.1126/science.6093263

Tsujimoto, Y., Ikegaki, N., & Croce, C. M. (1987). Characterization of the protein product of bcl-2, the gene involved in human follicular lymphoma. *Oncogene*.

Uhlik, M. T., Abell, A. N., Johnson, N. L., Sun, W., Cuevas, B. D., Lobel-Rice, K. E., … Johnson, G. L. (2003). Rac–MEKK3–MKK3 scaffolding for p38 MAPK activation during hyperosmotic shock. *Nature Cell Biology*, *5*(12), 1104–1110. https://doi.org/10.1038/ncb1071

Vandenabeele, P., Galluzzi, L., Vanden Berghe, T., & Kroemer, G. (2010). Molecular mechanisms of necroptosis: An ordered cellular explosion. *Nature Reviews Molecular Cell Biology*. https://doi.org/10.1038/nrm2970

Vanlangenakker, N., Bertrand, M. J. M., Bogaert, P., Vandenabeele, P., & Vanden Berghe, T. (2011). TNF-induced necroptosis in L929 cells is tightly regulated by multiple TNFR1 complex i and II members. *Cell Death and Disease*. https://doi.org/10.1038/cddis.2011.111

Varga, T., & Aplan, P. D. (2005). Chromosomal aberrations induced by double strand DNA breaks. *DNA Repair*. https://doi.org/10.1016/j.dnarep.2005.05.004

Vermezovic, J., Stergiou, L., Hengartner, M., D 'adda, F., & Fagagna, D. (2012). Differential regulation of DNA damage response activation between somatic and germline cells in *Caenorhabditis elegans*. *Cell Death and Differentiation*. https://doi.org/10.1038/cdd.2012.69

Veyhl, J., Dunn, R. J., Johnston, W. L., Bennett, A., Zhang, L. W., Dennis, J. W., … Culotti, J. G. (2017). The directed migration of gonadal distal tip cells in *Caenorhabditis elegans* requires NGAT-1, a ß1,4-N-acetylgalactosaminyltransferase enzyme. *PLoS ONE*. https://doi.org/10.1371/journal.pone.0183049

Vu, H. T., Kotla, S., Ko, K. A., Fujii, Y., Tao, Y., Medina, J., … Abe, J.-I. (2018). Ionizing Radiation Induces Endothelial Inflammation and Apoptosis via p90RSK-Mediated ERK5 S496 Phosphorylation. *Frontiers in Cardiovascular Medicine*. https://doi.org/10.3389/fcvm.2018.00023

Wajant, H., Mühlenbeck, F., & Scheurich, P. (1998). Identification of a TRAF (TNF receptor-associated factor) gene in *Caenorhabditis elegans*. *Journal of Molecular Evolution*. https://doi.org/10.1007/PL00006423

Wang, H., Lu, Q., Cheng, S., Wang, X., & Zhang, H. (2013). Autophagy activity contributes to programmed cell death in *Caenorhabditis elegans*. *Autophagy*. https://doi.org/10.4161/auto.26095

Wang, K., Yin, X. M., Chao, D. T., Milliman, C. L., & Korsmeyer, S. J. (1996). BID: A novel BH3 domain-only death agonist. *Genes and Development*. https://doi.org/10.1101/gad.10.22.2859

Wang, M. C., O'Rourke, E. J., & Ruvkun, G. (2008). Fat metabolism links germline stem cells and longevity in *C. elegans*. *Science*. https://doi.org/10.1126/science.1162011

Wang, P., Lindsay, J., Owens, T. W., Mularczyk, E. J., Warwood, S., Foster, F., … Gilmore, A. P. (2014). Phosphorylation of the Proapoptotic BH3-Only Protein Bid Primes Mitochondria for Apoptosis during Mitotic Arrest. *Cell Reports*. https://doi.org/10.1016/j.celrep.2014.03.050

Wang, S., Wu, L., Wang, Y., Luo, X., & Lu, Y. (2009). Copper-induced germline apoptosis in *Caenorhabditis elegans*: The independent roles of DNA damage response signaling and the dependent roles of MAPK cascades. *Chemico-Biological Interactions*. https://doi.org/10.1016/j.cbi.2009.03.012

Wang, X., Wang, J., Gengyo-Ando, K., Gu, L., Sun, C. L., Yang, C., … Xue, D. (2007). *C. elegans* mitochondrial factor WAH-1 promotes phosphatidylserine externalization in apoptotic cells through phospholipid scramblase SCRM-1. *Nature Cell Biology*. https://doi.org/10.1038/ncb1574

Wang, X., Wu, Y. C., Fadok, V. A., Lee, M. C., Gengyo-Ando, K., Cheng, L. C., … Xue, D. (2003). Cell Corpse Engulfment Mediated by *C. elegans* Phosphatidylserine Receptor Through CED-5 and CED-12. *Science*. https://doi.org/10.1126/science.1087641

Wang, X., Yang, C., Chai, J., Shi, Y., & Xue, D. (2002). Mechanisms of AIF-mediated apoptotic DNA degradation in *Caenorhabditis elegans*. *Science*. https://doi.org/10.1126/science.1076194

Wang, X., & Zhou, B. (2010). Dietary zinc absorption: A play of zips and znts in the gut. *IUBMB Life*. https://doi.org/10.1002/iub.291

Warnhoff, K., Roh, H. C., Kocsisova, Z., Tan, C. H., Morrison, A., Croswell, D., … Kornfeld, K. (2017). The Nuclear Receptor HIZR-1 Uses Zinc as a Ligand to Mediate Homeostasis in Response to High Zinc. *PLoS Biology*, *15*(1). https://doi.org/10.1371/journal.pbio.2000094

Watanabe, N., Nagamatsu, Y., Gengyo-Ando, K., Mitani, S., & Ohshima, Y. (2005). Control of body size by SMA-5, a homolog of MAP kinase BMK1/ERK5, in *C. elegans*. *Development (Cambridge, England)*, *132*(14), 3175–3184. https://doi.org/10.1242/dev.01895

Wei, Y., & Kenyon, C. (2016). Roles for ROS and hydrogen sulfide in the longevity response to germline loss in *Caenorhabditis elegans*. *Proceedings of the National Academy of Sciences*. https://doi.org/10.1073/pnas.1524727113

White, J. G., Southgate, E., Thomson, J. N., & Brenner, S. (1986). The Structure of the Nervous System of the Nematode *Caenorhabditis elegans*. *Philosophical Transactions of the Royal Society B: Biological Sciences*. https://doi.org/10.1098/rstb.1986.0056

Whitehead, K. J. (2004). Ccm1 is required for arterial morphogenesis: implications for the etiology of human cavernous malformations. *Development*. https://doi.org/10.1242/dev.01036

Willis, S. (2003). The Bcl-2-regulated apoptotic pathway. *Journal of Cell Science*. https://doi.org/10.1242/jcs.00754

Wu, W., Liu, P., & Li, J. (2012). Necroptosis: An emerging form of programmed cell death. *Critical Reviews in Oncology/Hematology*. https://doi.org/10.1016/j.critrevonc.2011.08.004

Wu, Y., Han, M., & Guan, K. L. (1995). MEK-2, a *Caenorhabditis elegans* MAP kinase kinase, functions in Ras-mediated vulval induction and other developmental events. *Genes and Development*. https://doi.org/10.1101/gad.9.6.742

Xie, T., Peng, W., Liu, Y., Yan, C., Maki, J., Degterev, A., … Shi, Y. (2013). Structural basis of RIP1 inhibition by necrostatins. *Structure*. https://doi.org/10.1016/j.str.2013.01.016

Xu, K., Tavernarakis, N., & Driscoll, M. (2001). Necrotic cell death in *C. elegans* requires the function of calreticulin and regulators of Ca2+ release from the endoplasmic reticulum. *Neuron*. https://doi.org/10.1016/S0896-6273(01)00432-9

Yang, J., Liu, X., Bhalla, K., Kim, C. N., Ibrado, A. M., Cai, J., … Wang, X. (1997). Prevention of apoptosis by Bcl-2: Release of cytochrome c from mitochondria blocked. *Science*. https://doi.org/10.1126/science.275.5303.1129

Yang, M., Sun, J., Sun, X., Shen, Q., Gao, Z., & Yang, C. (2009). *Caenorhabditis elegans* protein arginine methyltransferase PRMT-5 negatively regulates DNA damage-induced apoptosis. *PLoS Genetics*. https://doi.org/10.1371/journal.pgen.1000514

Yoder, J. H., Chong, H., Guan, K. I., & Han, M. (2004). Modulation of KSR activity in *Caenorhabditis elegans* by Zn ions, PAR-1 kinase and PP2A phosphatase. *EMBO Journal*, *23*(1), 111–119. https://doi.org/10.1038/sj.emboj.7600025

Yu, H., Lai, H., Lin, T., & Lo, S. (2015). Autonomous and non-autonomous roles of DNase II during cell death in *C. elegans* embryos. *Bioscience Reports*. https://doi.org/10.1042/BSR20150055

Yunger, E., Safra, M., Levi-Ferber, M., Haviv-Chesner, A., & Henis-Korenblit, S. (2017). Innate immunity mediated longevity and longevity induced by germ cell removal converge on the C-type lectin domain protein IRG-7. *PLoS Genetics*. https://doi.org/10.1371/journal.pgen.1006577

Zawistowski, J. S., Stalheim, L., Uhlik, M. T., Abell, A. N., Ancrile, B. B., Johnson, G. L., & Marchuk, D. A. (2005). CCM1 and CCM2 protein interactions in cell signaling: Implications for cerebral cavernous malformations pathogenesis. *Human Molecular Genetics*, *14*(17), 2521–2531. https://doi.org/10.1093/hmg/ddi256

Zeitoun-Ghandour, S., Charnock, J. M., Hodson, M. E., Leszczyszyn, O. I., Blindauer, C. A., & Starzenbaum, S. R. (2010). The two *Caenorhabditis elegans* metallothioneins (CeMT-1 and CeMT-2) discriminate between essential zinc and toxic cadmium. *FEBS Journal*. https://doi.org/10.1111/j.1742-4658.2010.07667.x

Zhang, D. W., Shao, J., Lin, J., Zhang, N., Lu, B. J., Lin, S. C., … Han, J. (2009a). RIP3, an energy metabolism regulator that switches TNF-induced cell death from apoptosis to necrosis. *Science*. https://doi.org/10.1126/science.1172308

Zhang, H., Kim, A., Abraham, N., Khan, L. A., Hall, D. H., Fleming, J. T., & Gobel, V. (2012). Clathrin and AP-1 regulate apical polarity and lumen formation during *C. elegans* tubulogenesis. *Development*, *139*(11), 2071–2083. https://doi.org/10.1242/dev.077347

Zhang, J., Clatterbuck, R. E., Rigamonti, D., Chang, D. D., & Dietz, H. C. (2001). Interaction between krit1 and icap1alpha infers perturbation of integrin beta1-mediated angiogenesis in the pathogenesis of cerebral cavernous malformation. *Hum Mol Genet*, *10*(25), 2953–2960. Retrieved from http://www.ncbi.nlm.nih.gov/pubmed/11741838

Zhang, J., Yang, C., Brey, C., Rodriguez, M., Oksov, Y., Gaugler, R., … Hashmi, S. (2009b). Mutation in *Caenorhabditis elegans* Kruppel-like factor, KLF-3 results in fat accumulation and alters fatty acid composition. *Exp Cell Res*, *315*(15), 2568–2580. https://doi.org/10.1016/j.yexcr.2009.04.025

Zhang, R., Li, X., & Boggon, T. J. (2015). Structural analysis of the KRIT1 ankyrin repeat and FERM domains reveals a conformationally stable ARD-FERM interface. *Journal of Structural Biology*. https://doi.org/10.1016/j.jsb.2015.10.006

Zhao, Y., Tan, C.H., Krauchunas, A., Scharf, A., Dietrich, N., Warnhoff, K., Yuan, Z., Druzhinina, M., Gu, S.G., Miao, L., Singson, A., Ellis, R.E., & Kornfeld, K. (2018). The zinc transporter ZIPT-7.1 regulates sperm activation in nematodes. *PLoS Biology*.

https://doi: 10.1371/journal.pbio.2005069.

Zheng, F., Zhang, J., Luo, S., Yi, J., Wang, P., Zheng, Q., & Wen, Y. (2016). miR-143 is associated with proliferation and apoptosis involving ERK5 in heLa cells. *Oncology Letters*. https://doi.org/10.3892/ol.2016.5016

Zhou, H. J., Qin, L., Zhang, H., Tang, W., Ji, W., He, Y., … Min, W. (2016a). Endothelial exocytosis of angiopoietin-2 resulting from CCM3 deficiency contributes to cerebral cavernous malformation. *Nature Medicine*. https://doi.org/10.1038/nm.4169

Zhou, Z., Rawnsley, D. R., Goddard, L. M., Pan, W., Cao, X. J., Jakus, Z., … Kahn, M. L. (2015). The Cerebral Cavernous Malformation Pathway Controls Cardiac Development via Regulation of Endocardial MEKK3 Signaling and KLF Expression. *Developmental Cell*, *32*(2), 168–180. https://doi.org/10.1016/j.devcel.2014.12.009

Zhou, Z., Tang, A. T., Wong, W.-Y., Bamezai, S., Goddard, L. M., Shenkar, R., … Kahn, M. L. (2016b). Cerebral cavernous malformations arise from endothelial gain of MEKK3–KLF2/4 signalling. *Nature*, *532*(7597), 122–126. https://doi.org/10.1038/nature17178

Zou, C.-G., Ma, Y.-C., Dai, L.-L., & Zhang, K.-Q. (2014). Autophagy protects *C. elegans* against necrosis during Pseudomonas aeruginosa infection. *Proceedings of the National Academy of Sciences*. https://doi.org/10.1073/pnas.1405032111

Zou, H., Henzel, W. J., Liu, X., Lutschg, A., & Wang, X. (1997). Apaf-1, a human protein homologous to *C. elegans* CED-4, participates in cytochrome c-dependent activation of caspase-3. *Cell*. https://doi.org/10.1016/S0092-8674(00)80501-2